Université de Montréal

INNERVATION CHOLINERGIQUE DU CORTEX CÉRÉBRAL CHEZ LE RAT ADULTE ET EN COURS DE DÉVELOPPEMENT : DISTRIBUTION QUANTIFIÉE ET ANALYSE ULTRASTRUCTURALE

par

NAGUIB MECHAWAR

Départements de physiologie et de pathologie et biologie cellulaire et Centre de recherche en sciences neurologiques

Faculté de Médecine

Thèse présentée à la Faculté des études supérieures
en vue de l'obtention du grade de Philosophiæ Doctor (Ph.D.)
en sciences neurologiques

juillet 2001

Université de Montréal

Faculté des études supérieures

Cette thèse de doctorat intitulée :

« Innervation cholinergique du cortex cérébral chez le rat adulte et en cours de développement : distribution quantifiée et analyse ultrastructurale »

présentée par

NAGUIB MECHAWAR

a été évaluée par un jury composé des personnes suivantes :

VINCENT CASTELLUCCI
.....
président-rapporteur

LAURENT DESCARRIES
.....
directeur de recherche

ALAIN BEAUDET
.....
membre du jury

MIRCEA STERIADE
.....
examinateur externe

VICTOR GISIGER
.....
représentant du doyen de la FES

SOMMAIRE

Cette thèse rassemble une série d'études immunocytochimiques en microscopie photonique et électronique ayant pour but de mieux connaître la distribution et l'ultrastructure des varicosités axonales des neurones cholinergiques (ACh) innervant le cortex cérébral du rat adulte et en cours de développement postnatal. Les arborisations et varicosités axonales ACh ont été identifiées à l'aide d'un anticorps monoclonal très sensible, spécifiquement dirigé contre la choline acétyltransférase, l'enzyme de synthèse de l'ACh (gracieuseté de C. Cozzari et B.K. Hartman).

Dans un premier temps, nous avons mis au point une méthode semi-informatisée de quantification des axones immunoréactifs et de leurs varicosités permettant de déterminer les densités d'axones (longueur par mm^3 de tissu) et de varicosités (nombre par mm^3 de tissu) dans différentes couches et aires corticales. Cette méthode nous a permis de chiffrer les densités régionale et laminaires dans trois aires primaires du cortex cérébral adulte: frontale (motrice), pariétale (sensorielle) et occipitale (visuelle). Ces données nous ont ensuite permis de déterminer par extrapolation la longueur totale de l'arborisation axonale cholinergique corticale et le nombre total de ses varicosités, de même que la longueur moyenne d'axone et le nombre moyen de varicosités axonales par neurone cholinergique qui se projette au cortex. Ces chiffres à eux seuls laissent supposer une influence ubiquitaire de l'ACh au sein du cortex cérébral. (Publié dans *The Journal of Comparative Neurology*, 2000)

Dans un deuxième temps, nous avons employé la même méthode pour examiner et mesurer la croissance de l'innervation cholinergique dans les trois mêmes régions du cortex cérébral à divers stades de leur développement postnatal.

Ce travail a révélé une installation précoce et rapide de l'innervation cholinergique, permis d'évaluer son taux de croissance comme étant maximal au cours des deux premières semaines suivant la naissance, et démontré certaines différences entre les aires en ce qui a trait à la durée requise pour atteindre la densité d'innervation adulte. Ainsi, l'innervation du cortex pariétal s'est avérée de la même densité que chez l'adulte dès la fin de la deuxième semaine, alors que celles des cortex frontal et surtout occipital n'atteignent leur valeur adulte qu'à la fin du premier mois après la naissance. Ces résultats viennent à l'appui d'un rôle possible de l'acétylcholine au cours du développement cortical, et soulignent la remarquable capacité de croissance des neurones cholinergiques individuels. (Sous presse au journal *Neuroscience*, 2001)

Dans un troisième temps, nous avons examiné au microscope électronique l'innervation cholinergique du cortex pariétal en développement, à trois âges postnataux: 8, 16 et 32 jours. Cette étude a montré que la plupart des caractéristiques intrinsèques de cette innervation en croissance étaient comparables à celles de l'adulte, incluant une fréquence de spécialisation synaptique très faible, de l'ordre de 17% des varicosités seulement. Cette constatation laisse supposer qu'une neurotransmission diffuse, à distance, de même qu'un niveau ambiant d'acétylcholine dans l'espace intercellulaire peuvent être impliqués dans les fonctions qui sont attribuées à ce neurotransmetteur/modulateur au cours du développement cortical. (Soumis à *The Journal of Comparative Neurology*, 2001)

Mots clés: Acétylcholine, innervation, axones, cortex cérébral, développement, immunocytochimie, choline acetyltransferase, quantification.

SUMMARY

This thesis presents a series of light- and electron-microscopic immunocytochemical studies aimed at a better understanding of the distribution and fine structure of cholinergic (ACh) axon varicosities in the cerebral cortex of the adult and developing rat. The cortical ACh innervation was visualized with a highly sensitive monoclonal antibody against rat brain choline acetyltransferase, the synthesizing enzyme of ACh (generous gift of C. Cozzari and B.K. Hartman).

Firstly, we developed a semi-computerized quantification method allowing to measure densities of immunoreactive axons (length per mm^3) and varicosities (number per mm^3) in different cortical areas and layers. Thus, we obtained the laminar and regional densities of ACh innervation in three primary cortical areas of adult rat: frontal (motor), parietal (somatosensory) and occipital (visual). These data allowed further extrapolation, in terms of total length of ACh axons and total number of ACh varicosities in cortex, as well as mean length of axon and mean number of varicosities per ACh neuron projecting to cortex. (Published in *The Journal of Comparative Neurology*, 2000)

Secondly, we used the same method to examine and measure the growth of the ACh innervation in the same cortical areas, at different stages of their postnatal development. This study revealed that the cortical ACh innervation develops early and rapidly, that its speed of growth is maximal during the first two weeks after birth, and that the time required to reach an adult density of innervation varies between areas. Thus, the ACh innervation in parietal cortex was already adult-like after two weeks, whereas those of the frontal and particularly occipital cortex continued their maturation until the end of the first postnatal month. These results support the roles and functions attributed to ACh during cortical development, and

underline the remarkable growth capacity of individual cholinergic neurons. (In press, *Neuroscience*, 2001)

Thirdly, we examined the ultrastructural features of the cholinergic innervation in the developing parietal cortex at three postnatal ages: 8, 16 and 32 days. This study demonstrated that most of the intrinsic characteristics of this growing innervation are comparable to those of adult, including a very low frequency of synaptic specializations (17% of varicosities only). This suggests that a diffuse transmission, as well as an ambient level of ACh in the intercellular space, could be involved in the functions attributed to this neurotransmitter/modulator during cortical development. (Submitted to *The Journal Comparative Neurology*, 2001)

Key words: Acetylcholine, innervation, axons, cerebral cortex, development, immunocytochemistry, choline acetyltransferase, quantification.

RÉSUMÉ VULGARISÉ

De nos jours, l'organisation en réseau des cellules nerveuses (neurones) du cerveau peut être étudiée en tenant compte de l'identité des diverses substances chimiques utilisées par les neurones comme transmetteurs d'information (neurotransmetteurs). On sait que cet échange d'information s'effectue au niveau de spécialisations membranaires jonctionnelles (synapses). Des travaux antérieurs de notre laboratoire ont cependant permis de comprendre qu'il peut également dépendre d'une diffusion de transmetteur dans l'espace intercellulaire, à partir de sites de libération dépourvus de telles jonctions. On parle alors de neuromodulation plutôt que de neurotransmission au sens strict du terme.

Grâce à l'immunocytochimie, il est possible d'identifier dans le tissu nerveux les prolongements neuronaux de type axonal et leurs renflements ou varicosités, qui représentent les sites de libération d'un neurotransmetteur/modulateur donné. C'est cette méthode que nous avons appliquée, en microscopie optique puis en microscopie électronique, pour visualiser les arborisations axonales contenant l'acétylcholine (cholinergiques) dans le cortex cérébral du rat. Il s'agit d'un sujet d'autant plus intéressant que l'acétylcholine est impliquée, entre autre, dans la plasticité neuronale, soit la capacité de remodelage des cellules nerveuses au cours du développement ou chez l'adulte.

Dans un premier temps, nous avons développé une méthode de comptage semi-informatisée, qui nous a permis de chiffrer les densités régionale et intra-régionale (couche par couche) de l'innervation cholinergique dans trois régions corticales du rat adulte: frontale (motrice), pariétale (sensorielle) et occipitale (visuelle). En plus des données ainsi recueillies, notre étude a suggéré un rôle particulier de l'acétylcholine dans le traitement de l'information sortant du cortex, de même que

celle y entrant. Elle a également permis de déterminer la longueur moyenne de l'arborisation axonale et le nombre moyen de varicosités axonales par neurone cholinergique qui se projette au cortex, ce qui devrait également améliorer nos connaissances des propriétés fonctionnelles et du rôle de l'acétylcholine dans cette région du cerveau.

Dans un deuxième temps, nous avons employé la même méthode pour examiner et mesurer la croissance de l'innervation cholinergique dans les trois mêmes régions du cortex cérébral à divers stades de leur développement postnatal. Ce travail a révélé une installation précoce et rapide de l'innervation cholinergique, évalué son taux de croissance comme étant maximal au cours des deux premières semaines suivant la naissance, et démontré certaines différences entre les aires en ce qui a trait à la durée requise pour atteindre la densité d'innervation adulte. Ces résultats viennent à l'appui d'un rôle possible de l'acétylcholine au cours du développement du cortex cérébral et soulignent les remarquables capacités de croissance des neurones cholinergiques individuels.

Finalement, nous avons examiné au microscope électronique l'innervation cholinergique du cortex pariétal en développement, à trois âges postnataux : 8, 16 et 32 jours. Cette étude a démontré que la plupart des caractéristiques intrinsèques de cette innervation en croissance se comparent à celles de l'adulte, incluant une fréquence de spécialisation synaptique très faible, de l'ordre de 17% des varicosités seulement. Cette constatation laisse supposer qu'une neurotransmission diffuse, à distance, de même qu'un niveau ambiant d'acétylcholine dans l'espace intercellulaire puissent être impliqués dans les fonctions qui lui sont attribuées au cours du développement cortical.

TABLE DES MATIÈRES

Chapitre V

LISTE DES TABLEAUX

Chapitre II

Chapitre III

Chapitre IV

LISTE DES FIGURES

Chapitre II

Chapitre III

Chapitre IV

LISTE DES ABRÉVIATIONS

5-HT	5-hydroxytryptamine (sérotonine)
ACh	Acétylcholine
AChE	Acétylcholinesterase
ANOVA	analyse de variance
BSA	*bovine serum albumin*
ChAT	choline acétyltransferase
DAB	*3,3' diaminobenzidine tetrahydrochloride*
EEG	électroencéphalogramme
Fr1	cortex fronral (moteur)
GABA	*gamma amino butyric acid*
HACU	*high-affinity choline uptake*
KPB	*potassium phosphate buffer*
NGF	*nerve growth factor*
NHS	*normal horse serum*
Oc1	cortex occipital (visuel)
Par1	cortex pariétal (somatosensoriel)
PBS	*phosphate buffered saline*
PFA	paraformaldéhyde
SNC	système nerveux central
vAChT	*vesicular ACh transporter*
VIP	*vasoactive intestinal polypeptide*
WGA-HRP	*wheat germ agglutinin-horse radish peroxidase*

Les mots font partie de nous plus que les nerfs. Nous ne connaissons notre cerveau que par ouï-dire.

- Paul Valéry

Tis strange, the mind, that fiery particle,
Should let itself be snuff'd out by an article.

- Byron

À mes parents pour 30 ans d'affection, et à Julie pour 10 ans d'amour.

REMERCIEMENTS

Si mes cinq années au doctorat ont été aussi agréables et enrichissantes, c'est grâce aux personnes suivantes, que je remercie de tout coeur:

D'abord et avant tout, Laurent Descarries, que je considère aujourd'hui plus comme un mentor qu'un directeur de recherche. Je le remercie tout particulièrement pour sa confiance, sa générosité, sa gentillesse, son enthousiasme, son sens critique, sa pédagogie et sa patience. C'est par l'exemple que ce grand perfectionniste et travailleur infatigable m'aura appris à forger les outils nécessaires pour continuer à faire ce que j'aime dans la vie.

Merci à Kenneth Watkins, Sylvia Garcia et Annie Vallée pour leurs nombreux conseils et leur précieuse aide technique, ainsi qu'à Gaston Lambert, Jean Léveillé et Giovanni Battista Filosi pour leur art.

Merci aux membres de mon jury d'avoir si gentiment accepté d'évaluer ma thèse.

Merci aux docteurs Costantino Cozzari et Boyd Hartman pour leur généreux don de l'anticorps anti-ChAT.

Merci à mes potes du labo, Mustapha Riad, Ariel Ase et Nicolas Aznavour, pour leur sens de l'humour et pour avoir toujours eu le cœur sur la main. Merci aussi à Annie, Cyrine, Audrey, Mélanie et Christine, les cinq sylphides du département, pour avoir été de fort agréables commensales.

Merci à tous les professeurs du CRSN pour leur disponibilité et la qualité de leur enseignement.

Enfin, un très gros merci à Julie, mon épouse, pour sa patience, sa compréhension et son beau sourire ☺.

Chapitre I

INTRODUCTION GÉNÉRALE

I.1 PRÉSENTATION DE L'OUVRAGE

Cette thèse comprend cinq chapitres. D'abord, une Introduction Générale (Chapitre I), qui situe le contexte dans lequel s'est insérée la présente recherche. Cette Introduction débute par une présentation des rôles principaux attribués à l'acétylcholine (ACh) au sein du néocortex adulte. Elle se poursuit par un bref survol des descriptions récentes, aux échelons cellulaire et subcellulaire, de l'innervation ACh corticale du rat. Des données actuelles sur la distribution des récepteurs cholinergiques dans le cortex cérébral sont ensuite présentées. Enfin, la dernière partie de l'introduction rappelle certains faits qui suggèrent une implication de l'ACh dans le développement cortical, ainsi que les connaissances actuelles sur le développement de cette innervation. Pour conclure, les objectifs de la recherche sont annoncés. Les trois chapitres qui suivent se présentent sous forme d'articles de recherche originaux. Finalement, une Discussion Générale (Chapitre V), traîtant des points majeurs découlant de l'ensemble de ces travaux, vient conclure l'ouvrage.

On retrouve en annexe deux articles pertinents au sujet de la thèse: un article de synthèse intitulé "Ultrastructural evidence for diffuse transmission by monoamine and acetylcholine neurons of the central nervous system", publié en 2000 dans un volume de la série *Progress in Brain Research*, et un article original, intitulé "Comparative analysis of the cholinergic innervation in the dorsal hippocampus of adult mouse and rat: a quantitative immunocytochemical study", à paraître sous peu dans le journal *Hippocampus*.

Cette thèse comprend aussi un sommaire des travaux présentés, ainsi qu'une bibliographie générale.

I.2 L'ACÉTYLCHOLINE DANS LE CORTEX CÉRÉBRAL ADULTE: IMPLICATIONS FONCTIONNELLES

I.2.1 Repères historiques

La première démonstration expérimentale d'une transmission nerveuse chimique est attribuée à Otto Loewi qui, en 1921, apporta la preuve qu'une substance libérée par le nerf vague affecte la rythmicité cardiaque (Loewi, 1921). Cette substance, qu'il nomma *Vagusstuff*, fut subséquemment rebaptisée acétylcholine (ACh), puis identifiée comme le neurotransmetteur libéré à la jonction neuromusculaire. Au cours des années trente, la mise en évidence d'une synthèse de l'ACh dans le cerveau des mammifères (Quastel et al., 1936) a permis de comprendre que l'ACh est aussi une molécule bioactive au sein du système nerveux central (SNC). Depuis, l'ACh a été impliquée dans une variété d'états, fonctions et dysfonctions du cortex cérébral. Nous nous attarderons ici brièvement aux rôles les mieux documentés de ce neurotransmetteur/modulateur dans cette région du cerveau.

I.2.2 Les rôles de l'acétylcholine corticale

Les premiers résultats faisant intervenir l'ACh comme transmetteur chimique dans le cortex cérébral remontent à MacIntosh et Oborin (1953), qui ont mesuré une libération spontanée d'ACh à la surface corticale. Ce n'est que dix ans plus tard que Krnjevic et Phillis (1963a,b), par suite d'enregistrements électrophysiologiques multiples combinés à l'application d'ACh par microiontophorèse, ont découvert l'existence de neurones corticaux sensibles à l'ACh (cholinoceptifs). La majorité de ces neurones, pour la plupart localisés dans les couches profondes du cortex, étaient excités par l'ACh de façon prolongée (réponse de type muscarinique; voir aussi

Krnjevic et al., 1971). Vers la même époque, la libération d'ACh par le cortex fut corrélée à l'activation corticale (Mitchell, 1963). Cette découverte fut rapidement approfondie par Jasper et collaborateurs, qui démontrèrent que des taux élevés d'ACh libérés à la surface du cortex étaient non seulement reliés à l'activation électrique accompagnant l'éveil, mais aussi à celle observée lors du sommeil paradoxal (Celesia et Jasper, 1966; Jasper et Tessier, 1971). En somme, ces chercheurs ont établi que les principaux niveaux d'activité corticale, tels que caractérisés par l'électroencéphalogramme (EEG), étaient directement corrélés aux niveaux d'ACh libérés au sein du cortex cérébral. Plus récemment, ces travaux pionniers ont été largement confirmés, mais aussi complétés par de nombreuses études *in vitro* et *in vivo* qui montrent des effets modulateurs de l'ACh sur les propriétés oscillatoires de la décharge de neurones corticaux individuels (interneurones inhibiteurs et neurones pyramidaux) ou en circuit (Buzsáki et al., 1988; Metherate et Ashe, 1991; Metherate et al., 1992; McCormick, 1992; Steriade et al., 1993; Détari, 2000).

L'un des états physiologiques où le rôle de l'ACh est des mieux documenté est l'état d'éveil, où le pattern d'activité corticale facilite l'accès aux stimuli sensoriels. Plusieurs travaux suggèrent que l'ACh corticale puisse être impliquée dans le traitement de ces informations extra-corticales. Lors de stimuli variés, il a été observé que l'ACh exerce des effets facilitateurs qui précisent et augmentent la sélectivité des réponses corticales. Cette modulation a d'abord été démontrée au sein du cortex visuel (Sillito et Kemp, 1983), puis des aires auditive (McKenna et al., 1988) et somatosensorielle (Donoghue et Carroll, 1987; Lamour et al., 1988; Rasmusson et Dykes, 1988). Puisque l'innervation ACh corticale est diffuse (voir I.3.2 et I.3.3), qu'il existe des neurones cholinoceptifs dans toutes les couches corticales et, qu'*in vitro*, du

moins, l'ACh peut inhiber la transmission synaptique (Kimura et Baughman, 1997), on peut se demander comment ce transmetteur/modulateur parvient à exercer une influence aussi sélective sur le traitement des informations sensorielles. La réponse réside peut-être dans l'hypothèse d'Hasselmo et collaborateurs, voulant que les effets de l'ACh sur la transmission synaptique varient selon la couche corticale à l'étude. Cette hypothèse a trouvé son appui expérimental dans des expériences *in vitro* effectuées sur le cortex piriforme (olfactif) et l'hippocampe. Dans les deux régions, ces auteurs ont constaté que l'ACh, par l'intermédiaire de récepteurs muscariniques, favorise le traitement d'informations extrinsèques (afférences) et inhibe l'activité intracorticale (Hasselmo et Bower, 1992; Hasselmo et Schnell, 1994). Récemment, Kimura et collaborateurs ont rapporté des données similaires pour le néocortex. Grâce à des marqueurs fluorescents sensibles au voltage, ils ont pu examiner, dans des tranches de cerveau de rat, la propagation de l'excitation corticale par suite de stimulations de la voie thalamo-corticale avec ou sans application simultanée d'ACh. Il s'est avéré que, dans le cortex visuel, l'ACh inhibe la propagation de l'excitation dans toutes les couches corticales sauf la couche IV, où se terminent les afférences thalamiques (Kimura et al., 1999). Ceci s'expliquerait par la prédominance d'effets nicotiniques excitateurs sur les arborisations thalamocorticales dans la couche granulaire (Kimura, 2000). Les récentes démonstrations d'actions nicotiniques rapides au niveau d'interneurones corticaux inhibiteurs (GABAergiques) chez le rat (Xiang et al., 1998; Porter et al., 1999) et chez l'homme (Alkondon et al., 2000) suggèrent une implication nicotinique additionnelle dans le contrôle fin de l'activité corticale.

Un mode d'action commun à plusieurs régions corticales semble donc exister, par lequel l'ACh favoriserait l'acquisition (ex.: Miranda et Bermudez-Rattoni, 1999) et

le traitement d'informations nouvelles. Ce même mécanisme pourrait rendre compte des effets permissifs de l'ACh sur la plasticité corticale, puisqu'un pattern altéré d'activité sensorielle afférente se traduit par une réorganisation de la carte sensorielle correspondante lors d'une exposition concomitante à l'ACh (Metherate et al., 1988; Tremblay et al., 1990; Juliano et al., 1991; Kilgard et Merzenich, 1998).

L'ACh a aussi été mise en cause dans des processus cognitifs comme l'attention (Voytko et al., 1994; Bucci et al., 1998; Dalley et al., 2001), l'apprentissage (Rigdon et Pirch, 1986; Pirch et al., 1992; Fine et al., 1997; Miranda et Bermudez-Rattoni, 1999) et la mémoire (Hasselmo et al., 1992), voire même l'expérience consciente (Perry et al., 1999). Ces processus font notamment défaut chez les patients atteints de la démence sénile de type Alzheimer, une maladie neurodégénérative qu'on sait accompagnée d'une réduction importante de l'innervation ACh corticale (Perry et al., 1978; Whitehouse et al., 1981; Bartus et al., 1982; Etienne et al., 1986). Finalement, on attribue à l'ACh un rôle dans le contrôle de la microcirculation locale, puisque la stimulation du noyau basalis entraîne dans le cortex cérébral une vasodilatation des microvaisseaux associée à la libération locale d'ACh (Kurosawa et al., 1989; voir aussi Vaucher et Hamel, 1995).

I.3 L'INNERVATION CHOLINERGIQUE DU CORTEX CÉRÉBRAL ADULTE

I.3.1 Sources de l'innervation cholinergique corticale

L'innervation cholinergique du néocortex des mammifères provient principalement de neurones magnocellulaires du prosencéphale basal, et plus spécifiquement du noyau basalis de Meynert (Rye et al., 1984; Saper, 1984). Chez le rat, ce noyau contient 7 000 à 9 000 neurones ACh qui se projettent au cortex (Rye

et al., 1984; Gritti et al., 1993). Leurs axones s'arborisent dans toutes les aires et les couches corticales (Lysakowski et al., 1989). Chez les rongeurs, une composante ACh intrinsèque au cortex s'ajoute à cette innervation extrinsèque sous forme d'interneurones bipolaires (Eckenstein et Thoenen, 1983; Eckenstein et Baughman, 1984; Levey et al., 1984). Ces interneurones, que l'on retrouve en plus grand nombre dans les couches pyramidales, co-localisent le polypeptide vasoactif intestinal (VIP) et l'acide gamma-amino-butyrique (GABA) (Chédotal et al., 1994a; Bayraktar et al., 1997). On estime que leur contribution à l'innervation corticale ACh est de l'ordre de 20 à 30% (Johnston et al., 1981; Eckenstein et Baughman, 1987).

I.3.2 Visualisation de l'innervation cholinergique corticale

Il est paradoxal que la plupart des études sus-mentionnées sur les fonctions de l'ACh dans le cortex cérébral aient été menées en l'absence de données qualitatives et quantitatives sur la distribution cellulaire et subcellulaire de cette innervation. Une telle lacune est sans doute imputable au nombre restreint des marqueurs cellulaires qui sont spécifiques aux neurones cholinergiques, ainsi qu'à l'absence de techniques suffisamment sensibles pour la mise en évidence de ces marqueurs au sein de régions cérébrales relativement éloignées des neurones d'origine (voir revue détaillée dans Umbriaco, 1996). À l'inverse, les autres innervations neuromodulatrices classiques du néocortex ont pu être décrites en détail chez le rat adulte, notamment par notre laboratoire. Ainsi, chez le rat, les distributions respectives des innervations à monoamine, à dopamine, sérotonine ou noradrénaline, ont été quantifiées par autoradiographie après capture et stockage de la monoamine tritiée correspondante dans des tranches de cerveau (Descarries et al., 1987; Audet et al., 1988, 1989). De

plus, leur ultrastructure a été caractérisée, d'abord par autoradiographie (Lapierre et al., 1973; Descarries et al., 1975, 1977), puis par immunocytochimie en microscopie électronique (Séguéla et al., 1988, 1989, 1990; voir aussi Cohen et al., 1995, 1997).

La production relativement récente d'anticorps monoclonaux à très haute affinité contre la choline acétyltransférase (ChAT; Cozzari et al., 1990), l'enzyme de synthèse de l'ACh, a permis de combler cette lacune. Depuis, l'ultrastructure des innervations ACh du néocortex (Chédotal et al., 1994b; Umbriaco et al., 1994; Vaucher et Hamel, 1995) et d'autres régions cérébrales (Umbriaco et al., 1995; Contant et al., 1996) ont été caractérisées chez le rat adulte. Ces descriptions ont révélé que ces innervations sont majoritairement asynaptiques, au sens qu'une très faible proportion de leurs terminaisons ou varicosités axonales présentent une jonction synaptique morphologiquement définie (pour une revue exhaustive, voir Annexe I). En particulier, Umbriaco et collaborateurs (1994) ont examiné en coupes sériées plus de 800 varicosités axonales ACh en provenance de toutes les couches du cortex pariétal du rat adulte. Cette étude a révélé que seulement 14% de ces terminaisons nerveuses faisaient synapse. Il a donc été proposé que, tout comme les monoamines (Descarries et al., 1975, 1977; Beaudet et al., 1976, 1978), l'ACh corticale puisse être libérée de façon diffuse et agir ainsi sur une grande variété de cibles cellulaires, plus ou moins éloignées des sites de libération (Umbriaco et al., 1994). À ce concept mieux connu sous le nom de transmission volumique (*volume transmission*), s'est ajouté celui d'un niveau ambiant de transmetteur, pour tenir compte des taux d'ACh mesurés en permanance dans le cerveau et des effets à grande échelle de l'ACh sur la physiologie corticale (Descarries et al., 1997; Descarries et Mechawar, 2000).

I.3.3 Les récepteurs cholinergiques dans le cortex cérébral

L'étude d'une innervation est d'autant plus intéressante qu'elle peut se compléter par celle de la distribution cellulaire et subcellulaire de ses récepteurs. Malheureusement, si l'on fait abstraction des études autoradiographiques de radioliaison, pour la plupart effectuées avec des ligands non sélectifs, il existe actuellement relativement peu de données sur la distribution des récepteurs tant muscariniques que nicotiniques dans le cortex cérébral.

Les récepteurs nicotiniques les plus répandus au sein du cortex cérébral sont les hétéro-pentamères résultant de l'agencement des sous-unités α4 et β2, et les homo-pentamères composés exclusivement de la sous-unité α7 (Sargent, 1993). Des anticorps sélectifs dirigés contre l'une ou l'autre de ces sous-unités ont été récemment employés pour l'examen de leur distribution cellulaire. Tel qu'attendu, les sous-unités α4 et β2 présentent un pattern de distribution similaire: elles sont toutes deux principalement localisées aux corps cellulaire et dendrites proximaux des neurones pyramidaux des couches II/III et V (Hill et al., 1993; Nakayama et al., 1995). À l'échelon subcellulaire, Hill et collaborateurs (1993) ont rapporté, par suite de marquages à l'or, que la sous-unité β2 se retrouvait sur la membrane plasmique de dendrites et de varicosités axonales. Toutefois, ces auteurs ont remarqué que l'immunoréactivité β2 était très rarement associée à des spécialisations jonctionnelles. La sous-unité α7 a également été localisée à la portion somatodendritique de neurones pyramidaux, mais aussi d'interneurones GABAergiques (Lubin et al., 1999). En microscopie électronique après marquage à l'or, ces auteurs ont observé la présence de ce récepteur dans des somas et dendrites, ainsi que des terminaisons axonales. Le marquage se retrouvait fréquemment associé à la membrane plasmique, mais souvent loin des spécialisations synaptiques. L'examen ultrastructural de doubles marquages

α7/GABA, en plus de confirmer l'expression du récepteur par des interneurones inhibiteurs, a démontré sa présence sur des épines dendritiques, tant à la base de ces épines que sur leurs jonctions postsynaptiques (Lubin et al., 1999).

Les sous-types réceptoriels m1, m2 et m4 sont les principaux récepteurs muscariniques du cortex cérébral, tel que démontré par les expériences immunocytochimiques de Levey et collaborateurs (1991). Le récepteur de type m1, de loin le plus répandu, est exprimé par des neurones de toutes les couches corticales, mais surtout des couches II/III et V. Le récepteur m2, exprimé par des fibres et des corps cellulaires, est particulièrement dense dans la couche IV et à l'interface des couches V et VI. Enfin, le récepteur de type m4 est faiblement exprimé entre les couches II/III et V (Levey et al., 1991).

Les données ultrastructurales sur la distribution subcellulaires des sous-types m1 et m2 dans le cortex cérébral proviennent essentiellement du laboratoire de Goldman-Rakic (Mrzljak et al., 1993, 1996, 1998). Ces études effectuées sur les cortex frontal et occipital du singe macaque, ont révélé que les récepteurs de type m1 et m2 pouvaient être associés aux densités postsynaptiques de jonctions synaptiques non cholinergiques. Comme il s'agit de marquages obtenus avec la diaminobenzidine, un chromogène diffusible, la réalité de cette localisation reste à confirmer. Ces auteurs ont également localisé le récepteur m2 à des terminaisons thalamo-corticales. Dans une étude subséquente où ils ont réussi des marquages à l'or pour le sous-type m2, ils ont souligné que l'immunoréactivité observée sur des cellules pyramidales et non pyramidales était exclusivement péri- et extra-synaptique (Mrzljak et al., 1998).

Dans l'ensemble, ces données ultrastructurales suggèrent fortement que la majorité des récepteurs nicotiniques et muscariniques corticaux pouvaient être activés par de l'ACh libérée à distance, qui vienne ainsi moduler la libération et/ou l'action d'acides aminés excitateurs et inhibiteurs, une influence déja bien démontrée en électrophysiologie (voir revues de Role et Berg 1996, et Jones et al., 1999).

I.4 L'ACÉTYLCHOLINE DANS LE CORTEX CÉRÉBRAL EN DÉVELOPPEMENT

I.4.1 Les rôles de l'acétylcholine corticale au cours du développement

En plus des nombreuses fonctions qui sont attribuées à l'ACh dans le cortex cérébral adulte, on reconnait depuis peu à l'ACh des effets morpho-fonctionnels au sein de cette région cérébrale en développement. En particulier, l'ACh semble contribuer à la forte plasticité observée durant la période critique.

Dans leur étude classique sur la déprivation monoculaire chez le chaton, Hubel et Wiesel ont démontré que la mise en place des circuits corticaux débute par une période critique survenant très tôt au cours du développement postnatal (Hubel et Wiesel, 1970). Cette période, dont la durée varie selon l'espèce et la région concernées, se caractérise par un potentiel maximal de plasticité. On utilise encore couramment ce modèle expérimental pour départager les facteurs extrinsèques vs intrinsèques responsables d'une telle plasticité. Au cours du développement, les afférences provenant du corps genouillé latéral, une fois leur cible corticale atteinte, se départagent en bandes oeil-spécifiques régulièrement alternées au sein du cortex visuel primaire. La suture d'une des paupières au cours de la période critique (entre les troisième et cinquième semaines postnatales dans ce cas-ci), provoque, après un

certain temps, un élargissement permanent des bandes correspondant à l'oeil ouvert et une réduction proportionelle de celles correspondant à l'oeil fermé. La même expérience, après la période critique, n'entraîne pas une telle alternance irrégulière de bandes thalamo-corticales. Bien qu'elle fasse actuellement l'objet d'une controverse (voir Crowley et Katz, 1999, 2000), l'hypothèse la plus répandue pour expliquer ce phénomène veut que les projections visuelles soient en compétition pour le territoire d'innervation. Ainsi, des mécanismes hebbiens seraient impliqués, par lesquels des afférences synchrones (du même oeil) seraient renforcées pour une cible donnée, alors que celles correspondant à l'autre oeil seraient affaiblies ou tout simplement éliminées. Une activité rétinienne spontanée avant l'ouverture des yeux serait à la base de cette ségégation initiale (Penn et al., 1998; Rossi et al., 2001), qui serait par la suite raffinée au cours de la période critique.

Les premières données expérimentales indiquant que l'ACh puisse être mise en jeu lors de la période critique proviennent des travaux de Bear et Singer, qui ont observé une réduction importante de la réponse plastique à la déprivation monoculaire chez le chaton, par suite de lésions combinées des afférences corticales cholinergiques et noradrénergiques (Bear et Singer, 1986). Une forte majorité des neurones enregistrés dans le cortex visuel de ces animaux présentait des réponses binoculaires, suggérant que la présence de ces neuromodulateurs soit nécessaire à la plasticité de la carte visuelle lors de la période critique. Ces résultats doivent cependant être interprétés avec prudence, puisque les lésions du prosencéphale basal étaient non sélectives et détruisaient de ce fait des projections basalo-corticales non cholinergiques (GABAergiques). Plus récemment, des données provenant du même laboratoire ont confirmé, par l'administration d'antagonistes des récepteurs cholinergiques,

l'implication de l'ACh dans la plasticité corticale au cours du développement. Ces données ont révélé en outre que l'influence permissive de l'ACh s'exerce par l'intermédiaire de récepteurs muscariniques du type M1 (Gu et Singer, 1993).

Le cortex somatosensoriel des rongeurs, qui ne possèdent pas de colonnes de dominance occulaire, constitue un autre modèle particulièrement propice à l'étude de la plasticité corticale au cours du développement. Chez ces animaux, chaque vibrisse est représentée dans la couche IV du cortex somatosensoriel contralatéral par un aggrégat de neurones (barillet) (Woolsey et van der Loos, 1970). La période critique pour l'établissement du cortex à barillets a lieu au cours de la première semaine postnatale. Récemment, il a été rapporté que des lésions sélectives des neurones ACh basalo-corticaux chez le rat nouveau-né entraînaient une réduction de l'élargissement des barillets épargnés, normalement observée après la destruction d'une rangée entière de follicules (Zhu et Waite, 1998). De telles lésions auraient aussi des conséquences directes sur développement morphologique du néocortex, puisqu'elles entraînent un retard dans la maturation des couches corticales (Höhmann et al., 1988), un pattern altéré d'expression des récepteurs glutamatergiques (Höhmann et al., 1999), ainsi qu'un développement anormal des dendrites apicaux des neurones pyramidaux (Robertson et al., 1998). Dans l'ensemble, ces résultats suggèrent que l'ACh exerce un rôle trophique, voire même tropique, au sein du cortex cérébral en développement. Toutefois, il faut souligner qu'ils ont été obtenus, pour la plupart, par suite de lésions à la 192-IgG saporine, une drogue susceptible d'agir également sur d'autres populations neuronales, du moins au cours du développement. En effet, la 192-IgG saporine se lie au récepteur à basse affinité (p75) du *nerve growth factor* (NGF), est alors internalisée et tue la cellule en bloquant la synthèse protéique (voir

Leanza et al., 1996). Les neurones ACh du prosencéphale basal sont connus pour exprimer ce récepteur chez l'adulte tout comme durant le développement. Cependant, cette expression ne leur est pas exclusive; en particulier, un bon nombre de neurones corticaux expriment le récepteur p75 avant même d'avoir amorcé leur migration finale (Koh et Loy, 1989; Koh et Higgins, 1991; voir aussi Conner et Varon, 1997).

D'autres études récentes, menées durant la période néonatale chez le rongeur, impliquent directement les récepteurs cholinergiques, muscariniques et nicotiniques (voir I.4.2), comme médiateurs de multiples effets de l'ACh sur la corticogénèse, via la prolifération neuronale (Ma et al., 2000) ou la formation de circuits corticaux (Broide et al., 1996; Roerig et al., 1997; Aramakis et al., 2000; Kojic et al., 2001). Soulignons particulièrement la récente mise en évidence de vagues lentes d'activité neuronale corrélée induites par des agonistes muscariniques dans des tranches de cortex pariétal immature. Ce phénomène, observé seulement entre la naissance et le sixième jour postnatal, pourrait sous-tendre la formation de colonnes corticales (Peinado, 2000). De toute évidence, il indique aussi que l'ACh a la capacité d'influencer directement l'activité des populations neuronales alors même que le cortex s'élabore.

I.4.2 Les paramètres cholinergiques dans le cortex cérébral en développement

Les données biochimiques, moléculaires et histochimiques en rapport avec le développement de l'innervation ACh corticale demeurent fragmentaires et parfois difficiles à concilier (revues dans Semba, 1992). Dans l'ensemble, elles suggèrent une croissance assez précoce (périnatale) de cette innervation, même si les études en

immunocytochimie de la ChAT jusqu'à maintenant ont plutôt fait état d'une croissance tardive (voir I.4.3).

Selon les dosages biochimiques effectuées par Coyle et Yamamura (1976), le contenu en ACh du cerveau entier augmente de façon stable au cours de la période postnatale pour atteindre des niveaux adultes quatre semaines après la naissance. Toutefois, il existe des différences régionales importantes, et chaque région contient un pourcentage variable des quantités retrouvées chez l'adulte. Ainsi, la teneur en ACh du cortex pariétal en développement représenterait environ 50% de celle de l'adulte. L'activité de la ChAT, mesurée dans la même région, s'est avérée très faible au cours de la première semaine postnatale (0.2 nMole/mg/h), pour s'accroître ensuite constamment entre le début de la deuxième semaine et l'âge adulte (4.6 nMole/mg/h). Ces mesures d'activité ChAT ont été corroborées par une étude semblable du cortex visuel chez le rat (McDonald et al., 1987). Comment concilier cette faible activité enzymatique avec les fortes concentrations d'ACh corticale au cours des stades précoces du développement? L'explication pourrait provenir du fait que les neurones du néocortex ont une faible activité cholinestérasique durant cette période (Lassiter et al., 1998). Une bonne partie de l'ACh corticale mesurées à la naissance pourrait aussi provenir de la périphérie, puisque l'ACh est synthétisée par le placenta, le sang et les organes périphériques (Wessler et al., 1998) et que la barrière hémato-encéphalique est encore perméable dans les jours qui suivent la naissance (Lossinsky et al., 1986). Cette perméabilité avait d'ailleurs été précédemment démontrée dans le cas des monoamines circulantes (Loizou et al., 1970; Dupin et al., 1976; Lidow, 1998), mais la démonstration reste à venir pour l'ACh.

Deux autres marqueurs cholinergiques ont été examinés par autoradiographie quantitative, soit le transporteur à haute affinité pour la choline (HACU) et le transporteur vésiculaire de l'ACh (vAChT). Curieusement, dès la fin de la période embryonnaire, les densités de liaison obtenues avec le vésamicol (vAChT) sont très proches (88%) de celles mesurées dans le cortex adulte. Ces densités montrent une augmentation importante de la naissance au quatorzième jour postnatal (128%), pour ensuite redescendre à des valeurs adultes (Aubert et al., 1996). Vu la disponibilité récente d'anticorps dirigés contre le vAChT (Arvidsson et al., 1997; Ichikawa et al., 1997; Roghani et al., 1998; Schäfer et al., 1998), ces données surprenantes pourront bientôt faire l'objet de comparaisons avec des profils de distribution obtenus par immunocytochimie de la protéine. À l'inverse, le développement du HACU semble beaucoup moins précoce, puisque la densité de liaison à l'hemicholinium-3 augmente graduellement à partir de la fin de la première semaine postnatale seulement (Happe et Murrin, 1992; voir aussi Zahalka et al. 1993).

L'étude de récepteurs de l'ACh par autoradiographie (radioliaison), transfert de Northern, hybridation *in situ* ou immunocytochimie a révélé l'expression de différents sous-types muscariniques et sous-unités nicotiniques au sein du cortex cérébral en développement (Prusky et Cynader, 1990; Buwalda et al., 1995; Höhmann et al., 1995; Ostermann et al., 1995; Zoli et al., 1995; Aubert et al., 1996; Broide et al., 1996; Shacka et Robinson, 1998; Zhang et al., 1998). On notera toutefois l'absence complète d'études sur la distribution ultrastructurale de ces récepteurs au cours du développement. Tel que mentionné précédemment, non seulement ces récepteurs sont-ils fonctionnels dans le cortex immature (Roerig et al., 1997; Ma et al., 2000), mais leur présence semble indispensable à la mise en place des circuits corticaux (Gu

et Singer, 1993; Broide et al., 1996; Aramakis et al., 2000; Kojic et al., 2001). Il serait donc d'un très grand intérêt de savoir où ils sont situés à l'échelon subcellulaire, afin de mieux comprendre les mécanismes mis en cause.

I.4.3 Développement de l'innervation cholinergique corticale

À ce jour, aucune description détaillée du développement de l'innervation ACh basalo-corticale n'a été rapportée. À défaut d'outils sensibles pour marquer la ChAT, le marquage histochimique de l'acétylcholinesterase (AChE) a généralement été employé pour visualiser les axones cholinergiques dans le cortex en développement (Krnjevic et Silver, 1966; Höhmann et Ebner, 1985; Kostovic, 1986; Henderson, 1991; Kiss et Patel, 1992; Nyakas et al., 1994). Toutefois, il est bien connu que l'expression de cette enzyme de dégradation n'est pas exclusive aux neurones cholinergiques, particulièrement au cours des premières semaines postnatales, alors que les afférences thalamiques et certains neurones corticaux expriment l'AChE de façon transitoire (Robertson et al., 1985; Kutscher, 1991; Sendemir et al., 1996). Il est intéressant de noter que les projections thalamo-corticales présentent, au cours de la même période, un phénotype sérotoninergique transitoire (Lebrand et al., 1996). En effet, sans être capables de synthétiser la sérotonine, les neurones thalamiques de projection expriment, entre autre, les transporteurs membranaire et vésiculaire de la sérotonine, ce qui leur donne la capacité de stocker et de libérer ce transmetteur. La correspondance temporelle entre ce phénotype emprunté et l'expression transitoire d'AChE par les mêmes fibres est frappante. Même si la signification biologique de ces phénomènes reste inconnue, il se pourrait que l'un et l'autre soient interreliés.

Le développement des projections basalo-corticales a également fait l'objet d'études par marquage axonal rétrograde et antérograde. Après injection de conjugué agglutinine du germe de blé-peroxydase de raifort (WGA-HRP) dans le cortex visuel de ratons un jour après la naissance, Dinopoulos et collaborateurs (1989) ont marqué de façon rétrograde des neurones du prosencéphale basal ayant la même morphologie et la même localisation que les neurones immunoréactifs pour la ChAT. Cependant, ces auteurs ont accordé une signification limitée à leurs propres observations: "...accumulating data showing the relatively late development of this system in the neocortex minimizes its importance in early developmental processes..." (Dinopoulos et al., 1989). Une autre étude intéressante a aussi été menée sur le cortex visuel, cette fois avec le marqueur fluorescent DiI, dont le transport axonal est antérograde (Calarco et Robertson, 1995). Dès la naissance, des injections de ce marqueur dans le prosencéphale basal ont permis de confirmer qu'un certain nombre de projections issues de ce noyau avaient déja atteint le cortex occipital (matière blanche). Au cours des trois ou quatre jours suivants, ces auteurs ont observé que des fibres marquées avaient graduellement infiltré les couches profondes du cortex, pour ensuite s'arboriser jusqu'à présenter une densité comparable à l'adulte vers la fin de la deuxième semaine postnatale. Dans ces deux cas cependant, l'utilisation de marqueurs non spécifiques limitait la portée des résultats en ce qui a trait à l'innervation cholinergique.

Jusqu'à nos propres travaux, les données en immunocytochimie de la ChAT sur la genèse de l'innervation ACh corticale ont laissé croire à un développement plutôt tardif, survenant surtout à partir de la fin de la deuxième semaine postnatale chez le rat. Ainsi, Dori et Parnavelas (1989) ont rapporté la présence, au milieu de la

deuxième semaine postnatale, de quelques fibres et interneurones faiblement marqués. Selon ces auteurs, ces éléments continuaient ensuite de croître graduellement jusqu'à ce qu'un pattern d'innervation adulte soit observé vers la cinquième semaine après la naissance. Une étude plus récente, menée dans le cortex temporal, a rapporté la présence d'interneurones bipolaires et de fibres variqueuses immunoréactives pour la ChAT à partir de la fin de la deuxième semaine postnatale (Gould et al., 1991).

Ces descriptions immunocytochimiques sont difficiles à concilier avec les multiples données expérimentales montrant que la plupart des paramètres cholinergiques sont exprimés de façon précoce au sein du cortex en développement. Il se pourrait, comme le suggèrent les marquages rétrogrades et antérogrades ci-haut mentionnés, que les projections basalo-corticales aient déja commencé d'atteindre le cortex à la naissance, et que l'absence de données immunocytochimiques positives dans les jours suivant la naissance soit imputable à une faible sensibilité des anticorps utilisés.

I.5 OBJECTIFS DE RECHERCHE

Dans ce contexte, et ayant à notre disposition un anticorps à très haute affinité contre la ChAT purifiée à partir du cerveau de rat (Cozzari et al., 1990), trois objectifs de recherche principaux ont été poursuivis en vue d'arriver à une meilleure compréhension des caractéristiques structurales et ultrastructurales de l'innervation ACh corticale chez le rat adulte et en cours de développement.

En l'absence de données quantifiées sur l'innervation ACh, le premier objectif consistait à quantifier l'innervation ACh dans les différentes couches de trois aires corticales chez le rat adulte: les cortex frontal (moteur), pariétal (somatosensoriel) et occipital (visuel). Pour ce faire, il nous fallait mettre au point une méthode de quantification permettant de mesurer la longueur d'axone ACh ainsi que le nombre de varicosités axonales ACh à partir de coupes de cerveau de rat immunomarquées pour la ChAT.

Notre deuxième objectif était de quantifier, à l'aide de cette méthode, la croissance et la maturation de l'innervation ACh au sein des trois mêmes régions corticales en cours de développement.

Finalement, nous savions pouvoir produire, à l'échelon ultrastructural, une description princeps de l'innervation ACh corticale en croissance, en mettant l'accent sur les caractéristiques intrinsèques et relationelles de ses varicosités axonales.

Chapitre II

CHOLINERGIC INNERVATION IN ADULT RAT CEREBRAL CORTEX: A QUANTITATIVE IMMUNOCYTOCHEMICAL DESCRIPTION

(*J Comp Neurol* 428:305-318)

En tant que premier auteur, j'ai réalisé les expériences, analysé les résultats et contribué de façon majeure à toutes les étapes de la rédaction de l'article.

CHOLINERGIC INNERVATION IN ADULT RAT CEREBRAL CORTEX: A QUANTITATIVE IMMUNOCYTOCHEMICAL DESCRIPTION

Naguib MECHAWAR [1], Costantino COZZARI [2] and Laurent DESCARRIES [1]

[1] Départements de pathologie et biologie cellulaire et de physiologie, and Centre de recherche en sciences neurologiques, Faculté de médecine, Université de Montréal, Montréal, Québec, Canada H3C 3J7;

and

[2] Istituto di Biologia Cellulare CNR, 00137 Roma, Italia

(43 text pages including figure legends; 2 tables and 7 figures)

Abbreviated title: **ACh innervation in cerebral cortex**

Associate editor: Dr. Oswald STEWARD

KEYWORDS acetylcholine, ChAT, neocortex, axons, varicosities, immunocytochemistry

Correspondence: Laurent DESCARRIES m.d.
Département de pathologie et biologie cellulaire
Université de Montréal
CP 6128, Succursale Centre-ville
Montréal, QC, Canada H3C 3J7
tel. (514) 343-7070
fax (514) 343-5755

Grant sponsor: Medical Research Council of Canada; Grant number: MT-3544.

ABSTRACT

A method for determining the length of acetylcholine (ACh) axons and number of ACh axon varicosities (terminals) in brain sections immunostained for choline acetyltransferase (ChAT) was used to estimate the areal and laminar densities of this innervation in the frontal (motor), parietal (somatosensory) and occipital (visual) cortex of adult rat. The number of ACh varicosities per length of axon (4 per 10 μm) appeared constant in the different layers and areas. The mean density of ACh axons was the highest in the frontal cortex (13.0 m/mm^3 versus 9.9 and 11.0 m/mm^3 in the somatosensory and visual cortex, respectively), as was the mean density of ACh varicosities (5.4 x 10^6/mm^3 versus 3.8 and 4.6 x 10^6/mm^3). In all three areas, layer I displayed the highest laminar densities of ACh axons and varicosities (e.g. 13.5 m/mm^3 and 5.4 x 10^6/mm^3 in frontal cortex). The lowest were those of layer IV in the parietal cortex (7.3 m/mm^3 and 2.9 x 10^6/mm^3). The lengths of ACh axons under a 1 mm^2 surface of cortex were 26.7, 19.7 and 15.3 m in the frontal, parietal and occipital areas, respectively, for corresponding numbers of 11.1, 7.7 and 6.4 x 10^6 ACh varicosities. In the parietal cortex, this meant a total of 1.2 x 10^6 synaptic ACh varicosities under a 1 mm^2 surface, 48% of which in layer V alone, according to previous electron microscopic estimates of synaptic incidence. In keeping with the notion that the synaptic component of ACh transmission in cerebral cortex is preponderant in layer V, these quantitative data suggest a role for this innervation in the processing of cortical output as well as input. Extrapolation of particular features of this system in terms of total axon length and number of varicosities in whole cortex, length of axons and number of varicosities per cortically projecting neuron, and concentration of ACh per axon varicosity, should also help in arriving at a better definition of its roles and functional properties in cerebral cortex.

Ever since the first demonstration of its spontaneous release from mammalian cerebral cortex (MacIntosh and Oborin, 1953), the neurotransmitter/ modulator acetylcholine (ACh) has been implicated in a variety of neural states and functions: wakefulness and sleep (Richter and Crossland, 1949; Jasper and Tessier, 1971; Jiménez-Capdeville and Dykes, 1996), cortical activation (Krnjevic and Phillis, 1963a,b; Mitchell, 1963; Celesia and Jasper, 1966; Buzsàki et al., 1988; Metherate et al., 1992), modulation of sensory information (Sillito and Kemp, 1983; Donoghue and Carroll, 1987; Lamour et al., 1988; McKenna et al., 1988; Rasmusson and Dykes, 1988), plasticity of sensory maps (Bear and Singer, 1986; Metherate et al., 1988; Tremblay et al., 1990; Juliano et al., 1991; Kilgard and Merzenich, 1998), attention (Voytko et al., 1994; Bucci et al., 1998), memory (Hasselmo et al., 1992), learning (Rigdon and Pirch, 1986; Pirch et al., 1992; Fine et al., 1997; Miranda and Bermudez-Rattoni, 1999), and conscious awareness (Perry et al., 1999) (for selected reviews, see McCormick, 1992; Hasselmo and Bower, 1993; Hasselmo, 1995; Dykes, 1997; Baxter and Chiba, 1999; Sarter and Bruno, 2000). A substantial loss of cortical choline acetyltransferase (ChAT) activity (e.g. Perry et al., 1978; Etienne et al., 1986) and a selective degeneration of ChAT-positive nucleus basalis neurons (Davies and Maloney, 1976; Whitehouse et al., 1981) have been correlated with the cognitive deficits seen in patients with Alzheimer's disease (Bartus et al., 1982; but see Gilmor et al., 1999).

In the rat, there is combined retrograde axonal tracing and ChAT-immunocytochemical evidence that most of the cortical ACh innervation stems from the magnocellular nuclei of the basal forebrain (Saper, 1984; Rye et al., 1984). A small projection to medial frontal cortex, issued by a subset of midbrain neurons co-localizing substance P, has also been described (Vincent et al., 1983). A third

component arises from intrinsic bipolar interneurons, at least in rodents (Eckenstein and Thoenen, 1983; Eckenstein and Baughman, 1984; Levey et al., 1984). Following lesions of the ACh basal forebrain neurons, it has been estimated that these interneurons account for 20-30% of ChAT activity (Johnston et al., 1981) and as many as 20% of ChAT-immunoreactive terminals in the neocortex (Eckenstein and Baughman, 1987). According to more recent immunocytochemical studies, 88% of these interneurons would co-localize γ-aminobutyric acid (Bayraktar et al., 1997), and roughly a third, vasoactive intestinal polypeptide (Chédotal et al., 1994a).

In an extensive light microscope immunocytochemical study, Lysakowski and collaborators (1989) have shown differences in the interareal as well as interlaminar distribution of ChAT-immunoreactive fibers throughout the cerebral cortex of rat. These authors reported as many as thirteen distinct laminar patterns and emphasized the similarity between cortical areas with comparable function. Unlike the cortical monoamine innervations, which have been the subject of detailed quantitative descriptions by autoradiography after tritiated monoamine uptake (e.g. Audet et al., 1988, 1989), this and other studies having examined the distribution of the cortical ACh innervation remained essentially qualitative, or semi-quantitative at best (Stichel and Singer, 1987; Garofalo et al., 1992, 1993), because of the recognized limitations of ChAT-immunocytochemistry for visualizing ACh axons in addition to ACh nerve cell bodies. As for acetylcholinesterase histochemistry, it has never been applicable for such quantitative purposes, even in modified versions, since groups of noncholinergic neurons clearly express this degradative enzyme (Butcher et al., 1975; Robertson and Gorenstein, 1987).

Ten years ago, a highly sensitive monoclonal antibody against purified rat brain ChAT was produced and characterized by one of us (C.C.), which allowed for an excellent immunocytochemical visualization of ACh axons at the electron as well as light microscopic level (Cozzari et al., 1990). With further use of this antibody (e.g. Umbriaco et al., 1994), it became clear that, at the light microscopic level, it might permit an integral detection and hence a quantification of the ACh innervation in cerebral cortex (or other brain regions).

A method for ChAT-immunostaining and semi-computerized analysis of the data was therefore developed, which fulfilled this prerequisite and allowed to measure the length of ACh axons and number of ACh axon varicosities in histological sections of the rat brain. This method is here described and illustrated with results on the densities of ACh axons and of axon varicosities in the different layers and full thickness of the frontal (motor), parietal (somatosensory) and occipital (visual) cortex of adult rat. Similar data from a companion study at various stages of postnatal development will soon be reported. Preliminary results on both topics have been published in abstract form (Mechawar and Descarries, 1998, 1999).

MATERIALS AND METHODS

Tissue processing

All experiments abided by the policies and guidelines of the Canadian Council on Animal Care and the regulations of the Animal Care Committee at the Université de Montréal. The study was carried out on 8 adult male, Sprague-Dawley rats (body weight: 250 ± 50 g), purchased from Charles River, Canada (St-Constant, Quebec, Canada). All rats were deeply anesthetized with sodium pentobarbital (80 mg/kg, i.p.) and perfused through the heart with 50 ml of ice-cold sodium phosphate-buffered

saline (PBS; 50 mM; pH 7.4) followed by 400-500 ml of 4% paraformaldehyde (PFA) in 0.1 M sodium phosphate buffer (PB; pH 7.4; 24°C) for light microscopy (n = 7), or 200 ml of 4% PFA, 100 ml of 4% PFA + 0.5% glutaraldehyde, and 200 ml of 4% PFA, for electron microscopy (n = 1). The brain was then rapidly removed, postfixed overnight in PFA alone at 4°C, and washed in PBS. Transverse vibratome sections (50 μm-thick), including primary motor, somatosensory and visual cortex, were cut from 6 of the 7 brains to be processed for light microscopic immunocytochemistry, and alternate sections were stained with cresyl violet to delimit cortical layers. The seventh brain was split on the midline, and the cortex of each hemisphere flattened between glass slides, to be examined in sections tangential to the surface. Transverse sections from the eighth brain were prepared for electron microscopic immunocytochemistry.

ChAT-immunocytochemistry

The mouse monoclonal antibody against purified rat brain ChAT was utilized as described in detail in earlier studies (e.g. Umbriaco et al., 1994, 1995; Contant et al., 1996). At room temperature, the free-floating sections were thoroughly rinsed in PBS and pre-incubated for 2 hours in a blocking solution of PBS containing 2% normal horse serum (NHS; Vector, Burlingame, CA), 1% bovine serum albumin (BSA; Sigma, St-Louis, MO) and 0.2% Triton X-100 (light microscopy only). They were then incubated overnight in this same solution containing 2 μg/ml of monoclonal anti-ChAT antibody.

Immunostaining was carried out at room temperature with the ABC method (Shi et al., 1988). After rinses in PBS and then in 0.1 M potassium phosphate

buffer (KPB; pH 7.4), sections were incubated for 2 hours in biotinylated horse anti-mouse, rat-adsorbed, secondary antibody (Vector), diluted 1/200 in KPB containing 2% NHS and 1% BSA, followed by the avidin-biotin complex procedure (ABC Kit, Vectastain Elite; Vector) for 2 hours. For light microscopy, the labeling was revealed for 2.5 min in a 0.05% solution of 3,3'-diaminobenzidine (DAB; Sigma) containing 0.01% $CoCl_2$, 0.01% $NiSO_4$, 0.01% $(NH_4)_2SO_4$, to which 0.005% H_2O_2 was added. Sections were then rinsed several times with KPB, air-dried on gelatin-coated slides, dehydrated with ethanol, cleared with toluene and mounted with DPX (Fluka; Sigma). Control experiments included omission of the primary or secondary antibodies.

Sections destined for electron microscopy were processed as above but developed for 2 min without nickel/cobalt enhancement. They were osmicated, dehydrated with ethanol and propylene oxide, and flat-embedded in Durcupan (Fluka; Sigma) according to standard procedures. Ultrathin (60-80 nm) sections from the lower half of the parietal cortex were cut with an ultramicrotome, collected on 150-mesh grids, stained with lead citrate, and examined with a Philips CM100 electron microscope.

Length of ChAT-immunostained axons

Measurements of the length of ChAT-immunostained axons were obtained from the primary motor (Fr1), somatosensory (Par1) and visual (Oc1) cortex of 5 rats (Fig. 1), using a microcomputer-based image analysis system (MacIntosh Quadra 950; NIH Image software, version 1.61) connected to a light microscope (Leitz Orthoplan; 25 X PlanApo objective lens) via a video camera (Panasonic WV-BD400; 768 x 493 pixels for 1.7 cm^2). At this working magnification (X 645), three steps of focusing were required to visualize the immunostained axon network across

the full depth of 50 μm-thick sections. A preliminary step in quantifying this network was therefore to determine the proportion of its total length that was visualized in one of these three planes of focus.

For this particular purpose, large photomontages were produced (X 645), respectively corresponding to a superficial, middle and deep plane of focus through the depth of 240 μm-wide vertical strips across the full cortical thickness (Figs. 2A), and representing each cortical area in 2 rats. Twenty-five square sampling windows, 100 μm in side (64.5 mm in side at the magnification of the photomontages), were then arbitrarily positioned in different layers of the three areas, as exemplified in Figs. 2A and 2B. The full extent of the immunostained fiber network within each window was then drawn on transparent film, by successive tracing of the network in the three planes of focus (Fig. 2C). Similar drawings were also prepared from the superficial plane of focus only. The fiber length in each window was then measured with the aid of the image analysis system. The drawings were captured and digitized, and their lines reduced to a uniform width of 1 pixel, using the " skeletonize " function of the NIH Image program (Fig. 2D). All closed surfaces in the network were cut open by removing one pixel from these outlines, the total length was measured and corrected for the number of removed pixels, and this value was converted to μm based on a prior calibration of the system with a microscopic scale. The length of immunostained axons visualized in one plane of focus was then found to be a fixed proportion of total length in the section (44.6% ± 0.76 s.e.m).

Sampling in a single plane of focus was therefore used for an extensive survey of the three cortical areas in 5 rats. Again on large photomontages produced at X 645, length of axons was measured in squares, 64.5 mm in side, this time aligned in

rows perpendicular to the cortical surface, within which a maximal number of squares (1-6) was fitted in each layer. Respective tissue areas of 0.15, 0.16 and 0.10 mm^2 were thus sampled in the frontal, parietal and occipital cortex of each rat, for a total of 0.41 mm^2 per rat. The length values were corrected to the full thickness of sections (x 2.24), and a further correction was introduced to compensate for angulation of the fibers in the sections (x 1/cos 45; Soghomonian et al., 1987), assuming their random orientation (but see Methodological considerations in Discussion). The resulting values were extrapolated to tissue volume (mm^3), to provide an average axon density for each layer and for the whole thickness of each cortical area. They were also expressed in actual length (meters) of axons under 1 mm^2 of cortical surface, by taking into account the thickness of the different layers in each cortical area.

Number of ChAT-immunostained axon varicosities

To derive the number of ChAT-immunostained axon varicosities from the length measurements of ChAT-immunostained axons, the average number of these dilations per unit length of axon was determined. The varicosities were defined as darkly stained axonal dilations > 0.5 μm in transverse diameter. From each layer of three cortical areas in 3 rats, 25 axon segments running in the transverse plane of section were selected (total n = 1050; > 10 mm of axon per rat), and the number of varicosities counted on these fibers at a final magnification of 1000 X. The fibers were then drawn on transparent film, the tracings skeletonized and measured for length as described above, and the average number of varicosities per μm of axon (N/μm) determined from total axon length in each layer of each area. The same calculation was also performed on an additional group of 50 fibers, located in layer I of the frontal (n = 25) and layer IV of the parietal area (n = 25), that were visualized

in sections tangential to the cortical surface. The product of N/μm by the length of axons in 1 mm^3 , or by the length of axons under 1 mm^2 of cortical surface, then provided the corresponding densities ($10^6/mm^3$) or actual numbers (10^6) of axon varicosities.

Complementary experiments

Two sets of data were acquired to demonstrate that the above described experimental conditions allowed for a maximal visualization of the ChAT-immunoreactive fiber network, at least at the light microscopic level. In the first, a series of adjacent transverse sections from the parietal cortex of one rat was incubated with a concentration of 2 μg/ml of the primary monoclonal anti-ChAT antibody, and the density of immunostained fibers was measured in layer I after labeling with DAB (see above) for increasing durations of 1.5, 2.5, 3.5 and 5 minutes. Since, throughout this time range, the density of immunoreactive fibers did not vary in length but only in intensity of immunostaining, a second series of sections was processed with increasing concentrations of 0.02, 0.2, 2 and 4 μg/ml of the anti-ChAT antibody and revealed for 2.5 min, the duration which provided the best contrast at the concentration of 2 μg/ml.

Statistical analysis

The laminar densities of ChAT-immunostained axons and axon varicosities were tabulated as means ± s.e.m. per mm^3 of tissue (n = 5). An interlaminar mean ± s.e.m. was also obtained from each cortical area (n = 5). The statistical comparisons between layers and areas were made by one-way ANOVA ($\alpha = 0.05$) followed by one- or two-tailed Student's t test ($\alpha = 0.005$).

RESULTS

Visualization of the cortical ACh innervation

As illustrated in Fig. 3, the concentration of 2 μg/ml of primary anti-ChAT antibody chosen for the present study provided for the detection of a maximal length of ChAT-immunoreactive fibers in the cortex. Omission of the primary or secondary antibodies resulted in total lack of immunostaining (not illustrated).

The regional and laminar distribution of ChAT-immunoreactive elements in the three cortical areas (Fig. 4) was in good agreement with earlier immunocytochemical descriptions based on the use of other anti-ChAT antibodies (e.g., Eckenstein et al., 1988; Lysakowski et al., 1989). In general, however, a richer network of immunostained fibers was seemingly visualized with the present antibody (see also Cossette et al., 1993; Umbriaco et al., 1994). Every layer in each cortical area was pervaded by an intricate network of fine, varicose, branching fibers. The orientation of these fibers appeared to be random, except in layers I and VI. In layer I, a number of axonal branches of fine caliber ran in the transverse plane, parallel to the pial surface. In the depth of layer VI, certain larger and smoother fibers also ran in this plane, immediately above or within the callosal radiations, whereas others, visualized as dotted profiles, seemed to run orthogonal to the transverse plane. All layers but layer I also displayed ChAT- positive, ovoid-shaped bipolar interneurons with radially oriented dendrites, that were more numerous in layers II/III and V. At distances greater than 60 μm from the soma, the arborizing dendrites of these cells could no longer be distinguished from surrounding immunoreactive axons. As for their axonal arborization, it could not even be identified as such in the midst of the rich network of ChAT-immunostained fibers.

Area-specific differences in the laminar distribution of the immunostained axon network were readily apparent, as illustrated in Figure 4A-C. In the parietal and occipital cortex (Figs. 4B and 4C), layers I and V showed the densest innervation, while layers II/III, IV and VI were less densely innervated. In contrast with these sensory areas, the frontal cortex (Fig. 4A) exhibited a more homogeneous distribution of ChAT-immunostained fibers. Whether in the transverse or the tangential plane, there was no hint of a barrel pattern in the posteromedial barrel subfield of the parietal cortex.

Quantification of ACh axon network

As shown in Figure 5A and Table 1, the density of ChAT-immunostained axons in the frontal, parietal and occipital cortex ranged from 7.3 m/mm^3 in layer IV of the parietal cortex to 13.5 m/mm^3 in layer I of the frontal cortex. In all three areas, layers I and V displayed comparably high densities. In the frontal cortex, the other layers were also high, whereas there was a striking laminar heterogeneity in the two sensory areas, with lower values in layers II/III, IV and VI of the parietal cortex, and layers IV and VI of the occipital cortex ($p < 0.005$ compared to layer I). The density in these layers was also lower than that in layer V ($p < 0.01$), except in layer VI of the parietal area where it was significantly higher that in layers II/III and IV. The mean (interlaminar) axon density in the frontal cortex (13.0 m/mm^3) was significantly higher than those of the parietal and the occipital cortex (9.9 and 11.0 m/mm^3, respectively) ($p < 0.01$).

Taking into account layer thickness in each area, the length of axon under a cortical surface of 1 mm^2 ranged from 1.4 m in layer I of the occipital cortex to 10.0 m in layer V of the frontal cortex (Table 1). Irrespective of the cortical area, it was always the lowest in layer I and the highest in layer V. The total length of ChAT-

immunostained axons under 1 mm^2 was 26.7 m and 19.7 m in the frontal and the parietal cortices, respectively, and 15.3 m in the occipital cortex, owing to the lesser thickness of this cortex.

Quantification of ACh axon varicosities

It was of particular interest to determine the number of dilations borne by the ChAT-immunostained axons (Fig. 6), since they represent the presumed sites of ACh release (Fig. 7). The number of axon varicosities per unit length of axon (N/μm) showed no significant differences between the different layers and areas (Table 1), nor between axons visualized in the transverse or tangential plane of section. It averaged 0.39 and 0.41 in transverse sections of the parietal and of the frontal and occipital cortex, respectively, and 0.42 in tangential sections of the parietal and frontal cortex. As a consequence, the laminar profiles of density for varicosities closely matched those of the axons (Fig. 5B). Values ranged from 2.9 x $10^6/mm^3$ in layer IV of the parietal cortex to 5.5 x $10^6/mm^3$ in layer I of the occipital cortex. As in the case of the axons, the highest interlaminar mean density for varicosities was that of the frontal cortex (5.4 x $10^6/mm^3$), and those of the parietal and the occipital cortex were lower (3.8 and 4.6 x $10^6/mm^3$). When considering layer thickness, the number of varicosities ranged from 0.60 x 10^6 in layer I of the occipital cortex to 4.10 x 10^6 in layer V of the frontal cortex. The number of ChAT-immunostained varicosities under 1 mm^2 of cortical surface was 11.07, 7.70 and 6.36 x 10^6 in the frontal, parietal and occipital areas, respectively.

From these values, it was possible to determine the number of ChAT-immunostained axon varicosities endowed with a synaptic specialization (Table 2). With the same antibody, the synaptic incidence of these varicosities had already been determined in the different layers and whole thickness of adult rat parietal

cortex, using electron microscopic immunocytochemistry in serial thin sections (Umbriaco et al., 1994). When multiplied by the corresponding laminar densities or the number of axon varicosities under 1 mm^2 of cortical surface, these proportions yielded the corresponding numbers of synaptic ChAT-immunostained varicosities. As shown in Table 2, layer V contained the highest density of synaptic ACh varicosities (0.92 x $10^6/mm^3$) and layer IV the lowest (0.32 x $10^6/mm^3$), based on respective synaptic incidence proportions of 21% and 11%. Layer I contained only 0.07 x 10^6 synaptic varicosities under 1 mm^2, 5.7% of the total number (1.23 x 10^6) and 11.9% of the number in layer V (0.59 x 10^6). Layer V accounted for almost half of the synaptic ChAT-immunostained varicosities (48%) in the parietal cortex, and the combination of layers V and VI for 75.6% of the total. In keeping with the interlaminar average previously calculated from the proportion of synaptic ACh varicosities in the different layers of this cortex (14% in Umbriaco et al., 1994), the average synaptic incidence determined from the total number of synaptic varicosities under 1 mm^2 of parietal cortex is thus estimated at 16.0%.

DISCUSSION

Methodological considerations

Previous immunocytochemical descriptions with the antibody against purified rat brain ChAT (Cozzari et al., 1990) have illustrated its specificity and high affinity. Indeed, in these studies, this antibody provided not only for a selective visualization of the same cell bodies and dendrites as previously identified with different anti-ChAT antibodies (e.g., Chédotal et al., 1994a; Molnar et al., 1998; Oakman et al., 1999), but also for a strong immunostaining of their axonal arborizations in all terminal fields, such as the cerebral cortex (Chédotal et al.,

1994b; Umbriaco et al., 1994), hippocampus (Umbriaco et al., 1995; Deller et al., 1999), neostriatum (Contant et al., 1996) and cerebellum (Jaarsma et al., 1996). Moreover, the visualization of the axon terminals (varicosities) could then be achieved in conditions of tissue fixation suitable for electron- as well as light-microscopic characterization.

There was clear evidence that the present experimental conditions led to complete detection of the cortical cholinergic axon network, at least at the light microscopic level. First, the same, maximal length of ChAT-immunostained axons was measured in sections incubated at the working concentration of primary antibody (2 μg/ml), or with a two-fold higher concentration. Second, irrespective of the duration of the labeling with DAB, the same length of fibers was detected at this working concentration. Third, a full penetration of immunoreagents through the thickness of the vibratome (50-μm-thick) sections was indicated by the fact that, with an 25 X objective lens of 0.7 numerical aperture, a comparably dense network of immunostained fiber was visible when focusing at the center versus both surfaces of sections. Moreover, in tracing the network in successive planes of focus, there were no indications of discontinuous immunostaining along individual fibers.

The two-step sampling technique used for the quantification also ensured that the totality of the fiber network across each section would be taken into account. By successive hand tracing of the immunoreactive axon pattern visible in the three focal planes through each section, it could be ascertained that all and only these fibers, whether black or of various shades of gray, were recorded from a sampling window, while avoiding redundancy. Such a level of discrimination could not be provided by current computerized automated analysis programs designed to extract image features above a specified treshold (e.g., Mize et al., 1988). On the other

hand, this procedure was tedious. It was therefore of practical interest to establish that tracings at a single depth of focus yielded a constant proportion of the whole network. This allowed to proceed with a more extensive sampling and for statistical validation of the results.

In determining the number of axon varicosities, fiber dilations were considered as varicosities if their transverse diameter was greater than 0.5 μm. This diameter for cortical ACh axon varicosities was consistent with earlier electron microscopic measurements of their average diameter in the parietal cortex (Umbriaco et al., 1994), whether determined from single (0.52 μm) or from serial thin sections (0.59 μm). This same study has shown that intervaricose axon segments belonging to cortical ACh terminals measure 0.2 μm in transverse diameter. As the mean number of varicosities per length of ChAT-immunostained axon showed minimal variations between layers and cortical areas (means/μm ± s.d.: 0.41 ± 0.01; 0.39 ± 0.05 and 0.41 ± 0.01, in the frontal, parietal and occipital cortex, respectively), a fixed number of 4 varicosities per 10 μm might be used in future studies of adult brain to infer the number of varicosities from measurements of axon length. From these ratios and the average size of cortical ACh varicosities, it may also be inferred that the average length of intervaricose axon segments is approximately 2 μm.

The measurement of axon length in straight rows of relatively large windows across the whole thickness of cortex ensured an extensive and reliable sampling of each cortical layer and area. The correction of axon length for angulation, assuming a random orientation of these fibers, may have led to a slight overestimation in layer I and/or layer VI, in which medio-lateral trajectories were visible in the transverse plane. Conversely, in lower layer VI, the presence of orthogonally oriented axons might have resulted in slight underestimation.

However, in both instances, these trajectories represented a minimal fraction of the whole network, much as the few fibers measured in the upper cortical layers that were presumably not axons but ramifications of thin varicose dendrites from ChAT-immunoreactive interneuron, or at least those which co-localize VIP in cerebral cortex (see Hajós et al., 1988). It was beyond the scope of the present study to determine the overall contribution of these interneurons to the total cholinergic innervation of the cortex (but see Johnston et al., 1981; Eckenstein and Baughman, 1987; Eckenstein et al., 1988).

Because of the tight relationship between length of axons and number of axon varicosities irrespective of the cortical layer and area examined, both densities of axons and varicosities could be referred to as *density of innervation*. Length of axons and number of varicosities were first expressed as densities per mm^3 in order to facilitate the comparison with previous estimates for other chemically-defined systems. These measurements were also extrapolated to real length and number under a cortical surface of 1 mm^2, for the layers and the whole thickness of each cortex, in order to better appreciate differences mainly imputable to layer and cortical thickness. For example, the parietal cortex was 28% thicker than the occipital cortex, and this was better reflected by real axonal length (19.7 m vs 15.3 m) than interlaminar average density (9.9 m/mm^3 vs 11.0 m/mm^3). In the frontal cortex, transversely cut sections may not have been strictly orthogonal to the curving surface, leading to some overestimation of cortical thickness. However, based on simple geometrical considerations, this should have been less than 10% at the middle level sampled in the present study.

It is noteworthy that among putative markers of cholinergic innervation density, ChAT activity showed the tightest correlation with the present

measurements of ChAT-immunoreactive innervation density. In the occipital cortex, notably, the amount of ChAT activity (McDonald et al., 1987) was almost identical in its laminar distribution to the pattern displayed and quantified in the present study. In conditions of cholinergic denervation or reinnervation, however, this relationship might no longer hold true, owing to adaptive changes in the activity of the enzyme (e.g., Cossette et al., 1993). Immunocytochemistry with recently produded antibodies against the vesicular transporter of ACh may also be used to visualize the cholinergic innervation (Arvidsson et al., 1997; Ichikawa et al., 1997; Roghani et al., 1998; Schäfer et al., 1998). Thus far, however, evidence is still lacking that these antibodies provide for the integral immunocytochemical detection of an ACh innervation in CNS tissue.

Areal and laminar distribution of the ACh innervation

The distributional patterns revealed by the present study were in general agreement with the previous description of Lysakowski and collaborators (1989), except for their report of a barrel-like disposition of ChAT-immunoreactive fibers in the posteromedial barrel field area of the parietal cortex. No such pattern was observed in the present study, whether in tangential or in transverse sections (see also Cossette et al., 1993; Umbriaco et al., 1994), a finding to be taken into account in the interpretation of experimental results on cholinergic parameters in this cortical area.

Of the three areas examined, the frontal (primary motor) displayed the most homogeneous distribution and highest mean density (interlaminar) of ACh innervation. This was largely imputable to the lack of a well-defined layer IV (see below) and the preponderance of layer V (almost 37% of the whole cortical thickness), which received a dense innervation in each area. The primary sensory

areas, parietal and occipital, showed some similarities in both distributional pattern and density of ACh innervation. Their lower mean density than in frontal cortex (parietal: ↓23.8 %; occipital: ↓15.4 %) seemed mainly due to the presence of a well-developed granular layer IV, in which laminar density was low. When considering the amount of innervation underneath 1 mm^2 of cortical surface, the occipital cortex received 22.3 % less ACh innervation than the parietal cortex, and 42.7 % less than the frontal cortex, mostly because of its lesser thickness.

The average density of 4.6 x 10^6 axon varicosities per mm^3 measured in the three areas here examined demonstrated that the ACh innervation is not only widespread, but also the most abundant of all modulatory systems in cerebral cortex. Indeed, it corresponds to 2.4 times the number of axon varicosities of the dopamine innervation in its area of densest distribution (anterior cingulate cortex; Descarries et al., 1987), more than 4 times that of the widespread noradrenaline innervation (Audet et al., 1988), and is slightly superior to the mean for the serotonin innervation in the frontal and parietal areas (4.5 x 10^6; Audet et al., 1989). The average density of ACh innervation may also be envisaged relative to the total number of axon terminals, estimated to be in the order of 1.2 x 10^9 in the rat cerebral cortex (Sirevaag and Greenough, 1987, and personal communication). It may then be inferred that there is 1 ACh varicosity per 260 cortical nerve endings, compared to 1 per 270 for serotonin, 1 per 1200 for noradrenaline, and 1 per 8 000 for dopamine (layer VI only) varicosities in the same cortical areas.

In mammalian neocortex, ACh has long been known to exert long-latency and prolonged excitatory effects mediated by muscarinic receptors (Krnjevic et al., 1971). More recently, fast excitatory actions mediated by nicotinic receptors have also been described, in ferret, rat and human neocortical tissue (Roerig et al., 1997;

Xiang et al., 1998; Porter et al., 1999; Alkondon et al., 2000). Laminar profiles of binding obtained in the rat cerebral cortex with [^{3}H]ACh or with nicotinic ([^{3}H]nicotine, [^{3}H]methylcarbamylcholine, [^{125}I]α-bungarotoxin) or muscarinic ([^{3}H]pirenzepine, [^{3}H]AFDX 116 and 384, [^{3}H]4-DAMP, [^{3}H]QNB) radioligands were all distinct from the laminar distribution of the ACh innervation (Clarke et al., 1985; Quirion et al., 1989; Fuchs and Schwark, 1993; Séguéla et al., 1993; Aubert et al., 1996). According to immunocytochemical descriptions carried out with specific antibodies against nicotinic subunits or muscarinic receptor subtypes, the closest match with the ACh innervation is probably that of the α4 and β2 nicotinic subunits, the co-assembly of which forms the predominant nicotinic receptor in the CNS (Sargent, 1993). Labeling of both these subunits involves neuronal cell bodies and dendrites in the different cortical layers (Hill et al., 1993; Nakayama et al., 1995), and predominantly neuronal cell bodies in layer II/III and layer V pyramidal neurons, in keeping with earlier *in situ* hybridization data having shown neurons with the corresponding mRNAs in all cortical layers (Wada et al., 1989). These results would seem to indicate that, in the cerebral cortex, the α4β2 nicotinic receptor acts primarily as a somatodendritic heteroreceptor, presumably activated by ACh diffusing from neighboring ACh varicosities.

Among muscarinic receptors, the closest match with the ACh innervation is that of the m2 subtype, which has long been thought to be a terminal autoreceptor regulating ACh release. In rat cortex, immunoreactivity to this receptor has been described as the strongest in layer V and upper layers IV and VI, and mainly associated with fibers and occasionally perikarya (Levey et al., 1991). Basal forebrain cholinergic and non-cholinergic cell bodies also display m2 receptor immunoreactivity and the corresponding mRNA (Levey et al., 1995). However, a

subsequent study in normal and cholinergically deafferented frontal cortex of rhesus monkey has shown that the contribution of the nucleus basalis ACh neurons to cortical m2-immunoreactivity was minimal (Mrzljak et al., 1998), emphasizing the heteroreceptor role of the m2 receptor subtype. Furthermore, after gold immunolabeling for electron microscopy, the same study demonstrated that the m2 receptor is located at peri- and extra-synaptic sites within pyramidal as well as non pyramidal neurons (Mrzljak et al., 1998), leading to the conclusion that muscarinic as well as nicotinic ACh receptors might be activated by ACh having diffused from its release sites (Umbriaco et al., 1994; Descarries et al., 1997).

In primary as well as associative cortical areas, modulatory actions of ACh have been described mainly as muscarinic-like facilitatory effects on input processing. In rat frontal cortex, ACh released by basal forebrain afferents has been implicated in the generation (Rigdon and Pirch, 1986) and modulation (Pirch et al., 1992) of conditioned neuronal responses. In cat parietal and occipital cortex, facilitatory effects of iontophoresed ACh on somatosensory and visual responses have been documented to be predominant (Silito and Kemp, 1983; Tremblay et al., 1990). It has also been shown that, in rat piriform cortex and hippocampus, ACh selectively suppresses intrinsic cortical activity, thus favoring responsiveness to extrinsic input (Hasselmo and Bower, 1992; Hasselmo and Schnell, 1994). Recent optical recordings of Kimura et al. (1999), indicating that ACh blocks the spread of excitation in all layers of the visual cortex, are consistent with this view. The fact that such suppressive effects are the weakest in layer IV and not exerted on thalamocortical afferents would seem congruent with the low density of ACh innervation in this layer. Taken together, these observations support the suggestion that, in the primary sensory areas at least, ACh can shift the balance of cortical

activity in favor of extrinsic inputs (Hasselmo and Bower, 1993). As a consequence, it may be speculated that perception of new incoming information should be enhanced (e.g., Jacob and Juliano, 1995), accounting for the proposed involvement of ACh in attention (see Baxter and Chiba, 1999) and in the shaping or reshaping (plasticity) of sensory maps (e. g. Dykes, 1997; Kilgard and Merzenich, 1998).

In view of the abundance of ACh innervation in all layers of the frontal cortex and layer V of the parietal and the occipital cortex, the possibility should also be considered that ACh might exert similar (and not only secondary) influences on the selection and processing of cortical output. In support of this hypothesis are the demonstrated effects of ACh or of cholinergic agonists on the activity and adaptation of pyramidal cell firing in motor as well as other regions of cerebral cortex (Krnjevic and Phillis, 1963a; Woody and Gruen, 1987; Barkai and Hasselmo, 1994). Also noteworthy are the observations of Ivliev (1999) showing that microinjection of atropine in the motor cortex of freely moving rat has a dose-dependent effect on the motor component of a conditioned behavior, suppressing the inhibition of concurrent movements during learning.

It should also be noted that, whatever effects are attributed to ACh on information processing in the cerebral cortex, these should be pronounced in layer I, in which the distal dendritic arborizations of pyramidal neurons are located and the ACh innervation is the densest of all layers (see Vogt, 1991). This may be viewed as a further argument in favor of a modulatory effect of ACh on cortical output.

The previous electron microscopic demonstration in serial sections that less than 15% of ChAT-immunostained axon terminals (varicosities) in adult rat parietal cortex displayed the membrane differentiation of typical synapses has led to the suggestion that transmission by diffusion might be a major mode of ACh action in

cerebral cortex (Umbriaco et al., 1994 ; Descarries et al., 1997; Descarries and Mechawar, 2000). It has also been suggested that in a region with such a widespread and relatively dense ACh innervation, an ambient level of ACh might be permanently maintained in the extracellular space and contribute to the modulation of cortical information processing by ACh (Descarries et al., 1997; Descarries, 1998; Testylier et al., 1999). Conversely, the synaptic ACh varicosities in cerebral cortex might have more to do with direct influences of ACh on intracortical circuitry and cortical output, in keeping with their increased density and total number in layer V, at least in the parietal cortex (Table 2).

Extent and content of ACh neurons projecting to cortex

The present quantitative data reveal unexpected features of the cholinergic innervation in cerebral cortex, in terms of its overall extent but also of its cytological and biochemical characteristics at the single neuron level. Assuming comparable densities of innervation in all cortical areas, and given an estimated volume of 670 mm^3 for the whole cerebral cortex of adult rat (Paxinos and Watson, 1986) and averages of 11.3 m/mm^3 and 4.6 x 10^6 varicosities/mm^3 for length of axons and number of varicosities in the frontal, parietal and occipital areas, it may be calculated that the adult rat cortex contains some 7.6 kilometers of ACh axons and 3.1 billion ACh varicosities. When broken down to the contribution of each nucleus basalis ACh neuron projecting to cortex (7 000 - 9 000 according to Rye et al., 1984, and Gritti et al., 1993), this allows the inference that, in cortex alone, each of these neurons has an axonal arborization averaging almost 1 meter in length and bearing close to 400 000 varicosities.

ACh levels have been measured in adult rat parietal cortex (Johnston and Coyle, 1980; Ni et al., 1995), in which the volume of individual ACh varicosities is

also known from the earlier serial section electron microscopic study of Umbriaco et al. (1994). Since ACh is likely to be highly concentrated in synaptic vesicles and hence in axon varicosities as opposed to intervaricose segments, the average concentration of ACh per cortical varicosity may be calculated to be about 45 mM. By analogy with hippocampal axon terminals of the same diameter (Harris and Sultan, 1995), it may also be assumed that cortical ACh varicosities contain an average of 200 small spherical vesicles, 40 nm in diameter. If the concentration of ACh is 100-fold higher in synaptic vesicles than axoplasm, it may be further extrapolated that an average of 13 500 ACh molecules (642 mM) is present in these vesicles. Interestingly, such a concentration is in the same range as that measured for the larger (70-90 nm) synaptic vesicles of *Torpedo*'s electric organ (400-800 mM; Parsons et al., 1993), and equivalent to the number of ACh molecules in one quantum at the motor endplate (Miledi et al., 1983).

Concluding remarks

This quantitative evaluation of the length of ACh axons and number of ACh axon varicosities in three areas of adult rat neocortex demonstrates that this innervation is the most abundant of all cortical neuromodulatory systems. In addition to its ubiquitous distribution, variations in its regional and laminar density are consequent with the proposed roles of ACh in cortical information processing. Current knowledge on the ultrastructural features of ACh varicosities and the distribution of ACh receptors in cerebral cortex strongly suggests that such effects be at least partly dependent on ACh diffusing from its release sites. Speculations on the role of ACh in refining cortical input as well as cortical output are justified by the data on the laminar distribution and synaptic features of this innervation. In addition to their potential value for future assessments of the

cortical ACh innervation in different experimental settings, these quantified results also provide insights on the extent and content of individual cholinergic neurons projecting to the cerebral cortex.

Acknowledgments

The authors thank Julie Poupart and Jean-François Pujol for useful suggestions during the development of the method, Yves Lepage for advice in the statistical analysis of the results, and Robert W. Dykes and Mustapha Riad for their critical reading of the manuscript. They are also grateful to Kenneth C. Watkins for the electron microscopy, and Giovanni Battista Filosi and Gaston Lambert for their help in the preparation of the illustrations. N.M. is the recipient of a doctoral research studentship from the MRC of Canada.

LITERATURE CITED

Alkondon M, Pereira EFR, Eisenberg HM, Albuquerque EX. 2000. Nicotinic receptor activation in human cerebral cortical interneurons: a mechanism for inhibition and disinhibition of neural networks. J Neurosci 20:66-75.

Arvidsson U, Riedl M, Elde R, Meister B. 1997. Vesicular acetylcholine transporter (VAChT) protein: a novel and unique marker for cholinergic neurons in the central and peripheral nervous system. J Comp Neurol 378:454-467.

Aubert I, Cécyre D, Gauthier S, Quirion R. 1996. Comparative ontogenic profile of cholinergic markers, including nicotinic and muscarinic receptors, in the rat brain. J Comp Neurol 369:31-55.

Audet MA, Descarries L, Doucet G. 1989. Quantified regional and laminar distribution of the serotonin innervation in the anterior half of adult rat cerebral cortex. J Chem Neuroanat 2:29-44.

Audet MA, Doucet G, Oleskevich S, Descarries L. 1988. Quantified regional and laminar distribution of the noradrenaline innervation in the anterior half of the adult rat cerebral cortex. J Comp Neurol 274:307-318.

Barkai E, Hasselmo ME. 1994. Modulation of the input/output function of rat piriform cortex pyramidal cells. J Neurophysiol 72:644-658.

Bartus RT, Dean RL, Beer B, Lippa AS. 1982. The cholinergic hypothesis of geriatric memory dysfunction. Science 217:408-417.

Baxter MG, Chiba AA. 1999. Cognitive functions of the basal forebrain. Curr Opin Neurobiol 9:178-183.

Bayraktar T, Staiger JF, Acsady L, Cozzari C, Freund TF, Zilles K. 1997. Co-localization of vasoactive intestinal polypeptide, γ-aminobutyric acid and choline acetyltransferase in neocortical interneurons of the adult rat. Brain Res 757:209-217.

Bear MF, Singer W. 1986. Modulation of visual cortical plasticity by acetylcholine and noradrenaline. Nature 320:172-176.

Bucci DJ, Holland PC, Gallagher M. 1998. Removal of cholinergic input to rat posterior parietal cortex disrupts incremental processing of conditionned stimuli. J Neurosci 18:8038-8046.

Butcher LL, Talbot K, Bilezikjian L. 1975. Acetylcholinesterase neurons in dopamine-containing regions of the brain. J Neural Transm 37:127-153.

Buzsàki G, Bickford RG, Ponomareff G, Thal LJ, Mandel R, Gage FH. 1988. Nucleus basalis and thalamic control of neocortical activity in the freely moving rat. J Neurosci 8:4007-4026.

Celesia GG, Jasper HH. 1966. Acetylcholine released from cerebral cortex in relation to state of activation. Neurology 16:1053-1063.

Chédotal A, Cozzari C, Faure MP, Hartman BK, Hamel E. 1994a. Distinct choline acetyltransferase (ChAT) and vasoactive intestinal polypeptide (VIP) bipolar neurons project to local blood vessels in the rat cerebral cortex. Brain Res 646:181-193.

Chédotal A, Umbriaco D, Descarries L, Hartman BK, Hamel E. 1994b. Light and electron microscopic immunocytochemical analysis of the neurovascular relationships of choline acetyltransferase and vasoactive intestinal polypeptide nerve terminals in the rat cerebral cortex. J Comp Neurol 343:57-71.

Clarke PB, Schwartz RD, Paul SM, Pert CB, Pert A. 1985. Nicotinic binding in rat brain: autoradiographic comparison of [^{3}H]acetylcholine, [^{3}H]nicotine, and [^{125}I]α-bungarotoxin. J Neurosci 5:1307-1315.

Contant C, Umbriaco D, Garcia S, Watkins KC, Descarries L. 1996. Ultrastructural characterization of the acetylcholine innervation in adult rat neostriatum. Neuroscience 71:937-947.

Cossette P, Umbriaco D, Zamar N, Hamel E, Descarries L. 1993. Recovery of choline acetyltransferase activity without sprouting of the residual acetylcholine innervation in adult rat cerebral cortex after lesion of the nucleus basalis. Brain Res 630:195-206.

Cozzari C, Howard J, Hartman B. 1990. Analysis of epitopes on choline acetyltransferase (ChAT) using monoclonal antibodies (Mabs). Soc Neurosci Abstr 16:200.

Davies P, Maloney AJ. 1976. Selective loss of central cholinergic neurons in Alzheimer's disease. Lancet 2:1403.

Deller T, Katona I, Cozzari C, Frotscher M, Freund TF. 1999. Cholinergic innervation of mossy cells in the rat fascia dentata. Hippocampus 9:314-320.

Descarries L. 1998. The hypothesis of an ambient level of acetylcholine in the central nervous system. J Physiol (Paris) 92:215-220.

Descarries L, Mechawar N. 2000. Ultrastructural evidence for diffuse transmission by monoamine and acetylcholine neurons in the central nervous system. In: Agnati LF, Fuxe K, Nicholson C, Sykova E, editors: Volume Transmission Revisited. Prog Brain Res, Vol 125, Elsevier, Amsterdam (in press).

Descarries L, Gisiger V, Steriade M. 1997. Diffuse transmission by acetylcholine in the CNS. Prog Neurobiol 53:603-625.

Descarries L, Lemay B, Doucet G, Berger B. 1987. Regional and laminar density of the dopamine innervation in adult rat cerebral cortex. Neuroscience 21:807-824.

Donoghue JP, Carroll KL. 1987. Cholinergic modulation of sensory responses in rat primary somatic sensory cortex. Brain Res 408:367-371.

Dykes RW. 1997. Mechanisms controlling neuronal plasticity in somatosensory cortex. Can J Physiol Pharmacol 75:535-545.

Eckenstein F, Baughman RW. 1984. Two types of cholinergic innervation in cortex, one co-localized with vasoactive intestinal polypeptide. Nature 309:153-155.

Eckenstein F, Baughman RW. 1987. Cholinergic innervation in cerebral cortex. In: Jones EG, Peters A, editors: Cerebral Cortex, Vol. 6, Plenum Press, New York, pp. 29-160.

Eckenstein F, Thoenen H. 1983. Cholinergic neurons in the rat cerebral cortex demonstrated by immunohistochemical localization of choline acetyltransferase. Neurosci Lett 36:211-215.

Eckenstein FP, Baughman RW, Quinn J. 1988. An anatomical study of cholinergic innervation in rat cerebral cortex. Neuroscience 25:457-474.

Etienne O, Robitaille Y, Wood P, Gauthier S, Nair NPV, Quirion R. 1986. Nucleus basalis neuronal loss, neuritic plaques and choline acetyltransferase activity in advanced Alzheimer's disease. Neuroscience 19:1279-1291.

Fine A, Hoyle C, Maclean CJ, Levatte TL, Baker HF, Ridley RM. 1997. Learning impairments following injection of a selective cholinergic immunotoxin, ME20.4 IgG-saporin, into the basal nucleus of Meynert in monkeys. Neuroscience 81:331-343.

Fuchs JL, Schwark HD. 1993. Distribution of [^{3}H]QNB and [^{125}I]α-bungarotoxin binding and acetylcholinesterase activity in visual system and hippocampal structures of eleven mammalian species. J Comp Neurol 329:427-437.

Garofalo L, Ribeiro-da-Silva A, Cuello AC. 1992. Nerve growth factor-induced synaptogenesis and hypertrophy of cortical cholinergic terminals. Proc Natl Acad Sci USA 89:2639-2643.

Garofalo L, Ribeiro-da-Silva A, Cuello AC. 1993. Potentiation of nerve growth factor-induced alterations in cholinergic fibre length and presynaptic terminal size in cortex of lesioned rats by the monosialoganglioside GM1. Neuroscience 57:21-40.

Gilmor ML, Erickson JD, Varoqui H, Hersh LB, Bennett DA, Cochran EJ, Mufson EJ, Levey AI. 1999. Preservation of nucleus basalis neurons containing choline acetyltransferase and the vesicular acetylcholine transporter in the elderly with mild cognitive impairment and early Alzheimer's disease. J Comp Neurol 411:693-704.

Gritti I, Mainville L, Jones BE. 1993. Codistribution of GABA- with acetylcholine-synthesizing neurons in the basal forebrain of the rat. J Comp Neurol 329:438-457.

Hajós F, Zilles K, Gallatz K, Schleicher A, Kaplan I, Werner L. 1988. Ramification patterns of vasoactive intestinal polypeptide (VIP)-cells in the rat primary visual cortex. Anat Embryol 178:197-206.

Harris KM, Sultan P. 1995. Variation in the number, location and size of synaptic vesicles provides an anatomical basis for the nonuniform probability of release at hippocampal CA1 synapses. Neuropharmacology 34:1387-1395.

Hasselmo ME. 1995. Neuromodulation and cortical function: modeling the physiological basis of behavior. Behav Brain Res 67:1-27.

Hasselmo ME, Bower JM. 1992. Cholinergic suppression specific to intrinsic not afferent fiber synapses in rat piriform (olfactory) cortex. J Neurophysiol 67:1222-1229.

Hasselmo ME, Bower JM. 1993. Acetylcholine and memory. Trends Neurosci 16:218-222.

Hasselmo ME, Schnell E. 1994. Laminar selectivity of the cholinergic suppression of synaptic transmission in rat hippocampal region CA1: computational modeling and brain slice physiology. J Neurosci 14:3898-3914.

Hasselmo ME, Anderson BP, Bower JM. 1992. Cholinergic modulation of cortical associative memory function. J Neurophysiol 67:1230-1246.

Hill JA, Zoli M, Bourgeois J-P, Changeux J-P. 1993. Immunocytochemical localization of a neuronal nicotinic receptor: the β2-subunit. J Neurosci 13:1551-1568.

Ichikawa T, Ajiki K, Matsuura J, Misawa H. 1997. Localization of two cholinergic markers, choline acetyltransferase and vesicular acetylcholine transporter in the central nervous system of the rat: in situ hybridization histochemistry and immunohistochemistry. J Chem Neuroanat 13:23-39.

Ivliev DA. 1999. The effects of atropine microinjections into the motor cortex of rats on the development of a motor habit. Neurosci Behav Physiol 29:371-375.

Jaarsma D, Dino MR, Cozzari C, Mugnaini E. 1996. Cerebellar choline acetyltransferase positive mossy fibers and their granule and unipolar brush cell targets: a model for central cholinergic nicotinic neurotransmission. J Neurocytol 25:829-842.

Jacobs SE, Juliano SL. 1995. The impact of basal forebrain lesions on the ability of rats to perform a sensory discrimination task involving barrel cortex. J Neurosci 15:1099-1109.

Jasper HH, Tessier J. 1971. Acetylcholine liberation from cerebral cortex during paradoxical (REM) sleep. Science 172:601-602.

Jiménez-Capdeville ME, Dykes RW. 1996. Changes in cortical acetylcholine release in the rat during day and night : differences between motor and sensory areas. Neuroscience 71:567-579.

Johnston MV, Coyle JT. 1980. Ontogeny of neurochemical markers for noradrenergic, GABAergic, and cholinergic neurons in neocortex lesioned with methylazoxymethanol acetate. J Neurochem 34:1429-1441.

Johnston MV, McKinney M, Coyle JT. 1981 Neocortical cholinergic innervation: A description of extrinsic and intrinsic components in the rat. Exp Brain Res 43:159-172.

Juliano SL, Ma W, Eslin D. 1991. Cholinergic depletion prevents expansion of topographic maps in somatosensory cortex. Proc Natl Acad Sci USA 88:780-784.

Kilgard MP, Merzenich MM. 1998. Cortical map reorganization enabled by nucleus basalis activity. Science 279:1714-1718.

Kimura F, Fukuda M, Tsumoto T. 1999. Acetylcholine suppresses the spread of excitation in the visual cortex revealed by optical recording : possible differential effect depending on the source of input. Eur J Neurosci 11:3597-3609.

Krnjevic K, Phillis JW. 1963a. Acetylcholine-sensitive cells in the cerebral cortex. J Physiol (London) 166:296-327.

Krnjevic K, Phillis JW. 1963b. Pharmacological properties of acetylcholine-sensitive cells in the cerebral cortex. J Physiol (London) 166:328-350.

Krnjevic, K, Primain R, Renaud L. 1971. The mechanism of excitation by acetylcholine in the cerebral cortex. J Physiol (London) 215:247-268.

Lamour Y, Dutar P, Jobert A, Dykes RW. 1988. An iontophoretic study of single somatosensory neurons in rat granular cortex serving the limbs: a laminar analysis of glutamate and acetylcholine effects on receptive-field properties. J Neurophysiol 60:725-750.

Levey AI, Edmunds SM, Hersch SM, Wiley RG, Heilman CJ. 1995. Light and electron microscopic study of m2 muscarinic acetylcholine receptor in the basal forebrain of the rat. J Comp Neurol 351:339-356.

Levey AI, Kitt CA, Simonds WF, Price DL, Brann MR. 1991. Identification and localization of muscarinic acetylcholine receptor proteins in brain with subtype-specific antibodies. J Neurosci 11:3218-3226.

Levey AI, Wainer BH, Rye DB, Mufson EJ, Mesulam M-M. 1984. Choline acetyltransferase-immunoreactive neurons intrinsic to rodent cortex and distinction from acetylcholinesterase-positive neurons. Neuroscience 13:341-353.

Lysakowski A, Wainer BH, Bruce G, Hersh LB. 1989. An atlas of the regional and laminar distribution of choline acetyltransferase immunoreactivity in rat cerebral cortex. Neuroscience 28:291-336.

MacIntosh FC, Oborin PE. 1953. Release of acetylcholine from intact cerebral cortex. Abstr. XIX Int. Physiol. Congr. Montreal: The Congress, pp. 580-581.

McCormick DA. 1992. Neurotransmitter actions in the thalamus and cerebral cortex and their role in neuromodulation of thalamocortical activity. Prog Neurobiol 39:337-388.

McDonald JK, Speciale SG, Parnavelas JG. 1987. The laminar distribution of glutamate decarboxylase and choline acetyltransferase in the adult and developing visual cortex of the rat. Neuroscience 21:825-832.

McKenna TM, Ashe JH, Hui GK, Weinberger NM. 1988. Muscarinic agonists modulate spontaneous and evoked unit discharge in auditory cortex of cat. Synapse 2:54-68.

Mechawar N, Descarries L. 1998. Early postnatal development of the cholinergic innervation in the rat cerebral cortex. Soc Neurosci Abstr 24: 1338.

Mechawar N, Descarries L. 1999. Quantitative data on the cholinergic innervation in adult rat parietal cortex. Soc Neurosci Abstr 25:190.

Metherate R, Cox CL, Ashe JH. 1992. Cellular bases of neocortical activation: modulation of neural oscillations by the nucleus basalis and endogenous acetylcholine. J Neurosci 12:4701-4711.

Metherate R, Tremblay N, Dykes RW. 1988. Transient and prolonged effects of acetylcholine on responsiveness of cat somatosensory cortical neurons. J Neurophysiol 59:1253-1276.

Miledi R, Molenaar PC, Polak RL. 1983. Electrophysiological and chemical determination of acetylcholine release at the frog neuromuscular junction. J Physiol (London) 334:245-254.

Miranda MI, Bermúdez-Rattoni F. 1999. Reversible inactivation of the nucleus basalis magnocellularis induces disruption of cortical acetylcholine release and

acquisition, but not retrieval, of aversive memories. Proc Natl Acad Sci USA 96:6478-6482.

Mitchell JF. 1963. The spontaneous and evoked release of acetylcholine from the cerebral cortex. J Physiol (London) 165:98-116.

Mize RR, Holdefer RN, Nabors LB. 1988. Quantitative immunocytochemistry using an image analyzer. I. Hardware evaluation, image processing and data analysis. J Neurosci Meth 26:1-24.

Molnar M, Tongiorgi E, Avignone E, Gonfloni S, Ruberti F, Domenici L, Cattaneo A. 1998. The effects of anti-nerve growth factor monoclonal antibodies on developing basal forebrain neurons are transient and reversible. Eur J Neurosci 10:3127-3140.

Mrzljak L, Levey AI, Belcher S, Goldman-Rakic PS. 1998. Localization of the m2 muscarinic acetylcholine receptor protein and mRNA in cortical neurons of the normal and cholinergically deafferented rhesus monkey. J Comp Neurol 390:112-132.

Nakayama H, Shioda S, Okuda H, Nakashima T, Nakai Y. 1995. Immunocytochemical localization of nicotinic acetylcholine receptor in rat cerebral cortex. Mol Brain Res 32:321-328.

Ni J-W, Matsumoto K, Li H-B, Murakami Y, Watanabe H. 1995. Neuronal damage and decrease of central acetylcholine level following permanent occlusion of bilateral common carotid arteries in rat. Brain Res 673:290-296.

Oakman SA, Faris PL, Cozzari C, Hartman BK. 1999. Characterization of the extent of pontomesencephalic cholinergic neurons' projections to the thalamus: comparison with projections to midbrain dopaminergic groups. Neuroscience 94:529-547.

Parsons SM, Prior C, Marshall IG. 1993. Acetylcholine transport, storage and release. Int Rev Neurobiol 35:279-390.

Paxinos G, Watson C. 1986. The Rat Brain in Stereotaxic Coordinates, second edition. Academic Press Australia.

Perry EK, Tomlinson BE, Blessed G, Bergmann K, Gibson PH, Perry RH. 1978. Correlation of cholinergic abnormalities with senile plaques and mental test scores in senile dementia. Brit Med J 2:1457-1459.

Perry E, Walker M, Grace J, Perry R. 1999. Acetylcholine in mind: a neurotransmitter correlate of consciousness? Trends Neurosci 22:273-280.

Pirch JH, Turco K, Rucker HK. 1992. A role for acetylcholine in conditioning-related responses of rat frontal cortex neurons: microiontophoretic evidence. Brain Res 586:19-26.

Porter JT, Cauli B, Tsuzuki K, Lambolez B, Rossier J, Audinat E. 1999. Selective excitation of subtypes of neocortical interneurons by nicotinic receptors. J Neurosci 19:5228-5235.

Quirion R, Araujo D, Regenold W, Boksa P. 1989. Characterization and quantitative autoradiographic distribution of [^{3}H]acetylcholine muscarinic receptors in mammalian brain, apparent labelling of an M_2-like receptor sub-type. Neuroscience 29:271-289.

Rasmusson DD, Dykes RW. 1988. Long-term enhancement of evoked potentials in cat somatosensory cortex by co-activation of the basal forebrain and cutaneous receptors. Exp Brain Res 70:276-286.

Richter D, Crossland J. 1949. Variation in acetylcholine content of the brain with physiological state. Am J Physiol 159:247-255.

Rigdon GC, Pirch JH. 1986. Nucleus basalis involvement in conditioned neuronal responses in the rat frontal cortex. J Neurosci 6:2535-2542.

Robertson RT, Gorenstein C. 1987. 'Non-specific' cholinesterase-containing neurons of the dorsal thalamus project to medial limbic cortex. Brain Res 404:282-292.

Roerig B, Nelson DA, Katz LC. 1997. Fast synaptic signaling by nicotinic acetylcholine and serotonin 5-HT_3 receptors in developing visual cortex. J Neurosci 17:8353-8362.

Roghani A, Shirzadi A, Butcher LL, Edwards RH. 1998. Distribution of the vesicular transporter for acetylcholine in the rat central nervous system. Neuroscience 82:1195-1212.

Rye DB, Wainer BH, Mesulam M-M, Mufson EJ, Saper CB. 1984. Cortical projections arising from the basal forebrain : a study of cholinergic and noncholinergic components employing combined retrograde tracing and immunohistochemical localization of choline acetyltransferase. Neuroscience 13:627-643.

Saper CB. 1984. Organization of the cerebral cortical afferent systems in the rat. II. Magnocellular basal nucleus. J Comp Neurol 222:313-342.

Sargent PB. 1993. The diversity of neuronal nicotinic acetylcholine receptors. Annu Rev Neurosci 16:403-443.

Sarter M, Bruno JP. 2000. Cortical cholinergic inputs mediating arousal, attentional processing and dreaming: differential afferent regulation of the basal forebrain by telencephalic and brainstem afferents. Neuroscience 95:933-952.

Schäfer MK-H, Eiden LE, Weihe E. 1998. Cholinergic neurons and terminal fields revealed by immunohistochemistry for the vesicular acetylcholine transporter. I. Central nervous system. Neuroscience 84:331-359.

Séguéla P, Wadiche J, Dineley-Miller K, Dani JA, Patrick JW. 1993. Molecular cloning, functional properties, and distribution of rat brain α_7: a nicotinic cation channel highly permeable to calcium. J Neurosci 13:596-604.

Shi ZR, Itzkowitz SH, Kim YS. 1988. A comparison of three immunoperoxidase techniques for antigen detection in colorectal carcinoma tissues. J Histochem Cytochem 36:317-322.

Sillito AM, Kemp JA. 1983. Cholinergic modulation of the functional organization of the cat visual cortex. Brain Res 289:143-155.

Sirevaag AM, Greenough WT. 1985. Differential rearing effects on rat visual cortex synapses. III. Neuronal and glial nuclei, boutons, dendrites, and capillaries. Brain Res 424:320-332.

Soghomonian J-J, Doucet G, Descarries L. 1987. Serotonin innervation in adult rat neostriatum. I. Quantified regional distribution. Brain Res 425:85-100.

Stichel CC, Singer W. 1987. Quantitative analysis of the choline acetyltransferase-immunoreactive axonal network in the cat primary visual cortex: I. Adult cats. J Comp Neurol 258:91-98.

Testylier G, Maalouf M, Butt AE, Miasnikov AA, Dykes RW. 1999. Evidence for homeostatic adjustments of rat somatosensory cortical neurons to changes in extracellular acetylcholine concentrations produced by iontophoretic administration of acetylcholine and by systemic diisopropylfluorophosphate treatment. Neuroscience 91:843-870.

Tremblay N, Warren RA, Dykes RW. 1990. Electrophysiological studies of acetylcholine and the role of the basal forebrain in the somatosensory cortex of the cat. II. Cortical neurons excited by somatic stimuli. J Neurophysiol 64:1212-1222.

Umbriaco D, Watkins KC, Descarries L, Cozzari C, Hartman BK. 1994. Ultrastructural and morphometric features of the acetylcholine innervation in adult rat parietal cortex. An electron microscopic study in serial sections. J Comp Neurol 348:351-373.

Umbriaco D, Garcia S, Beaulieu C, Descarries L. 1995. Relational features of acetylcholine, noradrenaline, serotonin and GABA axon terminals in the stratum radiatum of adult rat hippocampus (CA1). Hippocampus 5:605-610.

Vincent SR, Satoh K, Armstrong DM, Fibiger HC. 1983. Substance P in the ascending cholinergic reticular system. Nature 306:688-691.

Vogt BA. 1991. The role of layer I in cortical function. In: Peters A, Jones EG, editors: Cerebral Cortex, Vol. 9, Plenum Press, New York, pp. 49-80.

Voytko ML, Olton DS, Richardson RT, Gorman LK, Tobin JR, Price DL. 1994. Basal forebrain lesions in monkeys disrupt attention but not learning and memory. J Neurosci 14:167-186.

Wada E, Wada K, Boulter J, Deneris E, Heinemann S, Patrick J, Swanson LW. 1989. Distribution of alpha2, alpha3, alpha4, and beta2 neuronal nicotinic receptor subunit mRNAs in the central nervous system: a hybridization histochemical study in the rat. J Comp Neurol 284:314-335.

Whitehouse PJ, Price DL, Clark AW, Coyle JT, DeLong MR. 1981. Alzheimer disease : evidence for selective loss of cholinergic neurons in the nucleus basalis. Ann Neurol 10:122-126.

Woody CD, Gruen E. 1987. Acetylcholine reduces net outward currents measured in vivo with single electrode voltage clamp techniques in neurons of the motor cortex of cats. Brain Res 424:193-198.

Xiang Z, Huguenard JR, Prince DA. 1998. Cholinergic switching within neocortical inhibitory networks. Science 281:985-988.

Table 1

ACh AXONS AND AXON VARICOSITIES IN ADULT RAT CEREBRAL CORTEX

LAYERS		AXONS		AXON VARICOSITIES		
Number	Height	Density	Length under 1 mm^2	Number per unit length	Density	Number under 1 mm^2
	(mm)	(m/mm^3)	(m)	(N/μm)	($10^6/mm^3$)	(10^6)
A- FRONTAL CORTEX						
I	0.14	13.5	1.9	0.40	5.4	0.76
II/IV	0.51	12.6	6.4	0.42	5.3	2.70
V	0.76	13.2	10.0	0.41	5.4	4.10
VI	0.65	12.9	8.4	0.42	5.4	3.51
I-VI	**t = 2.06**	**m = 13.0**	**t = 26.7**	**m = 0.41**	**m = 5.4**	**t = 11.07**

Table 1 (continued)

B- PARIETAL CORTEX

I	0.14	12.8	1.8	0.38	4.9	0.69
II/III	0.35	8.1	2.8	0.37	3.0	1.05
IV	0.24	7.3	1.8	0.40	2.9	0.70
V	0.64	11.2	7.2	0.39	4.4	2.82
VI	0.61	10.0	6.1	0.40	4.0	2.44
I-VI	**t = 1.98**	**m = 9.9**	**t = 19.7**	**m = 0.39**	**m = 3.8**	**t = 7.70**

Table 1 (continued)

C- OCCIPITAL CORTEX

I	0.11	12.7	1.4	0.43	5.5	0.60
II/III	0.19	11.5	2.2	0.40	4.6	0.87
IV	0.30	10.0	3.0	0.40	4.0	1.20
V	0.46	12.3	5.6	0.42	5.2	2.39
VI	0.37	8.4	3.1	0.42	3.5	1.30
I-VI	**t = 1.43**	**m = 11.0**	**t = 15.3**	**m = 0.41**	**m = 4.6**	**t = 6.36**

Mean values from 5 rats. See Materials and Methods for sampling procedure and treatment of the data, and Fig. 4A-C for illustration of the three cortical areas investigated: frontal, primary motor, Fr1; parietal, primary somatosensory, Par1; occipital, primary visual, Oc1. Totals (t) and means (m) are for the whole cortical thickness (I-VI). The laminar densities of axons and axon varicosities are graphically represented in Fig. 5AB. Length of axons and number of varicosities under 1 mm^2 take into account the thickness of the different layers in each cortical area.

Table 2

SYNAPTIC ACh AXON VARICOSITIES IN THE PARIETAL CORTEX

Layer	Incidence (%)	Density ($10^6/mm^3$)	Number under 1 mm^2 (10^6)
I	10	0.49	0.07 (5.7%)
II/III	14	0.42	0.15 (12.2%)
IV	11	0.32	0.08 (6.5%)
V	21	0.92	0.59 (48.0%)
VI	14	0.56	0.34 (27.6%)
I-VI	**mean = 14**	**mean = 0.54**	**total = 1.23**

Incidence (%) refers to the proportion of synaptic ACh varicosities in each layer, as determined by Umbriaco et al. (1994). Density and number under 1 mm^2 are extrapolated from the values in Table 1.

Fig. 1. Schematic representation of the cortical areas sampled for length of ChAT-immunostained axons and number of ChAT-immunostained varicosities: primary motor (Fr1), primary somatosensory (Par1) and primary visual (Oc1). These areas are depicted at transverse levels corresponding to stereotaxic planes A-11.2, A-9.2 and A-2.7 mm, according to the atlas of Paxinos and Watson (1986).

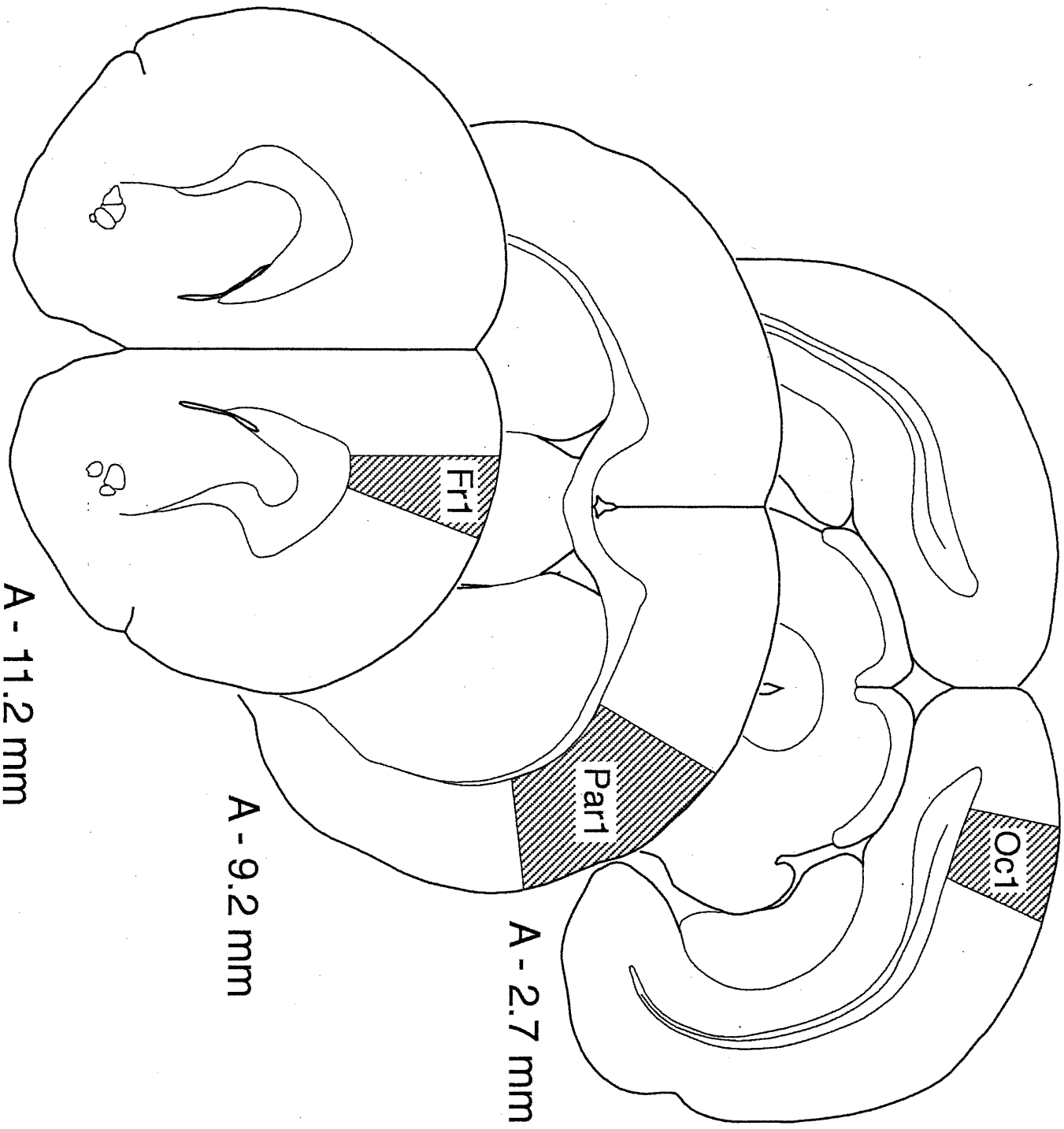
Oc1
Par1
Fr1
A - 2.7 mm
A - 9.2 mm
A - 11.2 mm

Fig. 2A-D. Illustration of the methodology employed to estimate the length of ChAT-immunoreactive axons from 50-μm-thick transverse sections across the cerebral cortex (e.g.: primary somatosensory area, Par 1). The three panels of **2A** are line drawing renditions of the immunoreactive axon network, as visualized in three planes of light microscopic focusing through the depth of a strip of cortex running from the pial surface to the bottom of layer VI (layers designated in roman numerals). Note that the density of the immunostained axon network is similar in all three planes of focus. The small square area in layer IV, delineated in the first panel, represents one of the small, sampling windows, 100 μm in side, in which the length of the immunoreactive axon network was actually measured. Figs. **2B, 2C,** and **2D** illustrate successive steps in the treatment of the data from that sampling window, at the very magnification (X 645) at which the digitized images of each plane of focus were actually captured and printed for analysis (for details, see Materials and Methods). Fig. **2B** is a photomicrograph of the axonal network in the superficial plane of focus (see corresponding drawing in first panel of A). Fig. **2C** is a telescopic view of the immunoreactive axon network through the depth of the section, as drawn by successive tracing of the three planes of focusing. Fig. **2D** is the computerized transformation of this drawing, after linearization with the " skeletonize " function of the image analysis program. Scale bar in D: 10 μm.

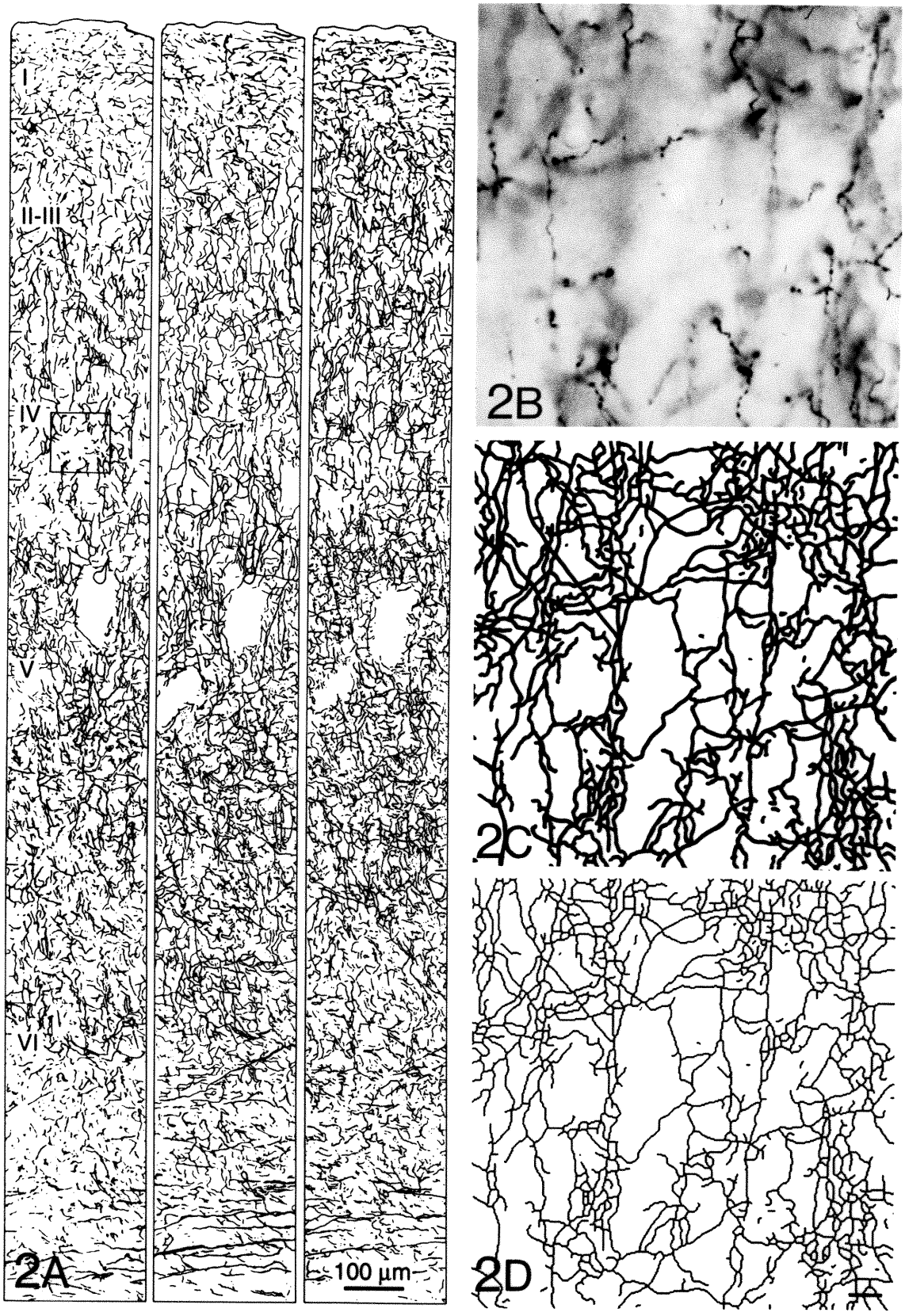
I
II-III
IV
V
VI
2A
100 µm
2B
2C
2D

Fig. 3. Graph of the relationship between the length of ChAT- immunoreactive axons measured in the cortex (density of axons) and the concentration of primary antibody used for their immunocytochemical detection. Mean ± s.d. from two sampling windows in layer I of the parietal cortex, at each of the four concentrations tested: 0.02, 0.2, 2 and 4 μg/ml. Note the plateau attained at the 2 μg/ml concentration used for the present study.

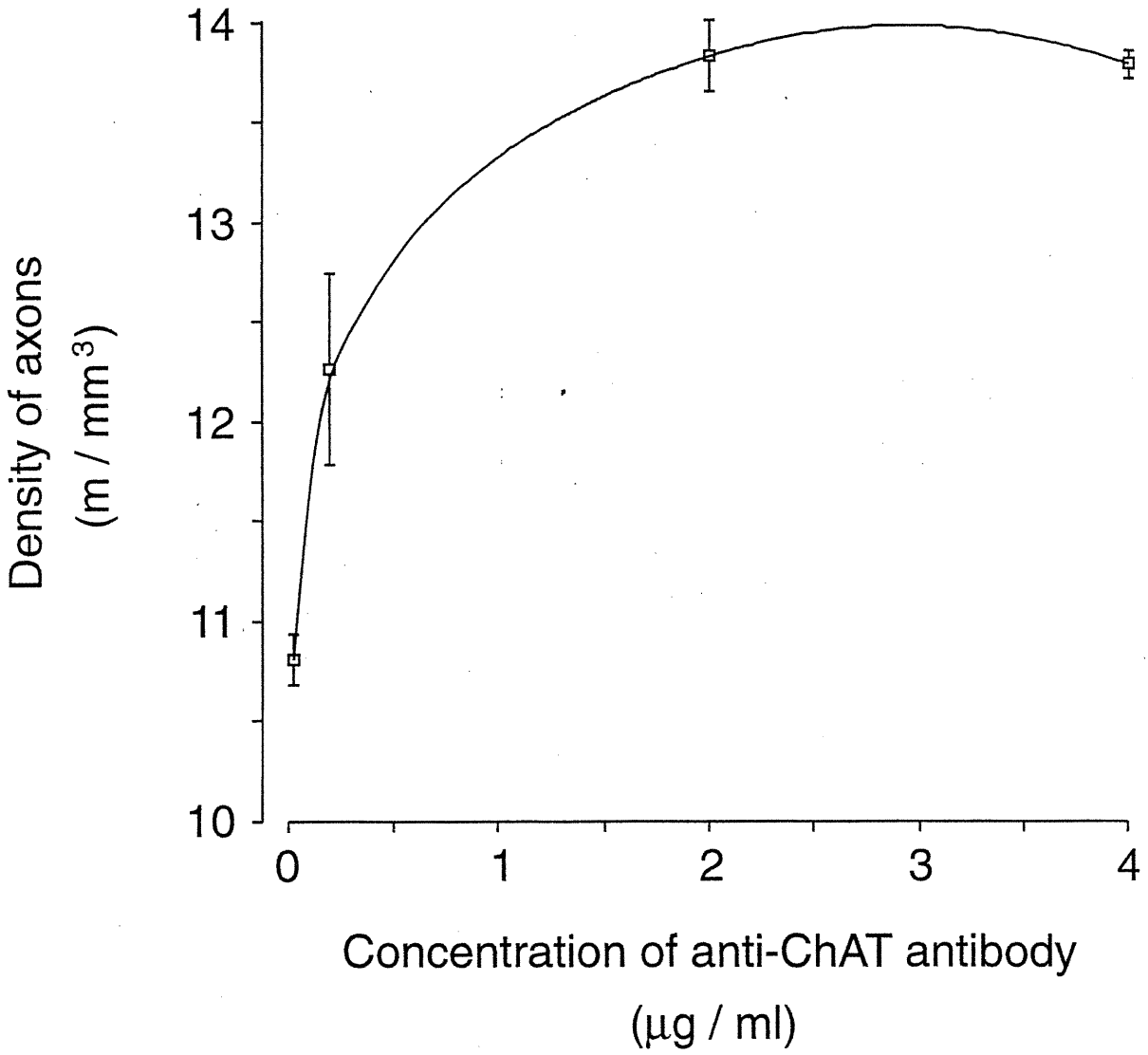
Density of axons
(m / mm3)
14
13
12
11
10
0
1
2
3
4
Concentration of anti-ChAT antibody
(µg / ml)

Fig. 4A-C. Low power micrographs illustrating the laminar distribution of ChAT-immunopositive fibers in transverse sections from the three cortical areas investigated: frontal, primary motor, Fr1 (**4A**); parietal, primary somatosensory, Par1 (**4B**); occipital, primary visual, Oc1 (**4C**). Narrow strips from adjacent Nissl-stained sections used in delimiting the cortical layers (I-VI) are also shown. In each area, small, fusiform, bipolar cholinergic interneurons, with their vertically oriented dendrites, are scattered in layers II-VI, in addition to the intricate network of fine varicose fibers pervading the whole cortical thickness. Smooth and thick, transversely oriented fibers are also visible immediately above the callosal radiations in the lower part of layer VI. X 70.

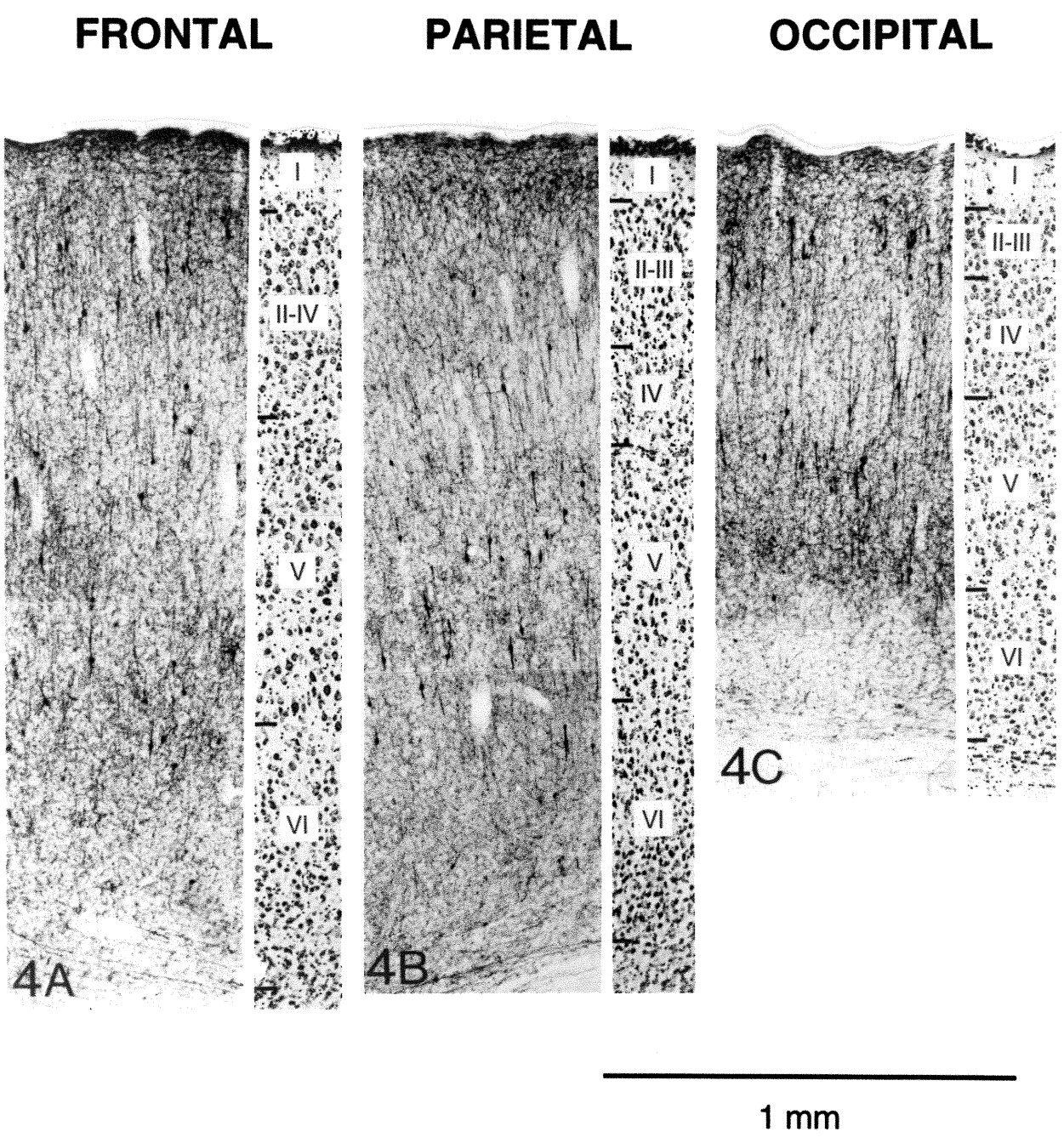
FRONTAL
PARIETAL
OCCIPITAL
I
II-IV
V
VI
4A
I
II-III
IV
V
VI
4B
I
II-III
IV
V
VI
4C
1 mm

Figs. 5AB. Densities of ACh axons (**A**) and axon varicosities (**B**) in the different layers (I-VI) of the frontal, parietal and occipital cortex. See Materials and Methods for sampling procedure and treatment of the data. Mean values (± s.e.m) from five rats. * indicates statistically significant differences from layer I by one-tailed Student's t test ($p < 0.005$). Same data as in Table 1.

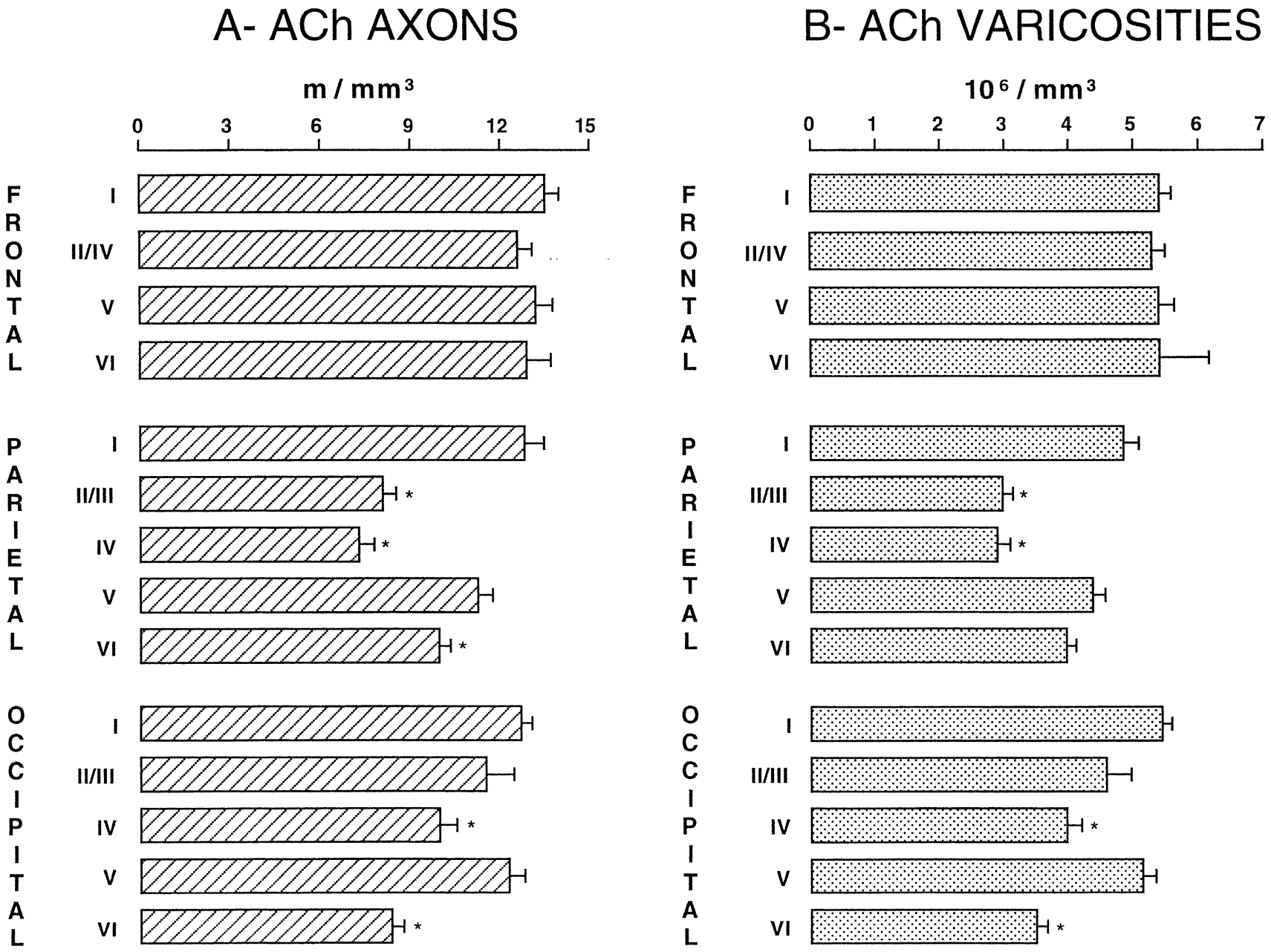
A- ACh AXONS
m / mm3
0
3
6
9
12
15
FRONTAL
I
II/IV
V
VI
PARIETAL
I
II/III
IV
V
VI
OCCIPITAL
I
II/III
IV
V
VI
B- ACh VARICOSITIES
10 6 / mm3
0
1
2
3
4
5
6
7
FRONTAL
I
II/IV
V
VI
PARIETAL
I
II/III
IV
V
VI
OCCIPITAL
I
II/III
IV
V
VI

Fig. 6. Relatively high light microscopic magnification illustrating gross morphological features of the ChAT-immunoreactive axon network in cerebral cortex (layers II-III of the parietal cortex). These varicose axon branches seemingly run in every direction. Smaller and larger varicosities may be observed on the same axonal branches (thin and thick arrows). When coursing in the plane of focus, the short and narrow axon segments between the varicosities are also seen to be immunostained. Occasional bifurcations are visible (arrowhead). X 900. Scale bar: 10 μm.

Fig. 7. Electron micrograph illustrating the ultrastructural features of cortical ACh varicosities (middle layers of the parietal cortex). The immunostained profile (center) is identified as a varicosity by its content in aggregated synaptic vesicles. No part of its plasma membrane shows any differentiation suggestive of a synaptic contact. The patchy distribution of the diffusible DAB immunoprecipitate is not to be taken as biologically significant. This ACh varicosity is juxtaposed to two dendritic branches (d), an immunonegative axonal varicosity (av), and a few small, unidentifiable profiles. X 24 000. Scale bar: 0.5 μm.

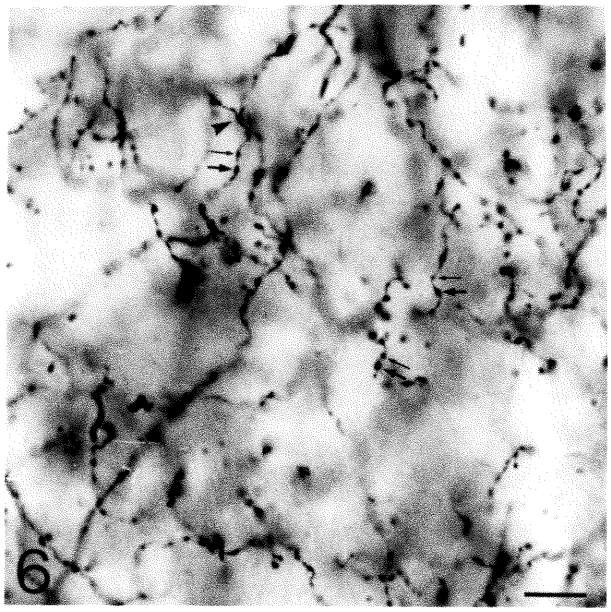
6

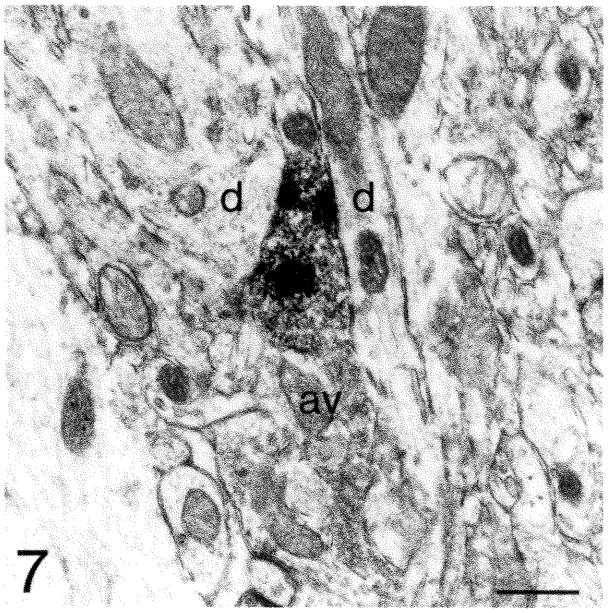
d
d
av
7

Chapitre III

THE CHOLINERGIC INNERVATION DEVELOPS EARLY AND RAPIDLY IN THE RAT CEREBRAL CORTEX : A QUANTITATIVE IMMUNOCYTOCHEMICAL STUDY

(Sous presse au journal *Neuroscience*)

En tant que premier auteur, j'ai réalisé les expériences, analysé les résultats et contribué de façon majeure à toutes les étapes de la rédaction de l'article.

Section Editor : Dr Constantino Sotelo

THE CHOLINERGIC INNERVATION DEVELOPS EARLY AND RAPIDLY IN THE RAT CEREBRAL CORTEX : A QUANTITATIVE IMMUNOCYTOCHEMICAL STUDY

N. MECHAWAR and L. DESCARRIES

Départements de pathologie et biologie cellulaire et de physiologie, and

Centre de recherche en sciences neurologiques, Faculté de médecine,

Université de Montréal, Montréal, Québec, Canada H3C 3J7

Correspondence: Laurent DESCARRIES m.d.
Département de pathologie et biologie cellulaire
Université de Montréal
CP 6128, Succursale Centre-ville
Montréal, QC, Canada H3C 3J7

tel. (514) 343-7070
fax (514) 343-5755
E-mail: laurent.descarries@umontreal.ca

LIST OF ABBREVIATIONS

ACh: acetylcholine

BSA: bovine serum albumin

ChAT: choline acetyltransferase

DAB: 3,3'-diaminobenzidine

Fr1: primary motor cortex

KPB: potassium phosphate buffer

NGF: nerve growth factor

NHS: normal horse serum

Oc1: primary visual cortex

Par1: primary somatosensory cortex

PBS: phospate buffered saline

PFA: paraformaldehyde

vAChT: vesicular acetylcholine transporter

KEYWORDS : neocortex – acetylcholine – choline acetyltransferase – axons – axon varicosities – innervation

Running title : Cholinergic innervation in developing neocortex

ABSTRACT

A recently developed method for determining the length of cholinergic axons and number of cholinergic axon varicosities (terminals) in brain sections immunostained for choline acetyltransferase was used to estimate the areal and laminar densities of the cholinergic innervation in rat frontal (motor), parietal (somatosensory) and occipital (visual) cortex at different postnatal ages. This cortical innervation showed an early beginning, a few immunostained fibers being already present in the cortical subplate at birth. In the first two postnatal weeks, it developed rapidly along three parameters: a progressive increase in the number of varicosities per unit length of axon, and a lengthening and branching of the axons. Between postnatal days 4 and 16, the number of varicosities increased steadily from 2 to 4 per 10 μm of cholinergic axon. The mean densities of cholinergic axons increased from 1.4 to 9.6, 1.7 to 9.3 and 0.7 to 7.2 m/mm^3, and the corresponding densities of varicosities from 0.4 to 3.9, 0.4 to 3.5, and 0.2 to 2.6 x $10^6/mm^3$ in the frontal, parietal and occipital areas, respectively. The rate of growth was maximal during these first two weeks, after which the laminar pattern characteristic of each area appeared to be established. Adult values were almost reached by P16 in the parietal cortex, but maturation proceeded further in the frontal and particularly in the occipital cortex.

These quantitative data on the ingrowth and maturation of the cholinergic innervation in postnatal rat cerebral cortex substantiate a role for acetylcholine in the development of this brain region and emphasize the striking growth capacity of individual cholinergic neurons.

The development of the mammalian cerebral cortex is driven by the combined influences of intrinsic and extrinsic factors. Among the latter, much attention has been devoted to ingrowing cortical afferents, and notably thalamic axons. Increasing evidence that neuromodulatory inputs also play a role in shaping cortical circuitry has been brought forward in recent years. In particular, a number of investigations have shown that monoamines have pronounced effects on the morphology and physiology of maturing cortical neurons (see Levitt et al., 1997). The neurotransmitter/modulator acetylcholine (ACh), which has long been implicated in a variety of cortical states and functions in the adult, is currently considered as a permissive factor for cortical plasticity during development (Gu and Singer, 1993; Robertson et al., 1998; Zhu and Waite, 1998).

Knowing when and how an innervation develops is obviously crucial for understanding its properties and roles in corticogenesis. Previous studies have provided detailed qualitative descriptions of the sequence of innervation by serotonin, noradrenaline and dopamine cortical afferents in the rat (Lidov and Molliver, 1982; Verney et al., 1984; Kalsbeek et al., 1988). To this day, however, the study of developing cortical ACh afferents has proven more difficult, mainly because of the lack of cholinergic markers of sufficient specificity or sensitivity. Histochemistry has revealed the presence of fibers containing acetylcholinesterase in rat cortex at different pre- and postnatal ages (Kiss and Patel, 1992; Nyakas et al., 1994; see also De Carlos et al., 1995), but the significance of these results was limited by the known expression of this degradative enzyme in non cholinergic neurons, particularly during development (Kristt and Waldman, 1982; Kutscher, 1991). Retrograde and anterograde tracing experiments indicated that a few basal forebrain axons had reached the occipital cortex at birth (Dinopoulos et al., 1989;

Calarco and Robertson, 1995), but again the cholinergic nature of these afferents could not be established. Prior immunocytochemical investigations using antibodies against choline acetyltransferase (ChAT), the synthesizing enzyme of ACh, led to the belief that the ACh innervation develops relatively late postnatally in the rat cerebral cortex, i.e. mainly from the latter part of the second week (Dori and Parnavelas, 1989; Gould et al., 1991; for review, see Semba, 1992). However, in these early studies, the available data on the ingrowth and proliferation of cortical ACh axons remained somewhat sketchy.

Owing to the availability of a highly sensitive monoclonal antibody (Cozzari et al., 1990) raised against purified rat brain ChAT, we undertook a detailed examination of the developmental sequence of the ACh innervation in the frontal, parietal and occipital cortex of postnatal rat. To document our observations with data amenable to correlation with other parameters (cholinergic and others) of cortical growth, we used a quantification method, recently developed in our laboratory (Mechawar et al., 2000a), which allows to estimate the length of ACh axons and number of ACh varicosities (terminals) per volumetric unit of tissue from ChAT-immunostained sections. Preliminary reports of this study have been published in abstract form (Mechawar and Descarries, 1998; Mechawar et al., 2000b).

EXPERIMENTAL PROCEDURES

Tissue processing. All experiments abided by the policies and guidelines of the Canadian Council on Animal Care and the regulations of the Animal Care Commitee at the Université de Montréal. All efforts were made to minimize the number of animals used and their suffering. The study was carried out on 15 male

Sprague-Dawley rats (Charles River St-Constant, Québec, Canada), purchased on the day of birth (P0) or at known postnatal ages and kept with their lactating mothers. At P0 and postnatal days P4, P8, P16 and P32, 3 rats per age were deeply anesthetized with sodium pentobarbital (80 mg/kg, i.p.), and perfused through the heart with ice-cold phosphate-buffered saline (PBS; 50 mM; pH 7.4; 5-50 ml) followed by 4% paraformaldehyde in 0.1 M sodium phosphate buffer (PFA; pH 7.4; 24° C; 100-500 ml). Immediately after, the brains were rapidly dissected out, postfixed overnight in 4% PFA at 4°C, and cut into consecutive 50 µm-thick transverse sections (Lancer vibratome). Sections were cut at anatomical levels equivalent to the stereotaxic planes A-11.2 (Fr1), A-9.2 (Par1) and A-2.7 (Oc1) of adult rat (Paxinos and Watson, 1986). Structural landmarks were chosen which were present beneath the cortical areas of interest throughout development (Paxinos et al., 1991). Thus, Fr1 was analyzed from sections immediately rostral to the appearance of the *genu corpus callosum*, Par1 from sections immediately rostral to the *globus pallidus*, and Oc1 from sections in which the medial geniculate nucleus was the widest. The sections were then processed for ChAT-immunocytochemistry or stained with cresyl violet.

ChAT-immunocytochemistry. The protocol allowed for a maximal detection of ChAT-immunostained axons in 50 µm-thick rat brain sections (Mechawar et al., 2000a; see also Umbriaco et al., 1994, 1995, and Contant et al., 1996). In brief, after a 30 min incubation in 0.3 % H_2O_2 to eliminate endogenous peroxidase activity, the sections were incubated sequentially in 1) a blocking solution of PBS containing 2% normal horse serum (NHS; Vector, Burlingame, CA), 1% bovine serum albumin (BSA; Sigma, St-Louis, MO), and 0.2% Triton X-100 (2 h); 2) the same solution containing 2 µg/ml of mouse monoclonal antibody against purified rat brain ChAT

(Cozzari et al., 1990) (overnight); and 3) a 1/200 dilution of biotinylated horse anti-mouse antibody (Vector), in KPB containing 2% NHS and 1% BSA (2 h). This was followed by the avidin-biotin complex procedure (ABC Kit, Vectastain Elite; Vector) (2 h), and the labeling was revealed with a 0.05% solution of 3,3'-diaminobenzidine (DAB; Sigma) containing 0.01% $CoCl_2$, 0.01% $NiSO_4$, 0.01% $(NH_4)_2SO_4$, to which 0.005% H_2O_2 was added (2.5 min). The immunostained sections were mounted on gelatin-coated slides. Control experiments included omission of the primary or secondary antibodies, which completely abolished the immunostaining.

Length of ChAT-immunostained axons. Measurements were made at P4, P8, P16 and P32. The length of ChAT-immunostained axons was determined as detailed previously (Mechawar et al., 2000a), using a microcomputer-based image analysis system. In brief, this system consisted of a Macintosh Quadra 950 (NIH Image software 1.61) connected to a Leitz Orthoplan microscope via a Panasonic WV-BD400 video camera. At the working magnification providing distinct light microscopic visualization of the immunostained axon network (25 X PlanApo objective lens), three steps of focusing (superficial, intermediate and deep) were required to observe the network across the full thickness of 50 µm-thick sections. However, because an equivalent proportion of the total network was detected in each plane of section (45%; Mechawar et al., 2000a), measurements were made in the superficial plane of focus only.

To this effect, 240 µm-wide vertical strips, extending from the pial surface to the bottom of layer VI, were digitized, printed and assembled as large photomontages in each area (final magnification: 645 X). The boundaries of cortical layers were determined with the aid of adjacent Nissl-stained sections, and square sampling windows, 64.5 mm in side (10 000 μm^2 of tissue), were drawn in a straight

row perpendicular to the cortical surface so as to fit a maximal number of squares (1 to 6) within each layer. At P4, the marginal zone and cortical plate were treated as a single layer. All immunostained axon trajectories within the confines of each window were then drawn by hand on transparent film. These tracings were digitized, their lines reduced to a uniform width (1 pixel) with the "skeletonize" function of the program, all closed outlines cut open by removal of 1 pixel, and their lenght measured in micrometers, based on a prior calibration of the system with a microscopic scale. The resulting values were corrected for angulation of the fibers in the sections, assuming their random orientation (x 1/cos 45; Soghomonian et al., 1987), and extrapolated to the full thickness of the sections (x 2.2). Lastly, they were converted to cubic millimeter of tissue, to provide a density of ACh axons (m/mm^3) for each layer and cortical area, and also expressed in actual length of axons (m) under 1 mm^2 of cortical surface, to account for the increasing cortical thickness with age.

Axon length measurements were thus obtained from 3 rats at each age, 1 section per cortical area in each rat, and, within each section, a tissue area ranging from 0.05, 0.05 and 0.04 mm^2 at P4 to 0.15, 0.16 and 0.10 mm^2 at P32, in the frontal, parietal and occipital cortex, respectively.

Number of ChAT-immunostained axon varicosities. The image analysis system was also used to estimate the average number of axon varicosities per unit length of ChAT-immunostained axons in each layer and cortical area at the different ages. For this purpose, 10 immunostained axon segments running for at least 20 μm in the plane of focus were drawn as above from every layer in each rat, at a final magnification of 1 000 X (total n = 1 470). The axon varicosities, defined as axon dilations > 0.5 μm in transverse diameter, were counted on prints of these axons,

the length of which was then measured as already described with the image analyzer. This diameter for cortical ACh axon varicosities was consistent with earlier electron microscopic measurements in the developing (Mechawar and Descarries, 2001) and adult rat parietal cortex (Umbriaco et al., 1994). The latter study had also established that inter-varicose segments belonging to these axons average 0.2 μm in transverse diameter.

Data analysis. For each area, the number of varicosities per μm of ACh axon was expressed as as an interlaminar mean ± SEM (n = 3 at each age, except for P60: n = 5; Fig. 5). Knowing the actual length of ChAT-immunostained axons and the average number of axon varicosities per unit length (N/μm), laminar and regional densities of ACh innervation could be calculated in number of axon varicosities per cubic mm of tissue ($10^6/mm^3$), or actual number under 1 mm^2 of cortical surface (Figs. 6-8). The P60 data, used as end points, were from a previous publication (Mechawar et al., 2000a). Statistical comparisons between the values at different ages and the corresponding adult values were made with a Kruskal-Wallis followed by Wilcoxon-Mann-Whitney test. Differences were considered significant when $p < 0.05$.

RESULTS

Figures 1-3 provide overviews of the ChAT-immunostained innervation in the frontal, parietal and occipital cortex at the different postnatal ages examined. Figure 4 illustrates the development of this innervation at a magnification comparable to that used for its quantification, within a different layer of each area. At birth (P0), scattered growth cone-tipped ChAT-immunostained axons were

already present in every area (not illustrated; but see Fig. 4A,E). These ACh afferents appeared to reach the frontal and parietal cortex via the anterior cingulate gyrus and, to a lesser extent, the external capsule. Confined to the subplate, they were seen in greater number in the frontal and parietal area than the occipital. Most of these fibers were unbranched and showed a few, irregularly spaced, varicosities. At P4, their number had more than doubled, many infiltrated the upper cortical layers (marginal zone and cortical plate), and their varicosities were more numerous. The fibers were still noticeably less numerous in the occipital than the frontal and the parietal cortex. At this age, a few faintly stained interneurons were visible in all three areas, and some were also present that were darker and more numerous in the upper layers of the anterior cingulate cortex. At P8, all cortical layers in each area displayed many strongly immunoreactive interneurons and an intricate network of varicose axons. At P16, the laminar pattern of ACh innervation was adult-like in each area, but continued to increase in density to reach adult density at P32 or P60. At none of the ages examined were there any indications of a barrel pattern in layer IV of the primary somatosensory area.

In all three areas and cortical layers, the number of varicosities per micrometer of ChAT-immunostained axon increased sharply between P4 and P16 and stabilized thereafter to its adult value (Fig. 5). At the onset of this period, it corresponded to 2.2-2.5 varicosities per 10 μm of axon. Four days later (P8), it had increased to 3.0-3.4 per 10 μm, in parallel with the density of axons. It then plateaued to its adult ratio (4.0) at P16, while the laminar density of axons had almost reached its adult value in the parietal area, but not in the frontal and the occipital areas (see below). Although the length of ACh axons underwent a similar increase in all three areas during the first two postnatal weeks (Table 1), the early rostro-caudal gradient of

innervation was evidenced by a mean regional density of varicosities at P4 that was twice as high in the frontal (0.35 x 10^6/mm^3) and parietal cortex (0.37 x 10^6/mm^3) than the occipital (0.16 x 10^6/mm^3) (see I-VI in Figs. 6-8). At P8, when ACh axons had proliferated in all layers of each area, this gradient was no longer found, with virtually identical mean densities in all three areas (1.4, 1.6 and 1.5 x 10^6/mm^3). During the period of fastest growth, between P4 and P16, the mean density of axons increased almost seven-fold in the frontal cortex (1.4 to 9.6 m/mm^3), more than five-fold in the parietal cortex (1.7 to 9.3 m/mm^3), and ten-fold in the occipital cortex (0.7 to 7.2 m/mm^3). This was reflected by proportional increases in the regional densities of varicosities, which went from 0.4 to 3.9, 0.4 to 3.5, and 0.2 to 2.6 x 10^6/mm^3 in the frontal, parietal and occipital areas, respectively (Figs. 6-8). The values under 1 mm^2, which took into account the increasing thickness of the cortex (Figs. 1-3), displayed even greater increases (Table 1 and Figs. 6-8), with respective axon lengths and numbers of varicosities from 1.4 to 15.6 m and 0.4 to 6.4 x 10^6 in the frontal cortex, 1.9 to 17.8 m and 0.4 to 6.6 x 10^6 in the parietal cortex, and 0.4 to 8.5 m and 0.1 to 3.1 x 10^6 in the occipital cortex (Figs. 6-8). Whereas nearly adult values were reached by P16 in the parietal cortex (Fig. 7), maturation proceeded further in the frontal and particularly in the occipital cortex. In the frontal cortex, the mean density of varicosities increased by 34% over P16 to reach adult value by P32 (Fig. 6). In the occipital cortex, the increase over P16 was 49% at P32 and 71% in the adult (P60). At no time were there any indications of an overproduction or elimination of ACh axons or varicosities. As previously reported (Mechawar et al., 2000a), the regional density attained in the adult frontal cortex was significantly higher than in the parietal and occipital cortex.

In all three regions, layer I received the densest innervation throughout development and into adulthood, even though, because of its reduced thickness, it contained the lowest amount of ACh fibers and varicosities under 1 mm^2. The greatest amount of ACh innervation under 1 mm^2 was that of layer V at all ages in each region. Within each area, the laminar increases in density of axons and axon varicosities displayed similar temporal profiles, i.e., a comparable rate of growth (Table 1 and Figs. 6-8).

DISCUSSION

The validity of the quantitative ChAT-immunocytochemical approach for determining ACh axon length and number of axon varicosities in cerebral cortex has been established and discussed in detail elsewhere (Mechawar et al., 2000a). The present study in postnatal rat revealed unexpected features of the developing neocortical ACh innervation that may be critical to understanding its properties and functions. In the frontal, parietal and occipital areas, this innervation was shown to develop early and rapidly, according to three major parameters of growth: an increase in the number of varicosities per unit length of axon and a lengthening and branching of the axons. The rate of growth was maximal and parallel for all parameters during the first two weeks, after which the number of varicosities per unit length of axon remained constant, the characteristic laminar pattern of each region was established, but maturation proceeded further at a different pace in each region. As expressed in areal and laminar densities of axons and number of axon varicosities, the data substantiated a role for ACh in the developing cortex and emphasized the striking growth capacity of individual ACh neurons innervating this brain region.

In all three areas, the first two postnatal weeks were clearly the period of maximal increase in terms of regional and laminar density of ACh innervation. All layers in each cortical area conformed to this temporal sequence, during which the number of varicosities per unit length of ACh axon increased steadily, a phenomenon previously noticed in the case of developing ACh axons in cat striate cortex (Stichel and Singer, 1987), and other ingrowing cortical afferents in the rat (Lidov and Molliver, 1982; Kalsbeek et al., 1988). The sequential analysis of our quantitative data demonstrated that this increase occurred in parallel with the rapid proliferation of axon branches in all cortical layers and areas. The average ratio of 4 varicosities per 10 μm of ACh axon reached after two weeks remained constant afterward (Mechawar et al., 2000a), and therefore appeared to be an intrinsic feature of these neurons, as also measured in the hippocampus of adult rat and mouse (N. Aznavour, N. Mechawar, and L. Descarries, unpublished observations). This constancy also implied that differences in density of ACh innervation later observed between layers of a given area and/or between areas mainly reflected a lesser or greater lengthening and branching of ACh axons, and was thus presumably regulated by extrinsic, local factors (e.g., Castellani and Bolz, 1997; Dantzker and Callaway, 1998).

The development of the cortical ACh innervation did not seem to involve any overproduction/elimination of axons, a process clearly demonstrated for certain populations of developing corticofugal (Stanfield et al., 1982) and cortico-cortical (Innocenti, 1981, 1995) projections. Establishment of the characteristic laminar patterns displayed by this ACh innervation was likely to involve a differential distribution of trophic molecules. Unfortunately, little is known about the role of such molecules in the formation of transmitter-specific innervations in the cerebral

cortex (Sanes and Yamagata, 1999). NGF could be a candidate of choice for ACh neurons, since, in basal forebrain, these neurons are known to express high- and low-affinity NGF receptors during development and into adulthood (Koh and Loy, 1989; Li et al., 1995). However, during the first two postnatal weeks, NGF expression in rat neocortex appears mostly restricted to cells in the cingulate and retrosplenial areas and evolves along a rostro-caudal gradient (Conner and Varon, 1997). This suggests that NGF is more likely to act as a chemoattractant for ingrowing ACh axons than as a local factor involved in lamina-specific axonal branching.

The earlier establishment of an adult density of ACh innervation in the parietal cortex, or its protracted maturation in the frontal and especially the occipital cortex, had little to do with the densities to be reached, since the frontal attains a denser ACh innervation than the occipital cortex in the adult (Mechawar et al., 2000a). It might possibly relate with the degree of neuronal activity in the respective areas, in view of the earlier development of whisking and motor than visually-driven behaviors in rodents. Also noteworthy in this regard was the particularly rapid and extensive ACh innervation of layer I, which, in all three areas, was the most densely innervated throughout development and into adulthood. Interestingly, layer I has been shown to be the first generated (Marin-Padilla, 1998) and to develop synaptic connectivity in the rat cerebral cortex (Balslev et al., 1996). As for the abundant innervation of layer V in all regions, it has been previously correlated with a presumed role of ACh in modulating cortical output as well as extrinsic and intrinsic cortical input (Mechawar et al., 2000a).

The above-described sequence of cholinergic innervation could account for previous measures of ACh function in the developing rat cerebral cortex. In the

frontal and parietal cortex, tissue ChAT activity has been shown to be low at birth and to rise progressively to adult levels by the end of the first postnatal month (Coyle and Yamamura, 1976; Thal et al., 1991; Zahalka et al., 1993). A similar temporal profile of ChAT activity has been demonstrated for all layers of the occipital cortex by McDonald et al. (1987). It has also been shown that cortical levels of high-affinity choline uptake increase in parallel with ChAT activity (Johnston, 1988; Happe and Murrin, 1992; but see Zahalka et al., 1993). Other cholinergic parameters appear more precocious, as if transiently independent of the basalo-cortical ACh innervation. In particular, concentration of ACh (Coyle and Yamamura, 1976; see also Pedata et al., 1983) and binding for the vesicular acetylcholine transporter (vAChT; Aubert et al., 1996), which reach adult levels between the second and third postnatal weeks, are already measured at half these values in the newborn cortex. It remains to be determined whether this precocious capacity for ACh storage in cortex reflects a transient expression of vAChT by non-cholinergic cells, as previously demonstrated for the serotonin plasma membrane and the vesicular monoamine transporters in the developing cerebral cortex (Lebrand et al., 1996). In the case of ACh itself, its particularly high concentration in the newborn cortex might be a consequence of the absence of a fully developed blood-brain barrier (e.g., Loizou, 1970; Dupin et al., 1976; Lidow, 1998). This barrier, which is immature well into postnatal life in rodents (Lossinsky et al., 1986), would normally be impermeable to ACh synthesized in the blood, peripheral organs, or placenta (for review of non-neuronal ACh, see Wessler et al., 1998). Such a permeability could also account for the existence of a variety of nicotinic receptors or mRNA for nicotinic subunits throughout rat cerebral cortex as early as mid- to late embryonic ages (Ostermann et al., 1995; Zoli et al., 1995; Aubert et al., 1996;

Zhang et al., 1998). The gradual appearance and patterning of muscarinic receptors in postnatal cortex, on the other hand, would seem more dependent on the presence of ACh axons (Aubert et al., 1996).

ACh has been proposed to act as an enhancer of functional plasticity during the early postnatal period, (Bear and Singer, 1986; Gu and Singer, 1993; Zhu and Waite, 1998), and might be critical for the subsequent cytodifferentiation and refinement of cortical connectivity (Höhmann et al., 1988, 1991a, 1991b; Roerig et al., 1997; Robertson et al., 1998) and/or shaping of cortical maps (Höhmann et al., 1995; Broide et al., 1996, Aramakis et al., 2000). The recent demonstration that ACh mediates the propagation of slow waves of electrical activity in the developing neocortex might be relevant in this respect. This newly observed phenomenon, restricted to the first postnatal week, has been proposed to be involved in cortical column formation (Peinado, 2000).

While the present quantitative data substantiate a role for ACh in the developing cortex, they also emphasize the striking growth capacity of ACh neurons innervating this brain region. It has been estimated that 14 000 – 18 000 nucleus basalis ACh neurons project to adult rat cerebral cortex (Rye et al., 1984; Gritti et al., 1993), while the mean length of their individual axonal arborization is in the order of 0.5 meter.* Based on the proportion of cortical ACh innervation which is installed within the first two weeks, and leaving aside the 20-30% fraction which presumably arises from interneurons (Johnston et al., 1981; Eckenstein and Baughman, 1987), it can now be inferred that, during the first two weeks after birth, each basalo-cortical ACh neuron produces daily an average of 2 cm of axon bearing 9 000 varicosities, i.e., more than 1 mm of axon and 400 varicosities per hour. These figures will need to be taken into account in future investigations of

the biophysical and metabolic requirements of such a rapid and extensive neuronal growth.

AKNOWLEDGEMENTS

This study was supported by grant MT-3544 from the MRC of Canada. N. M. is the recipient of a doctoral studentship from the MRC of Canada. The authors are grateful to Costantino Cozzari and Boyd K. Hartman for their generous gift of ChAT antibody. They also thank Nicolas Aznavour for valuable help in the preparation of Fig. 4, and Jean Léveillé and Gaston Lambert for photographic work.

* This value will correct a previous estimate (Mechawar et al., 2000a), where the length of ACh axons extrapolated for whole cortex (both hemispheres) had been mistakenly divided by the number of ACh cell bodies in one nucleus basalis only.

REFERENCES

Aramakis, V. B., Hsieh, C. Y., Leslie, F. M., Metherate, R., 2000. A critical period for nicotine-induced disruption of synaptic development in rat auditory cortex. J. Neurosci. 20, 6106-6116.

Aubert, I., Cécyre, D., Gauthier, S., Quirion, R., 1996. Comparative ontogenic profile of cholinergic markers, including nicotinic and muscarinic receptors, in the rat brain. J. Comp. Neurol. 369, 31-55.

Balslev, Y., Saunders, N. R., Møllgard, K., 1996. Synaptogenesis in the neocortical anlage and early developing neocortex of rat embryos. Acta Anat. 156, 2-10.

Bear, M. F., Singer, W., 1986. Modulation of visual cortical plasticity by acetylcholine and noradrenaline. Nature 320, 172-176.

Broide, R. S., Robertson, R. T., Leslie, F. M., 1996. Regulation of α_7 nicotinic acetylcholine receptors in the developing rat somatosensory cortex by thalamocortical afferents. J. Neurosci. 16, 2956-2971.

Calarco, C. A., Robertson, R. T., 1995. Development of basal forebrain projections to visual cortex: DiI studies in the rat. J. Comp. Neurol. 354, 608-626.

Castellani, V., Bolz, J., 1997. Membrane-associated molecules regulate the formation of layer-specific cortical circuits. Proc. Natl. Acad. Sci. USA 94, 7030-7035.

Conner, J. M., Varon, S., 1997. Developmental profile of NGF immunoreactivity in the rat brain: a possible role of NGF in the establishment of cholinergic terminal fields in the hippocampus and cortex. Dev. Brain Res. 101, 67-79.

Contant, C., Umbriaco, D., Garcia, S., Watkins, K. C., Descarries, L., 1996. Ultrastructural characterization of the acetylcholine innervation in adult rat neostriatum. Neuroscience 71, 937-947.

Coyle, J. T., Yamamura, H. I., 1976. Neurochemical aspects of the ontogenesis of cholinergic neurons in the rat brain. Brain Res. 118, 429-440.

Cozzari, C., Howard, J., Hartman, B., 1990. Analysis of epitopes on choline acetyltransferase (ChAT) using monoclonal antibodies (Mabs). Soc. Neurosci. Abstr. 16, 200.

Dantzker, J. L., Callaway, E. M., 1998. The development of local, layer-specific visual cortical axons in the absence of extrinsic influences and intrinsic activity. J. Neurosci. 18, 4145-4154.

De Carlos, J. A., Schlaggar, B. L., O'Leary, D. D. M., 1995. Development of acetylcholinesterase-positive thalamic and basal forebrain afferents to embryonic rat neocortex. Exp. Brain Res. 104, 385-401.

Dinopoulos, A., Eadie, L. A., Dori, I., Parnavelas, J. G. 1989. The development of basal forebrain projections to the rat visual cortex. Exp. Brain Res. 76, 563-571.

Dori, I., Parnavelas, J. G., 1989. The cholinergic innervation of the rat cerebral cortex shows two distinct phases in development. Exp. Brain Res, 76, 417-423.

Dupin, J. C., Descarries, L., De Champlain, J., 1976. Radioautographic visualization of central catecholamine neurons in newborn rat after intravenous administration of tritiated norepinephrine. Brain Res. 103, 588-596.

Eckenstein, F., Baughman, R. W., 1987. Cholinergic innervation in cerebral cortex. In: Jones, E. G., Peters, A. (Eds.), Cerebral Cortex, vol. 6. Plenum Press, New York, pp. 29-160.

Gould, E., Woolf, N. J., Butcher, L. L., 1991. Postnatal development of cholinergic neurons in the rat: I. Forebrain. Brain Res. Bull. 27, 767-789.

Gritti, I., Mainville, L., Jones, B. E., 1993. Codistribution of GABA- with acetylcholine-synthesizing neurons in the basal forebrain of the rat. J. Comp. Neurol. 329, 438-457.

Gu, Q., Singer, W., 1993. Effects of intracortical infusion of anticholinergic drugs on neuronal plasticity in kitten striate cortex. Eur. J. Neurosci. 5, 475-485.

Happe, H. K., Murrin, L. C., 1992. Development of high-affinity choline transport sites in rat forebrain: a quantitative autoradiography study with [^{3}H]hemicholinium-3. J. Comp. Neurol. 321, 591-611.

Höhmann, C. F., Brooks, A. R., Coyle, J. T., 1988. Neonatal lesions of the basal forebrain cholinergic neurons result in abnormal cortical development. Dev. Brain Res. 42, 253-264.

Höhmann, C. F., Kwiterovich, K. K., Oster-Granite, M. L., Coyle, J. T., 1991a. Newborn basal forebrain lesions disrupt cortical cytodifferentiation as visualized by rapid golgi staining. Cereb. Cortex 1, 143-157.

Höhmann, C. F., Wilson, W., Coyle, J. T. 1991b. Efferent and afferent connections of mouse sensory-motor cortex following cholinergic deafferentation at birth. Cereb. Cortex 1, 158-172.

Höhmann, C. F., Potter, E. D., Levey, A. I., 1995. Development of muscarinic receptor subtypes in the forebrain of the mouse. J. Comp. Neurol. 358, 88-101.

Innocenti, G. M., 1981. Growth and reshaping of axons in the establishment of visual callosal connections. Science 212, 824-827.

Innocenti, G. M., 1995. Exuberant development of connections, and its possible permissive role in cortical evolution. Trends Neurosci. 18, 397-402.

Johnston, M. V., 1988. Biochemistry of neurotransmitters in cortical development. In: Jones, E. G., Peters, A. (Eds.), Cerebral Cortex, vol. 7. Plenum Press, New York, pp. 211-236.

Johnston, M. V., McKinney, M., Coyle, J. T., 1981. Neocortical cholinergic innervation: a description of extrinsic and intrinsic components in the rat. Exp. Brain Res. 43, 159-172.

Kalsbeek, A., Voorn, P., Buijs, R. M., Uylings, H. B. M., 1988. Development of the dopaminergic innervation in the prefrontal cortex of the rat. J. Comp. Neurol. 269, 58-72.

Kiss, J., Patel, A. J., 1992. Development of the cholinergic fibres innervating the cerebral cortex of the rat. Int. J. Devl. Neuroscience 10, 153-170.

Koh, S., Loy, R., 1989. Localization and development of nerve growth factor-sensitive rat basal forebrain neurons and their afferent projections to hippocampus and neocortex. J. Neurosci. 9, 2999-3018.

Krisst, D. A., Waldman, J. V., 1982. Developmental reorganization of acetylcholinesterase-rich inputs to somatosensory cortex of the mouse. Anat. Embryol. 164, 331-342.

Kutscher, C. L., 1991 Development of transient acetylcholinesterase staining in cells and permanent staining in fibers in cortex of rat brain. Brain Res. Bull. 27, 641-649.

Lebrand, C., Cases, O., Adelbrecht, C., Doye, A., Alvarez, C., El Mestikawy, S., Seif, I., Gaspar, P., 1996. Transient uptake and storage of serotonin in developing thalamic neurons. Neuron 17, 823-835.

Levitt, P., Harvey, J. A., Friedman, E., Simansky, K., Murphy, E. H., 1997. New evidence for neurotransmitter influences on brain development. Trends Neurosci. 20, 269-274.

Li, Y., Holtzman, D. M., Kromer, L. F., Kaplan, D. R., Chua-Couzens, J., Clary, D. O., Knüsel, B., Mobley, W. C., 1995. Regulation of TrkA and ChAT expression in developing rat basal forebrain: evidence that both exogenous and endogenous NGF regulate differentiation of cholinergic neurons. J. Neurosci. 15, 2888-2905.

Lidov, H. G. W., Molliver, M. E., 1982. An immunohistochemical study of serotonin neuron development in the rat: ascending pathways and terminal fields. Brain Res. Bull. 8, 389-430.

Lidow, M. S., 1998. Cocaine abuse and corticogenesis. Trends Neurosci. 21, 19-20.

Loizou, L. A., 1970. Uptake of monoamines into central neurons and the blood-brain barrier in infant rats. Brit. J. Pharmacol. 40, 800-813.

Lossinsky, A. S., Vorbrodt, A. W., Wisniewski, H. M., 1986. Characterization of endothelial cell transport in the developing mouse blood-brain barrier. Dev. Neurosci. 8, 61-75.

Marin-Padilla, M., 1998. Cajal-Retzius cells and the development of the neocortex. Trends Neurosci. 21, 64-71.

McDonald, J. K., Speciale, S. G., Parnavelas, J. G., 1987. The laminar distribution of glutamate decarboxylase and choline acetyltransferase in the adult and developing visual cortex of the rat. Neuroscience 21, 825-832.

Mechawar, N., Descarries, L., 1998. Early postnatal development of the cholinergic innervation in the rat cerebral cortex. Soc. Neurosci. Abstr. 24, 1338.

Mechawar, N., Descarries, L., 2001. Ultrastructural features of cholinergic axon varicosities in the developing parietal cortex of rat. Soc. Neurosci. Abstr. 27, in press.

Mechawar, N., Cozzari, C., Descarries, L., 2000a. Cholinergic innervation in adult rat cerebral cortex: a quantitative immunocytochemical description. J. Comp. Neurol. 428, 305-318.

Mechawar, N., Kolta, A., Descarries, L., 2000b. Postnatal development of the cholinergic innervation in rat neocortex: a quantitative immunocytochemical study. Soc. Neurosci. Abstr. 26, 609.

Nyakas, C., Buwalda, B., Kramers, R. J. K., Traber, J., Luiten, P. G. M., 1994. Postnatal development of hippocampal and neocortical cholinergic and serotonergic innervation in rat: effects of nitrite-induced prenatal hypoxia and nimodipine treatment. Neuroscience 59, 541-559.

Ostermann, C.-H., Grunwald, J., Wevers, A., Lorke, D. E., Reinhardt, S., Maelicke, A., Schröder, H., 1995. Cellular expression of α4 subunit mRNA of the nicotinic acetylcholine receptor in the developing rat telencephalon. Neurosci. Lett. 192, 21-24.

Paxinos, G., Watson, C., 1986. The Rat Brain in Stereotaxic Coordinates. 2nd ed. Academic Press, Sydney.

Paxinos, G., Törk, I., Tecott, L. H., Valentino, K. L., 1991. Atlas of the Developing Rat Brain. Academic Press, San Diego, CA.

Pedata, F., Slavikova, J., Kotas, A., Pepeu, G., 1983. Acetylcholine release from rat cortical slices during postnatal development and aging. Neurobiol. Aging 4, 31-35.

Peinado, A., 2000. Traveling slow waves of neural activity: a novel form of network activity in developing neocortex. J. Neurosci. 20, RC54 (1-6).

Robertson, R. T., Gallardo, K. A., Claytor, K. J., Ha, D. H., Ku, K.-H., Yu, B. P., Lauterborn, J. C., Wiley, R. G., Yu, J., Gall, C. M., Leslie, F. M., 1998. Neonatal treatment with 192 IgG-saporin produces long-term forebrain cholinergic deficits and reduces dendritic branching and spine density of neocortical pyramidal neurons. Cereb. Cortex 8, 142-155.

Roerig, B., Nelson, D. A., Katz, L. C., 1997. Fast synaptic signaling by nicotinic acetylcholine and serotonin 5-HT_3 receptors in developing visual cortex. J. Neurosci. 17, 8353-8362.

Rye, D. B., Wainer, B. H., Mesulam, M.-M., Mufson, E. J., Saper, C. B., 1984. Cortical projections arising from the basal forebrain : a study of cholinergic and noncholinergic components employing combined retrograde tracing and immunohistochemical localization of choline acetyltransferase. Neuroscience 13, 627-643.

Sanes, J. R., Yamagata, M., 1999. Formation of lamina-specific synaptic connections. Curr. Op. Neurobiol. 9, 79-87.

Semba, K., 1992. Development of central cholinergic neurons. In: Björklund, A., Hökfelt, T., Tohyama, M. (Eds.), Handbook of Chemical Neuroanatomy, vol 10. Elsevier, Amsterdam, pp. 33-62.

Soghomonian, J.-J., Doucet, G., Descarries, L., 1987. Serotonin innervation in adult rat neostriatum: I. Quantified regional distribution. Brain Res. 425, 85-100.

Stanfield, B. B., O'Leary, D. D. M., Fricks, C., 1982. Selective collateral elimination in early postnatal development restricts cortical distribution of pyramidal tract axons. Nature 298, 371-373.

Stichel, C. C., Singer, W., 1987. Quantitative analysis of the choline acetyltransferase-immunoreactive axonal network in the cat primary visual cortex: II. Pre- and postnatal development. J. Comp. Neurol. 258, 99-111.

Thal, L. J., Gilbertson, E., Armstrong, D. M., Gage, F. H., 1991. Development of the basal forebrain cholinergic system: phenotype expression prior to target innervation. Neurobiol. Aging 13, 67-72.

Umbriaco, D., Watkins, K. C., Descarries, L., Cozzari, C., Hartman, B. K., 1994. Ultrastructural and morphometric features of the acetylcholine innervation in adult rat parietal cortex: an electron microscopic study in serial sections. J. Comp. Neurol. 348, 351-373.

Umbriaco, D., Garcia, S., Beaulieu, C., Descarries, L., 1995. Relational features of acetylcholine, noradrenaline, serotonin and GABA axon terminals in the stratum radiatum of adult hippocampus (CA1). Hippocampus 5, 605-610.

Verney, C., Berger, B., Baulac, M., Helle, K. B., Alvarez, C., 1984. Dopamine-β-hydroxylase-like immunoreactivity in the fetal cerebral cortex of the rat: Noradrenergic ascending pathwaya and terminal fields. Int. J. Dev. Neurosci. 2, 491-503.

Wessler, I., Kirkpatrick, C. J., Racké, K., 1998. Non-neuronal acetylcholine, a locally acting molecule, widely distributed in biological systems: expression and function in humans. Pharmacol. Ther. 77, 59-79.

Zahalka, E. A., Seidler, F. J., Lappi, S. E., Yanai, J., Slotkin, T. A., 1993. Differential development of cholinergic nerve terminal markers in rat brain regions: implications for nerve terminal density, impulse activity and specific gene expression. Brain Res. 601, 221-229.

Zhang, X., Liu, C., Miao, H., Gong, Z.-H., Nordberg, A., 1998. Postnatal changes of nicotinic acetylcholine receptor α2, α3, α4, α7 and β2 subunits genes expression in rat brain. Int. J. Devl. Neuroscience 6, 507-518.

Zhu, X. O., Waite, P. M. E., 1998. Cholinergic depletion reduces plasticity of barrel field cortex. Cereb. Cortex 8, 63-72.

Zoli, M., Le Novère, Hill Jr., J. A., Changeux, J.-P., 1995. Developmental regulation of nicotinic ACh receptor subunit mRNAs in the central and peripheral nervous system. J. Neurosci. 15, 1912-1939.

Table 1: LENGTH OF ACETYLCHOLINE AXONS IN DEVELOPING NEOCORTEX

		Frontal cortex		Parietal cortex		Occipital cortex	
Age	**Layer**	**Density** (m/mm^3)	**Length under 1 mm^2** (m)	**Density** (m/mm^3)	**Length under 1 mm^2** (m)	**Density** (m/mm^3)	**Length under 1 mm^2** (m)
P4	**MZ**	1.1	0.1	1.4	0.1	0.6	0.0
	CP	1.1	0.2	1.4	0.3	0.6	0.1
	V	1.4	0.5	1.3	0.4	0.7	0.1
	VI	1.6	0.6	2.3	1.1	0.8	0.2
		m = 1.4	**t = 1.4**	**m = 1.7**	**t = 1.9**	**m = 0.7**	**t = 0.4**
P8	**I**	5.6	0.4	8.1	0.7	6.2	0.4
	II/IV	3.4	0.8	3.3	1.0	3.7	0.6
	V	3.9	2.2	4.7	2.5	5.0	1.1
	VI	3.6	1.8	4.7	2.5	3.1	0.8
		m = 4.1	**t = 5.2**	**m = 5.2**	**t = 6.7**	**m = 4.5**	**t = 2.9**
P16	**I**	11.8	1.3	11.8	0.9	8.0	0.9
	II/III	8.0	2.8	7.0	2.0	6.0	0.8
	IV	-	-	8.2	2.1	6.0	0.8
	V	9.0	5.5	10.2	6.9	8.3	3.8
	VI	9.4	6.0	9.3	5.9	7.7	2.2
		m = 9.6	**t = 15.6**	**m = 9.3**	**t = 17.8**	**m = 7.2**	**t = 8.5**

Table 1 (continued)

		Frontal cortex		Parietal cortex		Occipital cortex	
Age	**Layer**	**Density**	**Length under 1 mm²**	**Density**	**Length under 1 mm²**	**Density**	**Length under 1 mm²**
		(m/mm³)	(m)	(m/mm³)	(m)	(m/mm³)	(m)
P32	**I**	13.9	2.0	12.6	1.8	12.1	1.3
	II/III	12.8	6.5	9.0	3.1	9.6	1.8
	IV	-	-	7.2	1.7	10.2	3.0
	V	13.3	10.1	11.2	7.2	11.6	5.4
	VI	12.3	8.0	10.0	6.1	8.0	2.9
		m = 13.1	**t = 26.6**	**m = 10.0**	**t = 19.9**	**m = 10.3**	**t = 14.4**
P60	**I**	13.5	1.9	12.8	1.8	12.7	1.4
	II/III	12.6	6.4	8.1	2.8	11.5	2.2
	IV	-	-	7.3	1.8	10.0	3.0
	V	13.2	10.0	11.2	7.2	12.3	5.6
	VI	12.9	8.4	10.0	6.1	8.4	3.1
		m = 13.0	**t = 26.7**	**m = 9.9**	**t = 19.7**	**m = 11.0**	**t = 15.3**

Mean values from 3 rats per age, except for the adult values (P60), from Mechawar et al., (2000a), which were from 5 rats. See Experimental Procedures for sampling technique and treatment of data. These length measurements of ChAT-immunostained axons are expressed as densities (m/mm³) or actual length (m) under 1 mm² of cortical surface. The corresponding laminar and areal densities and numbers of axon varicosities are graphically represented in Figs. 6-8. Interlaminar means (**m**) and totals (**t**), in bold characters, are for the whole cortical thickness.

Figs. 1-3. Low power micrographs illustrating the regional and laminar distribution of ChAT-immunostained fibers at P0 and different postnatal ages (P4, P8, P16, P32), as observed in transverse sections from the three neocortical areas investigated: frontal, primary motor, Fr1 (Fig. 1); parietal, primary somatosensory, Par1 (Fig. 2); occipital, primary visual, Oc1 (Fig. 3). In each area, scattered growth cone-tipped ChAT-immunopositive axons are visible in the subplate (SP) at birth. At P4, an increased number of immunostained axons is present, some of which pervade the cortical plate (CP) and marginal zone (MZ). A few faintly stained interneurons are also seen at this age in all three areas. At P8, numerous interneurons are strongly immunoreactive, and the varicose ACh axons form an intricate network in every cortical layer. The mature laminar pattern of ACh innervation is established at P16 in all areas, but increases further in density to its adult-like appearance at P32.

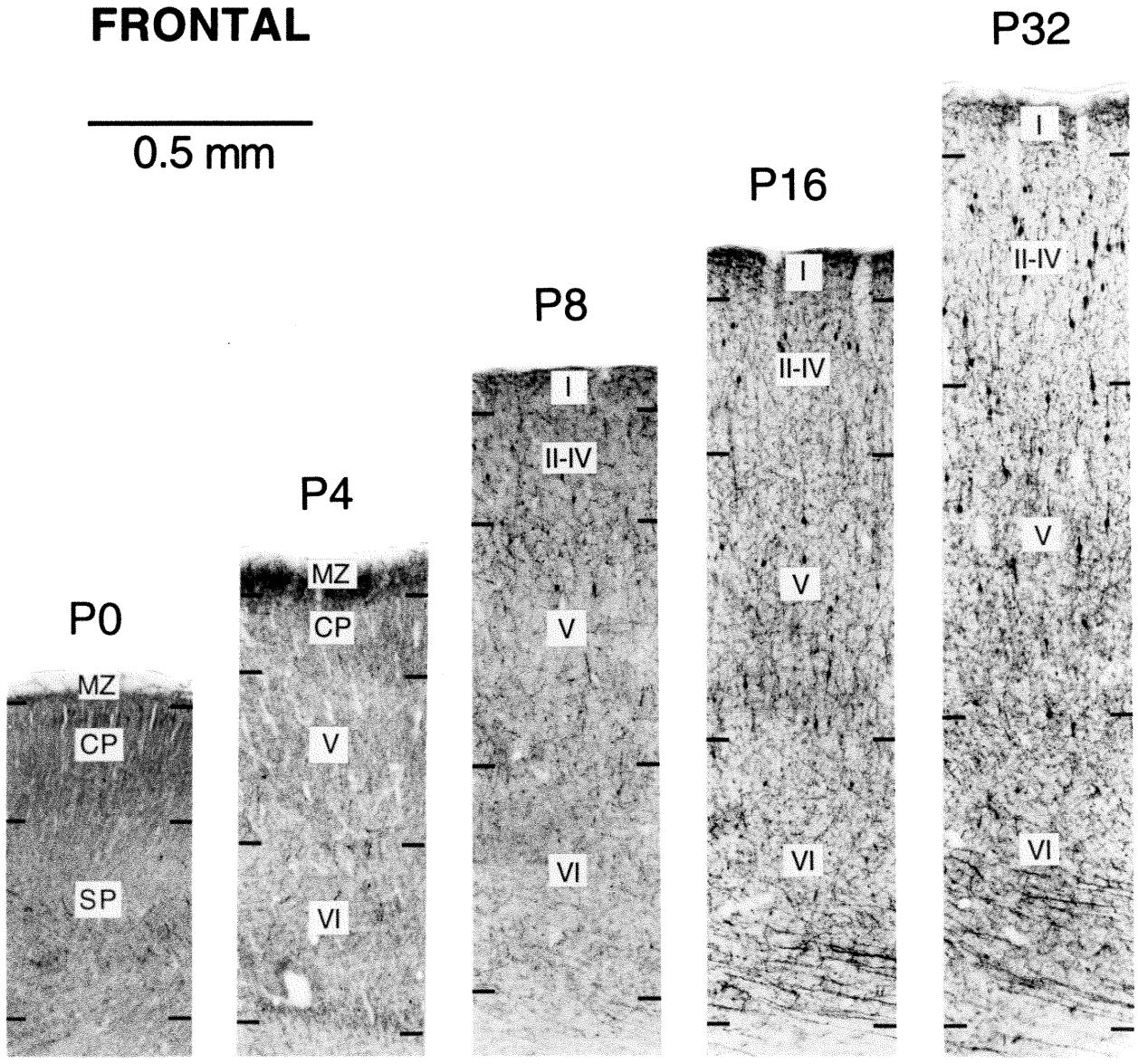
FRONTAL
0.5 mm
P0
MZ
CP
SP
P4
MZ
CP
V
VI
P8
I
II-IV
V
VI
P16
I
II-IV
V
VI
P32
I
II-IV
V
VI

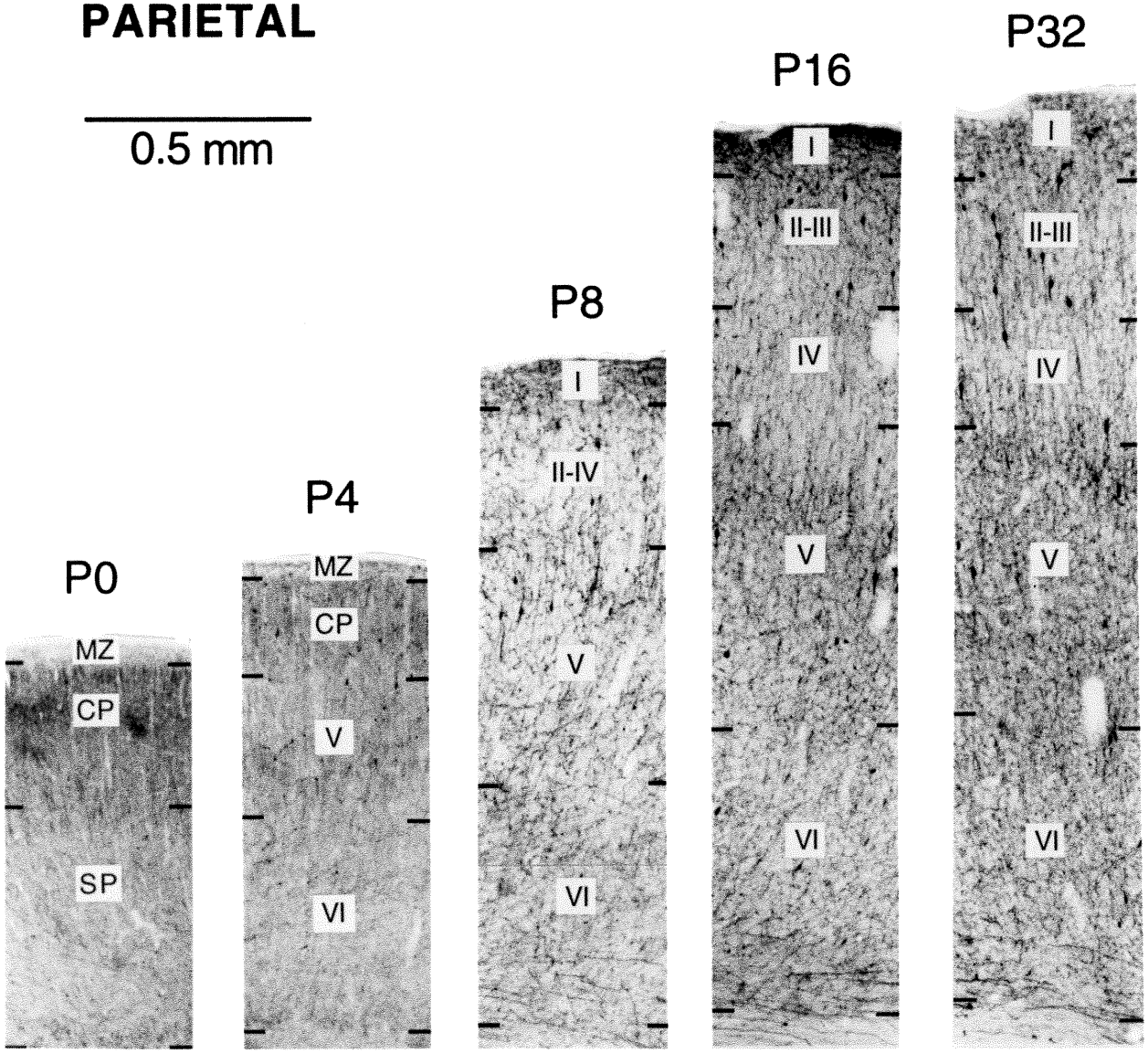
PARIETAL
0.5 mm
P0
MZ
CP
SP
P4
MZ
CP
V
VI
P8
I
II-IV
V
VI
P16
I
II-III
IV
V
VI
P32
I
II-III
IV
V
VI

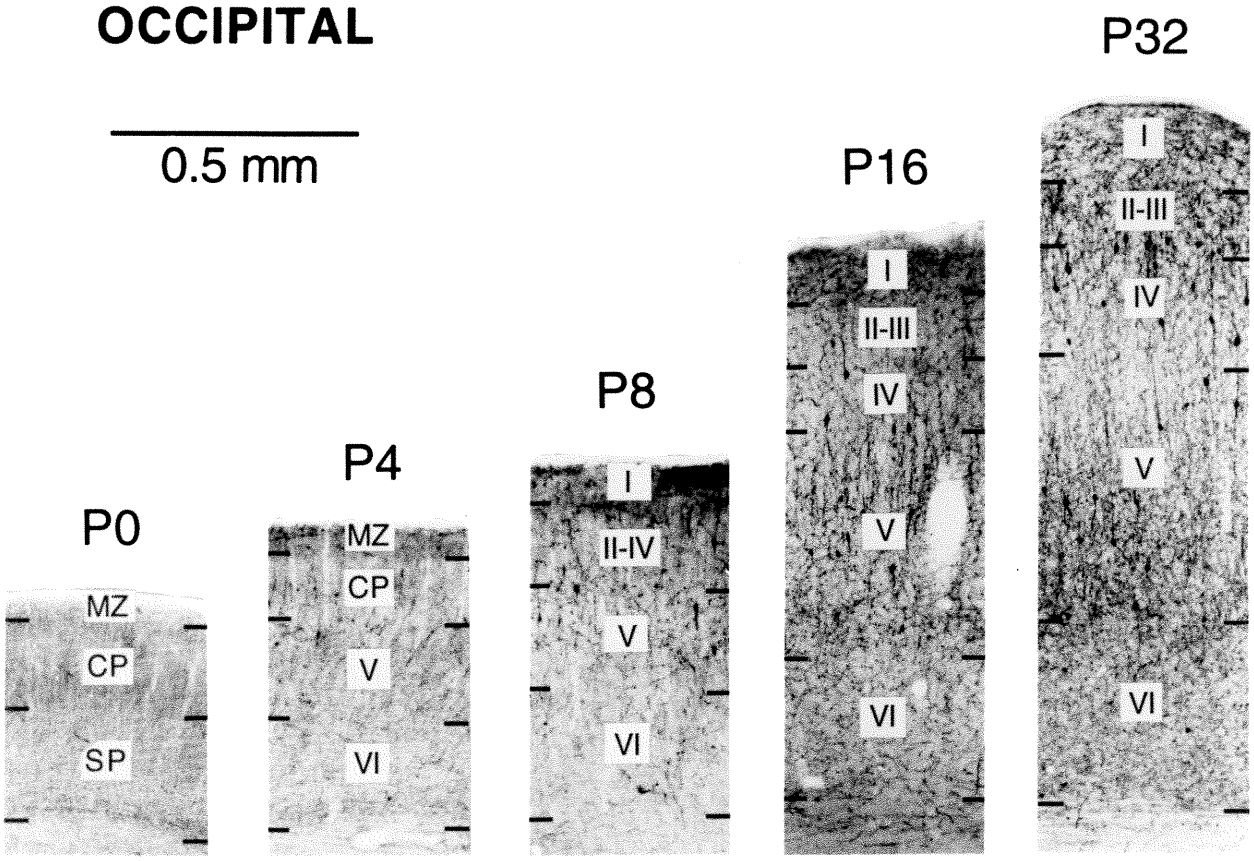
OCCIPITAL
0.5 mm
P0
MZ
CP
SP
P4
MZ
CP
V
VI
P8
I
II-IV
V
VI
P16
I
II-III
IV
V
VI
P32
I
II-III
IV
V
VI

Fig. 4. Digitized images of the ChAT-immunostained innervation in a given layer of the three cortical areas at the postnatal ages indicated. These images are equivalent to the sampling windows (100 x 100 μm) from which axon length was measured. In each case, the top of the figure is parallel to the cortical surface. Note the growth cone-tipped axons in A and E, and the interneurons in F and K. A progressive increase in density of ACh axons is visible at all ages in layers I of the frontal and V of the occipital cortex. In contrast, there is no further increase in density between P16 and P32 in layer IV of the parietal cortex. The contrast and brightness of some of these images were adjusted slightly for esthetic purposes. Scale bar in L: 20 μm.

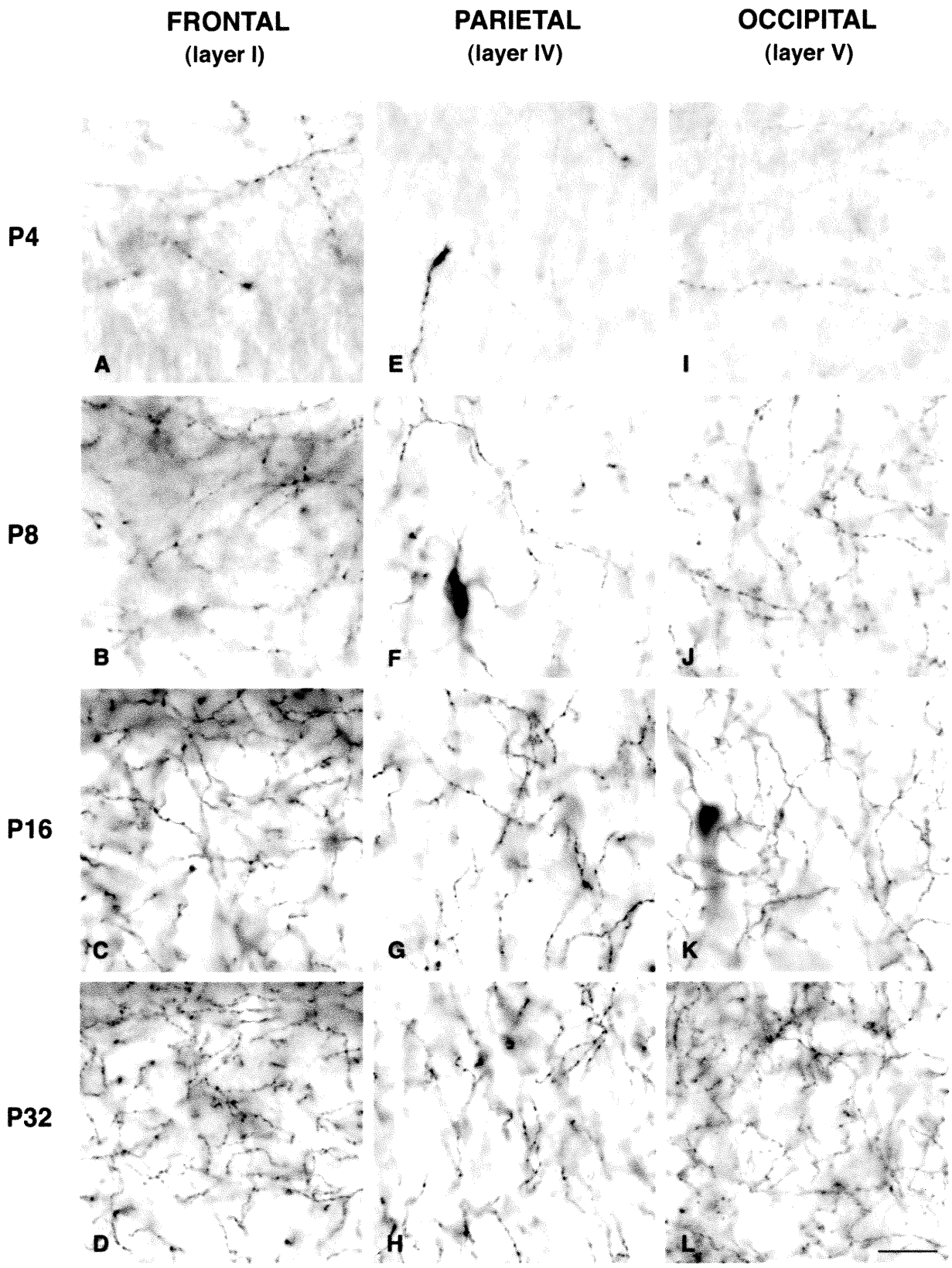
FRONTAL
(layer I)
PARIETAL
(layer IV)
OCCIPITAL
(layer V)
P4
P8
P16
P32
A
B
C
D
E
F
G
H
I
J
K
L

Fig. 5. Number of varicosities per μm of ChAT-immunostained axon in the frontal, parietal and occipital neocortex at different postnatal ages (P4 – P32) and the adult (P60). Interlaminar means (± SEM) from 3 rats per age, except for the adult values which are from 5 rats (Mechawar et al., 2000a). Note, in all areas, the sharp increase between P4 and P16, and the ensuing plateau at 4 varicosities per 10 μm of ACh axons. * $p < 0.05$ compared to P60, for all P4 and P8 values in the frontal, parietal and occipital cortex and the P16 and P32 values in the occipital cortex only.

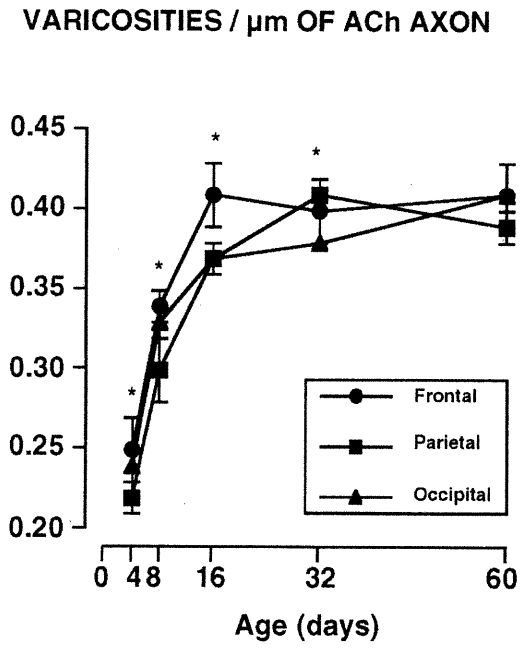
VARICOSITIES / µm OF ACh AXON
0.45
0.40
0.35
0.30
0.25
0.20
*
*
*
*
Frontal
Parietal
Occipital
0
4
8
16
32
60
Age (days)

Figs. 6-8. Laminar and regional densities (left graphs) and number of ACh axon varicosities under 1 mm^2 of cortical surface (right graphs) in the frontal (Fig. 6), parietal (Fig. 7) and occipital (Fig. 8) neocortex at the different postnatal ages (P4 - P32) and the adult (P60; data from Mechawar et al., 2000a). Means ± SEM from 3 rats per age, except at P60 (n = 5). The histograms show the data for the different layers (I, II/III or II/IV, V and VI) and the whole cortex (I-VI). On the left (densities), the means for whole cortex (I-VI) are interlaminar. On the right (actual numbers of varicosities under 1 mm^2), the value for whole cortex (I-VI) takes into account the relative thickness of each layer. * $p < 0.05$ compared to P60. The line graphs at bottom are based on the same values (error bars omitted), but depict the temporal profile of ACh innervation with greater clarity.

FRONTAL CORTEX

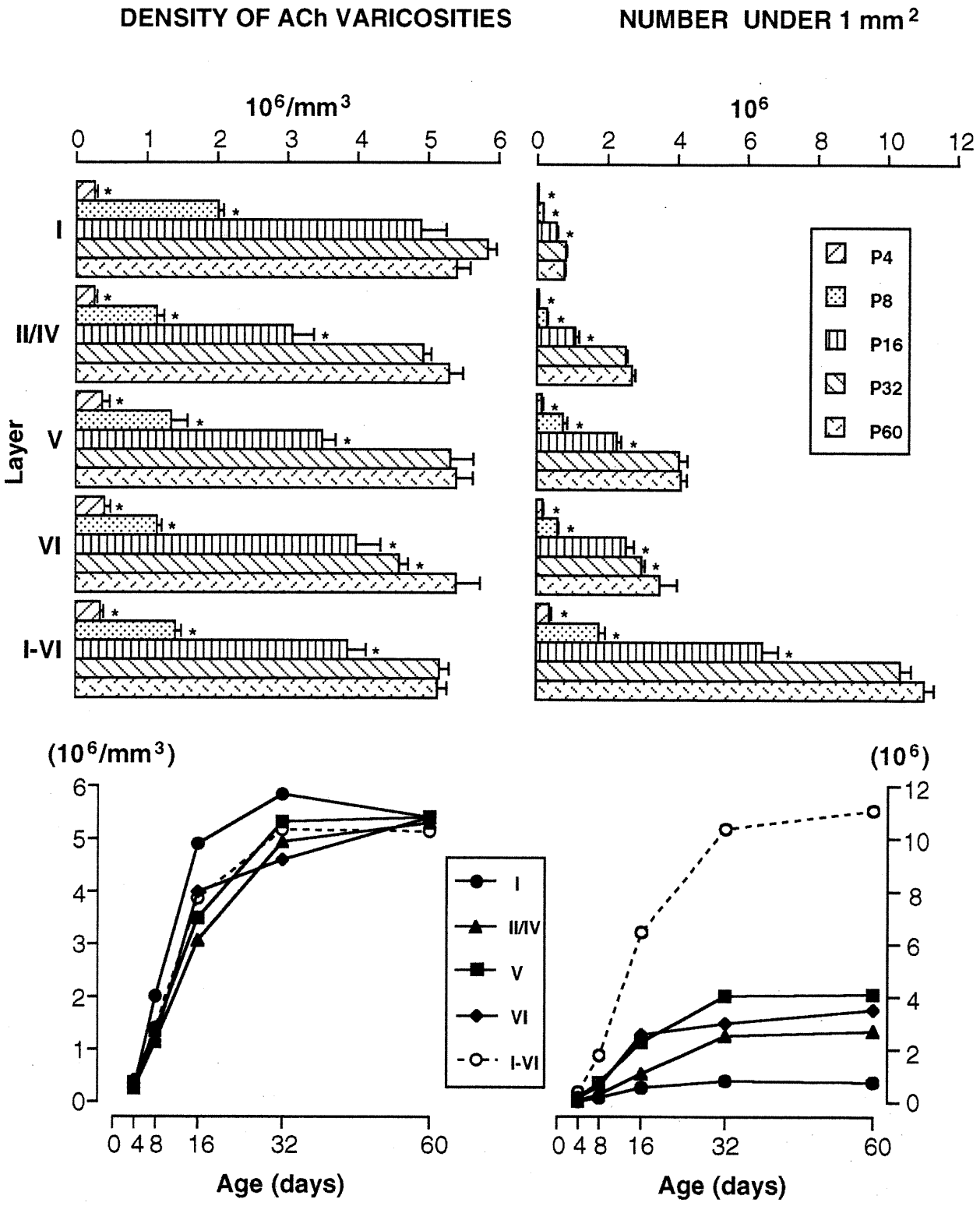

PARIETAL CORTEX

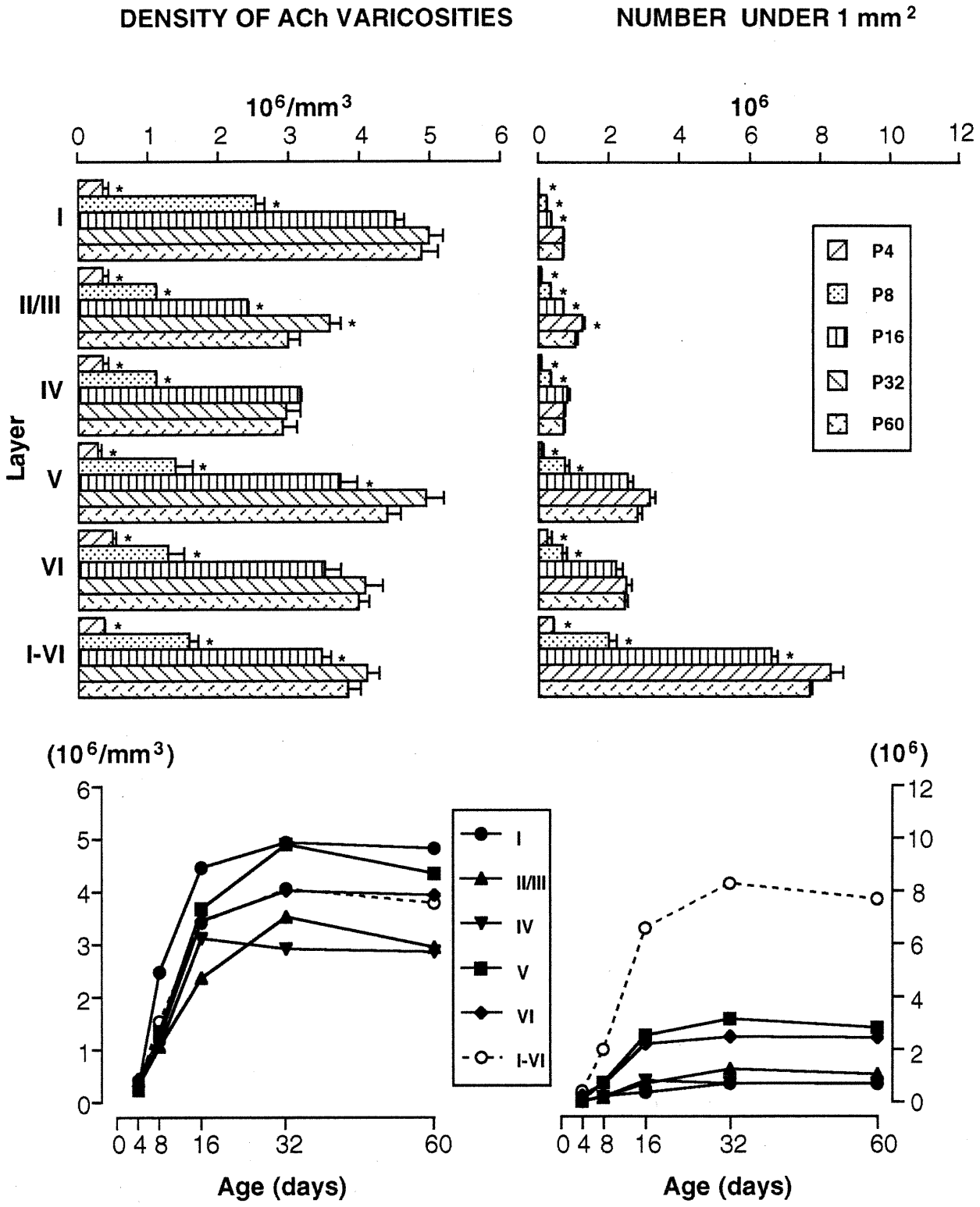

OCCIPITAL CORTEX

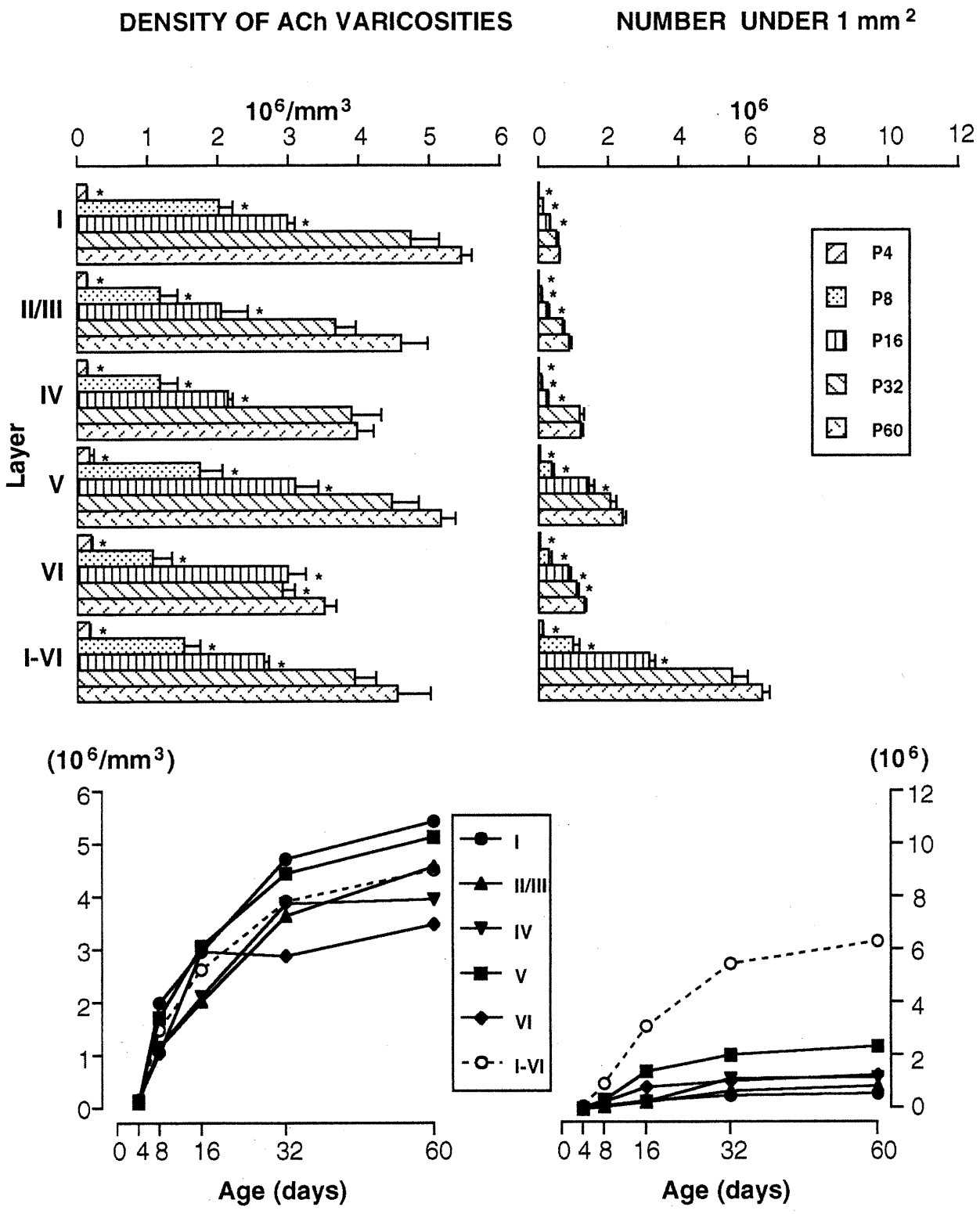

Chapitre IV

ULTRASTRUCTURAL FEATURES OF THE ACETYLCHOLINE INNERVATION IN THE DEVELOPING PARIETAL CORTEX OF RAT

(sous presse à *The Journal of Comparative Neurology*)

En tant que premier auteur, j'ai réalisé les expériences, analysé les résultats et contribué de façon majeure à toutes les étapes de la rédaction de l'article.

ULTRASTRUCTURAL FEATURES OF THE ACETYLCHOLINE INNERVATION IN THE DEVELOPING PARIETAL CORTEX OF RAT

Naguib MECHAWAR, Kenneth C. WATKINS, and Laurent DESCARRIES *

Départements de pathologie et biologie cellulaire et de physiologie,
and Centre de recherche en sciences neurologiques, Faculté de médecine,
Université de Montréal, Montréal, Québec, Canada H3C 3J7

(26 text pages including figure legends; 3 tables and 2 figures)

Abbreviated title: **ACh innervation in developing neocortex**

Associate editor: Dr. Oswald STEWARD

KEYWORDS: ChAT, neocortex, immunocytochemistry, electron microscopy, varicosities, axons

* Correspondence: Laurent DESCARRIES m.d.
Département de pathologie et biologie cellulaire
Université de Montréal (address same as above)

Aknowledgments: The authors are grateful to Costantino Cozzari and Boyd K. Hartman for their generous gift of ChAT antibody. They also thank Jean Léveillé and Gaston Lambert for photographic work.

Grant sponsor: Grant number NRF 3544 to L.D., and doctoral studentship to N.M., from the Canadian Institutes for Health Research.

ABSTRACT

To follow on a recent quantitative study of the developing cholinergic (ACh) innervation in rat neocortex, axon varicosities identified by electron microscopic immunocytochemistry with a highly sensitive antibody against choline acetyltransferase (ChAT) were examined in the primary somatosensory area (Par1) of rats at postnatal ages P8, P16 and P32. As visualized and measured in single thin sections, and compared to those of unlabeled varicosities selected at random in the same micrographs, the ChAT-immunostained profiles displayed intrinsic and relational features very similar to those previously described in the same cortical area of adult rat (Umbriaco et al., 1994. J. Comp. Neurol. 348:351-373). At the three postnatal ages, the immunoreactive profiles were comparable in shape, size and vesicular content in all cortical layers, but showed an increasing frequency of mitochondria with age, reaching 44% at P32. Synaptic junctions were observed on 6.3 to 8.7% of these sectional profiles, indicating an average synaptic incidence of 17% for whole varicosities, again comparable to that in the adult (14%). As in adult, the junctions made by the rare synaptic ChAT-immunostained varicosities were always single, usually symmetrical, and more frequently found on dendritic branches than spines. Thus, cortical ACh varicosities displayed intrinsic and relational features similar to adult ones as soon as this innervation was installed, suggesting that a diffuse mode of transmission and ambient level of ACh could play a major role in the diverse effects of this neuromodulator during cortical development.

The intricate network of varicose acetylcholine (ACh) axons pervading the adult rat neocortex supplies this region of the brain with its densest neuromodulatory input (Mechawar et al., 2000). The ubiquitous distribution of this innervation is consistent with the role(s) played by ACh in numerous cortical states and functions, among which wakefulness/sleep, modulation of sensory information, plasticity of sensory maps, attention, learning and memory are best documented (for selected reviews, see Hasselmo and Bower, 1993; Hasselmo, 1995; Dykes, 1997; Baxter and Chiba, 1999; Sarter and Bruno, 1999, 2000). On the basis of a growing number of studies, an involvement of cortical ACh during development has also been demonstrated. In particular, ACh seems to act as a permissive factor for the enhanced morpho-functional plasticity observed during the so-called 'critical period' of early postnatal life (Bear and Singer, 1986; Gu and Singer, 1993; Broide et al., 1996; Zhu and Waite, 1998; Aramakis et al., 2000). Further evidence implicating ACh in cortical development has been provided recently by *in vitro* experiments showing that, during the first postnatal week, muscarinic agonists induce slow waves of correlated neural activity in the parietal cortex (Peinado, 2000).

A light-microscopic quantitative immunocytochemical description of the developing ACh innervation in rat neocortex was achieved recently (Mechawar and Descarries, 2001a) with the use of a highly sensitive antibody against rat brain choline acetyltransferase (ChAT; Cozzari et al., 1990). This study showed that ACh axons reach the cortex early, i.e. perinatally, and then proliferate rapidly. The first two postnatal weeks represent the period of fastest growth for this innervation, which evolves along three parameters: the lengthening and branching of axons, and an increase in number of axon varicosities per unit length of axon (from 2 to 4 per 10 μm). Sixteen days after birth, the distribution and density of ACh axons and varicosities

have become equivalent to adult in the parietal cortex. In the frontal and occipital cortex, however, maturation continues during the latter part of the first month. It is likely that these growing axons are the source of the ACh measured in the developing cortex (Coyle and Yamamura, 1976), but, in the absence of prior data on their fine structural features during the early postnatal period, it remained to be demonstrated that they are properly equipped for transmitter release.

In previous electron microscopic studies of the ACh innervation in adult rat neocortex, ChAT immunoreactive varicosities were found to rarely display synaptic specializations. The average frequency with which these axon terminals engage in junctional relationships (synaptic incidence) was found to range between 9% (entorhinal) and 14% (frontal and parietal), as measured in serial thin sections (Chédotal et al., 1994; Umbriaco et al., 1994; Vaucher and Hamel, 1995; reviewed in Descarries and Mechawar, 2000). A much higher synaptic incidence (66%) was recently reported (Turrini et al., 2001) for layer V of rat parietal cortex, but the sampling in this study was presumably biased because of the use of an antibody against the vesicular ACh transporter, as suggested by the larger average dimensions of the examined sectional profiles. The ACh (ChAT-immunostained) innervations in other rat brain regions have similarly been shown to be predominantly asynaptic (Umbriaco et al., 1995; Contant et al., 1996). It has thus been proposed that, in the adult CNS, ACh acts mostly via diffuse (volume) transmission to exert widespread effects on a variety of cellular targets (Descarries et al., 1997). In this context, it was of particular interest to determine whether ACh varicosities were already endowed with such relational features during cortical development.

The present electron microscopic, ChAT-immunocytochemical study was therefore undertaken to address these and other issues regarding the ultrastructural characteristics of the growing ACh innervation in cerebral cortex. By comparing the intrinsic and relational features of these varicosities, as well as their immediate microenvironment, in rat parietal cortex at 8, 16 and 32 postnatal days, it was expected to detect morphological changes associated with maturation, and determine when they acquire the structural attributes of mature axon varicosities, including a low synaptic incidence. Some of the results have already been reported in abstract form (Mechawar and Descarries, 2001b).

MATERIALS AND METHODS

Tissue processing

All experiments abided by the policies and guidelines of the Canadian Council on Animal Care and the regulations of the Animal Care Commitee at the Université de Montréal. The study was carried out on 9 male Sprague-Dawley rats (Charles River, St-Constant, Québec, Canada), purchased at known ages and kept with their lactating mothers. At postnatal days P8, P16 and P32, 3 rats per age were deeply anesthetized with sodium pentobarbital (65 mg/kg, i.p.), and perfused through the heart with ice-cold phosphate-buffered saline (PBS; 50 mM; pH 7.4; 25-50 ml) followed by 100-150 ml of 4% paraformaldehyde (PFA) in 0.1 M sodium phosphate buffer (pH 7.4; 24° C), 100-150 ml of 4% PFA + 1% glutaraldehyde, and 150-200 ml of 4% PFA. Immediately after, the brain was dissected out, postfixed overnight in 4% PFA at 4°C, and cut into consecutive 50 µm-thick transverse sections (Lancer vibratome). With the aid of an atlas of the developing rat brain (Paxinos et al., 1991), sections immediately rostral to the *globus pallidus* were then selected at a

levels equivalent to stereotaxic plane A-9.2 in the Paxinos and Watson's stereotaxic atlas of the adult rat brain (1986), and processed for ChAT-immunocytochemistry. Adjacent sections were stained with cresyl violet to delimitate cortical layers.

ChAT-immunocytochemistry

The following protocol, allowing for an optimal detection of ChAT-immunostained axons in rat brain sections, has been previously described in detail (Umbriaco et al., 1994, 1995; Contant et al., 1996; Mechawar et al., 2000). In brief, after a 5 min immersion in a 1% solution of sodium borohydride, the sections were incubated sequentially in : 1) a blocking solution of PBS containing 2% normal horse serum (NHS; Vector, Burlingame, CA) and 1% bovine serum albumin (BSA; Sigma, St-Louis, MO) (2 h); 2) the same solution containing 2 µg/ml of mouse monoclonal antibody against purified rat brain ChAT (Cozzari et al., 1990) (overnight), and 3) a 1/200 dilution of biotinylated horse anti-mouse antibody (Vector), in KPB containing 2% NHS and 1% BSA (2 h). This was followed by the avidin-biotin complex procedure (ABC Kit, Vectastain Elite; Vector) (2 h), and revelation for 2 min in a 0.05% solution of 3,3'-diaminobenzidine (DAB; Sigma) prepared in Tris buffer (pH 7.4; 24° C), to which 0.005% H_2O_2 was added. Sections were then osmicated, dehydrated in ethanol and propylene oxide, and flat-embedded in Durcupan (Fluka; Sigma). Control experiments included omission of the primary or secondary antibodies, which completely abolished the immunostaining.

Electron microscopy

The examination was focused on the Par1 area of primary somatosensory cortex. Rectangular pieces of this area, spanning from the cortical surface to the

callosal radiations, were removed from the flat-embedded ChAT-immunostained section, glued to the tip of resin blocks, and sectioned ultrathin (90-100 nm) with a Porter-Blum MT-2 Ultra-Microtome. The sections were collected on Pioloform-coated, one-slot (2 x 0.6 mm) grids, stained with lead citrate, and examined with a Philips CM100 electron microscope at a uniform working magnification of 13 500 X. ChAT-immunostained varicosities were sampled randomly by taking a picture of every such profile in strips (at least 150 μm-wide) of tissue, from layer I to the bottom of layer VI, on both sides of each section. The varicosities were defined as round or ovoid axon dilations containing aggregated small vesicles (see Umbriaco et al., 1994). In each animal, the two or three sections scanned in this fashion amounted to an examined tissue surface of 1.5-2 mm^2. The cartesian coordinates from the microscope's stage readings were used to measure the distance of each varicosity from the pial surface. By comparison with adjacent Nissl sections, these depth values could then be assigned to the corresponding cortical layers.

In each rat (3 per age), the first 100 ChAT-immunostained varicosities thus selected were kept for further analysis (900 in total), and printed at a final magnification of 38 500 X, under standard photographic and darkroom conditions. With the aid of the public domain NIH Image program (1.61), these varicosity profiles were then measured for area, long axis, short axis and diameter [(long axis + short axis) / 2] and classified as containing or not one or more mitochondria. The proportion engaged in synaptic junction was tallied by categorizing the varicosity profiles as showing or not a junctional complex, i.e., a localized straightening of apposed plama membranes with a slight widening of the intercellular space and/or a pre- or postsynaptic thickening. The length of the junctions was measured, and the observed synaptic frequency converted to synaptic incidence for whole

varicosities by means of the stereological formula of Beaudet and Sotelo (1981), using the long axis as diameter of the profiles (Umbriaco et al., 1994). This formula takes into account the average size of varicosity profiles, the lenght of their junctional complexes and the thickness of the sections, to predict the probability of seeing a synapse if there is one on every varicosity. The synaptic incidence is then inferred by comparison with this predicted value. The reliability of this procedure has been validated experimentally by Umbriaco et al. (1994), who found almost identical values of synaptic incidence for a large population of ChAT-immunostained cortical varicosities examined in serial sections across their entire volume and which were also treated as a randomized single section sample.

The junctions made by ChAT-immunostained profiles were further characterized as symmetrical and asymmetrical, the synaptic targets identified, and the composition of their immediate microenvironment determined by identifying juxtaposed structural elements as axon varicosities, dendritic branches, dendritic spines, neurites (small axonal or dendritic processes) and miscellaneous (glia, myelinated axons, neuronal or glial cell bodies, blood vessels and unidentified processes), according to commonly accepted ultrastructural criteria (Peters et al., 1991).

The intrinsic and relational features of the ChAT-immunostained varicosities were also compared to those of a population of unlabeled axon varicosities randomly selected from the same electron micrographs. For this purpose, single profiles of unlabeled axon varicosities closest to a fixed mark on a transparent overlay were selected on the first 32-35 micrographs from each animal. A total of 100 unlabeled varicosity profiles per age could thus be analyzed for the same parameters as the ACh varicosities.

Statistical analysis

In each animal, an analysis of variance (ANOVA) was done to determine if the dimensions (area, long and short axes, diameter) and junctional features of ACh or unlabeled varicosities varied significantly between cortical layers. Since no such variations were found, averages ± s.d. were calculated for all parameters as presented in Tables 1-3. These figures were then tested for age-related differences with the non-parametric Kruskal-Wallis test (one-tail). Differences were considered statistically significant at $p < 0.05$ for both statistical tests.

RESULTS

Light microscopic distribution of ChAT-immunostaining

Immunostaining with the present anti-ChAT antibody visualized an intricate network of fine varicose fibers across the full thickness of the parietal cortex at P8, P16 and P32 (Fig. 1 A-C). Intensely labeled cells displaying the typical morphology of bipolar interneurons were also observed in every layer at all ages, being the most numerous in the pyramidal layers. The overall density of immunostained axons, moderate at P8, increased substantially in all layers to resemble the adult at P16 and P32. As reported in our recent quantitative light microscopic description of this developing innervation (Mechawar and Descarries, 2001a), between P8 and adulthood (>P60), the laminar density of ChAT-immunostained axons was consistently the highest in layers I and V, intermediate in layer II/III and the lowest in layers IV and VI of the parietal cortex. Moreover, in this as well as the other neocortical areas examined (frontal and occipital), the number of varicosities per unit lenght of ChAT-immunostained axon was then shown to rise from 3 to 4 per 10 µm.

Ultrastructural features

Regardless of the postnatal age or cortical layer examined, ACh varicosities shared similar ultrastructural characteristics (Fig. 2). Their sectional profiles arose from small diameter unmyelinated axons, were generally elliptic, contained numerous aggregated small and clear vesicles, and often one or more mitochondria. The diaminobenzidine immunoprecipitate was of variable density, confined to the axoplasm, and often lined the plasma membrane and the outer surface of organelles.

The dimensions of ACh varicosities did not vary significantly between P8 and P32 (Table 1). Their average sectional area was 0.16 μm^2, and their diameter 0.48 μm, with no significant difference between layers. Interestingly, similar values were measured from the population of randomly selected unlabeled varicosities (0.18 μm^2 and 0.48 μm). The aspect ratio was higher at all ages for ACh than unlabeled profiles, suggesting a more elliptic shape (Table 1). With age, the proportion of ChAT-immunostained profiles containing one or more mitochondria increased significantly, from 20.7% (P8) to 38.7% (P16) and 43.7% (P32). At each age, this percentage was higher than for unlabeled varicosities, but the statistical significance of this difference could not be established.

Junctional relationships

Immunostained varicosity profiles endowed with a synaptic junction were observed in every layer at all ages (Fig. 2). The average size of these synaptic profiles did not differ from that of their asynaptic counterparts. The proportion exhibiting a junction was consistently low, averaging 6.3%, 6.7% and 8.7% at P8, P16 and P32, respectively (Table 2). The corresponding synaptic incidences for whole varicosities, as extrapolated with the stereological formula Beaudet and Sotelo (1981), amounted to 13.2%, 15.6% and 22.2%. By comparison, the same

extrapolation performed on unlabeled profiles from the same material yielded considerably higher values, which increased significantly from 54.6% at P8 to > 100% at P16 and P32 (Table 2).

The synaptic junctions made by ACh varicosities were always single, almost always symmetrical (61/65; 94%), and made on either dendritic branches (71%) or spines (29%) (Table 2). The mean length of these junctions was 0.35 μm at P8, 0.28 μm at P16 and 0.24 at P32, without significant age- or layer-related difference.

Structural microenvironment

The composition of the immediate microenvironment of ACh and randomly selected unlabeled axon varicosities is presented in Table 3. At the three ages examined, there were mostly similarities between the two populations of varicosities.

At P8, dendritic branches were the most frequently observed element around both categories of profiles, followed by neurites (small dendritic or axonal profiles), other axon varicosities and dendritic spines. At P16 and P32, the neurites became more abundant, followed closely by dendritic branches and less numerous varicosities and dendritic spines. The only significant developmental trend was an increased number of dendritic spines next to unlabeled varicosities, in keeping with the significant increase in the number of synaptic contacts made by these varicosities on spines, which rises from 18% at P8 to 49% at P16 and 75% at P32. There was no such trend in the case of the ACh varicosities, which made synapse on spines with low frequencies of 27% at P8 and 16% at P32 (Table 2).

DISCUSSION

Previous ultrastructural descriptions have indicated that ChAT-immunostained (i.e. ACh) axon varicosities in different regions of adult rat brain share comparable morphometric and relational characteristics (Chédotal et al., 1994; Umbriaco et al., 1994; Umbriaco et al., 1995; Vaucher and Hamel, 1995; Contant et al., 1996). By revealing that varicosities borne by growing ACh axons in immature cortex already display similar characteristics, the present investigation provides strong evidence for the functionality of these putative release sites. It was beyond the scope of this study to distinguish between cortical ACh varicosities of intrinsic versus extrinsic origin. Nevertheless, the general ultrastructural features of these varicosities were compatible with the variety of roles and functions subserved by ACh during development.

As determined from single sections, the morphometric features of ACh varicosities in the developing parietal cortex were almost uniform from P8 to P32, in spite of a > 30% increase in the average number of these terminals per unit length of axon, and an almost tripling of their total number (from 1.6 to 4.1 x 10^6 per mm^3) in this cortical area (Mechawar and Descarries, 2001a). The average dimensions of these ACh profiles were slightly inferior to those measured in adult rat (Umbriaco et al., 1994). For example, their area and mean diameter averaged 0.16 μm^2 and 0.48 μm between P8 and P32, compared to 0.23 μm^2 and 0.52 μm in the adult. In view of their consistent size at all three postnatal ages examined, such small differences between developing and adult varicosities were likely to reflect sampling biases or variations in tissue fixation protocols. For all but one of the parameters examined, the dimensions of the developing ACh axon varicosities were very close to those of randomly selected unlabeled varicosities from their immediate surround. The

aspect ratio was the only measure which differed between the two populations, suggesting a slightly more elliptic shape of the ACh than other varicosities. In addition to their size and shape, as well as their content in organelles, the morphometric features of the developing cortical ACh varicosities strongly favored the view that, as soon as formed on their growing axons, they could be functional as transmitter storing and releasing sites.

The proportion of ACh profiles displaying one or more mitochondria increased significantly from 21% to 44% between P8 and P32, reaching a value very close to that previously found in the adult (38%; quoted in Contant et al., 1996). These figures were of particular interest in the light of an earlier report from Pedata and collaborators (1983), who measured a significant reduction in ACh release from slices of the developing but not adult parietal cortex submitted to protracted electrical stimulation. This exhaustion of developing ACh varicosities might have to do with a limited metabolic capacity due to their lesser content in mitochondria, especially since these organelles produce Acetyl CoA, one of two precursors required for the biosynthesis of ACh. This requirement for Acetyl CoA could also explain the relatively high content in mitochondria of ACh versus non ACh varicosities throughout development as well as in adult. It has been recently estimated that, during the first two postnatal weeks, each basalo-cortical ACh axon grows at a daily rate of 25 mm (Mechawar and Descarries, 2001a). Since mitochondria are carried along axons by fast transport at speeds up to 400 mm per day (Brady, 1991), the delay in their appearance as a full complement in developing ACh varicosities might reflect some lag in their formation by division in ACh nerve cell bodies.

As discovered in the adult, one of the major characteristics of the developing ACh varicosities, irrespective of the postnatal age examined, was the low frequency

with which they made morphologically defined synaptic junctions (average of 17% for the three ages examined). Even if the present material was viewed in single sections only, this finding was all the more striking that the corresponding proportions extrapolated for the population of randomly selected unlabeled varicosities were about 4 times higher at P8, and at least 6 times higher at P16 and P32. This raising proportion of unlabeled profiles observed in synaptic junction was a compelling argument in favor of the predominantly asynaptic nature of the ACh innervation during development.

Much as their intrinsic features, the synaptic incidence of the developing ACh varicosities was almost the same as in the adult, in which it was measured at 13.5% as extrapolated from single sections, and 14% in serial sections (Umbriaco et al., 1994). In contrast, unlabeled varicosities made synapse with an increasing frequency from P8 (55%) to P16 (102%), as expected from the peak in synaptogenesis which takes place between P14 and P26 in rat parietal cortex (Aghajanian and Bloom, 1967). The stable proportion of synaptic junctions formed by the developing ACh varicosities was all the more intriguing in that it implicated a vastly increasing number of varicosities in a rapidly changing environment. Such a stability could be indicative of a parallel increase in the growth of this innervation and the number of its synaptic targets.

As in the adult, the majority of synaptic ACh varicosities formed symmetrical junctions with dendritic branches more than dendritic spines at all postnatal ages. This was at variance with the unlabeled population of varicosities, in which the proportion of synapses on dendritic branches decreased significantly with age in favor of axo-spinous junctions. The low frequency of synaptic ACh varicosities did not allow to detect them in sufficient number at each postnatal age to statistically

establish any difference in the nature of their targets between cortical layers. However, as in the adult, layer V exhibited the highest synaptic incidence at all ages. In keeping with the paucity of synaptic ACh axon varicosities here shown in the developing neocortex as previously in the adult, fast excitatory actions mediated by nicotinic receptors have only been recorded recently from the developing (Roerig et al., 1997; Xiang et al., 1998; Porter et al., 1999) or adult neocortex (Alkondon et al., 2000). As most cortical neurons displaying such effects have been identified as GABA interneurons (see also Beaulieu and Somogyi, 1991 and Lubin et al., 1999), it is tempting to speculate that these represent the preferred target for a majority of synaptic ACh varicosities.

The true number of synaptic ACh varicosities in the developing parietal cortex may in fact be estimated from our previous quantitative data on the density of ACh innervation in this cortical region at the same postnatal ages (Mechawar and Descarries, 2001a). Based on the synaptic frequencies measured in the present study, it should amount to 0.3, 1.0 and 1.8 x 10^6 synaptic ACh varicosities under a 1 mm^2 surface of cortex, versus 1.7, 5.6 and 6.5 x 10^6 that are asynaptic, at P8, P16 and P32, respectively. The actual proportion (and thus number) which might synapse onto pyramidal neurons instead of GABA interneurons remains to be established.

The largely asynaptic nature of these ACh varicosities appears to be an inherent feature of this cortical innervation, which might subtend many of its properties, functions and roles during development as in the adult. In adult cortex, this relational feature has been taken as an indication that the ACh innervation might primarily function through a diffuse mode of transmission, in the sense of

being capable to influence a variety of functional targets within a relatively large expanse of tissue.

In this context, it was of particular interest to observe that dendritic branches and small neurites were the structures most frequently juxtaposed to the developing ACh axon varicosities, as also reported previously in the adult cortex (Umbriaco et al., 1994). As in other brain regions previously examined in this fashion, the major differences between the microenvironments of ACh and non ACh (randomly selected, unlabeled) varicosities could be accounted for by a high frequency of axo-spinous synapses made by the latter. At no time point in their development was a high frequency of other (unlabeled) axon varicosities observed around the ACh varicosities, as found in adult rat neostriatum or hippocampus, for instance (Umbriaco et al., 1995; Contant et al., 1996). The less frequent juxtaposition of ACh varicosities to other axon terminals in the neocortex can hardly be taken as an indication of a weaker influence of ACh on the release of other transmitters, since such effects are among the best documented for ACh in this brain region (for review, see Jones et al., 1999).

In view of the widespread distribution and relatively high density of this innervation, and of the molecular form of acetylcholinesterase present in the central as opposed to the peripheral nervous system, it has been postulated that, in cerebral cortex notably, most tissue elements might be exposed to a low ambient level of ACh, which could contribute to its function(s) in this brain region (see Umbriaco et al., 1994, Descarries et al., 1997 and Descarries, 1998). A similar mechanism could prevail during cortical development and account for the demonstrated effects of ACh on neuronal proliferation (Ma et al., 2000), cortical morphogenesis (Höhmann et al., 1991; Robertson et al., 1998) and plasticity of cortical sensory maps (Bear and Singer, 1986; Gu and Singer, 1993; Zhu and Waite, 1998; see also Peinado, 2000).

Most of these effects appear to be dependent on the activation of metabotropic muscarinic receptors, some of which have been demonstrated to be present in cortex as early as the late embryonic period (Höhmann et al., 1985; Aubert et al., 1996). An involvement of nicotinic receptors, which are also expressed early in cortical development (Zoli et al., 1995; Aubert et al., 1996), has also been demonstrated recently in the case of cortical plasticity (Broide et al., 1996; Aramakis et al., 2000). No data are currently available on the subcellular distribution of these receptors during cortical development, but several of the nicotinic subunits as well as muscarinic subtypes have been shown to be extrajunctional, at least in the adult (Hill et al., 1993; Mrzljak et al., 1998; Lubin et al., 1999). In this context, it is tempting to speculate that some of these receptors might be tonically activated by the ambient level of ACh during early cortical development, much as recently demonstrated to be the case for glycine receptors activated by non-synaptically released taurine (Flint et al., 1998).

In conclusion, the present study provides further morphological evidence that growing ACh axons might be the source of ACh released in the developing cerebral cortex. It also shows that this cortical innervation is predominantly asynaptic as soon as it develops, as already known to be the case for its serotonin and noradrenaline counterparts (Dori et al., 1996; Latsari et al., 2001), also mostly asynaptic in the adult (Descarries et al., 1975; Beaudet and Descarries, 1976; Descarries et al., 1977). It can thus be inferred that it is through diffuse (volume) transmission that these prototypical neuromodulatory innervations exert much of their influence(s) on the numerous neurobiological and physiological processes which shape the developing mammalian cerebral cortex.

References

Aghajanian GK, Bloom FE. 1967. The formation of synaptic junctions in developing rat brain: a quantitative electron microscopic study. Brain Res 6:716-727.

Alkondon M, Pereira EFR, Eisenberg HM, Albuquerque EX. 2000. Nicotinic receptor activation in human cerebral cortical interneurons: a mechanism for inhibition and disinhibition of neuronal networks. J Neurosci 20:66-75.

Aramakis VB, Hsieh CY, Leslie FM, Metherate R. 2000. A critical period for nicotine-induced disruption of synaptic development in rat auditory cortex. J Neurosci 20:6106-6116.

Aubert I, Cécyre D, Gauthier S, Quirion R. 1996. Comparative ontogenic profile of cholinergic markers, including nicotinic and muscarinic receptors, in the rat brain. J Comp Neurol 369:31-55.

Baxter MG, Chiba AA. 1999. Cognitive functions of the basal forebrain. Curr Opin Neurobiol 9:178-183.

Bear MF, Singer W. 1986. Modulation of visual cortical plasticity by acetylcholine and noradrenaline. Nature 320:172-176.

Beaudet A, Descarries L. 1976. Quantitative data on serotonin nerve terminals in adult rat neocortex. Brain Res 111:301-309.

Beaudet A, Sotelo C. 1981. Synaptic remodeling of serotonin axon terminals in rat agranular cerebellum. Brain Res 206:305-329.

Beaulieu C, Somogyi P. 1991. Enrichment of cholinergic synaptic terminals on GABAergic neurons and coexistence of immunoreactive GABA and choline acetyltransferase in the same synaptic terminals in the striate cortex of the cat. J Comp Neurol 304: 666-680.

Brady ST. 1991. Molecular motors in the nervous system. Neuron 7:521-533.

Broide RS, Robertson RT, Leslie FM. 1996. Regulation of α7 nicotinic acetylcholine receptors in the developing rat somatosensory cortex by thalamocortical afferents. J Neurosci 16:2956-2971.

Chédotal A, Umbriaco D, Descarries L, Hartman BK, Hamel E. 1994. Light and electron microscopic immunocytochemical analysis of the neurovascular relationships of choline acetyltransferase and vasoactive intestinal polypeptide nerve terminals in the rat cerebral cortex. J Comp Neurol 343:57-71.

Contant C, Umbriaco D, Garcia S, Watkins KC, Descarries L. 1996. Ultrastructural characterization of the acetylcholine innervation in adult rat neostriatum. Neuroscience 71:937-947.

Coyle JT, Yamamura HI. 1976. Neurochemical aspects of the ontogenesis of cholinergic neurons in the rat brain. Brain Res 118:429-440.

Cozzari C, Howard J, Hartman B. 1990. Analysis of epitopes on choline acetyltransferase (ChAT) using monoclonal antibodies (Mabs). Soc Neurosci Abstr 16:200.

Descarries L. 1998. The hypothesis of an ambient level of acetylcholine in the central nervous system. J Physiol (Paris) 92:215-220.

Descarries L, Mechawar N. 2000. Ultrastructural evidence for diffuse transmission by monoamine and acetylcholine neurons in the central nervous system. In: Agnati LF, Fuxe K, Nicholson C, Sykova E, editors: Volume Transmission Revisited. Prog Brain Res, Vol 125, Elsevier, Amsterdam 125:27-47.

Descarries L, Beaudet A, Watkins KC. 1975. Serotonin nerve terminals in adult rat neocortex. Brain Res 100:563-588.

Descarries L, Gisiger V, Steriade M. 1997. Diffuse transmission by acetylcholine in the CNS. Prog Neurobiol 53:603-625.

Descarries L, Watkins KC, Lapierre Y. 1977. Noradrenergic axon terminals in the cerebral cortex of rat. III. Topometric ultrastructural analysis. Brain Res 133:197-222.

Dori I, Dinopoulos A, Blue ME, Parnavelas JG. 1996. Regional differences in the ontogeny of the serotonergic projection to the cerebral cortex. Exp Neurol 138:1-14.

Dykes RW. 1997. Mechanisms controlling neuronal plasticity in somatosensory cortex. Can J Physiol Pharmacol 75:535-545.

Flint AC, Liu X, Kriegstein AR. 1998. Nonsynaptic glycine receptor activation during early neocortical development. Neuron 20:43-53.

Gu Q, Singer W. 1993. Effects of intracortical infusion of anticholinergic drugs on neuronal plasticity in kitten striate cortex. Eur J Neurosci 5:475-485.

Hasselmo ME. 1995. Neuromodulation and cortical function: modeling the physiological basis of behavior. Behav Brain Res 67:1-27.

Hasselmo ME, Bower JM. 1993. Acetylcholine and memory. Trends Neurosci 16:218-222.

Hill JA, Zoli M, Bourgeois J-P, Changeux J-P. 1993. Immunocytochemical localization of a neuronal nicotinic receptor: the β2-subunit. J Neurosci 13:1551-1568.

Höhmann CF, Pert CC, Ebner FF. 1985. Development of cholinergic markers in mouse forebrain. II. Muscarinic receptor binding in cortex. Dev Brain res 23:243-253.

Höhmann CF, Kwiterovich KK, Oster-Granite ML, Coyle JT. 1991. Newborn basal forebrain lesions disrupt cortical cytodifferentiation as visualized by rapid golgi staining. Cereb Cortex 1:143-157.

Jones S, Sudweeks S, Yakel JL. 1999. Nicotinic receptors in the brain: correlating physiology with function. Trends Neurosci 22:555-561.

Latsari M, Dori I, Antonopoulos J, Chiotelli M, Dinopoulos. 2001. The noradrenergic innervation of the developing and mature visual and motor cortex of the rat brain: a light and electron microscopic immunocytochemical analysis. J Comp Neurol (in press).

Lubin M, Erisir A, Aoki C. 1999. Ultrastructural immunolocalization of the α7 nAChR subunit in guinea pig medial prefrontal cortex. Ann NY Acad Sci 868:628-632.

Ma W, Maric D, Li B-s, Hu Q, Andreadis JD, Grant GM, Liu Q-Y, Shaffer KM, Chang YH, Zhang L, Pancrazio JJ, Pant HC, Stenger DA, Barker JL. 2000. Acetylcholine stimulates cortical precursor cell proliferation *in vitro* via muscarinic receptor activation and MAP kinase phosphorylation. Eur J Neurosci 12:1227-1240.

Mechawar N, Descarries L. 2001a. The cholinergic innervation develops early and rapidly in the rat cerebral cortex: a quantitative immunocytochemical study. Neuroscience (in press).

Mechawar N, Descarries L. 2001b. Ultrastructural features of acetylcholine axon varicosities in the developing parietal cortex of rat. Soc Neurosci Abstr 27, 1567.

Mechawar N, Cozzari C, Descarries L. 2000. Cholinergic innervation in adult rat cerebral cortex: a quantitative immunocytochemical description. J Comp Neurol 428:305-318.

Mrzljak L, Levey AI, Belcher S, Goldman-Rakic PS. 1998. Localization of the m2 muscarinic acetylcholine receptor protein and mRNA in cortical neurons of the normal and cholinergically deafferented rhesus monkey. J Comp Neurol 390:112-132.

Paxinos G, Watson C. 1986. The Rat Brain in Stereotaxic Coordinates, second edition. Academic Press Australia.

Paxinos G, Törk I, Tecott LH, Valentino KL. 1991. Atlas of the Developing Rat Brain. Academic Press, San Diego, CA.

Pedata F, Slavikova J, Kotas A, Pepeu G. 1983. Acetylcholine release from rat cortical slices during postnatal development and aging. Neurobiol Aging 4:31-35.

Peinado A. 2000. Traveling slow waves of neural activity: a novel form of network activity in developing neocortex. J Neurosci 20:RC54 (1-6).

Peters A, Palay SL, Webster HdeF. 1991. The Fine Structure of the Nervous System. Neurons and Their Supporting Cells. New York, Oxford, Oxford University Press.

Porter JT, Cauli B, Tsuzuki K, Lambolez B, Rossier J, Audinat E. 1999. Selective excitation of subtypes of neocortical interneurons by nicotinic receptors. J Neurosci 19:5228-5235.

Robertson RT, Gallardo KA, Claytor KJ, Ha DH, Ku K-H, Yu BP, Lauterborn JC, Wiley RG, Yu J, Gall CM, Leslie FM. 1998. Neonatal treatment with 192 IgG-Saporin produces long-term forebrain cholinergic deficits and reduces dendritic branching and spine density of neocortical pyramidal neurons. Cereb Cortex 8:142-155.

Roerig B, Nelson DA, Katz LC. 1997. Fast synaptic signaling by nicotinic acetylcholine and serotonin 5-HT_3 receptors in developing visual cortex. J Neurosci 17:8353-8362.

Sarter M, Bruno JP. 1999. Abnormal regulation of corticopetal cholinergic neurons and impaired information processing in neuropsychiatric disorders. Trends Neurosci 22:67-74.

Sarter M, Bruno JP. 2000. Cortical cholinergic inputs mediating arousal, attentional processing and dreaming: differential afferent regulation of the basal forebrain by telencephalic and brainstem afferents. Neuroscience 95:933-952.

Turrini P, Casu MA, Wong TP, De Koninck Y, Riberiro-Da-Silva A, Cuello AC. 2001. Cholinergic nerve terminals establish classical synapses in the rat cerebral cortex : synaptic patter and age-related atrophy. Neuroscience 105:277-285.

Umbriaco D, Garcia S, Beaulieu C, Descarries L. 1995. Relational features of acetylcholine, noradrenaline, serotonin and GABA axon terminals in the stratum radiatum of adult rat hippocampus (CA1). Hippocampus 5:605-610.

Umbriaco D, Watkins KC, Descarries L, Cozzari C, Hartman BK. 1994. Ultrastructural and morphometric features of the acetylcholine innervation in adult rat parietal cortex. An electron microscopic study in serial sections. J Comp Neurol 348:351-373.

Vaucher E, Hamel E. 1995. Cholinergic basal forebrain neurons project to cortical microvessels in the rat : electron microscopic study with anterogradely transported *Phaseolus vulgaris* leucoagglutinin and choline acetyltransferase immunocytochemistry. J Neurosci 15:7427-7441.

Xiang Z, Huguenard JR, Prince DA. 1998. Cholinergic switching within neocortical inhibitory networks. Science 281:985-988.

Zhu XO, Waite PME. 1998. Cholinergic depletion reduces plasticity of barrel field cortex. Cereb Cortex 8:63-72.

Zoli M, Le Novère N, Hill JA, Changeux J-P. 1995. Developmental regulation of nicotinic ACh receptor subunit mRNAs in the rat central and peripheral nervous systems. J Neurosci 15:1912-1939.

Table 1. Data for the number of single sectional profiles of varicosities indicated. The unlabeled profiles were selected at random from the same micrographs displaying the ACh (ChAT-immunostained) profiles, as explained in Materials and Methods. Means ± s.d. from 3 rats per postnatal age. In this and subsequent tables, * designates $p < 0.05$ for age-related differences, as analyzed by Kruskal-Wallis test.

Table 1. MORPHOMETRIC FEATURES OF ACh VERSUS RANDOMLY SELECTED UNLABELED AXON VARICOSITIES IN THE DEVELOPING PARIETAL CORTEX OF RAT

Postnatal age	P8		P16		P32	
	ACh	Unlabeled	ACh	Unlabeled	ACh	Unlabeled
Number examined	300	100	300	100	300	100
Dimensions						
Area (μm^2)	0.17 ± 0.02	0.18 ± 0.04	0.16 ± 0.01	0.17 ± 0.03	0.16 ± 0.02	0.19 ± 0.02
Diameter (μm)	0.49 ± 0.03	0.47 ± 0.05	0.46 ± 0.01	0.47 ± 0.03	0.48 ± 0.02	0.50 ± 0.02
Long axis (μm)	0.66 ± 0.02	0.59 ± 0.07	0.64 ± 0.04	0.61 ± 0.03	0.65 ± 0.03	0.65 ± 0.02
Short axis (μm)	0.32 ± 0.02	0.34 ± 0.03	0.30 ± 0.03	0.32 ± 0.03	0.31 ± 0.01	0.35 ± 0.03
Aspect ratio	2.18 ± 0.10	1.83 ± 0.16	2.30 ± 0.34	2.00 ± 0.15	2.18 ± 0.02	1.98 ± 0.18
% with mitochondria	20.7 ± 2.3 *	16.7 ± 6.8	38.7 ± 10.3 *	21.7 ± 4.0	43.7 ± 4.2 *	25.7 ± 1.5

Table 2. Data from the same single sectional profiles of varicosities as in Table 1 (means ± s.d. from 3 rats per postnatal age). The varicosity profiles were classified as showing or not a synaptic junction according to the criteria described in Materials and Methods. The synaptic incidence for the whole volume of varicosities was extrapolated by means of the stereological formula of Beaudet and Sotelo (1981), using the long axis as diameter of the profiles (Umbriaco et al., 1994).

Table 2. JUNCTIONAL FEATURES OF ACh VERSUS RANDOMLY SELECTED UNLABELED AXON VARICOSITIES IN THE DEVELOPING PARIETAL CORTEX OF RAT

Postnatal age	P8		P16		P32	
	ACh	Unlabeled	ACh	Unlabeled	ACh	Unlabeled
Synaptic incidence (%)						
Single sections	6.3 ± 1.5	24.7 ± 11.0	6.7 ± 2.5	43.7 ± 12.1	8.7 ± 2.1	49.0 ± 7.0
Whole volume	13.2 ± 3.2	54.6 ± 24.4 *	15.6 ± 5.9	102.4 ± 28.4 *	22.2 ± 5.4	119.6 ± 17.1 *
Synaptic targets (%)						
Dendritic branches	72.7 ± 11.7	81.7 ± 16.1 *	55.0 ± 14.2	51.3 ± 8.1 *	84.0 ± 18.3	24.7 ± 5.8 *
Dendritic spines	27.3 ± 11.7	18.3 ± 16.1 *	45.0 ± 14.2	48.7 ± 8.1 *	16.0 ± 18.3	75.3 ± 5.8 *

Table 3. Same single sectional profiles of varicosities as in Tables 1 and 2. The data presented under "Normalized frequency (%)" are the average number of juxtaposed elements for 100 varicosities in each group (means ± s.d. from 3 rats per postnatal age).

Table 3. MICROENVIRONMENT OF ACh VERSUS RANDOMLY SELECTED UNLABELED AXON VARICOSITIES IN THE DEVELOPING PARIETAL CORTEX OF RAT

Postnatal age	P8		P16		P32	
	ACh	Unlabeled	ACh	Unlabeled	ACh	Unlabeled
Normalized frequency (%)						
Axon varicosities	52.3 ± 9.4	56.7 ± 20.4	62.7 ± 34.5	78.3 ± 21.5	91.3 ± 7.02	85.0 ± 20.8
Dendritic branches	248 ± 11.5 *	243.3 ± 24.8	193.0 ± 40.1 *	201.7 ± 20.6	199.3 ± 12.7 *	216.0 ± 21.3
Dendritic spines	21.0 ± 7.6	24.7 ± 5.5 *	40.3 ± 20.5	46.0 ± 6.6 *	32.7 ± 4.5	60.7 ± 8.5 *
Neurites	224.3 ± 28.6	162.7 ± 28.3 *	251.3 ± 40.2	239.7 ± 28.0 *	207.7 ± 14.6	238.3 ± 10.2 *
Miscellaneous	133.3 ± 10.1	157.3 ± 19.4 *	112.0 ± 37.5	107.0 ± 32.4 *	128.7 ± 7.6	94.3 ± 12.5 *

Figure 1. Low power photomicrographs (X 70) illustrating the distribution of the ACh innervation in the primary somatosensory cortex (Par1 area) at postnatal ages P8 (A), P16 (B) and P32 (C). At P8 (A), as previously described (Mechawar and Descarries, 2001a), the thin varicose ChAT-immunostained axons already form an intricate network in every layer, and numerous interneurons are also strongly immunoreactive. In this cortical area, the mature laminar pattern of ACh innervation is established at P16 (B), and there is only a minimal increase in density to the adult-like appearance at P32 (C) (for details, see Mechawar and Descarries, 2001a).

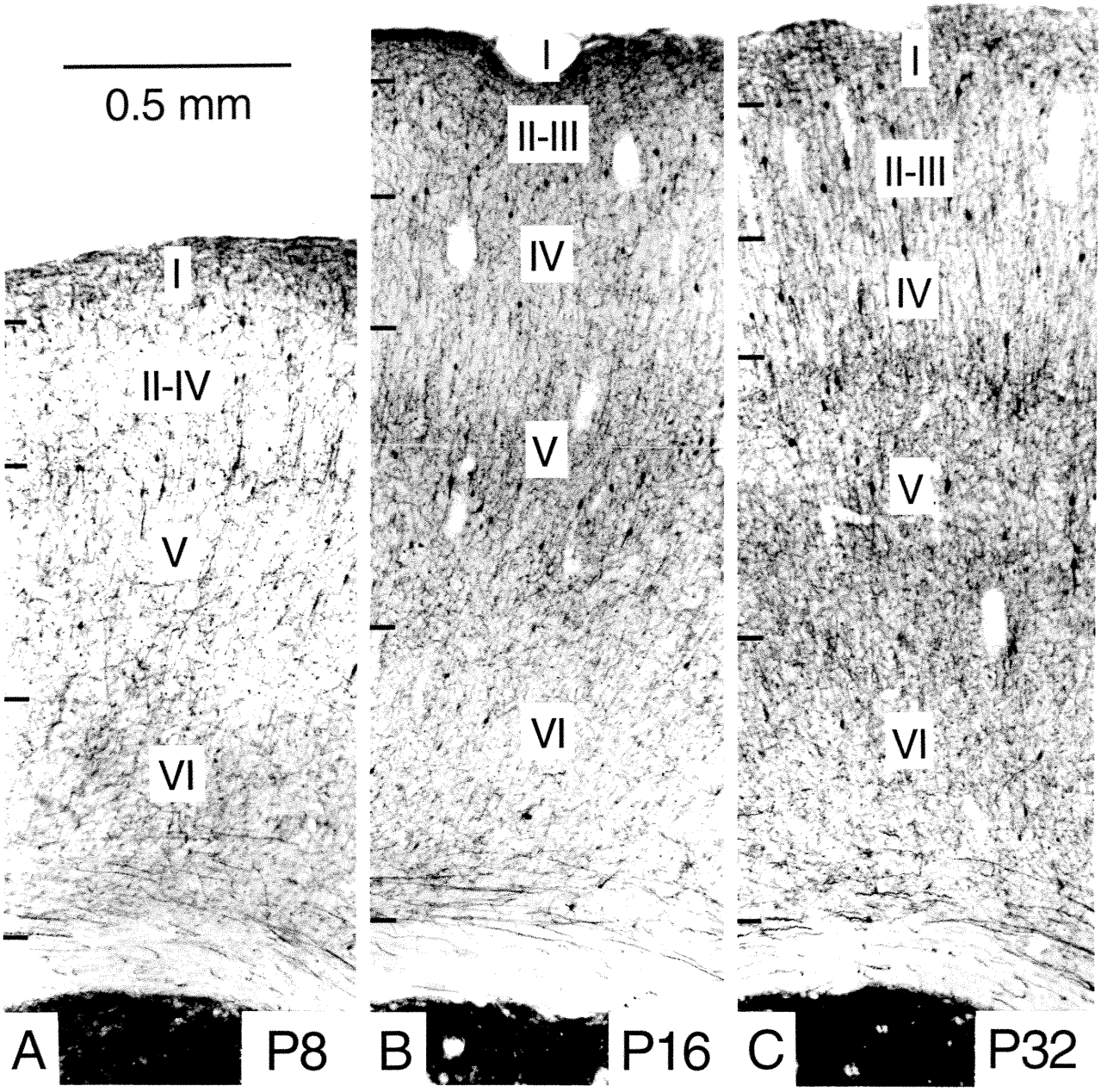
0.5 mm
I
II-IV
V
VI
A
P8
I
II-III
IV
V
VI
B
P16
I
II-III
IV
V
VI
C
P32

Figure 2A-I. Electron micrographs (X 30 000) of ACh (ChAT-immunostained) axon varicosities from the parietal cortex at postnatal ages P8 (A-C), P16 (D-F) and P32 (G-I). The labeled profiles are identified as axon varicosities by their content in aggregated synaptic vesicles. Most also display a mitochondrion (B, E, F-I). Their average size does not significantly differ from P8 to P32. Of the three ACh varicosities at P8 (A, B and C, respectively from layers VI, II-IV and V), only the third (C) displays a synaptic junction (between thin arrows), which is made with a dendritic branch (d). The same is true of the three varicosities at P16 (D, E and F, respectively from layers IV, VI and VI) ; the synapse in F (between thin arrows) is also made with a dendritic branch (d) and it is clearly symmetrical. In the P32 row (G, H, and I, respectively from layers I, V and V), the synapse made by the varicosity in I (between thin arrows) is of the perforated variety, asymmetrical, and made with a dendritic spine (**), which also receives two other synaptic varicosities (V_2 and V_3), unlabeled. Note the diverse structural microenvironment of these ACh varicosities at all ages. In A-C, all three varicosities are partly surrounded by dendritic branches (d). The one in D comes close to a capillary (L in lumen), from which it remains separated by an astrocyte (as). In E, the ACh varicosity is juxtaposed to the base of a dendritic trunk (dt). In G and H, direct apposition to dendritic branches (d) may be observed, as well as juxtaposition to a nerve cell body (N) in H. Scale bar (in I): 0.5 μm.

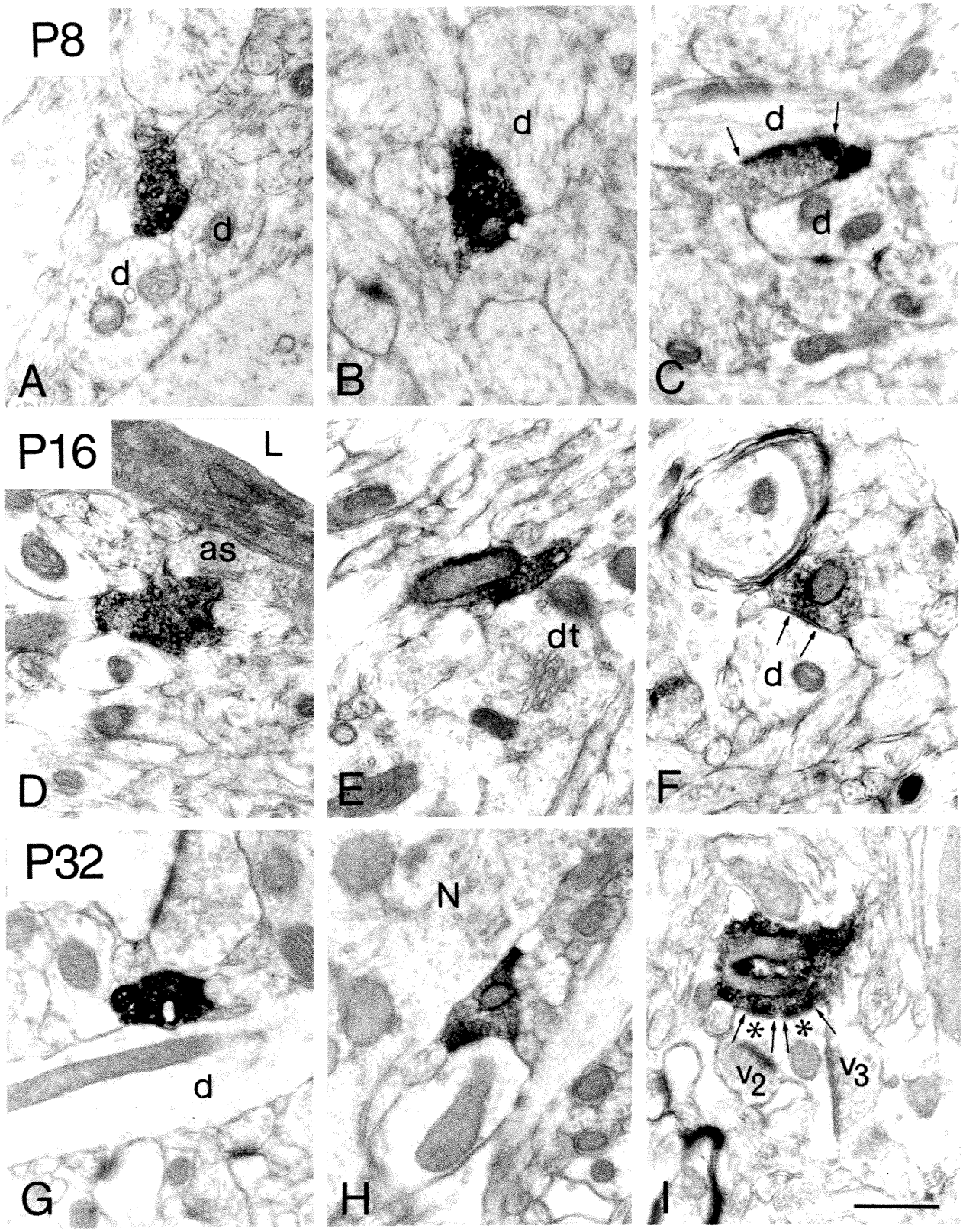
P8
d
d
A
d
B
d
d
C
P16
L
as
D
dt
E
d
F
P32
d
G
N
H
*
*
V2
V3
I

Chapitre V

DISCUSSION GÉNÉRALE

V.1 VISUALISATION, QUANTIFICATION ET CARACTÉRISATION ULTRASTRUCTURALE DE L'INNERVATION CHOLINERGIQUE CORTICALE: CONSIDÉRATIONS MÉTHODOLOGIQUES

V.1.1 L'anticorps

La disponibilité d'un anticorps monoclonal à très haute affinité contre la ChAT de cerveau de rat a été déterminante pour la réalisation des trois articles de recherche constituant l'essentiel du présent ouvrage. Même si la caractérisation et la spécificité immunologiques de cet anticorps n'ont fait l'objet que d'un seul résumé publié (Cozzari et al., 1990), elles ont été étudiées en détail (C. Cozzari et B. K. Hartman, communication personelle de deux manuscrits en préparation). Quant à sa spécificité immunocytochimique, elle a fait l'objet de nombreuses démonstrations formelles, surtout d'ordre neurocytologique, qui appartiennent maintenant à la littérature (ex.: Cossette et al., 1993; Chédotal et al., 1994a,b; Umbriaco et al., 1994, 1995; Contant et al., 1996; Jaarsma et al., 1996; Molnar et al., 1998; Deller et al., 1999; Oakman et al., 1999). L'affinité remarquable de cet anticorps pour la ChAT en fait un outil de détection très sensible, et donc idéal pour la visualisation immunocytochimique des projections axonales ACh plus ou moins éloignées des corps cellulaires d'origine.

V.1.2 La détection de l'innervation ACh en microscopie optique

L'utilisation de l'anticorps de Cozzari et Hartman a conduit à la visualisation immunocytochimique, en microscopie optique, d'un réseau relativement dense de fibres variqueuses au sein de toutes les couches et toutes les aires corticales examinées (voir ci-haut), de même que dans l'hippocampe (voir Annexe 2). La haute sensibilité de cet anticorps a aussi permis d'obtenir un marquage intense de fibres au sein du cortex cérébral en développement, notamment au cours de la première semaine postnatale, et ceci alors même que des études immunocytochimiques antérieures avec d'autres

anticorps dirigés contre la ChAT n'avaient révélé la présence de ces fibres qu'à partir de la fin de la deuxième semaine postnatale (Dori et Parnavelas, 1989; Gould et al., 1991).

V.1.3 Le marquage intégral en vue de la quantification

Les conditions immunocytochimiques employées pour nos marquages ont autorisé une visualisation optimale, en microscopie optique, du réseau axonal ACh cortical, et ceci dans toute l'épaisseur des coupes histologiques de 50 μm utilisées au cours de notre premier travail. L'élaboration et l'utilisation d'une véritable méthode de quantification par immunocytochimie d'une innervation requérait cependant une preuve expérimentale à l'effet que ces conditions qualitativement optimales correspondaient à une mise en évidence intégrale (maximale) de l'innervation à l'étude. C'est ce que nous ont montré les résultats obtenus en présence de concentrations croissantes d'anticorps et par suite de révélations pour des durées variables (voir Chapitre II). De plus, nous avons pu constater au cours de cette même étude que les mesures de longueur axonale obtenues de l'un ou l'autre des trois plans de mise au point nécessaires à la visualisation de toute l'épaisseur des coupes étaient une fraction constante des valeurs pour toute leur épaisseur. En conséquence, lors des études subséquentes, nous avons pu nous contenter de recueillir les données à partir d'un seul plan focal, ce qui a considérablement simplifié la méthode et permis le recueil de données à partir d'un plus grand nombre d'échantillons.

V.1.4 Avantages de la méthode de quantification

Toutes les données quantifiées au sein du cortex cérébral adulte et en cours de développement ont été acquises grâce à la mise au point de cette méthode semi-informatisée, incluant les modalités d'échantillonage, de collecte et de transformation

des données, tel que décrit en détail au Chapitre II. En bref, cette approche fournit une mesure de la longueur réelle d'axones et du nombre réel des varicosités axonales immunoréactives dans une surface et une épaisseur connues de tissu cérébral. Son avantage principal est de fournir des valeurs absolues, ce en quoi elle diffère de la plupart des méthodes précédemment utilisées pour la quantification par immunocytochimie d'axones et de varicosités, qui restent semi-quantitatives (relatives) (ex.: Stichel et Singer, 1987; Kritzer et Kohama, 1998). L'emploi subséquent de cette méthode pour la quantification de l'innervation ACh de l'hippocampe chez le rat et la souris a montré son applicabilité à d'autres régions cérébrales et d'autres espèces animales (Aznavour et al., 2001; voir Annexe 2). De plus, elle a récemment permis la détection de changements relativement subtils (20-30%) de densités d'innervation dans le cas de fibres à sérotonine au sein de différentes régions cérébrales chez un modèle de souris knockout (Ase et al., 2001), ce qui montre son applicabilité à d'autres systèmes immunocytochimiquement définis. Elle pourra donc s'avérer d'un intérêt général dans l'avenir, ouvrant la voie à l'étude quantitative d'un grand nombre de systèmes neuronaux, dans des conditions expérimentales très diverses (mutants, lésions, traitements pharmacologiques, etc.)

Afin de pouvoir convertir les données sur la longueur des axones ACh en nombre de varicosités axonales dans les différentes couches et régions du cortex cérébral, nous avons dû obtenir des mesures directes du nombre moyen de varicosités par unité de longueur d'axone cholinergique. Cette investigation a révélé la constance du nombre moyen de varicosités par longueur d'axone (4 par 10 μm) dans toutes les couches et aires examinées du cortex adulte, mais une croissance importante (du simple au double) de ce nombre dans le cortex en développement entre 4 et 16 jours après la naissance (voir Chapitre III). En possession de ce dernier renseignement, les mesures

de densité laminaire ou régionale d'axones (mètres/mm^3) ont pu être converties en densités de varicosités (millions/mm^3) tant au cours du développement que chez l'adulte. En outre, une telle expression des données en valeurs par unité de volume autorisait la corrélation avec de nombreux autres paramètres chiffrés d'ordre neurocytologique ou neurochimique. De plus, les données ont été exprimées par rapport à un volume cortical situé sous une surface de 1 millimètre carré. De cette façon, des longueurs réelles d'axone et des nombres réels de varicosités ont été produits, qui pouvaient notamment tenir compte du changement d'épaisseur du cortex au cours du développement. Finalement, puisque de telles données se prêtaient à une analyse statistique, les valeurs laminaires et régionales obtenues dans les trois aires corticales et aux différents âges postnataux ont pu être comparées entre elles.

V.1.5 La visualisation en microscopie électronique

Une fois l'innervation ACh corticale décrite et quantifiée au cours du développement, il devenait naturel de s'interroger sur ses propriétés ultrastructurales à ce stade. Il était particulièrement intrigant de savoir si la prépondérance de varicosités ACh asynaptiques est une caractéristique exclusive aux axones ACh chez adulte (Umbriaco et al., 1994), ou s'il s'agit d'une propriété inhérente de cette innervation, observable tout au cours de son propre développement. Encore une fois, l'anticorps anti-ChAT dont nous disposions permettait de répondre à cette questions. En effet, sa visualisation immunocytochimique est compatible avec une fixation tissulaire incluant le glutaraldéhyde en concentration suffisante pour obtenir une préservation adéquate de la structure fine du cortex. Nous avons donc entrepris de décrire, par immunocytochimie en microscopie électronique, l'innervation ACh du cortex pariéral du rat à trois âges postnataux (8, 16 et 32 jours). Cette région corticale constituait un objet d'étude d'autant plus approprié que l'innervation ACh s'y

développe plus rapidement qu'ailleurs, et qu'elle avait déjà fait l'objet d'une étude ultrastructurale extrêmement élaborée chez l'adulte (Umbriaco et al., 1994). Au cours de cette étude antérieure, plus de 800 varicosités ChAT-immunoréactives avaient été échantillonées à partir de toutes les couches corticales, puis décrites, mesurées et comparées à une population de varicosités axonales non marquées échantillonées au hasard à partir des mêmes micrographies. L'incidence synaptique de ces varicosités avait été déterminée de deux manières: 1) par observation directe à partir des coupes fines sériées à travers le volume entier des varicosités, et 2) à partir de coupes fines isolées choisies au hasard au travers de ces mêmes varicosités, grâce à la formule de Beaudet et Sotelo (1981), qui prend en compte le diamètre moyen des varicosités, la longueur des complexes de jonction et l'épaisseur des coupes fines. L'extrapolation à partir de cette formule ayant donné un résultat pratiquement identique à l'observation directe lorsque le plus grand diamètre des profils de coupe était utillisé comme diamètre moyen (Umbriaco et al., 1994), c'est avec assurance que nous y avons eu recours, avec cette modification, pour déterminer l'incidence synaptique dans le matériel examiné aux différents âges postnataux. En outre, comme dans plusieurs études précédentes du laboratoire, nous avons complété la description des caractéristiques et relationnelles des varicosités examinées par celle de leur microenvironnement cytologique immédiat, de manière à identifier les cibles potentielles d'un neurotransmetteur/modulateur libéré à partir de varicosités majoritairement asynaptiques et donc capable de diffusion dans l'espace extracellulaire.

V.2 DISTRIBUTION RÉGIONALE ET LAMINAIRE DE L'INNERVATION CHOLINERGIQUE CORTICALE CHEZ LE RAT ADULTE

V.2.1 Rappel des principaux résultats et implications fonctionnelles

Ayant mis au point une méthode de quantification semi-informatisée permettant de déterminer la longueur des axones et le nombre des varicosités (terminaisons) axonales cholinergiques dans des coupes de cerveau immunocolorées pour la choline acétyltransférase (ChAT), l'enzyme de biosynthèse de l'acétylcholine (ACh), nous avons déterminé la densité régionale et laminaire d'innervation ACh dans les cortex primaires frontal (moteur), pariétal (somatosensoriel) et occipital (visuel) du rat adulte. Le nombre de varicosités par unité de longeur d'axone s'est avéré constant (4 par 10 μm) dans ces aires corticales et leurs différentes couches. La plus forte densité moyenne d'axones et de varicosités a été retrouvée dans le cortex frontal (13.0 m/mm^3 d'axones comparativement à 9.9 et 11.0 m/mm^3 dans les cortex pariétal et occipital, respectivement; 5.4 x 10^6/mm^3 de varicosités comparativement à 3.8 et 4.6 x 10^6/mm^3). Dans les trois aires corticales, la couche I montrait les plus fortes densités d'axones et de varicosités ACh (13.5 m/mm^3 et 5.4 x 10^6/mm^3 dans le cortex frontal). Les plus faibles étaient celles de la couche IV du cortex pariétal (7.3 m/mm^3 et 2.9 x 10^6/mm^3). Les longeurs d'axone sous 1 mm^2 de surface corticale étaient respectivement de 26.7, 19.7 et 15.3 m dans les aires frontale, pariétale et occipitale, pour des nombres correspondants de varicosités de 11.1, 7.7 et 6.4 x 10^6. Selon l'estimation antérieure de l'incidence synaptique des varicosités ACh dans les différentes couches du cortex pariétal (Umbriaco et al., 1994), ces valeurs représentent un total de 1.2 x 10^6 varicosités ACh synaptiques sous 1 mm^2 de surface corticale, dont 48% résident dans la couche V. Sachant que la composante synaptique de l'innervation ACh corticale est prépondérante dans la couche V, nos données suggèrent un rôle de cette

neurotransmission/modulation dans le traitement de l'information sortante comme entrante du cortex. Une extrapolation des valeurs en termes de longueur totale d'axone et de nombre total de varicosités pour l'ensemble du cortex cérébral, de longueur d'axone et de nombre de varicosités par neurone ACh se projettant au cortex, ainsi que de concentration d'ACh par varicosité axonale, permet aussi d'en arriver à une meilleur définition du rôle et des propriétés de ce neurotransmetteur/modulateur dans le cortex.

V.2.2 Implications neurobiologiques

Ces données chiffrées sur l'innervation ACh du cortex cérébral laissent comprendre qu'il s'agit de la plus dense des innervations neuromodulatrices du néocortex (voir aussi l'Annexe 2). Par comparaison aux densités moyennes d'innervation mesurées précédemment pour les monoamines au sein des mêmes aires corticales, la densité régionale moyenne d'innervation ACh (4.6×10^6 varicosités/mm^3) s'avère plus de deux fois supérieure à celle de la dopamine, plus de quatre fois celle de la noradrénaline, et légèrement supérieure à celle de la sérotonine. L'avenir saura sans doute nous apprendre dans quelle mesure l'abondance respective de chacune de ces innervations traduit leur importance relative en termes de fonction corticale.

Connaissant le volume entier du cortex cérébral chez le rat, le nombre de neurones ACh se projettant au cortex, et faisant abstraction de la faible proportion de cette innervation qui provient des interneurones ACh, l'extrapolation de ces données laisse supposer que les neurones basalo-corticaux auraient une arborisation axonale totale de 7.6 kilomètres comportant 3.1 milliards de varicosités et, qu'en moyenne, individuellement, leur axone aurait une longueur d'environ un mètre et environ 400 000 varicosités. Tout en évoquant une image renouvelée du neurone cholinergique, ces

chiffres à eux seuls constituent un puissant argument en faveur d'une influence ubiquitaire de l'ACh au sein du cortex cérébral.

V.3 INNERVATION CHOLINERGIQUE À DIVERS STADES DU DÉVELOPPEMENT DU CORTEX CÉRÉBRAL CHEZ LE RAT

V.3.1 Rappel des principaux résultats et implications fonctionnelles

Grâce à la méthode de quantification mise au point chez l'adulte, et par suite de sa simplification par la collecte des données dans un seul plan focal, nous étions en position de pouvoir déterminer les densités régionale et laminaire d'innervation ACh des cortex frontal, pariétal et occipital du raton à divers âges après la naissance. Nous avons alors constaté l'apparition précoce de cette innervation, puisque quelques fibres immunoréactives pour la ChAT, dotées d'un cône de croissance, ont pu être observées dans la sous-plaque dès le jour de la naissance. Au cours des deux premières semaines, nous avons constaté que l'innervation ACh se développe rapidement en fonction de trois paramètres: un accroissement progressif du nombre de varicosités par unité de longueur d'axone, ainsi que l'allongement et l'arborisation progressive des axones. Entre les jours 4 et 16, le nombre de varicosités passe de 2 à 4 par 10 μm dans toutes les couches et aires corticales. Les densités moyennes d'axones augmentent respectivement de 1.4 à 9.6, 1.7 à 9.3 et 0.7 to 7.2 m/mm^3 et celles des varicosities de 0.4 à 3.9, 0.4 à 3.5 et 0.2 à 2.6 x 10^6/mm^3, dans les cortex frontal, pariétal et occipital. Le taux de croissance est maximal durant ces deux premières semaines, après quoi le pattern caractéristique de chaque aire semble établi. Les valeurs de densité adulte sont presqu'atteintes au jour 16 dans le cortex pariétal, mais le sont seulement plus tard (32 jours) dans les aires frontale et surtout occipitale. Ces données quantitatives

sur l'installation, la croissance et la maturation de l'innervation ACh dans le cortex cérébral en développement viennent étayer la possibilité d'un ou de plusieurs rôles de l'ACh au cours de cette période de plasticité morpho-fonctionnelle particulièrement intense. Elles soulignent également l'étonnante capacité de croissance des unités neuronales cholinergiques.

V.3.2 Implications neurobiologiques

Cette capacité phénoménale de croissance axonale était jusqu'ici insoupçonnée pour les neurones ACh basalo-corticaux. Au cours des deux premières semaines suivant la naissance, soit durant leur période de croissance maximale, ces neurones produisent quotidiennement environ 5 cm d'axone arborant 18000 varicosités, c'est-à-dire plus de 2 mm d'axone et 750 varicosités par heure. Fait à souligner, cette croissance est maximale durant une période considérée comme critique pour le développement du cortex cérébral. Les exigences d'une telle croissance neuronale aux plans métabolique et biophysique, ainsi que les mécanismes cellulaires et moléculaires qui en sont responsables, restent à élucider. Il serait intéressant de savoir si d'autres afférences neuromodulatrices du cortex cérébral présentent le même rythme et la même amplitude de croissance au cours du développement du cortex.

V.4 L'ULTRASTRUCTURE DE L'INNERVATION CHOLINERGIQUE DU CORTEX PARIÉTAL EN DÉVELOPPEMENT CHEZ LE RAT

V.4.1 Rappel des principaux résultats

Pour donner suite à l'étude quantitative du développement de l'innervation cholinergique du néocortex chez le rat, nous avons examiné par immunocytochimie en microscopie électronique de la ChAT des varicosités axonales du cortex pariétal

de rats agés de 8, 16 et 32 jours. Tels que visualisés en coupes fines isolées, et comparés à ceux de varicosiés non marquées choisies au hasard dans les mêmes micrographies, les profils immunoréactifs pour la ChAT ont montré des caractéristiques ultrastructurales intrinsèques et relationnelles très semblables à celles précédemment décrites dans le cortex adulte (Umbriaco et al., 1994). Aux trois âges postnataux, ces profils étaient comparables d'une couche corticale à l'autre, quant à leur forme, leur dimension et leur contenu vésiculaire. Seule la fréquence avec laquelle les profils contenaient une mitochondrie variait, augmentant avec l'âge pour atteindre 44% a P32. Des jonctions synaptiques ont été observées sur 6.3 à 8.7% de ces profils, indiquant une incidence synaptique moyenne de 16.7% pour les varicosités entières; une donnée aussi comparable à celle de l'adulte (14%). Comme chez l'adulte, les jonctions formées par les rares varicosités ACh synaptiques étaient toujours uniques, généralement symétriques et plus fréquemment trouvées sur des branches que des épines dendritiques. Les varicosités ACh corticales s'avèrent donc en vaste majorité asynaptiques (80-85%) dès lors que cette innervation s'installe dans le cortex, indiquant qu'il s'agit d'une caractéristique morphologique inhérente, et suggérant qu'un mode de transmission diffus ainsi qu'un niveau ambiant d'ACh dans l'espace extracellulaire puissent contribuer aux divers effets de ce neurotransmetteur/modulateur au cours du développement cortical.

V.4.2 Implications neurobiologiques

La nature fortement asynaptique des varicosités axonales ACh dès l'installation de cette innervation dans le cortex laisse supposer qu'il s'agit d'une caractéristique neurobiologique fondamentale inhérente à ces neurones. Elle pose la question des facteurs mis en cause, soit en termes de neurones d'origine vs territoire d'innervation,

soit en termes de déterminants moléculaires. Le territoire d'innervation n'est certes pas exclu en tant qu'élément de la relation, puisque dans le cas d'autres systèmes partiellement synaptiques, la proportion des varicosités qui font jonction dans un territoire donné est maintenue même lorsque ce territoire est innervé en excès (ex.: neostriatum ou hippocampe). Il faut cependant souligner que la proportion reste aussi la même lorsque cette hyperinnervation est issue de neurones qui, normalement, ne se projettaient pas à ce territoire (Daszuta et al., 1991). En termes de déterminants moléculaires, dont la nature reste à déterminer, il faut donc supposer l'existence de signaux rétrogrades qui pourraient alors informer le neurone du nombre de varicosités synaptiques versus asynaptiques qu'il lui faut produire.

V.4.3 Implications fonctionelles

Dans le cortex en développement comme adulte, la nature majoritairement non jonctionnelle de l'innervation ACh laisse supposer un mode de fonctionnement du type transmission diffuse, au sens d'une capacité d'action sur une variété de cibles fonctionnelles et d'une sphère d'influence de dimension considérable. Aucune donnée expérimentale ne permet actuellement de confirmer cette hypothèse dans le cas de l'ACh corticale. Par contre, la possibilité d'une transmission diffuse et d'un niveau ambiant d'ACh dans l'espace extracellulaire semble d'autant plus forte que les effets attribués à l'ACh dans le cortex cérébral en développement sont d'ordre très général, comme ceux sur la prolifération cellulaire et la plasticité des cartes sensorielles. Il apparaît peu vraisemblable qu'au moment où ces effets sont les plus manifestes, ils soient sous-tendus par un mode de communication interneuronale qui, quantitativement du moins, soit très peu représenté dans le cortex. À cet égard, deux types de données expérimentales pourraient s'avérer des plus instructives dans un proche avenir. D'une part, des renseignements fiables sur la localisation subcellulaire

des récepteurs cholinergiques dans le cortex; d'autre part, une connaissance des conséquences de l'absence de certains de ces récepteurs sur la morphogénèse et la plasticité corticale. Une histoire à suivre...

BIBLIOGRAPHIE GÉNÉRALE

Alkondon M, Pereira EFR, Eisenberg HM, Albuquerque EX. 2000. Nicotinic receptor activation in human cerebral cortical interneurons: a mechanism for inhibition and disinhibition of neural networks. J Neurosci 20:66-75.

Aramakis VB, Hsieh CY, Leslie FM, Metherate R. 2000. A critical period for nicotine-induced disruption of synaptic development in rat auditory cortex. J Neurosci 20:6106-6116.

Arvidsson U, Riedl M, Elde R, Meister B. 1997. Vesicular acetylcholine transporter (VAChT) protein: a novel and unique marker for cholinergic neurons in the central and peripheral nervous system. J Comp Neurol 378:454-467.

Ase AR, Reader TA, Hen R, Riad M, Descarries L. 2001. Region specific changes in density of serotonin transporter in the brain of 5-HT1A and 5-HT1B knockout mice and of serotonin innervation in the 5-HT1B knockout. J Neurochem (sous presse).

Aubert I, Cécyre D, Gauthier S, Quirion R. 1996. Comparative ontogenic profile of cholinergic markers, including nicotinic and muscarinic receptors, in the rat brain. J. Comp Neurol 369:31-55.

Audet MA, Descarries L, Doucet G. 1989. Quantified regional and laminar distribution of the serotonin innervation in the anterior half of adult rat cerebral cortex. J Chem Neuroanat 2:29-44.

Audet MA, Doucet G, Oleskevich S, Descarries L. 1988. Quantified regional and laminar distribution of the noradrenaline innervation in the anterior half of the adult rat cerebral cortex. J Comp Neurol 274:307-318.

Aznavour N, Mechawar N, Descarries L. 2001. Comparative analysis of cholinergic innervation in the dorsal hippocampus of adult mouse and rat: a quantitative immunocytochemical study. Hippocampus (sous presse).

Bartus RT, Dean RL, Beer B, Lippa AS. 1982. The cholinergic hypothesis of geriatric memory dysfunction. Science 217:408-417.

Bayraktar T, Staiger JF, Acsady L, Cozzari C, Freund TF, Zilles K. 1997. Co-localization of vasoactive intestinal polypeptide, γ-aminobutyric acid and choline acetyltransferase in neocortical interneurons of the adult rat. Brain Res 757:209-217.

Bear MF, Singer W. 1986. Modulation of visual cortical plasticity by acetylcholine and noradrenaline. Nature 320:172-176.

Beaudet A, Descarries L. 1976. Quantitative data on serotonin nerve terminals in adult rat neocortex. Brain Res 11:301-309.

Beaudet A, Descarries L. 1978. The monoamine innervation of rat cerebral cortex: synaptic and non synaptic axon terminals. neuroscience 3:851-860.

Beaudet A, Sotelo C. 1981. Synaptic remodeling of serotonin axon terminals in rat agranular cerebellum. Brain Res 206:305-329.

Broide RS, Robertson RT, Leslie FM. 1996. Regulation of α7 nicotinic acetylcholine receptors in the developing rat somatosensory cortex by thalamocortical afferents.

Bucci DJ, Holland PC, Gallagher M. 1998. Removal of cholinergic input to rat posterior parietal cortex disrupts incremental processing of conditionned stimuli. J Neurosci 18:8038-8046.

Buwalda B, de Groote L, Van der Zee EA, Matsuyama T, Luiten PGM. 1995. Immunocytochemical demonstration of developmental distribution of muscarinic acetylcholine receptors in rat parietal cortex. Dev Brain res 84:185-191.

Buzsáki G, Bickford RG, Ponomareff G, Thal LJ, Mandel R, Gage FH. 1988. Nucleus basalis and thalamic control of neocortical activity in the freely moving rat. J Neurosci 8:4007-4026.

Calarco CA, Robertson RT. 1995. Development of basal forebrain projections to visual cortex: DiI studies in the rat. J Comp Neurol 354:608-626.

Celesia GG, Jasper HH. 1966. Acetylcholine released from cerebral cortex in relation to state of activation. Neurology 16:1053-1063.

Chédotal A, Cozzari C, Faure MP, Hartman BK, Hamel E. 1994a. Distinct choline acetyltransferase (ChAT) and vasoactive intestinal polypeptide (VIP) bipolar neurons project to local blood vessels in the rat cerebral cortex. Brain Res 646:181-193.

Chédotal A, Umbriaco D, Descarries L, Hartman BK, Hamel E. 1994b. Light and electron microscopic immunocytochemical analysis of the neurovascular relationships of choline acetyltransferase and vasoactive intestinal polypeptide nerve terminals in the rat cerebral cortex. J Comp Neurol 343:57-71.

Cohen Z, Molinatti G, Hamel E. 1997. Astroglial and vascular interactions of noradrenaline terminals in the rat cerebral cortex. J Cereb Blood Flow Metab 17:894-904.

Cohen Z, Ehret M, Maitre M, Hamel E. 1995. Ultrastructural analysis of tryptophan hydroxylase immunoreactive nerve terminals in the rat cerebral cortex and hippocampus: their associations with local blood vessels. Neuroscience 66:555-569.

Conner JM, Varon S. 1997. Developmental profile of NGF immunoreactivity in the rat brain: a possible role of NGF in the establishment of cholinergic terminal fields in the hippocampus and cortex. Dev Brain Res 101:67-79.

Contant C, Umbriaco D, Garcia S, Watkins KC, Descarries L. 1996. Ultrastructural characterization of the acetylcholine innervation in adult rat neostriatum. Neuroscience 71:937-947.

Cossette P, Umbriaco D, Zamar N, Hamel E, Descarries L. 1993. Recovery of choline acetyltransferase activity without sprouting of the residual acetylcholine innervation in adult rat cerebral cortex after lesion of the nucleus basalis. Brain Res 630:195-206.

Coyle JT, Yamamura HI. 1976. Neurochemical aspects of the ontogenesis of cholinergic neurons in the rat brain. Brain Res 118:429-440.

Cozzari C, Howard J, Hartman B. 1990. Analysis of epitopes on choline acetyltransferase (ChAT) using monoclonal antibodies (Mabs). Soc Neurosci Abstr 16:200.

Crowley JC, Katz LC. 1999. Development of ocular dominance columns in the absence of retinal input. Nat Neurosci 2:1125-1130.

Crowley JC, Katz LC. 2000. Early development of ocular dominance columns. Science 290:1321-1324.

Dalley JW, McGaughy J, O'Connell MT, Cardinal RN, Levita L, Robbins TW. 2001. Distinct changes in cortical acetylcholine and noradrenaline efflux during contingent and noncontingent performance of a visual attentional task. J Neurosci 21:4908-4914.

Daszuta A, Chazal G, Garcia S, Oleskevich S, Descarries L. 1991. Ultrastructural features of serotonin neurons grafted to adult rat hippocampus: an immunocytochemical analysis of their cell bodies and axon terminals. Neuroscience 42:793-811.

Deller T, Katona I, Cozzari C, Frotscher M, Freund TF. 1999. Cholinergic innervation of mossy cells in the rat fascia dentata. Hippocampus 9:314-320.

Descarries L, Mechawar N. 2000. Ultrastructural evidence for diffuse transmission by monoamine and acetylcholine neurons in the central nervous system. In: Agnati LF, Fuxe K, Nicholson C, Sykova E, editors: Volume Transmission Revisited. Prog Brain Res, Vol 125, Elsevier, Amsterdam 125:27-47.

Descarries L, Beaudet A, Watkins KC. 1975. Serotonin nerve terminals in adult rat neocortex. Brain Res 100:563-588.

Descarries L, Gisiger V, Steriade M. 1997. Diffuse transmission by acetylcholine in the CNS. Prog Neurobiol 53:603-625.

Descarries L, Watkins KC, Lapierre Y. 1977. Noradrenergic axon terminals in the cerebral cortex of rat. III. Topometric ultrastructural analysis. Brain Res 133:197-222.

Descarries L, Lemay B, Doucet G, Berger B. 1987. Regional and laminar density of the dopamine innervation in adult rat cerebral cortex. Neuroscience 21:807-824.

Détari L. 2000. Tonic and phasic influence of basal forebrain unit activity on the cortical EEG. Beh Brain Res 115:159-170.

Dinopoulos A, Eadie LA, Dori I, Parnavelas JG. 1989. The development of basal forebrain projections to the rat visual cortex. Exp Brain Res 76:563-571.

Donoghue JP, Carroll KL. 1987. Cholinergic modulation of sensory responses in rat primary somatic sensory cortex. Brain Res 408:367-371.

Dori I, Parnavelas JG. 1989. The cholinergic innervation of the rat cerebral cortex shows two distinct phases in development. Exp Brain Res 76:417-423.

Dupin JC, Descarries L, De Champlain J. 1976. Radioautographic visualization of central catecholamine neurons in newborn rat after intravenous administration of tritiated norepinephrine. Brain Res 103:588-596.

Eckenstein F, Baughman RW. 1984. Two types of cholinergic innervation in cortex, one co-localized with vasoactive intestinal polypeptide. Nature 309:153-155.

Eckenstein F, Baughman RW. 1987. Cholinergic innervation in cerebral cortex. In: Jones EG, Peters A, editors: Cerebral Cortex, Vol. 6, Plenum Press, New York, pp. 29-160.

Eckenstein F, Thoenen H. 1983. Cholinergic neurons in the rat cerebral cortex demonstrated by immunohistochemical localization of choline acetyltransferase. Neurosci Lett 36:211-215.

Etienne O, Robitaille Y, Wood P, Gauthier S, Nair NPV, Quirion R. 1986. Nucleus basalis neuronal loss, neuritic plaques and choline acetyltransferase activity in advanced Alzheimer's disease. Neuroscience 19:1279-1291.

Fine A, Hoyle C, Maclean CJ, Levatte TL, Baker HF, Ridley RM. 1997. Learning impairments following injection of a selective cholinergic immunotoxin, ME20.4 IgG-saporin, into the basal nucleus of Meynert in monkeys. Neuroscience 81:331-343.

Gould, E., Woolf, N. J., Butcher, L. L., 1991. Postnatal development of cholinergic neurons in the rat: I. Forebrain. Brain Res. Bull. 27, 767-789.

Gritti I, Mainville L, Jones BE. 1993. Codistribution of GABA- with acetylcholine-synthesizing neurons in the basal forebrain of the rat. J Comp Neurol 329:438-457.

Gu Q, Singer W. 1993. Effects of intracortical infusion of anticholinergic drugs on neuronal plasticity in kitten striate cortex. Eur J Neurosci 5:475-485.

Happe HK, Murrin LC. 1992. Development of high-affinity choline transport sites in rat forebrain: a quantitative autoradiography study with [^{3}H]hemicholinium-3. J Comp Neurol 321:591-611.

Hasselmo ME, Bower JM. 1992. Cholinergic suppression specific to intrinsic not afferent fiber synapses in rat piriform (olfactory) cortex. J Neurophysiol 67:1222-1229.

Hasselmo ME, Schnell E. 1994. Laminar selectivity of the cholinergic suppression of synaptic transmission in rat hippocampal region CA1: computational modeling and brain slice physiology. J Neurosci 14:3898-3914.

Henderson Z. 1991. Early development of the nucleus basalis-cortical projection but late expression of its cholinergic function. Neuroscience 44:311-324.

Hill JA, Zoli M, Bourgeois J-P, Changeux J-P. 1993. Immunocytochemical localization of a neuronal nicotinic receptor: the β2-subunit. J Neurosci 13:1551-1568.

Höhmann CF, Ebner FF. 1985. Development of cholinergic markers in mouse forebrain. I. Choline acetyltransferase enzyme activity and acetylcholinesterase histochemistry. Dev Brain Res 23:225-241.

Höhmann CF, Brooks AR, Coyle JT. 1988. Neonatal lesions of the basal forebrain cholinergic neurons result in abnormal cortical development. Dev Brain Res 42:253-264.

Höhmann CF, Potter ED, Levey AI. 1995. Development of muscarinic receptor subtypes in the forebrain of the mouse. J Comp Neurol 358:88-101.

Höhmann CF, Wallace SA, Johnston MV, Blue ME. 1999. Effects of neonatal cholinergic basal forebrain lesions on excitatory amino acid receptors in neocortex. Int J Dev Neurosci 16:645-660.

Hubel DH, Wiesel TN. 1970. The period of susceptibility to the physiological effects of unilateral eyelid closure in kittens. J Physiol (Lond) 206:419-436.

Ichikawa T, Ajiki K, Matsuura J, Misawa H. 1997. Localization of two cholinergic markers, choline acetyltransferase and vesicular acetylcholine transporter in the central nervous system of the rat: in situ hybridization histochemistry and immunohistochemistry. J Chem Neuroanat 13:23-39.

Jaarsma D, Dino MR, Cozzari C, Mugnaini E. 1996. Cerebellar choline acetyltransferase positive mossy fibers and their granule and unipolar brush cell targets: a model for central cholinergic nicotinic neurotransmission. J Neurocytol 25:829-842.

Jasper HH, Tessier J. 1971. Acetylcholine liberation from cerebral cortex during paradoxical (REM) sleep. Science 172:601-602.

Johnston MV, McKinney M, Coyle JT. 1981 Neocortical cholinergic innervation: A description of extrinsic and intrinsic components in the rat. Exp Brain Res 43:159-172.

Jones S, Sudweeks S, Yakel JL. 1999. Nicotinic receptors in the brain: correlating physiology with function. Trends Neurosci 22:555-561.

Juliano SL, Ma W, Eslin D. 1991. Cholinergic depletion prevents expansion of topographic maps in somatosensory cortex. Proc Natl Acad Sci USA 88:780-784.

Kilgard MP, Merzenich MM. 1998. Cortical map reorganization enabled by nucleus basalis activity. Science 279:1714-1718.

Kimura F. 2000. Cholinergic modulation of cortical function: a hypothetical role in shifting the dynamics in cortical network. Neurosci Res 38:19-26.

Kimura F, Baughman RW. 1997. Distinct muscarinic receptor subtypes suppress excitatory and inhibitory synaptic responses in cortical neurons. J Neurophysiol 77:709-716.

Kimura F, Fukuda M, Tsumoto T. 1999. Acetylcholine suppresses the spread of excitation in the visual cortex revealed by optical recording : possible differential effect depending on the source of input. Eur J Neurosci 11:3597-3609.

Kiss J, Patel AJ. 1992. Development of the cholinergic fibres innervating the cerebral cortex of the rat. Int J Devl Neuroscience 10:153-170.

Koh S, Higgins GA. 1991. Differential regulation of the low-affinity nerve growth factor receptor during postnatal development of the rat brain. J Comp Neurol 313:494-508.

Koh S, Loy R. 1989. Localization and development of nerve growth factor-sensitive rat basal forebrain neurons and their afferent projections to hippocampus and neocortex. J Neurosci 9:2999-3018.

Kojic L, Gu Q, Douglas RM, Cynader MS. 2001. Laminar distribution of cholinergic- and serotonergic-dependent plasticity within kitten visual cortex. Dev Brain Res 126:157-162.

Kostovic I. 1986. Prenatal development of nucleus basalis complex and related fiber systems in man: a histochemical study. Neuroscience 17:1047-1077.

Kritzer MF, Kohama SG. 1998. Ovarian hormones influence the morphology, distribution, and density of tyrosine hydroxylase immunoreactive axons in the dorsolateral prefrontal cortex of adult rhesus monkeys. J Comp Neurol 395:1-17.

Krnjevic K, Phillis JW. 1963a. Acetylcholine-sensitive cells in the cerebral cortex. J Physiol (London) 166:296-327.

Krnjevic K, Phillis JW. 1963b. Pharmacological properties of acetylcholine-sensitive cells in the cerebral cortex. J Physiol (London) 166:328-350.

Krnjevic K, Silver A. 1966. Acetylcholinesterase in the developing forebrain. J Anat 100:63-89.

Krnjevic K, Primain R, Renaud L. 1971. The mechanism of excitation by acetylcholine in the cerebral cortex. J Physiol (London) 215:247-268.

Kurosawa M, Sato A, Sato Y. 1989. Well-maintained responses of acetylcholine release and blood flow in the cerebral cortex to focal electrical stimulation of the nucleus basalis of Meynert in aged rats. Neurosci Lett 100:198-202.

Kutscher CL. 1991 Development of transient acetylcholinesterase staining in cells and permanent staining in fibers in cortex of rat brain. Brain Res Bull 27:641-649.

Lamour Y, Dutar P, Jobert A, Dykes RW. 1988. An iontophoretic study of single somatosensory neurons in rat granular cortex serving the limbs: a laminar analysis of glutamate and acetylcholine effects on receptive-field properties. J Neurophysiol 60:725-750.

Lapierre Y, Beaudet A, Demianczuk N, Descarries L. 1973. Noradrenergic axon terminals in the cerebral cortex of rat. II. Quantitative data revealed by light and electron microscope radioautography of the frontal cortex. Brain Res 63:175-182.

Lassiter TL, Barone Jr S, Padilla S. 1998. Ontogenetic differences in the regional and cellular acetylcholinesterase and butyrylcholinesterase activity in the rat brain. Dev Brain Res 105:109-123.

Leanza G, Nilsson OG, Nikkhah G, Wiley RG, Björklund A. 1996. Effects of neonatal lesions of the basal forebrain cholinergic system by 192 immunoglobulin G-saporin: biochemical, behavioural and morphological characterization. Neuroscience 74:119-141.

Lebrand C, Cases O, Adelbrecht C, Doye A, Alvarez C, El Mestikawy S, Seif I, Gaspar P. 1996. Transient uptake and storage of serotonin in developing thalamic neurons. Neuron 17:823-835.

Levey AI, Kitt CA, Simonds WF, Price DL, Brann MR. 1991. Identification and localization of muscarinic acetylcholine receptor proteins in brain with subtype-specific antibodies. J Neurosci 11:3218-3226.

Levey AI, Wainer BH, Rye DB, Mufson EJ, Mesulam M-M. 1984. Choline acetyltransferase-immunoreactive neurons intrinsic to rodent cortex and distinction from acetylcholinesterase-positive neurons. Neuroscience 13:341-353.

Lidow MS. 1998. Cocaine abuse and corticogenesis. Trends Neurosci 21:19-20.

Loewi O. 1921. Über humorale übertragbarkeit der herznervenwirkung. I Mitteilung. Arch Ges Physiol 189:239-242.

Loizou LA. 1970. Uptake of monoamines into central neurons and the blood-brain barrier in infant rats. Brit J Pharmacol 40:800-813.

Lossinsky AS, Vorbrodt AW, Wisniewski HM. 1986. Characterization of endothelial cell transport in the developing mouse blood-brain barrier. Dev Neurosci 8:61-75.

Lubin M, Erisir A, Aoki C. 1999. Ultrastructural immunolocalization of the α7 nAChR subunit in guinea pig medial prefrontal cortex. Ann NY Acad Sci 868:628-632.

Lysakowski A, Wainer BH, Bruce G, Hersh LB. 1989. An atlas of the regional and laminar distribution of choline acetyltransferase immunoreactivity in rat cerebral cortex. Neuroscience 28:291-336.

Ma W, Maric D, Li B-s, Hu Q, Andreadis JD, Grant GM, Liu Q-Y, Shaffer KM, Chang YH, Zhang L, Pancrazio JJ, Pant HC, Stenger DA, Barker JL. 2000. Acetylcholine stimulates cortical precursor cell proliferation *in vitro* via muscarinic receptor activation and MAP kinase phosphorylation. Eur J Neurosci 12:1227-1240.

MacIntosh FC, Oborin PE. 1953. Release of acetylcholine from intact cerebral cortex. Abstr. XIX Int. Physiol. Congr. Montreal: The Congress, pp. 580-581.

McCormick DA. 1992. Neurotransmitter actions in the thalamus and cerebral cortex and their role in neuromodulation of thalamocortical activity. Prog Neurobiol 39:337-388.

McDonald JK, Speciale SG, Parnavelas JG. 1987. The laminar distribution of glutamate decarboxylase and choline acetyltransferase in the adult and developing visual cortex of the rat. Neuroscience 21:825-832.

McKenna TM, Ashe JH, Hui GK, Weinberger NM. 1988. Muscarinic agonists modulate spontaneous and evoked unit discharge in auditory cortex of cat. Synapse 2:54-68.

Metherate R, Ashe JH. 1991. Basal forebrain stimulation modifies auditory cortex responsiveness by an action at muscarinic receptors. Brain Res 559:163-167.

Metherate R, Cox CL, Ashe JH. 1992. Cellular bases of neocortical activation: modulation of neural oscillations by the nucleus basalis and endogenous acetylcholine. J Neurosci 12:4701-4711.

Metherate R, Tremblay N, Dykes RW. 1988. Transient and prolonged effects of acetylcholine on responsiveness of cat somatosensory cortical neurons. J Neurophysiol 59:1253-1276.

Miranda MI, Bermúdez-Rattoni F. 1999. Reversible inactivation of the nucleus basalis magnocellularis induces disruption of cortical acetylcholine release and acquisition, but not retrieval, of aversive memories. Proc Natl Acad Sci USA 96:6478-6482.

Mitchell JF. 1963. The spontaneous and evoked release of acetylcholine from the cerebral cortex. J Physiol (London) 165:98-116.

Molnar M, Tongiorgi E, Avignone E, Gonfloni S, Ruberti F, Domenici L, Cattaneo A. 1998. The effects of anti-nerve growth factor monoclonal antibodies on developing basal forebrain neurons are transient and reversible. Eur J Neurosci 10:3127-3140.

Mrzljak L, Levey AI, Goldman-Rakic P. 1993. Association of m1 and m2 muscarinic receptor proteins with asymmetric synapses i the primate cerebral cortex: morphological evidence for cholinergic modulation of excitatory neurotransmission. Proc Natl Acad Sci USA 90:5194-5198.

Mrzljak L, Levey AI, Rakic P. 1996. Selective expression of m2 muscarinic receptor in the parvocellular channel of the primate visual cortex. Proc Natl Acad Sci USA 93:7337-7340.

Mrzljak L, Levey AI, Belcher S, Goldman-Rakic PS. 1998. Localization of the m2 muscarinic acetylcholine receptor protein and mRNA in cortical neurons of the normal and cholinergically deafferented rhesus monkey. J Comp Neurol 390:112-132.

Nakayama H, Shioda S, Okuda H, Nakashima T, Nakai Y. 1995. Immunocytochemical localization of nicotinic acetylcholine receptor in rat cerebral cortex. Mol Brain Res 32:321-328.

Nyakas C, Buwalda B, Kramers RJK, Traber J, Luiten PGM. 1994. Postnatal development of hippocampal and neocortical cholinergic and serotonergic innervation in rat: effects of nitrite-induced prenatal hypoxia and nimodipine treatment. Neuroscience 59:541-559.

Oakman SA, Faris PL, Cozzari C, Hartman BK. 1999. Characterization of the extent of pontomesencephalic cholinergic neurons' projections to the thalamus: comparison with projections to midbrain dopaminergic groups. Neuroscience 94:529-547.

Ostermann C-H, Grunwald J, Wevers A, Lorke DE, Reinhardt S, Maelicke A, Schröder H. 1995. Cellular expression of α4 subunit mRNA of the nicotinic acetylcholine receptor in the developing rat telencephalon. Neurosci Lett 192:21-24.

Peinado A. 2000. Traveling slow waves of neural activity: a novel form of network activity in developing neocortex. J Neurosci 20:RC54 (1-6).

Penn AA, Riquelme PA, Feller MB, Shatz CJ. 1998. Competition in reticulogeniculate patterning driven by spontaneous activity. Science 279:2108-2112.

Perry E, Walker M, Grace J, Perry R. 1999. Acetylcholine in mind: a neurotransmitter correlate of consciousness? Trends Neurosci 22:273-280.

Perry EK, Tomlinson BE, Blessed G, Bergmann K, Gibson PH, Perry RH. 1978. Correlation of cholinergic abnormalities with senile plaques and mental test scores in senile dementia. Brit Med J 2:1457-1459.

Pirch JH, Turco K, Rucker HK. 1992. A role for acetylcholine in conditioning-related responses of rat frontal cortex neurons: microiontophoretic evidence. Brain Res 586:19-26.

Porter JT, Cauli B, Tsuzuki K, Lambolez B, Rossier J, Audinat E. 1999. Selective excitation of subtypes of neocortical interneurons by nicotinic receptors. J Neurosci 19:5228-5235.

Prusky G, Cynader M. 1990. The distribution of M1 and M2 muscarinic acetylcholine receptor subtypes in the developing cat visual cortex. Dev Brain Res 56:1-12.

Quastel JH, Tennenbaum M, Wheatley AHM. 1936. Choline ester formation in, and choline esterase activities of, tissues *in vitro*. Biochem J 30:1668-1681.

Rasmusson DD, Dykes RW. 1988. Long-term enhancement of evoked potentials in cat somatosensory cortex by co-activation of the basal forebrain and cutaneous receptors. Exp Brain Res 70:276-286.

Rigdon GC, Pirch JH. 1986. Nucleus basalis involvement in conditioned neuronal responses in the rat frontal cortex. J Neurosci 6:2535-2542.

Robertson RT, Tijerina AA, Gallivan ME. 1985. Transient patterns of acetylcholinesterase activity in visual cortex of the rat: normal development and the effects of neonatal monocular enucleation. Dev Brain Res 21:203-214.

Robertson RT, Gallardo KA, Claytor KJ, Ha DH, Ku K-H, Yu BP, Lauterborn JC, Wiley RG, Yu J, Gall CM, Leslie FM. 1998. Neonatal treatment with 192 IgG-Saporin produces long-term forebrain cholinergic deficits and reduces dendritic branching and spine density of neocortical pyramidal neurons. Cereb Cortex 8:142-155.

Roerig B, Nelson DA, Katz LC. 1997. Fast synaptic signaling by nicotinic acetylcholine and serotonin 5-HT_3 receptors in developing visual cortex. J Neurosci 17:8353-8362.

Roghani A, Shirzadi A, Butcher LL, Edwards RH. 1998. Distribution of the vesicular transporter for acetylcholine in the rat central nervous system. Neuroscience 82:1195-1212.

Role LW, Berg DK. 1996. Nicotinic receptors in the development and modulation of CNS synapses. Neuron 16:1077-1085.

Rossi FM, Pizzorusso T, Porciatti V, Marubio LM, Maffei L, Changeux J-P. 2001. Requirement of the nicotinic acetylcholine receptor b2 subunit for the anatomical and functional development of the visual system. Proc Natl Acad Sci USA 98:6453-6458.

Rye DB, Wainer BH, Mesulam M-M, Mufson EJ, Saper CB. 1984. Cortical projections arising from the basal forebrain : a study of cholinergic and noncholinergic components employing combined retrograde tracing and immunohistochemical localization of choline acetyltransferase. Neuroscience 13:627-643.

Saper CB. 1984. Organization of the cerebral cortical afferent systems in the rat. II. Magnocellular basal nucleus. J Comp Neurol 222:313-342.

Sargent PB. 1993. The diversity of neuronal nicotinic acetylcholine receptors. Annu Rev Neurosci 16:403-443.

Schäfer MK-H, Eiden LE, Weihe E. 1998. Cholinergic neurons and terminal fields revealed by immunohistochemistry for the vesicular acetylcholine transporter. I. Central nervous system. Neuroscience 84:331-359.

Séguéla P, Watkins KC, Descarries L. 1988. Ultrastructural features of dopamine axon terminals in the anteromedial and the suprarhinal cortex of adult rat. Brain res 442:11-22.

Séguéla P, Watkins KC, Descarries L. 1989. Ultrastructural relationships of serotonin axon terminals in the cerebral cortex of adult rat. J Comp Neurol 289:129-142.

Séguéla P, Watkins KC, Geffard M, Descarries L. 1990. Noradrenaline axon terminals in adult rat neocortex: an immunocytochemical analysis in serial thin sections. Neuroscience 35:249-264.

Semba K. 1992. Development of central cholinergic neurons. In: Björklund, A., Hökfelt, T., Tohyama, M. (Eds.), Handbook of Chemical Neuroanatomy, vol 10. Elsevier, Amsterdam, pp. 33-62.

Sendemir E, Erzurumlu RS, Jhaveri S. 1996. Differential expression of acetylcholinesterase in the developing barrel cortex of three rodent species. Cereb Cortex 6:377-387.

Sillito AM, Kemp JA. 1983. Cholinergic modulation of the functional organization of the cat visual cortex. Brain Res 289:143-155.

Steriade M, Amzica F, Nunez A. 1993. Cholinergic and noradrenergic modulation of the slow (~0.3 Hz) oscillation in neocortical cells. J Neurophysiol 70:1384-1400.

Stichel CC, Singer W. 1987. Quantitative analysis of the choline acetyltransferase-immunoreactive axonal network in the cat primary visual cortex: I. Adult cats. J Comp Neurol 258:91-98.

Tremblay N, Warren RA, Dykes RW. 1990. Electrophysiological studies of acetylcholine and the role of the basal forebrain in the somatosensory cortex of the cat. II. Cortical neurons excited by somatic stimuli. J Neurophysiol 64:1212-1222.

Umbriaco D. 1996. Caractérisation ultrastructurale de l'innervation cholinergique du cortex cérébral et de l'hippocampe. Études immunocytochimiques en microscopie électronique chez le rat adulte. Thèse de doctorat, Université de Montréal.

Umbriaco D, Watkins KC, Descarries L, Cozzari C, Hartman BK. 1994. Ultrastructural and morphometric features of the acetylcholine innervation in adult rat parietal cortex. An electron microscopic study in serial sections. J Comp Neurol 348:351-373.

Umbriaco D, Garcia S, Beaulieu C, Descarries L. 1995. Relational features of acetylcholine, noradrenaline, serotonin and GABA axon terminals in the stratum radiatum of adult rat hippocampus (CA1). Hippocampus 5:605-610.

Vaucher E, Hamel E. 1995. Cholinergic basal forebrain neurons project to cortical microvessels in the rat : electron microscopic study with anterogradely transported *Phaseolus vulgaris* leucoagglutinin and choline acetyltransferase immunocytochemistry. J Neurosci 15:7427-7441.

Voytko ML, Olton DS, Richardson RT, Gorman LK, Tobin JR, Price DL. 1994. Basal forebrain lesions in monkeys disrupt attention but not learning and memory. J Neurosci 14:167-186.

Wessler I, Kirkpatrick CJ, Racké K. 1998. Non-neuronal acetylcholine, a locally acting molecule, widely distributed in biological systems: expression and function in humans. Pharmacol Ther 77:59-79.

Whitehouse PJ, Price DL, Clark AW, Coyle JT, DeLong MR. 1981. Alzheimer disease : evidence for selective loss of cholinergic neurons in the nucleus basalis. Ann Neurol 10:122-126.

Woolsey TA, Van der Loos H. 1970. The structural organization of layer IV in the somatosensory region of the mouse cerebral cortex. Brain Res 17:205-242.

Xiang Z, Huguenard JR, Prince DA. 1998. Cholinergic switching within neocortical inhibitory networks. Science 281:985-988.

Zahalka EA, Seidler FJ, Lappi SE, Yanai J, Slotkin TA. 1993. Differential development of cholinergic nerve terminal markers in rat brain regions: implications for nerve terminal density, impulse activity and specific gene expression. Brain res 601:221-229.

Zhang X, Liu C, Miao H, Gong Z-H, Nordberg A. 1998. Postnatal changes of nicotinic acetylcholine receptor α2, α3, α4, α7 and β2 subunits genes expression in rat brain. Int J Devl Neuroscience 16:507-518.

Zhu XO, Waite PME. 1998. Cholinergic depletion reduces plasticity of barrel field cortex. Cereb Cortex 8:63-72.

Zoli M, Le Novère N, Hill JA, Changeux J-P. 1995. Developmental regulation of nicotinic ACh receptor subunit mRNAs in the rat central and peripheral nervous systems. J Neurosci 15:1912-1939.

LISTE DES PUBLICATIONS

Descarries L, **Mechawar N.** 2000. Ultrastructural evidence for diffuse transmission by monoamine and acetylcholine neurons in the central nervous system. In: *Volume Transmission Revisited*, Agnati LF, Fuxe K, Nicholson C and Sykova E eds., Prog Brain Res 125:27-47.

Mechawar N, Cozzari C, Descarries L. 2000. Cholinergic innervation in adult rat cerebral cortex: a quantitative immunocytochemical description. J Comp Neurol 428:305-318.

Mansour-Robaey S, **Mechawar N** , Radja F, Beaulieu C, Descarries L. 1998. Quantified distribution of serotonin transporter and receptors during the postnatal development of the rat barrel field cortex. Dev Brain Res 107:159-163.

Mechawar N, Anctil M. 1997. Melatonin in a primitive metazoan: seasonal changes of levels and immunohistochemical visualization in neurons. J Comp Neurol 387:243-254.

Articles sous presse

Mechawar N, Watkins KC, Descarries L. 2001. Ultrastructural features of the acetylcholine innervation in the developing parietal cortex of rat. J Comp Neurol.

Mechawar N, Descarries L. 2001. The cholinergic innervation develops early and rapidly in the rat cerebral cortex: a quantitative immunocytochemical study. Neuroscience.

Aznavour N, **Mechawar N**, Descarries L. 2001. Comparative analysis of cholinergic innervation in the dorsal hippocampus of adult mouse and rat: a quantitative immunocytochemical study. Hippocampus.

Pierret P, Vallée A, **Mechawar N**, Dower NA, Stone JC, Richardson PM, Dunn RJ. 2001. Cellular and subcellular localization of Ras Guanyl Nucleotide-Releasing Protein in the rat hippocampus. Neuroscience.

Pierret P, **Mechawar N**, Vallée A, Patel J, Priestley JV, Dunn RJ, Dower NA, Stone JC, Richardson PM. 2001. Presence of Ras Guanyl Nucleotide-Releasing Protein in striosomes of the mature and developing rat. Neuroscience.

Manuscrit en préparation

Meilleur S, Émond M, Renaud J, Aznavour N, **Mechawar N,** Descarries L, Mamer O, Carmant L, Psarropoulou C. 2001. Pentylenetetrazol-induced seizures in immature rats provoke long-term changes in adult hippocampal physiology. (préparé pour *The Journal of Neuroscience*)

ANNEXE I

ULTRASTRUCTURAL EVIDENCE FOR DIFFUSE TRANSMISSION BY MONOAMINE AND ACETYLCHOLINE NEURONS OF THE CENTRAL NERVOUS SYSTEM

(*Prog Brain Res* 125:27-47)

ULTRASTRUCTURAL EVIDENCE FOR DIFFUSE TRANSMISSION BY MONOAMINE AND ACETYLCHOLINE NEURONS OF THE CENTRAL NERVOUS SYSTEM

Laurent DESCARRIES [1] and Naguib MECHAWAR [2]

Départements de pathologie et biologie cellulaire [1, 2] et de physiologie [1], and Centre de recherche en sciences neurologiques [1,2], Faculté de médecine, Université de Montréal, Montréal, Québec, Canada H3C 3J7

Running title : **Diffuse transmission by MA and ACh neurons**

Correspondence: Laurent Descarries m.d.
Département de pathologie
Université de Montréal
C.P. 6128, Succ. Centre-ville
Montréal (Québec), Canada
H3C 3J7

Tel (514) 343-7070
Fax (514) 343-5755

E-mail: descarrl@alize.ere.umontreal.ca

Contents

Abbreviations

ACh, acetylcholine; AChE, acetylcholinesterase; DBH, dopamine-β-hydroxylase; ChAT, choline acetyltransferase; CNS, central nervous system; GABA, gamma-aminobutyric acid; MA, monoamine; NA, noradrenaline; TH, tyrosine hydroxylase; 5-HT, 5-hydroxytryptamine (serotonin); TpOH, tryptophane hydroxylase

INTRODUCTION

The present book highlights the view that, in addition to synaptic transmission, i.e. chemical transmission taking place at morphologically differentiated sites of membrane specialization, many central nervous system (CNS) neurons are capable of spreading transmitter more broadly, to various cellular targets, through what has come to be designated as "volume transmission". In mammalian CNS, this mode of neuronal communication was first envisaged on the basis of electron microscopic observations on autoradiographically identified serotonin (5-HT) and noradrenaline (NA) axon terminals (varicosities*) in adult rat cerebral cortex, which often lacked the membrane junctional complexes that are the hallmark of synapses (Descarries et al., 1975; Beaudet et al., 1976; Descarries et al., 1977). The proposal was then made that the monoamine (MA) transmitter released from such varicosities might not exert its effects solely on restricted areas of postsynaptic membrane specialization, but also diffuse in tissue and thus reach relatively distant targets endowed with receptive elements. It was also pointed out at the time that the largely asynaptic character of these innervations was hardly compatible with the preconceived notion of a fixed pattern of neuronal circuitry. Because of the known intra-axonal mobility of inner constituents (vesicular organelles and mitochondria), it was actually postulated that the varicosities themselves, lying free in the neuropil, were subjected to incessant movements of translocation and/or reshaping along their parent fibers, constantly modifying their position as release sites in relation to their immediate microenvironment. Thus, at the ultrastructural as well as cytological and anatomical levels, such neuronal systems appeared ideally built for achieving sustained and

adapted modulation and/or coordination of vast neuronal ensembles, in addition to cell-to-cell, point to point, direct transfer of information.

By the time of the first symposium on Volume Transmission, in September 1989, much of the early autoradiographic evidence in favor of the largely asynaptic character of the MA innervations in adult rat cerebral cortex had already been confirmed by detailed and systematic quantitative electron microscope immunocytochemical analyses (review in Descarries et al., 1991). Immunocytochemical data had also been produced in different laboratories regarding the ultrastructural relationships of dopamine (DA), NA and 5-HT axon varicosities in other regions of the rat brain (for reviews, see Beaudet and Descarries, 1987; Descarries et al., 1988; Soghomonian et al., 1988; Maley et al., 1990), but examination of the ultrastructure of these terminals in primate cerebral cortex had just begun (DeFelipe and Jones, 1988; De Lima et al., 1988). Moreover, despite the availability of specific antibodies against the biosynthetic enzyme of acetylcholine (ACh), choline acetyltransferase (ChAT; Crawford et al., 1982; Eckenstein and Thoenen, 1982; Levey et al., 1983), only qualitative information had been acquired about the relational features of cholinergic terminals in either the cerebral cortex or selected brain regions of rat, cat, dog, ferret or primate (for reviews, see Houser, 1990; Umbriaco, 1995). The immunocytochemical visualization of some of the receptors for the monoamines or ACh at the subcellular level was also in its early beginnings.

In the past ten years, considerable progress has been made on each of these fronts. As reviewed in the present chapter (see also Smiley, 1996), the relational features of MA axon terminals have been examined in the cerebral cortex of different mammalian species, including monkey and man. Other CNS regions in rat and other mammals have also been explored in this respect, notably the hippocampus and

neostriatum. In some of these studies, attempts were made to identify the synaptic targets of the identified terminals and/or to visualize the subcellular distribution of the receptors for their transmitter. Detailed ultrastructural investigations have been carried out on the ACh innervation of the cerebral cortex, hippocampus, neostriatum and olfactory bulb in rat, as well as the cerebral cortex in monkey and man. Lastly, some of these results have been brought together to propose the hypothesis of an ambient extracellular level of transmitter(s) in the CNS, at least in those anatomical regions richly innervated by the monoamines or ACh.

MONOAMINE INNERVATIONS

Most of the information acquired in recent years on the fine structural features and relationships of central MA axon terminals has been obtained by means of electron microscopic immunocytochemistry with specific antibodies against the biosynthetic enzymes, tyrosine hydroxylase (TH) and dopamine-β-hydroxylase (DBH), or against DA, NA or 5-HT themselves, coupled to protein with aldehydes to form immunogenic conjugates. In some of these studies, primary fixation of the CNS could thus be carried out by perfusion with relatively high concentrations of aldehydes, which improves the ultrastructural preservation of the tissue. Moreover, perhaps even more importantly, efforts were made to examine the immunostained axon terminals in serial as well as single thin sections for electron microscopy, allowing for detailed scrutiny of most if not the entire volume of varicosities and direct estimates of the frequency with which these terminals are engaged in synaptic junction (synaptic incidence; Fig. 1). In other instances, such estimates were inferred by linear transformation of the relationship between the frequency of observed synaptic junctions and the number of thin sections available for examination. A third approach was to determine synaptic incidence from the frequency in single thin sections by means of the stereological formula of Beaudet

and Sotelo (1981). This formula takes into account the average size of varicosity profiles, the length of their junctional complexes and the thickness of the sections to predict the probability of seeing a synapse if there is one on every varicosity. The synaptic incidence is then inferred by comparison with this predicted value. There is good evidence that such extrapolated incidences are reliable providing that the single section sampling of varicosities is of sufficient size. On numerous occasions, both a serial and a single thin section sampling of the same species of varicosities were indeed shown to yield similar values (e.g. Soghomonian et al., 1989; Oleskevich et al., 1991; Descarries et al., 1992; Ridet et al., 1992, 1993; Descarries et al., 1996). Furthermore, almost identical values were found by Umbriaco et al. (1994) in a large population of varicosities examined across their entire volume and which were also treated as a randomized single section sample.

Cerebral cortex and hippocampus

Except for discordant reports from one laboratory (Papadopoulos et al., 1987a, 1987b, 1989a, 1989b; Parnavelas and Papadopoulos, 1989; Paspalas and Papadopoulos, 1996), all other studies in which the synaptic incidence of MA terminals was determined in cerebral cortex of rat, monkey and man have confirmed the partly or largely asynaptic character of these innervations (see Table 1).

The DA innervation is undoubtedly the most synaptic, as now documented in the medial prefrontal, suprarhinal and occipital cortex of rat. Except in the study by Papadopoulos et al. (1989a), the junctions made by cortical DA varicosities have always been described as relatively small and mostly symmetrical. All available observations suggest important regional and perhaps laminar differences in the frequency with which these varicosities make synaptic junction (see Van Eden et al., 1987; Séguéla et al., 1988; Papadopoulos et al., 1989b; Verney et al., 1990). Attempts at identifying the

partners of synaptic DA varicosities in rat anteromedial, prefrontal and motor cortex have indicated that both pyramidal cell dendritic trees and a subpopulation of intrinsic GABA neurons were contacted (Verney et al., 1990). A similar conclusion has been reached with respect to the targets of synaptic DA terminals in the prefrontal, motor and entorhinal cortex of rhesus and cynomolgus monkeys (Goldman-Rakic et al., 1989; Sesack et al., 1995a, 1995b, 1998; Smiley et al., 1996; Erickson et al., 1999). In their study of rhesus monkey prefrontal cortex, Smiley et al. (1996) observed a synaptic incidence of 39% for 153 DA-immunostained varicosities completely examined in serial sections across their entire volume. They therefore concluded that, at least in this part of monkey cortex, DA presumably exerted effects via release from non synapsing varicosities and extracellular diffusion, in addition to synaptically targeted actions on specific neuronal populations. Also, a 9.8% proportion of synaptic DA varicosities has been reported recently for single sections of TH-immunostained terminals in the entorhinal cortex of cynomolgous monkey (Erickson et al., 1999). Assuming that these DA varicosities are of the same size as in rat, this should correspond to a synaptic incidence of about 20%.

Interestingly, there has also been an investigation of the distribution and synaptic connectivity of DA immunoreactive axons in human cortical tissue removed from the temporal pole and anterior lateral temporal surface (Brodmann's area 38 and anterior part of area 21) for tumor excision or the treatment of epilepsy (Smiley et al., 1997). Identification of synapses made by these varicosities was then reported to be "a tedious process", in which "approximately 100-200 immunoreactive profiles (e.g., 10-20 processes followed through 10 serial sections) had to be surveyed in order to find a convincing example". Although these terminals appeared to be slightly larger than their counterparts in the monkey (Smiley and Goldman-Rakic, 1996), such a frequency

in serial sections was highly suggestive of a low synaptic incidence (5-10%). Also noteworthy in this unique ultrastructural study was the fact that no axo-axonic specialization was found, even though an earlier report had mentioned (but not illustrated) the possible existence of such contacts in the medial and orbital prefrontal cortex of rat (Van Eden et al, 1987). It would be interesting to know if the synaptic incidence of presumed DA varicosities is similarly low in human cortical tissue resected for the treatment of partial seizures due to dysplasia. In two such cases, an increased density of TH-immunostained fibers has indeed been reported by Trottier et al. (1994) in the area of seizure propagation around dysplastic foci (area of seizure onset).

Presumably for methodological reasons, much less additional information has been gained on the relational features of the NA innervation in cerebral cortex since the extensive study by Séguéla et al. (1990) in the rat. Depending on the stringency of the criteria used in identifying the junctional complex, the synaptic incidence of cortical NA terminals was then evaluated at 17% and 26%, in a pooled sample of serially-sectioned NA-immunostained varicosities from the upper layers of primary motor (frontal), somatosensory (parietal) and visual (occipital) cortex. This was quite different from the earlier reports by Papadopoulos et al. (1987a, 1989), who had concluded that 88% and 89% of 125 and 800 serially sectioned NA-immunostained varicosities from all layers of the fronto-parietal and visual cortex made a synapse. It has never been determined if this discrepancy was due to a sampling bias or different criteria for defining synapses. In similarly prepared material from unspecified regions of rat cerebral cortex, Paspalas and Papadopoulos (1996) have later described direct contacts of NA varicosities with oligodendrocytes that frequently exhibited "a distinct accumulation of electron-dense material resembling membrane

differentiations found in symmetrical synapses". In a concurrent immunocytochemical study on the astroglial and vascular relationships of NA terminals in rat fronto-parietal cortex, Cohen et al. (1997) did not observe such contacts and evaluated the synaptic incidence at 7.1% from a population of 130 NA-immunostained profiles examined in single thin sections. These authors also noted the frequent juxtaposition of NA varicosities to astrocytic processes, a finding of particular interest in view of the earlier double immunolabeling study of Aoki (1992) in the rat visual cortex, which had shown occasional contacts (appositions) between presumed NA terminals (TH-immunostained) and astrocytic leaflets displaying β-adrenoreceptor immunoreactivity.

Using a similar approach, Aoki et al. (1998) have recently examined the topological relationship between DBH-immunostained terminals and α2A receptor immunoreactivity in the dorsolateral prefrontal cortex of cynomolgous monkey. Only 1 in 12 single sections of 564 NA varicosities from two monkeys were found to display morphologically identifiable synapses, and none of 79 profiles from layer VI included in that sampling. This should correspond to an average synaptic incidence of about 18% if these varicosities are of the same size as in rat. α2A receptors were visualized on dendritic spines bearing synaptic specializations, but also at sites along axons, dendritic shafts and astrocytic processes lacking identifiable junctions. The suggestion was therefore made that these receptors might be activated by diffuse transmission, and that noradrenergic modulation in prefrontal cortex should involve effects on glia, dendritic shafts and axons as well as synaptic interactions with the spines of pyramidal neurons.

As was the case for the NA innervation, the detailed study by Séguéla et al. (1989) of the 5-HT innervation in rat frontal, parietal and occipital cortex did not support the

earlier contention by Papadopoulos et al. (1987a, 1987b) that this cortical innervation is entirely synaptic (see Parnavelas and Papadopoulos, 1989). Values of 36% and 28% were obtained for the superficial and deep layers of the frontal cortex, respectively, and 46% and 37% for the parietal and the occipital cortex. A subsequent study by Cohen et al. (1995) yielded similar results. From a large population of single profiles of tryptophane hydroxylase (TpOH)-immunostained varicosities remote from the microvessels, synaptic incidences of 22% and 18% were then extrapolated for the fronto-parietal and the entorhinal cortex, respectively (Table 1).

Following an earlier study of visual cortex in which only profiles of 5-HT-immunostained varicosities endowed with a synaptic junction had been characterized (De Lima et al., 1988), the synaptic incidence of cortical 5-HT terminals was determined in both the sensorimotor (fronto-parietal) and prefrontal cortex of the monkey. In the sensory-motor cortex of cynomolgous monkey, DeFelipe and Jones (1988) found only 5 of 191 serially sectioned 5-HT-immunostained terminals making a synapse. Furthermore, around 4 pyramidal cells which showed basket formations in this material, they did not detect a single unequivocal specialization at the point of contact (apposition) by the 5-HT terminals. Similarly, in cat auditory cortex, DeFelipe et al. (1991) observed only 4 synapses made by 135 serially sectioned 5-HT-immunostained varicosities, 110 of which belonged to basket formations around GABA neurons. In layers I, III and V of the prefrontal cortex of rhesus monkey, Smiley and Goldman-Rakic (1996) reported that only 23% of 213 5-HT immunostained varicosities completely viewed in serial sections formed identifiable synapses. As previously shown in the rat (Séguéla et al., 1990), these 5-HT synapses were consistently asymmetric. Their preferred target in the monkey were dendritic shafts which usually belonged to somata with the morphological features of interneurons when followed in serial sections. In

fact, only 8% of such postsynaptic shafts were classified as pyramidal dendrites, further indicating that interneurons are the major recipients of 5-HT synapses. Ultrastructural data is still lacking about the 5-HT innervation of human cortex, even though Trottier et al. (1996) have already described a 5-HT hyperinnervation in addition to the altered pattern of catecholaminergic innervation previously reported in their two cases of focal cortical dysplasia.

In rat hippocampus, a systematic comparison of the ultrastructural features of NA, 5-HT, ACh and GABA terminals was carried out in the stratum radiatum of CA1 (Umbriaco et al., 1995). Relational features comparable to those in cerebral cortex were observed for all four species of terminals, with synaptic incidences of 16% and 23% extrapolated from single thin sections for the NA and the 5-HT varicosities, respectively (Table 1). This 23% value for the 5-HT endings was remarkably similar to previous estimates of 19.5% from single sections in the stratum radiatum and 18% from serial sections in the oriens layer of CA3, and 24% from single sections of the dentate gyrus (Oleskevich et al., 1991). It was also in keeping with the 12% incidence reported by Cohen et al. (1995) for TpOH-immunostained varicosities from the stratum lacunosum moleculare of the CA1 sector of dorsal hippocampus. As in the cerebral cortex, subpopulations of GABA neurons appear to be the preferred target of the synaptic 5-HT varicosities in rat hippocampus (Freund et al., 1990; Halasy et al., 1992). Here again, however, the low incidence of synapses formed by NA and 5-HT varicosities leads one to believe that these afferents exert their effects largely through diffuse transmission (for a recent review, see Vizi and Kiss, 1998).

Also worthy of note are the observations by Daszuta et al. (1991) indicating that after reinnervation and hyperinnervation of the previously 5-HT-denervated adult hippocampus by grafted midbrain 5-HT neurons, the proportion of 5-HT-

immunostained terminals engaged in synaptic contact in both the CA3 or the dentate sector of the outgrowth zone remains essentially the same as in intact tissue. Since the neurons which reinnervated the hippocampus were not necessarily destined to this region, these results suggest that the territory of innervation is the principle determinant of the frequency with which ingrowing 5-HT fibers make synaptic junction.

Neostriatum

Two studies carried out in the last ten years have provided definitive evidence for the partially synaptic character of both the DA and 5-HT innervation in adult rat neostriatum (Table 1). These original papers should be consulted for exhaustive reference to earlier literature. In the study of the DA innervation, results gathered over a 15 year period were finally published regarding the ultrastructural features of neostriatal axon terminals identified either by uptake autoradiography after intraventricular administration of [^{3}H]DA (single thin sections) (Fig. 2), or by DA immunocytochemistry in serial as well as single thin sections (Fig. 3) (Descarries et al., 1996). All three approaches yielded comparable values of synaptic incidence. Whether from the paraventricular zone or from a mediodorsal portion of the rostral half of neostriatum and examined in single or serial thin sections, 60%-70% of these DA varicosities were found to be asynaptic, and only 30-40% endowed with a synaptic membrane differentiation. The junctional complexes formed by striatal DA varicosities were invariably symmetrical. Approximately two thirds of these DA synapses were made on dendritic branches, one third on dendritic spines, and only 2-3% on cell bodies, as also found previously in a study of synaptic TH-immunolabeled boutons in the sensorimotor territory of squirrel monkey striatum (Smith et al., 1994).

These data in the rat were interpreted as indicative of a dual mode of transmission, i.e. diffuse as well as synaptic, for DA in neostriatum. Moreover, considering the extreme density of this innervation (see Doucet et al., 1986), the possibility was envisaged that a basal extracellular level of DA be permanently maintained around all cellular elements, owing to the spontaneous and evoked release from this multitude of asynaptic as well as synaptic varicosities. A subsequent report by Hanley and Bolam al. (1997) has added to the significance of this study. These investigators demonstrated that the synaptology of the nigrostriatal projection identified by TH immunostaining was essentially the same in both the patches of hyperdense and the matrix of dense striatal DA innervation. Thus, both diffuse and synaptic DA transmission are likely to be at play throughout the striatum, to participate in neostriatal and basal ganglia function(s) (and dysfunctions).

In the second study (Descarries et al., 1992), further characterization of the neostriatal 5-HT innervation was achieved during an ultrastructural investigation of the 5-HT hyperinnervation which takes place in adult rat neostriatum following its neonatal DA denervation by intraventricular administration of 6-hydroxydopamine. In normal controls, a synaptic frequency of 8% was extrapolated from single thin sections of 5-HT-immunostained varicosities in the dorsal third of rostral neostriatum, confirming earlier values of 13% and 10%, respectively obtained from single section autoradiographs of the paraventricular neostriatum after [^{3}H]5-HT uptake in vivo and serial sections from its mid-dorsal third after 5-HT-immunostaining (Soghomonian et al., 1988). Again, this proportion did not change (6% versus 8%) in spite of a twofold increase in the number of 5-HT axon terminals pervading the rostral portion of the neostriatum endogenously 5-HT hyperinnervated by rapheo-striatal 5-HT neurons.

Also of pertinence in the present context is the fact that knowing the synaptic incidence of DA and 5-HT terminals in adult rat neostriatum allows for estimating the actual number of these terminals engaged in synaptic contact. The density of these two innervations has indeed been measured in number of axon varicosities per cubic mm of tissue (Doucet et al., 1986; Mrini et al., 1995). Thus, it may be calculated that the 30%-40% proportion of DA varicosities making a synaptic junction corresponds to as many as 3-4 x 10^7 and 5-7 x 10^7 DA synapses per mm^3 in the DA islands and the matrix of the dorsolateral neostriatum, respectively, and 1.8-2.4 x 10^7 per mm^3 in the ventromedial neostriatum. The DA synapses are therefore likely to represent 1.8% to 7% of all striatal synapses. The synaptic 5-HT varicosities are 40 to 140 times less numerous. In the rostral neostriatum, for example, their 10% proportion corresponds to some 4.8 x 10^5 synapses per mm^3, i.e. approximately 1 in every 2000 striatal synapses.

Other brain regions

Data on the synaptic incidence of 5-HT terminals have also been obtained from many other regions of adult rat brain (Table 1). A study by Boulaich et al. (1994) has extrapolated values of 48% and 38% from single section of 5-HT-immunostained varicosities in the *suprachiasmatic and supraoptic nuclei of hypothalamus*. Furthermore, these proportions were then shown to be maintained following 5-HT denervation and either partial 5-HT reinnervation (suprachiasmatic) or hyperinnervation (supraoptic) by grafted embryonic 5-HT neurons. Thus, the synaptic incidence appears to remain constant in conditions of only limited as well as of excessive 5-HT reinnervation by 5-HT grafts.

In the *substantia nigra*, which receives one of the densest 5-HT innervation in CNS, a study by Moukhles et al. (1997) combined a quantitative evaluation of the density of this innervation by in vitro uptake autoradiography with [^{3}H]5-HT and its

ultrastructural characterization by electron microscopic 5-HT immunocytochemistry. Further indications of regional variability were thus obtained. In the pars reticulata, where their number amounts to 9×10^6 per mm^3, virtually all 5-HT varicosities were found to form synapses, whereas in the pars compacta, where the 5-HT innervation is slightly less dense ($6 \times 10^6/mm^3$), this proportion falls to 50%. This work also provided the basis for a comparative evaluation by fast-scan voltammetry of 5-HT release and uptake in a region of CNS where all 5-HT terminals are endowed with synaptic contact, as opposed to the dorsal raphe nucleus, a somatodendritic region with rare synaptic incidence (Bunin et al., 1998). The results supported the existence of diffuse 5-HT transmission in both regions, indicating that this mode of transmission might well apply to synaptic as well as asynaptic MA terminals.

Another region of interest is the *dorsal periaqueductal grey matter*, in which 5-HT has been shown to have anxiolytic (antiaversive) effects (Beckett et al., 1992; Nogueira and Graeff, 1995). In this region, the proportion of 5-HT-immunostained varicosities making a synaptic junction was recently evaluated at 23% in serial thin sections (Lovick et al., 1999). To our knowledge, it has not been determined if the 5-HT innervation displays similar features in the ventral periaqueductal grey, where it may be more directly involved in antinociception.

Data on serially-sectioned 5-HT-immunostained varicosities were also obtained from several regions of adult rat CNS in the course of developmental studies. The results at early postnatal ages must be regarded with caution, in view of the strong indications that numerous CNS neurons which do not synthetize 5-HT, including the thalamocortical projection neurons, take up and store 5-HT during the postnatal period in rodents (Lebrand et al., 1996, 1998; Cases et al., 1998; Hansson et al., 1998). These neurons can then be mistaken for 5-HT cells when labeled by ligand binding

autoradiography or 5-HT immunocytochemistry. However, results obtained after the age of 1 month are reliable because of the complete disappearance of this transient and partial 5-HT phenotype. Thus, a synaptic incidence of 42% may be inferred from the proportion reported by Dinopoulos et al. (1995) for single sections of 5-HT-immunostained terminals from the *lateral geniculate nucleus* in 35 day-old rat. Similarly, in adult rat, these authors have estimated the synaptic incidence of 5-HT terminals at 46%, 55%, 38% and 62% in the *basal forebrain* (nucleus of the horizontal limb of the diagonal band of Broca), superficial and deep layers of *superior colliculus* and *ventrolateral nucleus of thalamus*, respectively (Dinopoulos et al., 1997; Dori et al., 1998). In the superficial gray layer of the superior colliculus of the hamster, a value of 73% has been reported for serially-sectioned TH-immunostained profiles which were presumably noradrenergic, as most such profiles also stained for DBH in this region (Arce et al., 1994).

Spinal cord

Data have also become available regarding all three MA innervations in the rat spinal cord (Table 1). The spinal DA innervation has been examined in serial thin sections after DA-immunostaining (Ridet et al., 1992). Despite differences between anatomical levels and regions of the cord (Ridet et al., 1992), it was described as the most junctional. At cervical level, 34% of the DA varicosities were synaptic in the dorsal horn and 46% in the ventral horn. At thoracic level, the proportion reached 76% in the dorsal horn and > 100% in ventral horn, presumably because of the frequent occurrence of more than one synapse per DA terminal in this latter location. Around the central canal and in the intermediolateral cell column at thoracic level, 67% and >100% of the DA varicosities were synaptic, respectively.

The NA and 5-HT innervations also differed markedly between dorsal and ventral horn. In dorsal horn, whether estimated from single thin sections at lumbar and sacral levels or serial thin sections at cervical level, the synaptic incidence of NA-immunostained varicosities was in the order of 25-29% (Rajaofetra et al., 1992; Ridet et al., 1993). Around the central canal, the intermediolateral cell column and the ventral horn, it was much higher, at about 85%. Similarly, the 5-HT innervation in dorsal horn displayed a synaptic incidence of 37% in serial sections (Ridet et al., 1993), which apparently showed little variations in the different laminae of the dorsal horn or at different spinal cord levels (Marlier et al., 1991). In the intermediolateral cell column and anterior horn, however, the synaptic incidence of the 5-HT-immunostained varicosities was estimated at >100% (Poulat et al., 1992) and 95% (Ridet, 1994), respectively. Interestingly, as early as 1983, Maxwell et al. had reported a remarkably low synaptic incidence of 4% for 5-HT endings serially sectioned in the marginal zone (layer I of dorsal horn) of the rat spinal cord. These authors had concluded from this observation that non synaptic and diffuse transmission might be implicated in the antinociceptive effects of the descending 5-HT system. It should be pointed out that such data are quite distinct from earlier ultrastructural results in the cat, in which all the emphasis had been placed on the synaptic relationships of the 5-HT system in dorsal horn (Ruda and Gobel, 1980; Ruda et al., 1982; Light et al., 1983; Glazer and Basbaum, 1984).

ACETYLCHOLINE INNERVATIONS

It is only in the past ten years that an antibody against rat brain choline acetyltransferase (ChAT) has been available, which is sensitive enough to detect ACh axon terminals in vast number throughout the CNS of different mammals (Cozzari et

al., 1990). Many studies with other ChAT antibodies had previously allowed to describe some of the intrinsic and relational features of these terminals in rat, cat, or monkey brain (for reviews, see Houser et al., 1990; Umbriaco, 1995), but none had been aimed at a quantitative evaluation of their synaptic and/or appositional relationships (see in particular Armstrong, 1986; De Lima and Singer, 1986; Aoki and Kabak, 1992). As reviewed below, this has since been achieved for three major regions of the rat brain: cerebral cortex, hippocampus and neostriatum. An extensive report on rat olfactory bulb has also been published, as well as two studies with the previously available antibodies that managed to assess the synaptic incidence of the ACh terminals in monkey and human cerebral cortex.

Cerebral cortex and hippocampus

The ACh innervation of cerebral cortex is known to arise mainly from the nucleus basalis magnocellularis of Meynert (substantia innominata, Ch4), but also in rodents from intracortical neurons (Eckenstein and Thoenen, 1983; Levey et al., 1984; Lauterborn et al., 1993; Schafer et al., 1998) that may give origin to as many as 20% of these terminals (Eckenstein and Baughman, 1987). The intrinsic and relational features of ACh axon varicosities have been examined in detail in the primary somatosensory area (S1 or Par 1) of adult rat parietal cortex (Umbriaco et al., 1994). Eight hundred and twelve ChAT-immunostained terminals from the different layers of Par1 were scrutinized in long, uninterrupted series of thin sections across their whole volume. Several were actually reconstructed in three dimensions (see Fig. 8 in Umbriaco et al., 1994); about 200 were visualized as two or three varicosities along the same axon.

A totally unexpected finding was that, in every layer of Par1 cortex, only a low proportion of these ACh varicosities displayed a synaptic membrane differentiation

(junctional complex). As indicated in Table 1, their mean synaptic incidence across all layers was 14%. Only layer V showed a slightly higher proportion (21%). In general, cortical ACh varicosities were relatively small, averaging 0.57 μm in diameter. Those bearing a synaptic junction were slightly larger than their non synaptic counterparts (0.67 μm in diameter). Both junctional and non junctional ACh varicosities could be observed on the same axons. The junctional complexes formed by these terminals were single, almost always symmetrical, and occupied a small fraction of the total surface of varicosities (< 3%). Synaptic ACh varicosities usually contacted dendritic branches (76%), less often spines (24%), and none were seen on cell bodies.

Two subsequent investigations confirmed the low synaptic incidence of cortical ACh varicosities in the rat (Chédotal et al., 1994; Vaucher and Hamel, 1995). From single thin sections, values of 14% and 9% were then extrapolated for the frontoparietal cortex and the perirhinal cortex, respectively.

An extensive ChAT immunocytochemical study has also been performed by Mrzljak et al. (1995) in the prefrontal cortex of rhesus monkey. These authors then reported that among 100 serially sectioned ChAT immunoreactive boutons at the border of layers II and III, only 44% made synaptic contact. Fifty-six percent were without any visible junctional specialization, even if frequently juxtaposed to dendrites or spines receiving asymmetrical synapses. More recently, Smiley et al. (1997) carried out a similar study on two samples of human anterior temporal lobe removed at surgery. These investigators found 67% of 42 varicosities from layers I and II endowed with small but identifiable synaptic specializations. It remains to be determined whether such variations of synaptic incidence in cortex reflect sampling biases, regional differences or species differences. In any event, these results allow the inference that, in primates as well as rat cortex, the various modulatory actions of ACh are likely to

depend on both synaptic and non synaptic terminals delivering ACh to proximal and remote targets.

The data on the regional and laminar synaptic incidence of the cortical ACh innervation in rat parietal cortex assume further significance when viewed in relation with measurements of the density of this innervation, as expressed not only in length of ChAT-immunostained axons, but also in number of ChAT-immunostained varicosities per cubic mm of tissue (see Mechawar and Descarries, 1999). Thus, in the parietal cortex, the length of ChAT-immunostained axons per mm^3 of tissue is found to range from 13.33 m (layer V) to 9.47 m (layer IV) and to average of 11.94 m for the whole cortical thickness. The corresponding numerical densities for varicosities (x 10^6 per mm^3) range from 4.80 (layer V) to 3.49 (layer IV), with an average of 4.37 for the whole cortex. It may then be calculated that the parietal cortex is innervated by a total length of 23.89 m of ACh axons bearing 8.73 x 10^6 varicosities underneath a cortical surface of 1 mm^2. Based on the known proportions of synaptic ACh varicosities in each cortical layer (Umbriaco et al., 1994). only 1.38 x 10^6 of these varicosities would be synaptic (15.86%), for average numerical densities of 0.69 x 10^6 synaptic and 3.67 x 10^6 asynaptic ACh varicosities per mm^3 of cortex. Thus, synaptic ACh varicosities are likely to represent less than 1 in 1 450 of all cortical synapses. If release of ACh were to take place from synaptic varicosities only, such a small fraction would certainly make it difficult to account for the amounts of ACh collected from the cortical surface or concentrations measured intracortically with microdialysis.

In the previously mentioned study in which NA-, 5-HT- and ChAT- were compared to GAD-immunostained terminals in the stratum radiatum of CA1 (Umbriaco et al., 1995), the synaptic incidence of hippocampal ACh axon varicosities was found to be 7% and thus even lower than that of their NA and 5-HT counterparts.

Again, it would seem difficult to account for the current ACh measurements in hippocampus, if this transmitter were to be released by synaptic varicosities only. As in neocortex, the strong prevalence of asynaptic ACh varicosities in hippocampus could also account for the remarkable capacity of this innervation to regrow from grafts of cholinergic neurons after previous lesions, and then restore behavioral deficits in spatial learning and memory (e.g. Low et al., 1982; Nilsson et al., 1990).

Neostriatum

The ACh innervation of neostriatum is essentially intrinsic, being issued from a fraction of the large interneurons which represent less than 2% of the total neuronal population of this region (McGeer et al., 1971; Woolf, 1991). Yet, the ChAT immunoreactivity in neostriatum is one of the strongest in brain. Prior to our 1996 study (Contant et al., 1996), one could only imagine how profuse an axonal network might account for such labeling. This became immediately apparent when observing the multitude of ChAT-immunostained varicosities which pervaded the neostriatal neuropil in low power electron micrographs (Fig. 4A). As illustrated in Figs. 4B and 4C, these varicosities are particularly small, as their mean diameter (0.43 μm) was significantly less than that of their cortical congeneers and of striatal DA or 5-HT varicosities (all averaging about 0.6 μm in diameter). Once again, a vast majority were found to be asynaptic. In single thin section, only 2.7% exhibited a junctional complex compared with 57% for unlabeled varicosity profiles selected at random from the same electron micrographs. Stereological extrapolation to the whole volume of these ACh varicosities indicated a real synaptic incidence of less than 10% (Table 1), whereas that for the surrounding unlabeled varicosities was greater than 100% because of the frequent occurrence of multiple junctions. Direct apposition of ChAT-immunostained varicosities (Fig. 4A) was not uncommon, reflecting the extreme density of this ACh

innervation. Striatal ACh varicosities were also frequently found juxtaposed to unlabeled varicosities, many of which were synaptic, accounting for preterminal effects of ACh on the release of other tranmitters or vice versa (for references, see Contant et al., 1996).

Olfactory bulb

Another ultrastructural study has emphasized the asynaptic as well as synaptic character of an ACh innervation in adult rat CNS. In the main olfactory bulb, Kasa et al. (1995) have described a dual mode of innervation by ACh fibers, whereby ChAT-immunopositive terminals made occasional synapses with interneurons but never on relay cells. In the glomerular layer, notably, periglomerular cell dendrites were observed to receive asymmetrical synapses from ACh boutons, but the dendrites of mitral and tufted cells, although closely approached, were never contacted synaptically. In all other layers, occasional synaptic contacts were made on gemmules and/or dendritic spines of granule cells, but the vast majority of ChAT-immunopositive fibers were reported as "thin and with most of their varicosities (50 to 1) apparently lacking any synaptic specialization".

AMBIENT LEVEL OF MONOAMINES AND ACETYLCHOLINE IN THE CNS

An interesting complement to the diffuse transmission paradigm has been recently proposed on the basis of some of the above observations, at least for brain regions rich in one or the other of the largely asynaptic MA or ACh innervations (Descarries et al., 1995, 1996, 1997; Contant et al., 1996; Descarries, 1998). According to this hypothesis, a low level of ambient transmitter would be maintained throughout the extracellular space by the spontaneous and evoked release from predominantly asynaptic axon terminals, and presumably also by spillover from the minority that are

junctional. According to this hypothesis, reuptake and enzymatic degradation of the monoamines would primarily serve to keep their ambient level within physiological limits rather than totally eliminate them from synaptic clefts and the extracellular space. Brain acetylcholinesterase (AChE), which predominantly consists of the tetrameric G4 isoform, would play a similar role toward ACh, as suggested by the fact that, in skeletal muscle, this G4 form is concentrated outside and around endplates (Gisiger and Stephens, 1988) and, in contrast to the A12 form, does not significantly contribute to the rapid removal of ACh from synaptic clefts (for detailed discussion, see Descarries et al., 1997). In this context, individual release events would in fact correspond to local and transient fluctuations of this background level, i.e. signals superimposed on a preexisting state of information already determined, at least in part, by the same transmitter.

In many parts of CNS, microdialysis data seems consistent with the existence of low concentration, resting, ambient levels of monoamines and/or ACh in the extracellular space. Spontaneous dialysis outputs in the nanomolar range have been repeatedly measured for DA, NA, 5-HT and ACh in cerebral cortex, hippocampus or neostriatum of freely moving rat, even in the absence of MA reuptake blockers or AChE inhibitors (e.g. Smith et al., 1992; Testylier et al., 1996; Portas et al., 1998; Rowley et al., 1998). Experimental and theoretical models have been proposed to evaluate the extracellular diffusion of transmitters and answer the often-asked question of the distance that can be reached by these molecules in living brain (e.g. Nicholson and Syková, 1998). In the case of DA, it is usually agreed that a 10 μm distance might be attained within 50 milliseconds (Wightman and Zimmerman, 1990). This is no small domain of influence at the subcellular level. Based on currently available estimates of the density of DA innervation in striatum (Doucet et al., 1986), and the observation of a

comparable density of ACh innervation, a sphere of striatal neuropil with a radius of 10 μm should contain about 400 DA and 400 ACh axon terminals, five to ten times more unidentified terminals, and at least several thousand dendritic spines. If DA or ACh diffuse that far, one can easily understand why there may be such a variety of receptor subtypes for these transmitters, and presumably different subtypes on any single neuron.

A low ambient level of transmitter could regulate the expression and/or functional state of high-affinity receptor subtypes located on neurons releasing the corresponding transmitter (autoreceptors) or other neurons (heteroreceptors), glial cells and microvessels. Changes of this ambient level, affecting these widely distributed receptors, could be the ones to mediate many of the behavioral effects produced by drugs acting on the MA transporters, the choline transporter or AChE. The existence of the ambient level could also explain why some of the motor and cognitive deficits attributed to losses of MA or of ACh in CNS become manifest only when a major proportion of release sites have disappeared and even low background levels are no longer maintained. Similarly, it could account for the beneficial effects of substitution and pharmacological therapies, or of grafts of non neuronal cells engineered to release transmitter (e.g. Winkler et al., 1995; Dickinson-Anson et al., 1998), which obviously take place in the absence of restored synaptic connectivity.

CONCLUDING REMARKS

As illustrated by the present symposium, a wealth of evidence has accumulated to confirm the reality and heuristic value of the "volume transmission" paradigm. In its largest acceptance, this diffuse mode of transmission may now be considered to apply not only to neuronal populations characterized by a paucity of synaptic junctions, but also to wholly junctional ones, such as the glycine-, GABA- and glutamate-containing

neurons, which display spillover of their transmitter (see Chapter 21). Using immunoelectron microscopy, many of the receptors for these aminoacidergic transmitters, as well as for monoamines, ACh and neuropeptides, have been visualized in extrasynaptic membrane locations, on neuronal somata, dendrites, axons and axon terminals, as well as glia and endothelial cells, often remote from the corresponding release sites (see Chapter 14). The spread of various molecules, including DA, 5-HT, neuropeptides, cytokines and growth factors, has been documented in intact brain tissue following in vivo administration (see Chapter 7). The ambient level hypothesis has provided a framework for explaining some of the sustained and regulatory as well as trophic-like effects of transmitters on a prolonged time scale. Experimental techniques are being developed to investigate such effects and broad transmission by diffusion may now be envisaged not only in terms of cell-to-cell transfer of information, but also of coordination and synchronization of the activity of vast cellular ensembles, (e.g. Riehle et al., 1997; Fisahn et al., 1998; Testylier et al., 1999). A striking example of this progress is to be found in the current thinking on the implication of ACh in cortical functions and dysfunctions (Perry et al., 1999). Initially regarded as the canonical transmitter, exciting cortical neurons much as it did muscle fibers at the neuromuscular junction, ACh is now viewed as a major integrator of neuronal activity, whose widespread actions in the human cortex might in fact be essential for the maintenance of conscious experience. The "volume transmission" paradigm has been central to this evolution.

Acknowledgements

The authors thank Drs. Michel Geffard (Bordeaux, France), Boyd K. Hartman (Minneapolis, MN) and Costantino Cozzari (Rome, Italy) for generous gifts of antibodies. They also acknowledge the technical assistance of Sylvia Garcia and K.C. Watkins with the electron microscopy. They are also grateful to Gaston Lambert for photographic work. Their research work is currently supported by grant MT-3544 to L.D. and a studentship to N.M. from the Medical Research Council of Canada.

Title page footnote

* For lack of better words, the eponyms "terminal" and "varicosity" are used interchangeably to designate axonal enlargements containing aggregated synaptic vesicles and endowed or not with morphologically defined membrane specializations of synaptic contact (junctional complex).

References

Aoki, C. (1992) β-adrenergic receptors: astrocytic localization in the adult visual cortex and their relation to catecholamine axon terminals as revealed by electron microscopic immunocytochemistry. J. Neurosci., 12: 781-792.

Aoki, C. and Kabak, S. (1992) Cholinergic terminals in the cat visual cortex: Ultrastructural basis for interaction with glutamate-immunoreactive neurons and other cells. Vis. Neurosci., 8: 177-191.

Aoki, C., Venkatesan, C., Go, C.G., Forman, R. and Kurose, H. (1998) Cellular and subcellular sites for noradrenergic action in the monkey dorsolateral prefrontal cortex as revealed by the immunocytochemical localization of noradrenergic receptors and axons. Cereb. Cortex, 8: 269-277.

Arce, E.A., Bennett-Clarke, C.A. and Rhoades, R.W. (1994) Ultrastructural organization of the noradrenergic innervation of the superficial gray layer of the hamster's superior colliculus. Synapse, 18: 46-54.

Armstrong, D.M. (1986) Ultrastructural characterization of choline acetyltransferase-containing neurons in the basal forebrain of rat: Evidence for a cholinergic innervation of intracerebral blood vessels. J. Comp. Neurol. 250: 81-92.

Beaudet, A. and Descarries, L. (1987) Ultrastructural identification of serotonin neurons. In H.W.M. Steinbusch (Ed.), Monoaminergic Neurons: Light Microscopy and Ultrastructure, John Wiley & Sons, Chichester, pp. 265-313.

Beaudet, A and Sotelo C. (1981) Synaptic remodeling of serotonin axon terminals in rat agranular cerebellum. Brain Res., 206: 305-329.

Beckett, S.R.G., Lawrence, C.A., Marsden, C.A. and Marshall, P.W. (1992) Attenuation of chemically-induced defence responses by 5-HT1 receptor agonists administered into the periaqueductal grey. Psychopharmacology, 108: 110-114.

Boulaich, S., Daszuta, A., Geffard, M. and Bosler, O. (1994) Synaptic connectivity of serotonin graft efferents in the suprachiasmatic and supraoptic nuclei of the hypothalamus. Exp. Brain Res., 101: 353-364.

Bunin, M.A. and Wightman, R.M. (1998) Quantitative evaluation of 5-hydroxytryptamine (Serotonin) release and uptake: An investigation of extrasynaptic transmission. J. Neurosci., 18: 4854-4860.

Cases, O., Lebrand, C., Giros, B., Vitalis, T., De Maeyer, E., Caron, M.G., Price, D.L., Gaspar, P. and Seif, I. (1998) Plasma membrane transporters of serotonin, dopamine, and norepinephrine mediate serotonin accumulation in atypical locations in the developing brain of monoamine oxidase A knock-outs. J. Neurosci., 18: 6914-6927.

Chédotal, A., Umbriaco, D., Descarries, L., Hartman, B.K. and Hamel, E. (1994) Light and electron microscopic immunocytochemical analysis of the neurovascular relationships of choline acetyltransferase (ChAT) and vasoactive intestinal polypeptide (VIP) nerve terminals in the rat cerebral cortex. J. Comp. Neurol., 343: 57-71.

Cohen, Z., Ehret, M., Maître, M. and Hamel, E. (1995) Ultrastructural analysis of tryptophan hydoxylase immunoreactive nerve terminals in the rat cerebral cortex and hippocampus: their associations with local blood vessels. Neuroscience, 66: 555-569.

Cohen, Z., Molinatti, G. and Hamel, E. (1997) Astroglial and vascular interactions of noradrenaline terminals in the rat cerebral cortex. J. Cereb. Blood Flow Metab., 17: 894-904.

Contant, C., Umbriaco, D., Garcia, S., Watkins, K.C. and Descarries, L. (1996) Ultrastructural characterization of the acetylcholine innervation in adult rat neostriatum. Neuroscience, 71: 37-947.

Cozzari, C., Howard, J. and Hartman, B. (1990) Analysis of epitopes on choline acetyltransferase (ChAT) using monoclonal antibodies (Mabs). Soc. Neurosci. Abstr., 16: 200.

Crawford, G.D., Correa, L. and Salvaterra, P.M. (1982) Interaction of monoclonal antibodies with mammalian choline acetyltransferase. Proc. Natl. Acad. Sci. U.S.A., 79: 7031-7035.

Daszuta, A., Chazal, G., Garcia, S., Oleskevich, S. and Descarries, L. (1991) Ultrastructural features of serotonin neurons grafted to adult rat hippocampus: An immunocytochemical analysis of their cell bodies and axon terminals. Neuroscience, 42: 793-811.

DeFelipe, J. and Jones, E.G. (1988) A light and electron microscopic study of serotonin-immunoreactive fibers and terminals in the monkey sensory-motor cortex. Exp. Brain Res., 71: 171-182.

DeFelipe, J., Hendry, S.H.C., Hashikawa, T. and Jones, E.G. (1991) Synaptic relationships of serotonin-immunoreactive terminal baskets of GABA neurons in the cat auditory cortex. Cereb. Cortex, 1: 117-133.

De Lima A.D. and Singer, W. (1986) Cholinergic innervation of the cat striate cortex: A choline acetyltransferase immunocytochemical analysis. J. Comp. Neurol. 250: 324-338.

De Lima, A.D., Bloom, F.E., and Morrison, J.H. (1988) Synaptic organization of serotonin-immunoreactive fibers in primary visual cortex of the macaque monkey. J. Comp. Neurol., 274: 280-294.

Descarries, L. (1998) The hypothesis of an ambient level of acetylcholine in the central nervous system. J. Physiol. (Paris), 92: 215-220.

Descarries, L. and Umbriaco, D. (1995) Ultrastructural basis of monoamine and acetylcholine function in CNS. Semin. Neurosci., 7: 309-318.

Descarries, L., Doucet, G., Lemay, B., Séguéla, P. and Watkins, K.C. (1988) Structural basis of cortical monoamine function. In M. Avoli, T.A. Reader, R.W. Dykes and P. Gloor (Eds.), Neurotransmitters and Cortical Function. From Molecules to Mind, Plenum Press, New York, pp. 321-332.

Descarries, L., Gisiger, V. and Steriade, M. (1997) Diffuse transmission by acetylcholine in the CNS. Progr. Neurobiol., 53: 603-625.

Descarries, L., Séguéla, P. and Watkins, K.C. (1991) Nonjunctional relationships of monoamine axon terminals in the cerebral cortex of adult rat. In K. Fuxe and L.F. Agnati (Eds.), Volume Transmission in the Brain: Novel Mechanisms for Neural Transmission, Raven Press, New York, pp. 53-62.

Descarries, L., Soghomonian, J.-J., Garcia, S., Doucet, G., Bruno, J.P. (1992) Ultrastructural analysis of the serotonin hyperinnervation in adult rat neostriatum following neonatal dopamine denervation with 6-hydroxydopamine. Brain Res., 569: 1-13.

Descarries, L., Umbriaco, D., Contant, C and Watkins, K.C. (1995) A new hypothesis of acetylcholine (ACh) function in densely ACh-innervated regions of the brain. IVth IBRO World Congr. Neurosci. Abstr. A3.15, p. 101.

Descarries, L., Watkins, K.C., Garcia, S., Bosler, O. and Doucet, G. (1996) Dual character, asynaptic and synaptic, of the dopamine innervation in adult rat neostriatum: A quantitative autoradiographic and immunocytochemical analysis. J. Comp. Neurol., 375: 167-186.

Dickinson-Anson, H., Aubert, I., Gage, F.H. and Fisher, L.J. (1998) Hippocampal grafts of acetylcholine-producing cells are sufficient to improve behavioural performance following a unilateral fimbria-fornix lesion. Neuroscience, 84: 771-781.

Dinopoulos, A. Dori, I.E. and Parnavelas, J.G. (1995) Serotonergic innervation of the lateral geniculate nucleus of the rat during postnatal development: A light and electron microscopic immunocytochemical analysis. J. Comp. Neurol., 363: 532-544.

Dinopoulos, A. Dori, I.E. and Parnavelas, J.G. (1997) The serotonin innervation of the basal forebrain shows a transient phase during development. Dev. Brain Res., 99: 38-52.

Dori, I.E, Dinopoulos, A. and Parnavelas, J.G. (1998) The development of the synaptic organization of the serotonergic system differs in brain areas with different functions. Exp. Neurol., 154: 113-125.

Doucet, G., Descarries, L. and Garcia, S. (1986) Quantification of the dopamine innervation in adult rat neostriatum. Neuroscience, 19: 427-445.

Eckenstein, F. and Thoenen, H. (1982) Production of specific antisera and monoclonal antibodies to choline acetyltransferase: characterization and use for identification of cholinergic neurons. EMBO J., 1: 363-368.

Eckenstein, F. and Thoenen, H. (1983) Cholinergic neurons in the rat cerebral cortex demonstrated by immunohistochemical localization of choline acetyltransferase. Neurosci. Lett., 36: 211-215.

Eckenstein, F. and Baughman R.W. (1987) Cholinergic innervation in cerebral cortex. In E.G. Jones and A. Peters (Eds.), Cerebral Cortex. Further Aspects of Cortical Function, Including Hippocampus, Vol. 6, Plenum Press, New York, pp. 129-160.

Erickson, S.L., Sesack, S.R. and Lewis, D.A. (1999) The dopamine innervation of monkey entorhinal cortex: postsynaptic targets of tyrosine hydroxylase terminals. Synapse, in press.

Fisahn, A., Pike, F.G., Buhl, E.H. and Paulsen, O. (1998) Cholinergic induction of network oscillations at 40 Hz in the hippocampus in vitro. Nature, 394:186-189.

Freund, T.F., Gulyas, A.I., Acsady, L., Gorcs, T. and Toth, K. (1990) Serotonergic control of the hippocampus via local inhibitory interneurons. Proc. Natl. Acad. Sci. U.S.A., 87: 8501-8505.

Gisiger, V. and Stephens, H.R. (1988) Localization of the pool of G_4 acetylcholinesterase characterizing fast muscles and its alteration in murine muscular dystrophy. J. Neurosci. Res., 19: 62-78.

Glazer, E.J. and Basbaum, A.I. (1984) Axons which take up [^{3}H]serotonin are presynaptic to enkephalin immunoreactive neurons in cat dorsal horn. Brain Res., 298: 386-391.

Goldman-Rakic, P.S., Leranth, C., Williams, S.M., Mons, N. and Geffard, M. (1989) Dopamine synaptic complex with pyramidal neurons in primate cerebral cortex. Proc. Natl. Acad. Sci. U.S.A., 86: 9015-9019.

Halasy, K., Miettinen, R., Szabat, E. and Freund, T.F. (1992) GABAergic interneurons are the major postsynaptic targets of median raphe afferents in the rat dentate gyrus. Eur. J. Neurosci., 4: 144-153.

Hansson, S.R., Mezey, É. and Hoffman, B.J. (1998) Serotonin transporter messenger RNA in the developing rat brain: Early expression in serotonergic neurons and transient expression in non-serotonergic neurons. Neuroscience, 83: 1185-1201.

Houser, C.R. (1990) Cholinergic synapses in the central nervous system: studies of the immunocytochemical localization of choline acetyltransferase. J. Electron Microsc. Tech., 15: 2-19.

Kasa, P., Hlavati, I., Dobo, E., Wolff, A., Joo, F. and Wolff, J.R. (1995) Synaptic and non-synaptic cholinergic innervation of the various types of neurons in the main olfactory bulb of adult rat: Immunocytochemistry of choline acetyltransferase. Neuroscience, 67: 667-677.

Lauterborn, J.C., Isackson, P.J., Montalvo, R. and Gall, C.M. (1993) In situ hybridization localization of choline acetyltransferase mRNA in adult rat brain and spinal cord. Mol. Brain Res., 17: 59-69.

Lebrand, C., Cases, O., Adelbrecht, C., Doye, A., Alvarez, C., El Mestikawy, S., Seif, I. and Gaspar, P. (1996) Transient uptake and storage of serotonin in developing thalamic neurons. Neuron, 17: 823-835.

Lebrand, C., Cases, O., Wehrlé, R., Blakely, R.D., Edwards, R.H. and Gaspar, P. (1998) Transient developmental expression of monoamine transporters in the rodent forebrain. J. Comp. Neurol., 401: 506-524.

Levey, A.I., Armstrong, D.M., Atweh, S.F., Terry, R.D. and Wainer, B.H. (1983) Monoclonal antibodies to choline acetyltransferase: production, specificity, and immunohistochemistry. J. Neurosci., 3: 1-9.

Levey, A.I., Wainer, B.H., Rye, D.B., Mufson, E.J. and Mesulam, M.-M. (1984) Choline acetyltransferase-immunoreactive neurons intrinsic to rodent cortex and distinction from acetylcholinesterase-positive neurons. Neuroscience, 13: 341-353.

Light, A.R., Kavookjian, A.M. and Petrusz, P. (1983) The ultrastructure and synaptic connections of serotonin-immunoreactive terminals in spinal laminae I and II. Somatosensory Res., 1: 33-50.

Lovick, T.A., Parry, D.M., Stezhka, V.V. and Lumb, B.M. (1999) Serotonergic transmission in the periqueductal grey matter in relation to aversive behaviour: Morphological evidence for direct modulatory effects on identified output neurones. Neuroscience, in press.

Low, W.C., Lewis, P.R., Bunch, S.T., Dunnett, S.B., Thomas, S.R., Iversen, S.D., Björklund, A. and Stenevi, U. (1982) Functional recovery following neural transplantation of embryonic septal nuclei in adult rats with septohippocampal lesions. Nature, 300: 260-262.

Maley, B.E., Engle, M.G., Humphreys, S., Vascik, D.A., Howes, K.A., Newton, B.W. and Elde, R.P. (1990) Monoamine synaptic structure and localization in the central nervous system. J. Electr. Microsc. Tech., 15: 20-33.

Marlier, L., Sandillon, F., Poulat, P., Rajaofetra, N., Geffard, M. and Privat, A. (1991) Serotonergic innervation of the dorsal horn of rat spinal cord: light and electron microscopic immunocytochemical study. J. Neurocytol., 20: 310-322.

Maxwell, D.J., Leranth, C. and Verhofstad, A.A.J. (1983) Fine structure of serotonin-containing axons in the marginal zone of the rat spinal cord. Brain Res., 266: 253-259.

McGeer, P.L., McGeer, E.G., Fibiger, H.C. and Wickson V. (1971) Neostriatal choline acetylase and cholinesterase following selective brain lesions. Brain Res., 35: 308-314.

Mechawar, N. and Descarries, L. (1999) Quantitative data on the cholinergic innervation in adult rat parietal cortex. Soc. Neurosci. Abstr., 25: xxx.

Moukhles, H., Bosler, O., Bolam, J.P., Vallée, A., Umbriaco, D., Geffard, M. and Doucet, G. (1997) Quantitative and morphometric data indicate precise cellular interactions between serotonin terminals and postsynaptic targets in rat substantia nigra. Neuroscience, 76: 1159-1171.

Mrini, A., Soucy, J.-P., Lafaille, F., Lemoine, P. and Descarries, L. (1995) Quantification of the serotonin hyperinnervation in adult rat neostriatum after neonatal 6-hydroxydopamine lesion of nigral dopamine neurons. Brain Res., 669: 303-308.

Mrzljak, L., Levey, A.I. and Goldman-Rakic, P.S. (1993) Association of m1 and m2 muscarinic receptor proteins with asymmetric synapses in the primate cerebral cortex: morphological evidence for cholinergic modulation of excitatory neurotransmission. Proc. Natl. Acad. Sci. U.S.A., 90: 5194-5198.

Mrzljak, L., Pappy, M., Leranth, C. and Goldman-Rakic, P.S. (1995) Cholinergic synaptic circuitry in the macaque prefrontal cortex. J. Comp. Neurol., 357:603-617.

Nicholson, C. and Syková, E. (1998) Extracellular space structure revealed by diffusion analysis. Trends Neurosci., 21: 207-215.

Nilsson, O.G., Brundin, P. and Björklund, A. (1990) Amelioration of spatial memory impairment by intrahippocampal grafts of mixed septal and raphe tissue in rats with combined cholinergic and serotonergic denervation of the forebrain. Brain Res., 515: 193-206.

Nogueira, R.L. and Graeff, F.G. (1995) Role of 5-HT receptors in the modulation of dorsal periaqueductal gray matter of the rat. Pharmac. Biochem. Behav., 52: 1-6.

Oleskevich, S., Descarries, L, Watkins, K.C., Séguéla, P. and Daszuta, A. (1991) Ultrastructural features of the serotonin innervation in adult rat hippocampus: an immunocytochemical description in single and serial thin sections. Neuroscience, 42: 777-791.

Papadopoulos, G.C., Parnavelas, J.G. and Buijs, R.M. (1987a) Monoaminergic fibers form conventional synapses in the cerebral cortex. Neurosci. Lett., 76: 275-279.

Papadopoulos, G.C., Parnavelas, J.G. and Buijs, R.M. (1987b) Light and electron microscopic immunocytochemical analysis of the serotonin innervation of the rat visual cortex. J. Neurocytol., 16: 883-892.

Papadopoulos, G.C., Parnavelas, J.G. and Buijs, R.M. (1989a) Light and electron microscopic immunocytochemical analysis of the noradrenaline innervation of the rat visual cortex. J. Neurocytol., 18: 1-10.

Papadopoulos, G.C., Parnavelas, J.G. and Buijs, R.M. (1989b) Light and electron microscopic immunocytochemical analysis of the dopamine innervation of the rat visual cortex. J. Neurocytol., 18: 303-310.

Parnavelas, J.G. and Papadopoulos, G.C. (1989) The monoaminergic innervation of the cerebral cortex is not diffuse and nonspecific. Trends Neurosci., 12: 315-319.

Paspalas, C.D. and Papadopoulos, G.C. (1996) Ultrastructural relationships between noradrenergic nerve fibers and non-neuronal elements in the rat cerebral cortex. Glia, 17: 133-146.

Perry, E., Walker, M., Grace, J. and Perry, R. (1999) Acetylcholine in mind: A neurotransmitter correlate of consciousness. Trends Neurosci., 22: 273-280.

Portas, C.M., Bjorvatn, B., Fagerland, S., Gronli, J. Mundal, V., Sorensen, E. and Ursin, R. (1998) On-line detection of extracellular levels of serotonin in dorsal raphe nucleus and frontal cortex over the sleep/wake cycle in freely moving rat. Neuroscience, 83:807-814.

Poulat, P., Marlier, L., Rajaofetra, N. and Privat, A. (1992) 5-Hydroxytryptamine, substance P and thyrotropin-releasing hormone synapses in the intermediolateral cell column of the rat thoracic spinal cord. Neurosci. Lett., 136: 19-22.

Rajaofetra, N., Ridet, J.-L., Poulat, P., Marlier, L., Sandillon, F., Geffard, M. and Privat, A. (1992) Immunocytochemical mapping of noradrenergic projections to the rat spinal cord with an antiserum against noradrenaline. J. Neurocytol., 21: 481-494.

Ridet, J.-L. (1994) Organisation ultrastructurale et plasticité des systèmes monoaminergiques dans la moelle épinière du rat. Thèse de doctorat. Université de Montpellier II – Sciences et Techniques du Languedoc.

Ridet, J.-L., Sandillon, F., Rajaofetra, N., Geffard, M. and Privat, A. (1992) Spinal dopaminergic system of the rat: light and electron microscopic study using an antiserum against dopamine, with particular emphasis on synaptic incidence. Brain Res., 598: 233-241.

Ridet, J.-L., Rajaofetra, N., Teilhac, J.R., Geffard, M. and Privat, A. (1993) Evidence for nonsynaptic serotonergic and noradrenergic innervation of the rat dorsal horn and possible involvement of neuron-glia interactions. Neuroscience, 52: 143-157.

Riehle, A., Grun, S., Diesmann, M. and Aertsen, A. (1997) Spike synchronization and rate modulation differentially involved in motor cortical function. Science, 278: 1950-1953.

Rowley, H.L., Kilpatrick, I.C., Needham, P.L. and Heal, D.J. (1998) Elevation of extracellular cortical noradrenaline may contribute to the antidepressant activity of zotepine: An in vivo microdialysis study in freely moving rats. Neuropharmacology, 37: 937-944.

Ruda, M.A. and Gobel, S. (1980) Ultrastructural characterization of axonal endings in the substantia gelatinosa which take up [^{3}H]serotonin. Brain Res., 184: 57-83.

Ruda, M.A., Coffield, J. and Steinbusch, H.W.M. (1982) Immunocytochemical analysis of serotonergic axons in laminae I and II of the lumbar spinal cord of the cat. J. Neurosci., 2: 1660-1671.

Schafer, M.K., Eiden, L.E. and Weihe, E. (1998) Cholinergic neurons and terminal fields revealed by immunohistochemistry for the vesicular acetylcholine transporter. I. Central nervous system. Neuroscience, 84: 331-359.

Séguéla, P., Watkins K.C. and Descarries, L. (1988) Ultrastructural features of dopamine axon terminals in the anteromedial and suprarhinal cortex of adult rat. Brain Res., 442: 11-22.

Séguéla, P., Watkins, K.C. and Descarries, L. (1989) Ultrastructural relationships of serotonin axon terminals in the cerebral cortex of the adult rat. J. Comp. Neurol., 289: 129-142.

Séguéla, P., Watkins, K.C., Geffard, M. and Descarries, L. (1990) Noradrenaline axon terminals in adult rat neocortex: an immunocytochemical analysis in serial thin sections. Neuroscience, 35: 249-264.

Sesack, S.R., Bressler, C.N. and Lewis, D.A. (1995a) Ultrastructural associations between dopamine terminals and local circuit neurons in the monkey prefrontal cortex: A study of calretinin-immunoreactive cells. Neurosci. Lett., 200: 9-12.

Sesack, S.R., Snyder, C.L. and Lewis, D.A. (1995b) Axon terminals immunolabeled for dopamine or tyrosine hydroxylase synapse on GABA-immunoreactive dendrites in rat and monkey cortex. J. Comp. Neurol., 363: 264-280.

Sesack, S.R., Hawrylak, V.A., Melchitzky, D.S. and Lewis, D.A. (1998) Dopamine innervation of a subclass of local circuit neurons in monkey prefrontal cortex: ultrastructural analysis of tyrosine hydroxylase and parvalbumin immunoreactive structures. Cereb. Cortex, 8: 614-622.

Smiley, J.F. (1996) Monoamines and acetylcholine in primate cerebral cortex: What anatomy tells us about function. Rev. Brasil. Biol., 56 (Suppl. 1) 153-164.

Smiley, J.F. and Goldman-Rakic, P.S. (1993) Heterogeneous targets of dopamine synapses in monkey prefrontal cortex demonstrated by serial section electron microscopy: a laminar analysis using the silver-enhanced diaminobenzidine sulfide (SEDS) immunolabeling technique. Cereb. Cortex, 3: 223-238.

Smiley, J.F. and Goldman-Rakic, P.S. (1996) Serotonergic axons in monkey prefrontal cerebral cortex synapse predominantly on interneurons as demonstrated by serial section electron microscopy. J. Comp. Neurol., 367: 431-443.

Smiley, J.F., Williams, S.M., Szigeti, K. and Goldman-Rakic, P.S. (1992) Light and electron microscopic characterization of dopamine-immunoreactive axons in human cerebral cortex. J. Comp. Neurol., 32: 325-335.

Smiley, J.F., Morrell, F., Mesulam, M.-M. (1997) Cholinergic synapses in human cerebral cortex: an ultrastructural study in serial sections. Exp. Neurol., 144: 361-368.

Smith, A.D., Olson, R.J. and Justice, J.B. Jr. (1992) Quantitative microdialysis of dopamine in the striatum: effect of circadian variation. J. Neurosci. Meth., 44: 33-41.

Smith, Y., Bennett, B.D., Bolam, J.P., Parent, A. and Sadikot, A.F. (1994) Synaptic relationships between dopaminergic afferents and cortical thalamic input in the sensorimotor territory of the striatum in monkey. J. Comp. Neurol., 344: 1-19.

Soghomonian, J.-J., Beaudet, A. and Descarries L. (1988) Ultrastructural relationships of central serotonin neurons. In N.N. Osborne and M. Hamon (Eds.), Neuronal Serotonin, John Wiley & Sons, London, pp. 57-92.

Soghomonian, J.-J., Descarries, L. and Watkins, K.C. (1989) Serotonin innervation in adult rat neostriatum. II. Ultrastructural features: a radioautographic and immunocytochemical study. Brain Res., 481: 67-86.

Testylier G. and Dykes, R.W. (1996) Acetylcholine release from frontal cortex in the waking rat measured by microdialysis without acetylcholinesterase inhibitors: effects of diisopropylfluorophosphate. Brain Res., 740: 307-315.

Testylier, G., Maalouf, M., Butt, A.E., Miasnikov, A.A. and Dykes, R.W. (1999) Evidence for homeostatic adjustments of rat somatosensory cortical neurons to changes in extracellular acetylcholine concentrations produced by iontophoretic administration of acetylcholine and systemic diisopropylfluorophosphate treatment. Neuroscience, 91: 843-870.

Trottier, S., Evrard, B., Biraben, A. and Chauvel, P. (1994) Altered patterns of catecholaminergic fibers in focal cortical dysplasia in two patients with partial seizures. Epilepsy Res., 19: 161-179.

Trottier, S., Evrard, B., Vignal, J.P. and Chauvel, P. (1996) The serotonergic innervation of the cerebral cortex in man and its changes in focal cortical dysplasia. Epilepsy Res., 25: 79-106.

Umbriaco, D. (1995) Caractérisation ultrastructurale de l'innervation cholinergique du cortex cérébral et de l'hippocampe. Études immunocytochimiques en microscopie électronique chez le rat adulte. Thèse de doctorat, Université de Montréal.

Umbriaco, D., Watkins, K.C., Descarries, L., Cozzari C. and Hartman, B.K. (1994) Ultrastructural and morphometric features of the acetylcholine innervation in adult rat parietal cortex. An electron microscopic study in serial sections. J. Comp. Neurol., 348: 351-373.

Umbriaco, D., Garcia, S., Beaulieu, C. and Descarries, L. (1995) Relational features of acetylcholine, noradrenaline, serotonin and GABA axon terminals in the stratum radiatum of adult rat hippocampus (CA1). Hippocampus, 5: 605-620.

Van Eden, C.G., Hoorneman, E.M.D., Buijs, R.M., Matthijssen, M.A.H., Geffard, M. and Uylings, H.B.M. (1987) Immunocytochemical localization of dopamine in the prefrontal cortex of the rat at the light and electron microscopical level. Neuroscience, 22: 849-862.

Vaucher, E. and Hamel, E. (1995) Cholinergic basal forebrain neurons project to cortical microvessels in the rat: electron microscopic study with anterogradely transported *Phaseolus vulgaris* leucoagglutinin and choline acetyltransferase immunocytochemistr. J. Neurosci., 15: 7427-7441.

Verney, C., Alvarez, C., Geffard, M. and Berger, B. (1990) Ultrastructural double-labelling study of dopamine terminals and GABA-containing neurons in rat anteromedial cerebral cortex. Eur. J. Neurosci., 2: 960-972.

Vizi, E.S. and Kiss, J.P. (1998) Neurochemistry and pharmacology of the major hippocampal transmitter systems: synaptic and nonsynaptic interactions. Hippocampus, 8: 566-607.

Wightman, R.M. and Zimmerman, J.B. (1990) Control of dopamine extracellular concentration in rat striatum by impulse flow and uptake. Brain Res. Rev., 15: 135-144.

Winkler, J., Suhr, S.T., Gage, F.H., Thal, L.J. and Fisher, L.J. (1995) Essential role of neocortical acetylcholine in spatial memory. Nature, 375:484-487.

Woolf, N.J. (1991) Cholinergic systems in mammalian brain and spinal cord. Progr. Neurobiol., 37: 475-524.

Table 1- SYNAPTIC INCIDENCE OF MONOAMINE (DA, NA, 5-HT) AND ACETYLCHOLINE (ACh) AXON TERMINALS IN MAMMALIAN CNS

		DA	NA	5-HT	ACh
CEREBRAL CORTEX					
Rat	medial prefrontal	93% [1]	-	-	-
	suprarhinal	56% [1]	-	-	-
	frontal	-	7% [2]	32% [3], 22% [4]	14% [5]
	parietal	-	17% or 26% [6]	46% [3]	14% [7]
	occipital	90% [8]		37% [3]	-
	entorhinal	-	-	18% [4]	9% [9]
Cat	auditory	-	-	3% [10]	-
Monkey	sensory-motor	-	-	2-3% [11]	-
	prefrontal	39% [12]	18% [13]	23% [14]	44% [15]
	entorhinal	20% [16]	-	-	-
Human	anterolateral temporal	5-10% [17]	-	-	67% [18]
HIPPOCAMPUS *(Rat)*					
	CA1		16% [19]	23% [19], 12% [4]	7% [19]
	CA3		-	19% [20]	-
	DG		-	24% [20]	-

NEOSTRIATUM *(Rat)*	30-40% [21]		10%-13% [22]	9% [23]
OTHER BRAIN REGIONS *(Rat)*				
suprachiasmatic nucleus	-	-	48% [24]	-
supraoptic nucleus	-	-	38% [24]	-
substantia nigra, compacta		-	50% [25]	-
substantia nigra, reticulata		-	~100% [25]	-
dorsal periaqueductal grey	-	-	23% [26]	-
lateral geniculate nucleus	-	-	42% [27]	-
basal forebrain (NHL)	-	-	46% [28]	-
superior colliculus				
superficial layers	-	-	55% [29]	-
deep layers	-	-	38% [29]	-
ventrolateral n. of thalamus	-	-	62% [29]	-
SPINAL CORD *(Rat)*				
dorsal horn, cervical	34% [30]	25%-29% [31,32]	37% [32]	-
dorsal horn, thoracic	76% [30]	-	-	-
central canal	67% [30]	87% [31]	-	-
intermediolat. cell column	>100% [30]		>100% [33]	-
ventral horn	~100% [30]	85% [31]	95% [34]	-

Caption of Table 1

The synaptic incidences (%) were obtained by extrapolation from single thin sections or incomplete series of serial sections, or by observation of varicosities entirely examined in serial sections. The latter values were given priority whenever available. The superscripts refer to the following studies: [1] Séguéla et al., 1988; [2] Cohen et al., 1997; [3] Séguéla et al., 1989; [4] Cohen et al., 1995; [5] Chédotal et al., 1994; [6] Séguéla et al., 1990; [7] Umbriaco et al., 1994; [8] Papadopoulos et al., 1989b; [9] Vaucher and Hamel, 1995; [10] DeFelipe et al., 1991; [11] DeFelipe and Jones, 1988; [12] Smiley and Goldman-Rakic, 1993; [13] Aoki et al., 1998; [14] Smiley and Goldman-Rakic, 1996; [15] Mrzljak et al., 1995; [16] Erickson et al., 1999; [17] Smiley et al., 1992; [18] Smiley et al., 1997; [19] Umbriaco et al., 1995; [20] Oleskevich et al., 1991; [21] Descarries et al., 1996; [22] Soghomonian et al. 1989; [23] Contant et al., 1996; [24] Boulaich et al., 1994; [25] Moukhles et al., 1997; [26] Lovick et al., 1999; [27] Dinopoulos et al., 1995; [28] Dinopoulos et al, 1997; [29] Dori et al., 1998; [30] Ridet et al., 1992; [31] Rajaofetra et al., 1992; [32] Ridet et al., 1993; [33] Poulat et al., 1992; [34] Ridet, 1994.

Figure 1. Schematic representation of current methods for determining the frequency with which a given population of axon varicosities makes synaptic specializations (synaptic incidence). As illustrated by the three-dimensional reconstruction on the left (modified from Umbriaco et al., 1994), the immunostained terminals are visualized as sectional profiles, 0.5 – 1 μm in diameter (D), in ultrathin sections, approximately 0.1 μm in thickness (t). When present, the junctional complex occupies a small portion of the surface of varicosities (width: ls). From single sections (1), synaptic incidence may be extrapolated by means of the stereological formula of Beaudet and Sotelo (1981), as explained in the text. When partial or incomplete series of sections are available (2), synaptic incidence may be inferred by linear transformation of the relationship between the frequency of observed synaptic junctions and the number of sections available for examination. When complete series are available (3), synaptic incidence may be determined by direct observation.

ESTIMATING SYNAPTIC INCIDENCE FROM ELECTRON MICROGRAPHS

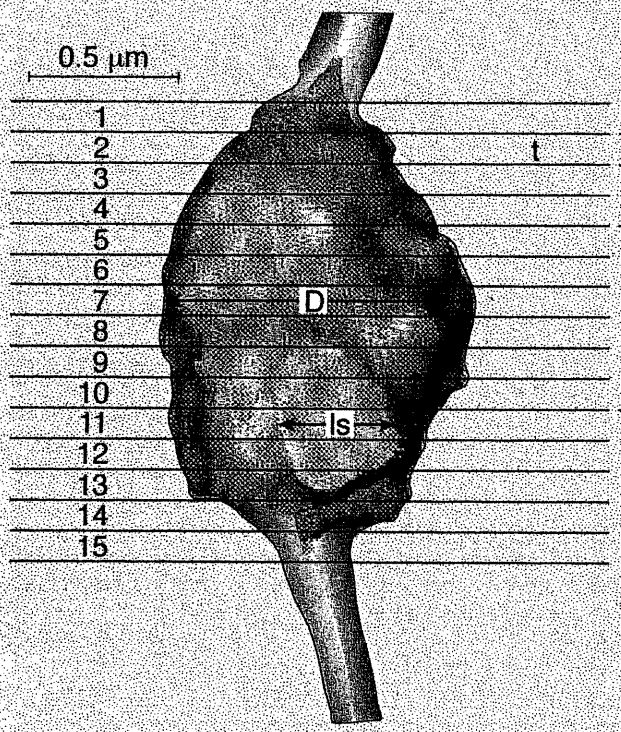

① SINGLE SECTION

Observed synaptic frequency (%)

$$\left(\frac{ls}{D} \times \frac{2}{\pi}\right) + \left(\frac{t}{D}\right)$$

(Adapted from Beaudet and Sotelo, 1981)

② INCOMPLETE SERIES

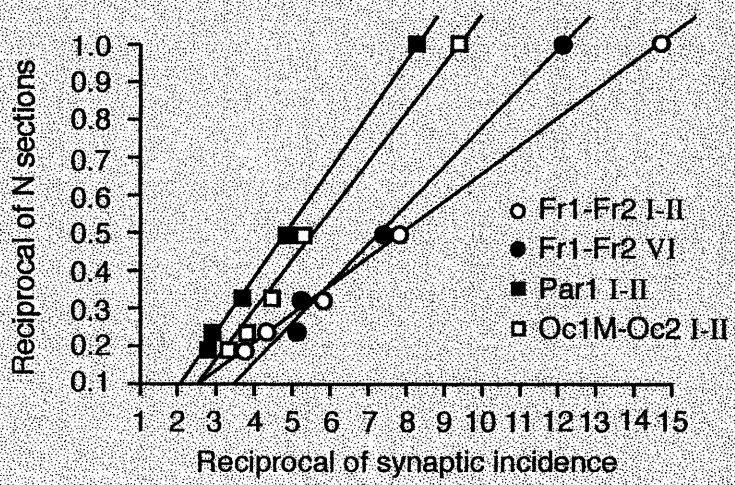

(From Séguéla et al., 1988)

③ COMPLETE SERIES

DIRECT READING (%)

Figure 2A-D. Electron microscope autoradiographs from rat paraventricular neostriatum after intraventricular administration of tritiated dopamine ([^{3}H]DA). Following prolonged autoradiographic exposure (42 weeks) and revelation with the physical developer paraphenelenediamine, accumulations of small and thin silver grains are detected over DA axon terminals (varicosities) laden with [^{3}H]DA. **A-** At very low magnification (X 3 500), these labeled sites are visible in large number (e.g. arrows) throughout the neuropil, between cell bodies which, in vast majority, exhibit the morphological features of spiny type I projection neurons (e.g. N). Scale bar: 5 µm. **B-D** illustrate ultrastructural characteristics of the labeled DA terminals at a higher magnification. Scale bars: 0.5 µm. In **B**, two elongated [^{3}H]DA-labeled varicosities display a rather uniform population of mostly round, small and clear vesicles, associated with a mitochondrion. Neither of these profiles shows any membrane differentiation even suggestive of a synaptic contact. As most of their labeled counterparts, these two varicosities are directly apposed to dendritic branches (db); the left-sided one is also apposed to a neuronal cell body (N) and to another axonal varicosity (av), unlabeled, containing dense core vesicles. In **C**, a larger [^{3}H]DA-labeled varicosity contains several mitochondria in addition to aggregated small vesicles. It forms a distinct symmetrical synaptic junction (between arrows) on a degenerating profile (D), presumably dendritic, while being also juxtaposed to a neuronal cell body (N). In **D**, another synaptic [^{3}H]DA-labeled varicosity is also directly apposed to a neuronal cell body (N). It makes a small symmetrical junction (between arrows) with the dendritic spine on its right (sp), also contacted synaptically by an unlabeled axonal varicosity (av). Above the labeled varicosity, another unlabeled axonal varicosity (av) shows a cristalline array of small clear vesicles. (Reproduced with permission from Descarries et al., 1996).

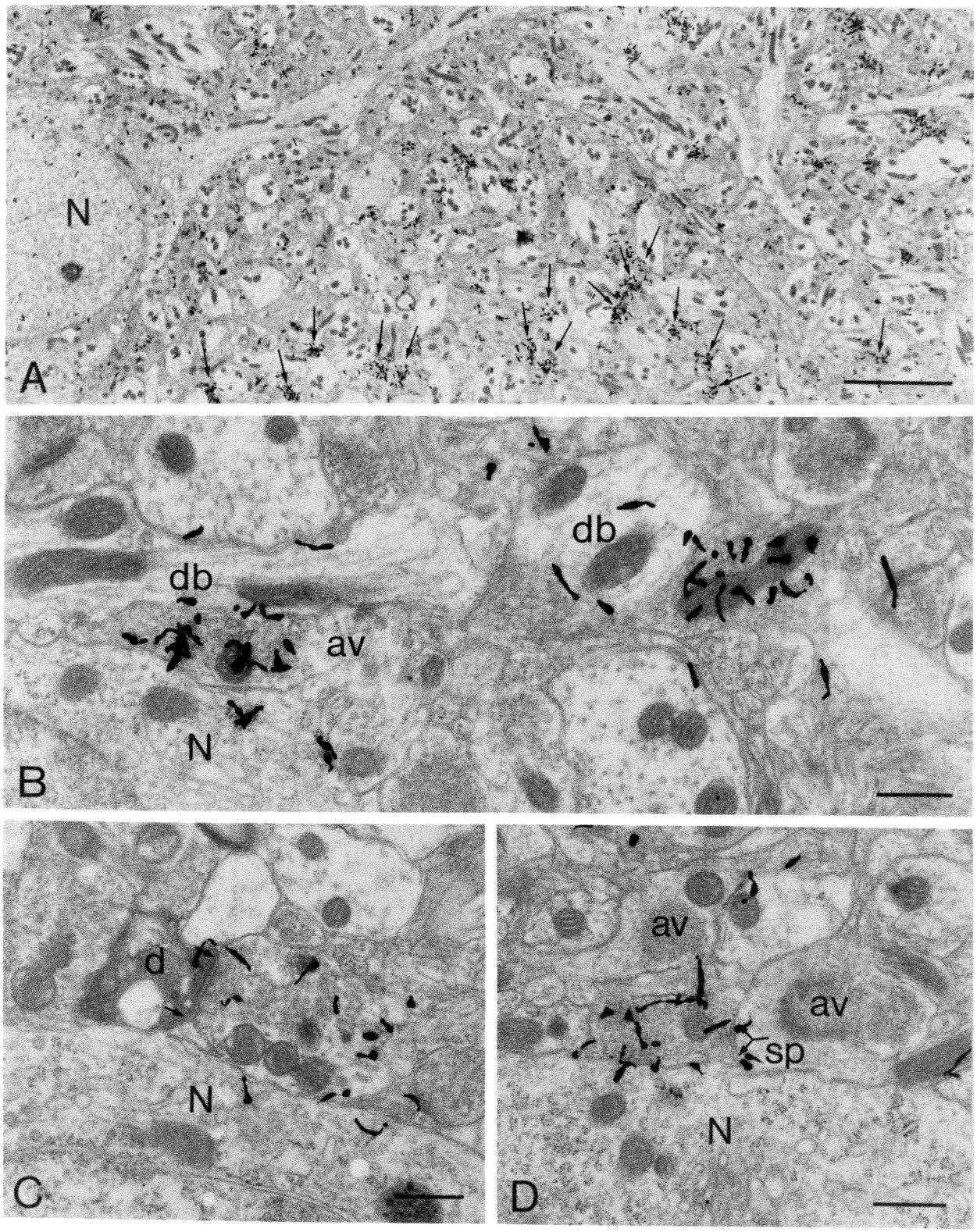
N
A
db
av
N
B
db
d
N
C
av
av
sp
N
D

Figure 3A-F. Six from a series of 10 thin sections across a DA immunoreactive axonal varicosity from the mediodorsal neostriatum (diaminobenzidine labeling). This DA varicosity (V in **A**) makes synaptic contact on the neck of a dendritic spine (sp in **C**) which receives an asymmetrical synapse on its head. The junctional complex formed by the DA varicosity on the spine neck is visible in **B** to **D** (between arrows in **C**). In **C**, the synaptically contacted spine neck may be observed in continuity with its parent dendrite (db). The large asymmetrical contact on the head of the spine (visible from B to F) is formed by an unlabeled varicosity containing small round and clear vesicles. In **E** and **F** (asterisk in **F**), the thin axonal segment leading into the DA varicosity may be observed. Scale bar: 1 μm. (Reproduced with permission from Descarries et al., 1996).

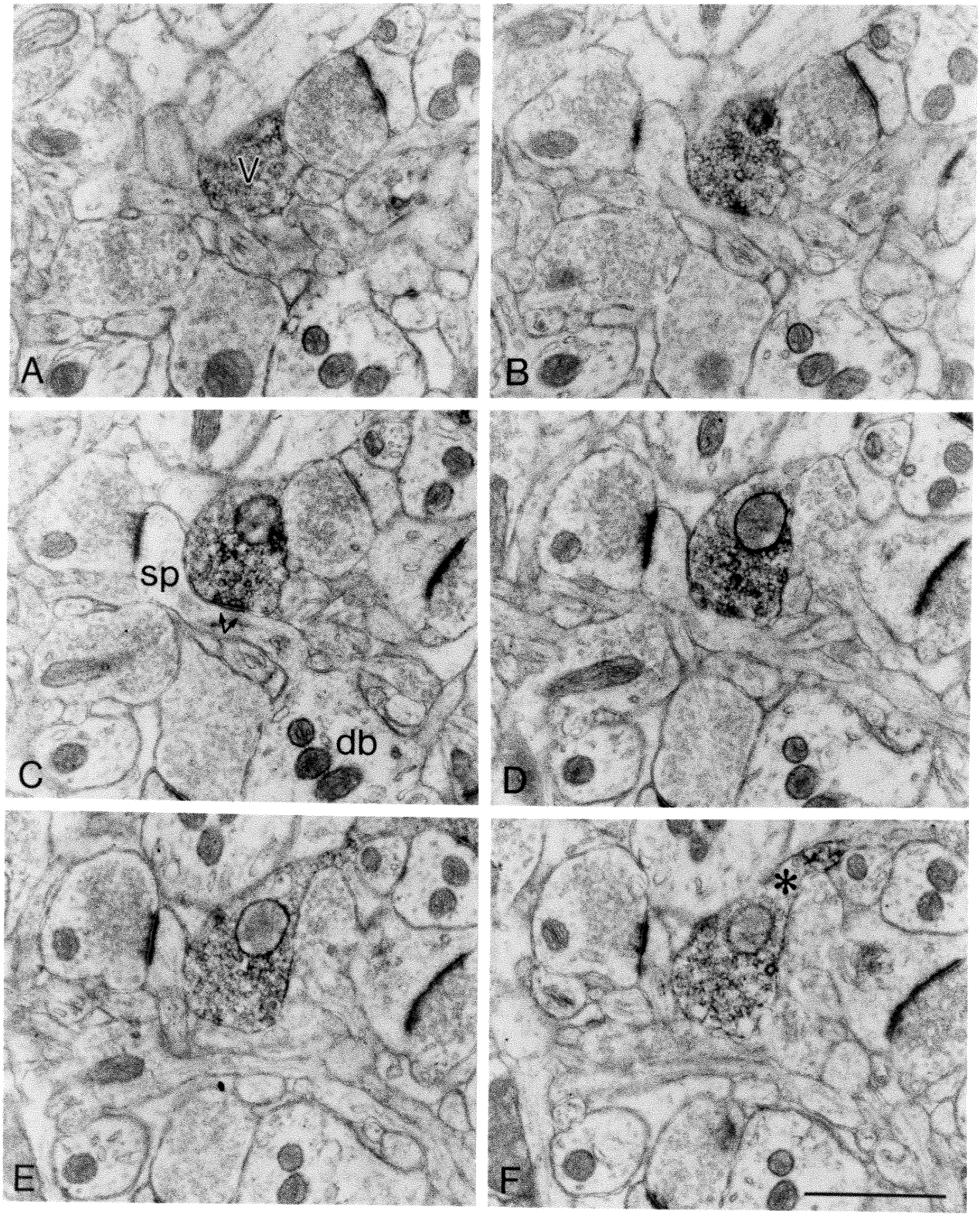
A
V
B
C
sp
db
D
E
F
*

Figure 4A-C. Electron micrograph from the center of neostriatum after ChAT immunostaining (diaminobenzinine labeling). **A-** At low magnification (X 10 000), the density of this ACh innervation may be appreciated. Within this single field, numerous sectional profiles of ChAT-immunostained axonal varicosities are seen (e.g. arrows). These immunostained profiles are generally smaller than their unlabeled counterparts. They are occasionally juxtaposed to one another (pair of vertical arrows). Scale bar: 1 μm. **B** and **C** illustrate some of the intrinsic and relational features of neostriatal ChAT-immunostained terminals. Scale bars: 0.5 μm. In **B**, two immunostained varicosities (V) filled with small vesicles are seen in continuity with their intertwining parent axons. In this section, the upper varicosity exhibits a mitochondrion, as usual devoid of immunostaining. Also note the presence of a few small vesicles in the parent axon. Even though both of these varicosities are juxtaposed to a dendritic branch, neither shows any membrane differentiation suggestive of synaptic junction. Note the small immunoreactive axon segment at arrow. In **C**, the ChAT-immunoreactive varicosity (V) displays a synaptic membrane specialization (between thin arrows) on a dendritic spine (sp). This asymmetrical junction is characterized by linearity of the apposed membranes, slight enlargement of the intercellular space and the presence of a postsynaptic density. (Reproduced with permission from Contant et al., 1996).

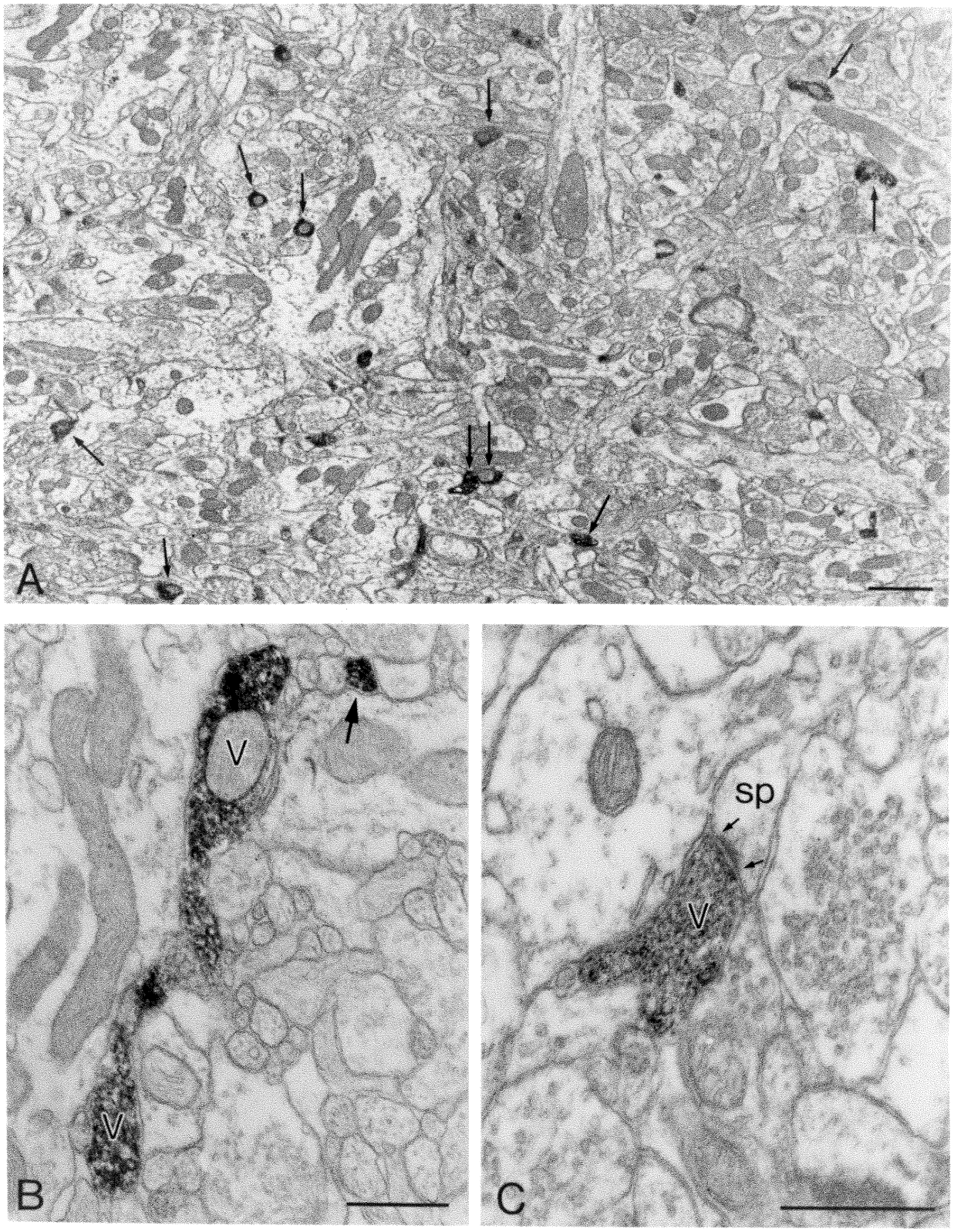
A
V
V
B
sp
V
C

ANNEXE II

COMPARATIVE ANALYSIS OF THE CHOLINERGIC INNERVATION IN THE DORSAL HIPPOCAMPUS OF ADULT MOUSE AND RAT : A QUANTITATIVE IMMUNOCYTOCHEMICAL STUDY

(Sous presse au journal *Hippocampus*)

COMPARATIVE ANALYSIS OF THE CHOLINERGIC INNERVATION IN THE DORSAL HIPPOCAMPUS OF ADULT MOUSE AND RAT: A QUANTITATIVE IMMUNOCYTOCHEMICAL STUDY

Nicolas AZNAVOUR, Naguib MECHAWAR and Laurent DESCARRIES

Départements de pathologie et biologie cellulaire et de physiologie,

and Centre de recherche en sciences neurologiques,

Faculté de médecine, Université de Montréal, Montréal, Québec, Canada H3C 3J7

(37 text pages including figure legends; 1 table and 5 figures)

Abbreviated title: **ACh innervation in mouse and rat hippocampus**

KEYWORDS acetylcholine – axons – varicosities – ChAT – distribution immunocytochemistry

Correspondence: Laurent DESCARRIES m.d.
Département de pathologie et biologie cellulaire
Université de Montréal
CP 6128, Succursale Centre-ville
Montréal, QC, Canada H3C 3J7
tel. (514) 343-7070
fax (514) 343-5755
E mail: laurent.descarries@umontreal.ca

Grant sponsor: Medical Research Council of Canada; Grant number: MT-3544.

ABSTRACT

To obtain quantitative data on the distribution of the acetylcholine (ACh) innervation in the dorsal hippocampus of adult mouse (C57/B6) and rat (Sprague-Dawley), a semi-computerized method was used to measure the length of immunostained axons in hippocampal sections processed for light microscopic immunocytochemistry with a highly sensitive antibody against choline acetyltransferase (ChAT). The results could be expressed in density of axons (meters per mm^3) for the different layers and regions of dorsal hippocampus (CA1, CA3, DG), and also in density of axon varicosities (millions per mm^3), after having determined the average number of varicosities per unit length of ChAT-immunostained axon (4 varicosities / 10 μm). In mouse, the mean regional densities of ACh innervation were thus measured at 13.9, 16.1 and 15.8 meters of axons, for 5.6, 6.4, and 6.3 million varicosities per mm^3 of tissue, in CA1, CA3 and DG, respectively. The values were comparable in rat, except for CA1, in which the densities were lower than in mouse by 40% in the stratum lacunosum, and 20% in the stratum radiatum. Otherwise, the laminar patterns of innervation were similar in the two species, the highest densities being found in the stratum lacunosum moleculare of CA3, pyramidale of both CA1 and CA3, and moleculare of DG. These quantitative data will be of particular interest to evaluate changes in mutant mice, or mice and rats subjected to experimental conditions affecting the cholinergic phenotype.

INTRODUCTION

The neurotransmitter/modulator acetylcholine (ACh) has long been recognized as playing a role in cognitive functions involving hippocampus, such as learning, memory and attention (Becker et al., 1981; Hasselmo and Schnell, 1994; Maeda et al., 1994; Acquas et al., 1996; Kim and Levin, 1996; Fujii et al., 2000; Yun et al., 2000). ACh transmission in hippocampus is impaired in Alzheimer's disease (e.g., Davies and Maloney, 1976; Bartus, 1982), certain forms of epilepsy (Mizuno and Kimura, 1996; Bertrand and Changeux, 1999; Berkowic and Steinlein, 1999; Steinlein, 2000), and schizophrenia (Freedman et al., 1997; Lindstrom, 1997; Adler et al., 1998; Freedman et al., 1999; Breese et al., 2000; Leonard et al., 2000).

The hippocampal ACh innervation originates mainly from neuronal cell bodies in the medial septal nucleus and nucleus of the vertical limb of the diagonal band of Broca (Mc Kinney et al., 1983; Rye et al., 1984; Amaral and Kurz, 1985; Nyakas et al., 1987; Woolf, 1991). A second, intrinsic component, arises from bipolar interneurons, at least in rodents (Houser et al., 1983; Frotscher et al., 1986; Blaker et al., 1988). After selective lesions of the basal forebrain ACh neurons, it has been estimated that ACh interneurons account for 5-10% of the choline acetyltransferase (ChAT) activity in dorsal hippocampus (Gage et al., 1983). Further studies have however indicated that these interneurons are unable to compensate for losses of extrinsic ACh input (Blaker et al., 1988; Frotscher, 1988).

ACh exerts its effects via muscarinic and nicotinic receptors that are widely distributed in hippocampus (reviewed in van der Zee and Luiten, 1999). At the single cell level, hippocampal ACh has been shown to depolarize a majority of

pyramidal neurons (Cole and Nicoll, 1984; Madison et al., 1987; Benson et al., 1988) and GABA interneurons (McQuiston and Madison, 1999a, 1999b; Ji and Dani, 2000), and to modulate glutamate and GABA release (Radcliffe and Dani 1998; Radcliffe et al., 1999; Alkondon et al., 1999). These widespread effects of ACh have been shown to underlie several types of large-scale synchronous neuronal activities, such as those manifested by the characteristic hippocampal β and θ rhythms (Jones and Yakel, 1997; Williams and Kauer, 1997; Cobb et al., 1999; Chapman and Lacaille, 1999; Shimono et al., 2000; Wyble et al., 2000).

Further elucidation of the physiological and pathological roles of the ACh innervation in hippocampus would greatly benefit from the availability of quantitative data on its distributional features. Yet, previous descriptions have remained essentially qualitative, or at best semi-quantitative, in mouse (Kitt et al. 1994; Schwegler et al. 1996) as well as rat (Lysakowski et al. 1989; Henderson et al. 1998). This lack of information is presumably due, at least in part, to the low sensitivity of commercially available ChAT antibodies, which appear more suited for the detection of ACh neuronal cell bodies than that of their axons and varicosities. Likewise, it remains to be demonstrated that the recently produced antibodies against the vesicular transporter for ACh provide for an integral immunocytochemical detection of this innervation (Roghani et al. 1996; Weihe et al. 1996; Arvidsson et al. 1997; Ichikawa et al. 1997; Schäfer et al. 1998; Wong et al., 1999). As for acetylcholinesterase (AChE) histo- or immunocytochemistry, it is hardly reliable for quantitative purposes, because of the widespread expression of AChE by non cholinergic neurons (Butcher et al. 1975; Robertson and Gorenstein 1987).

To fill this gap, we made use of a highly sensitive antibody against whole rat ChAT (Cozzari et al., 1990), which provides for a full light microscopic immunocytochemical visualization of ACh axon networks throughout rat brain (Umbriaco et al., 1994). In combination with a semi-computerized method for measuring the length of ChAT-immunostained axons in tissue sections, and separate counts of the average number of varicosities per unit length of ChAT-immunostained axon, it was thus possible to determine the regional and laminar densities of ACh axons and varicosities in adult and developing rat cerebral cortex (Mechawar et al., 2000; Mechawar and Descarries, 2001). In the present study, a similar approach was taken to measure and compare the density of the ACh innervation in CA1, CA3 and DG of the adult mouse and rat dorsal hippocampus. Preliminary data for the mouse have already been reported in abstract form (Aznavour et al., 2000).

MATERIALS AND METHODS

Tissue

All experiments abided by the policies and guidelines of the Canadian Council on Animal Care and the regulations of the Animal Care Committee at the Université de Montréal. The study was carried out on 6 adult male C57/B6 mice (body weight: 50 ± 10 g), and 6 adult male Sprague-Dawley rats (body weight : 250 ± 50 g), purchased from Charles River Canada (St-Constant, Quebec, Canada). After deep anesthesia with sodium pentobarbital (80 mg/kg, i.p.), these animals were respectively perfused through the heart with 25 or 50 ml of ice-cold phosphate

buffered saline (PBS; 50mM; pH 7.4), followed by 250-300 ml or 400-500 ml of 4% paraformaldehyde (PFA) in 0.1 M sodium phosphate buffer (PB; pH 7.4; 24°C). The brain was rapidly removed, postfixed overnight in PFA at 4°C, and washed in PBS. 20-µm-thick vibratome sections were then cut across the dorsal hippocampus, at transverse levels respectively equivalent to stereotaxic planes interaural A 1.98 mm in the mouse (Franklin and Paxinos, 1997) and bregma – 3.7 mm in the rat (Swanson, 1992). The sections were then processed for light microscopic immunocytochemistry as described below, or stained with cresyl violet to delimit hippocampal regions and layers.

ChAT-immunocytochemistry

The mouse monoclonal antibody against purified rat brain ChAT was used as previously described in detail (Umbriaco et al., 1994; Mechawar et al., 2000). At room temperature, the free-floating sections were rinsed (3 x 10 min), pre-incubated for 2 h in a blocking solution of PBS containing 2% normal horse serum (NHS; Vector, Burlingame, CA), 1% bovine serum albumin (BSA; Sigma, St. Louis, MO) and 0.2% Triton X-100, and incubated overnight in the same solution containing 2 µg/ml of monoclonal anti-ChAT antibody.

Immunostaining was performed at room temperature with the ABC method (Shi et al., 1988). After rinses in PBS (2 x 10 min) and a 10 min rinse in 0.1 M potassium phosphate buffer (KPB; pH 7,4), sections were incubated for 2 h in biotinylated horse anti-mouse, secondary antibody (Vector), diluted 1/200 in KPB containing 2% NHS and 1% BSA, followed by the avitidin-biotin complex procedure (ABC Kit, Vectastain Elite; Vector) for 2 h. The labeling was revealed for 2.25 min in a 0.05% solution of 3,3'-diaminobenzidine (Sigma) containing 0.01% $CoCl_2$,

0.01% $NiSO_4$, 0.01% $(NH_4)_2SO_4$, to which 0.005% H_2O_2 was added. Sections were rinsed in KPB (3 x 10 min), air-dried on gelatin-coated slides, dehydrated in ethanol, cleared in toluene, and mounted with DPX (Fluka; Sigma).

Length of ChAT-immunostained axons

The length of ChAT-immunostained axons was measured in three major sectors of hippocampus: CA1, CA3 and DG. This was done with the aid of a computer-based image analysis system: Macintosh Quadra 950, connected to a light microscope (Leitz Orthoplan; 25 X PlanApo objective lens) via a video camera (Panasonic WV-BD400; 768 x 493 pixels for 1,7 cm^2). For each animal, a 240 µm-wide vertical strip across the three hippocampal regions was captured as a series of images (645 X) that were assembled on the screen as a photomontage (Adobe Photoshop 5.5 software). Because of the relative thinness of the sections and depth of focus of the objective, all immunostained fibers across the sections were visible. Square sampling windows, 50 µm x 50 µm (0.0025 mm^2), were randomly positioned in each layer of each region, so as to fit 3 sampling windows per layer, as illustrated in Fig. 1. Using an Intuos Graphics Tablet (Wacom, Vancouver, WA), the axonal network was then drawn on the screen for each sampling window, i.e. in a total hippocampal surface of 0.0825 mm^2 per animal.

The length of the drawn axon networks was measured with the NIH Image software (1.61; public domain). The lines of the drawings were reduced to a uniform thickness of 1 pixel with the "skeletonize" function of the program, closed surfaces were cut open by removal of 1 pixel, and the length measurement (plus the number of removed pixels) was converted to micrometers, based on a prior calibration of the system with a microscopic scale. A correction (x 1/cos 45;

Soghomonian et al. 1987) was then introduced to compensate for angulation of the fibers, assuming their random orientation in the section, and the values were extrapolated to 1 mm^3 of tissue, to be expressed as average density of axons (meters per mm^3) for each layer, interlaminar mean for each hippocampal region, and interregional mean for whole dorsal hippocampus.

Number of ChAT-immunostained axon varicosities

The average number of ACh axon varicosities per unit length of axon was determined for each layer and the 3 regions of hippocampus in 3 mice and 3 rats. Varicosities were defined as axon dilations greater than 0.5 μm in transverse diameter (Umbriaco et al., 1994), as such dilations have been shown to display all subcellular attributes of axon terminals in the rat hippocampus (Umbriaco et al., 1995). In each region, the number of such dilations for 25 axon segments per layer was counted directly at the light microscope (1000 X; 1650 counts). The laminar, regional and mean hippocampal densities of axon varicosities (10^6 per mm^3) were calculated by multiplying the densities of ACh axons by the average number of varicosities per unit length.

Statistics

The laminar densities of ChAT-immunostained axons and axon varicosities were tabulated as means ± s.d. per mm^3 of tissue (n = 6). The statistical comparisons among layers of one species and between layers from a given region in mouse and rat were made by one-way ANOVA (α=0.05) followed by two-tailed Student's t test (α=0.05).

RESULTS

Visualization of ACh neurons

Previous studies have shown that the present experimental conditions provide for a specific and maximal immunocytochemical labeling of ChAT-immunoreactive axons in the rat CNS (e.g. Umbriaco et al., 1994; Mechawar et al., 2000). In mouse as well as in rat hippocampus, the nickel-cobalt enhanced ChAT-immunostaining resulted in intense darkening of a few neuronal cell bodies and of a dense network of fine varicose axons against a light background (Figs. 1-3). Individual axons could be followed without discontinuity across the thickness (20 μm) of the sections, attesting to the full penetration of immunoreagents in tissue.

Laminar distribution of hippocampal ACh innervation in mouse and rat

In both species, there were only a few small, round or ovoid, immunopositive cell bodies within hippocampus (Figs. 1A and 1B). In mouse, these neurons (2 or less per section) were mostly seen in the strata radiatum and lacunosum moleculare of CA1, and moleculare of DG but not in CA3. Their proximal dendrites were observed on rare occasions (Fig. 2C). In rat, immunostained nerve cell bodies were slightly more numerous (2-4 per section), and often typically bipolar, with their primary dendrites oriented perpendicular to the hippocampal surface (Fig. 3C). These neurons were mostly located in the stratum lacunosum moleculare of CA1, and, less often, in the strata radiatum, oriens and pyramidale of CA1, and the strata moleculare and granulare of DG. As in mouse, they were never seen in the polymorph layer of DG or in CA3.

The more or less intricate branching network of ChAT-immunoreactive axons pervaded all layers of each hippocampal region in both species (Figs. 1-3). These varicose fibers showed no predilection for the immediate vicinity of microvessels, nor any pericellular arrangement suggestive of particular relationships with specific neuronal types. In all layers, the varicose enlargements were comparably spaced along fibers, smaller and larger varicosities were visible along the same fibers, and there were no indications of regional or laminar segregation on the basis of their size. Overall, the laminar distribution of these fibers appeared consistent with earlier descriptions in mouse (Kitt et al., 1994) and rat (Lysakowski et al., 1989).

There were many more species similarities than differences when comparing, region by region, the laminar distribution of ACh axons (Figs. 2 and 3). In CA1 (Figs. 2A and 3A), a three-layered pattern was characteristic of the stratum pyramidale, with denser bands of varicose axons on its inner and outer borders. In contrast, the three neuropil layers, oriens, radiatum and lacunosum moleculare, were more homogeneously innervated, notwithstanding some density differences (see below). A narrow band of denser innervation was also found at the border between the strata lacunosum moleculare and radiatum. In CA3 (Figs. 2B and 3B), there was no stratification in the stratum pyramidale. The confinement of immunostained fibers between the closely packed immunonegative cell bodies in this layer produced a dark crescentic zone, riddled on its inner face with pale silhouettes outlined by varicose fibers. Inserted between this dark crescent and a stratum radiatum as densely innervated as in CA1, the less densely innervated stratum lucidum stood out as a light zone. The DG of mice

and rat also displayed a layered pattern, consisting of alternating bands of lesser and higher density of ACh innervation on either side of the stratum granulare (Figs. 2A and 3A). These bands differed in thickness between the two species, resulting in a different overall apearance. Compared to mice, both dorsal and ventral lips of the rat DG displayed a much thicker light zone in the inner third of the molecular layer and dark zone immediately above the granular layer. In both species, a narrow band of dense innervation was also present immediately underneath the granular layer, delimiting the hilus. Within the molecular layer in both species, there were hints of a discreet three-sublayer pattern (Figs. 2A and 3A), as already reported for the rat (Lysakowski et al., 1989).

Quantitative data on hippocampal ACh innervation in mouse and rat

The densities of ACh axons and axon varicosities (laminar, regional, whole hippocampus), respectively expressed in meters of axons and millions of varicosities per cubic millimeter of tissue, are given in Table 1 for both species. The mean number of axon varicosities per unit length of axon was not significantly different among hippocampal layers or regions within and between the two species (interlaminar means of 0.41 μm ± 0.02 s.d. and 0.40 μm ± 0.02 s.d., respectively). A fixed ratio of 4 varicosities per 10 μm of axon was therefore used to infer the densities of axon varicosities from the densities of axons, as listed in Table 1 and depicted in Figs. 4 and 5. Either parameter could indeed serve as index of ACh innervation density.

In mouse, the mean density of ACh axons and axon varicosities was significantly lower in CA1 than CA3 and DG, the latter two showing similar values (Table 1 and Fig. 4). Within each region, there were statistically significant

differences between layers (Fig. 4). In CA1, stratum pyramidale was the most densely innervated (17.9 m of axons or 7.2 million varicosites per mm^3), and lacunosum moleculare the least (10.8 m; 4.3 x 10^6). Radiatum and oriens displayed intermediate values. In CA3, on the contrary, stratum lacunosum moleculare had the highest density (20.2 m; 8.1 x 10^6). Pyramidale (19.6 m; 7.8 x 10^6) and oriens (16.7 m; 6.7 x 10^6) followed, also more densely innervated than in CA1. Stratum radiatum was moderately innervated (as in CA1), and lucidum had the lowest density (10.4 m; 4.2 x 10^6). In DG, stratum moleculare showed a high density (19.8 m; 7.9 x 10^6), while those of granulare (13.6 m; 5.4 x 10^6) and polymorph (13.9 m; 5.6 x 10^6) were intermediate.

In rat, as in mouse, the lowest mean regional density was that of CA1, the values for CA3 and DG were similar, and there were statistically significant differences between layers in all three regions (Table 1 and Fig. 5). In CA1, stratum pyramidale was again the most densely innervated (16.9 m of axons or 6.8 million varicosities per mm^3), and lacunosum moleculare the least (6.4 m; 2.6 x 10^6), the latter values being significantly lower than in mouse. The oriens values were intermediate, as in mouse (14.7 m; 5.9 x 10^6). Radiatum was also moderately innervated, but at lower densities than in mouse (10.6 m; 4.2 x 10^6). In CA3, the laminar densities were very similar to those in mouse. The values for stratum lacunosum moleculare were almost three fold greater than in CA1 (18.8 m; 7.5 x 10^6), those of pyramidale even higher (20.3 m; 8.1 x 10^6), and those of oriens also high (17.8 m; 7.1 x 10^6). Stratum radiatum was moderately innervated (13.2 m; 5.3 x 10^6), and lucidum had the lowest density (10.6 m; 4.2 x 10^6). Rat DG was also very similar to that of the mouse, with a stratum moleculare having a

high density (19.5 m; 7.8 x 10^6), whereas those of granulare (13.4 m; 5.4 x 10^6) and polymorph (13.8 m; 5.5 x 10^6) were intermediate. In brief, only CA1 showed a marked interspecies difference in ACh innervation, accounted for by the particularly low densities in strata lacunosum moleculare and radiatum.

DISCUSSION

Methodological considerations

Previous immunocytochemical descriptions with the present ChAT antibody have demonstrated its specificity throughout rat brain (Umbriaco et al., 1994), including hippocampus (Umbriaco et al., 1995; Deller et al., 1999). The fact that this antibody allows for a maximal detection of ACh axons and their varicosities under the present experimental conditions has been previously established, at least in adult rat neocortex (Mechawar et al., 2000). Visualization of the ACh innervation in mouse hippocampus and cerebral cortex appeared as selective and extensive as in the rat, with strong immunostaining of a dense axonal network as well as a few intrinsic nerve cell bodies and dendrites.

An unbiased stereological technique, such as the optical disector method, could not be used for the present quantitative purposes. In view of the size of the objects to be measured and counted (axons and axon varicosities), this would have required an electron microcopic approach, while none of the currently available antibodies against ChAT or against the vesicular ACh transporter provide for a complete immunocytochemical detection of ACh fibers in material processed for electron microscopy. We therefore opted for a two-dimensional light microscopic

method yielding reasonable estimates, and which had the advantage of allowing for extensive anatomical sampling (Benes and Lange, 2001).

The sampling windows from which the measurements were obtained were randomly located in relation to the layers and regions examined, and sufficiently large to ensure a reliable sampling of each layer across CA1, CA3 and the DG. Visual inspection of other hippocampal areas, in the same and other transverse sections, showed that the level examined was representative of the whole dorsal hippocampus, except for its rostral tip. The semi-computerized technique used for collecting the data ensured that all and only immunostained fibers were being measured across the full thickness of the sections. Although tedious, this procedure was the only way to obtain sufficient gray shade discrimination for tracing some of the more lightly stained axon segments between the darker varicosities. The mathematical correction for angulation, assuming a random orientation of the fibers in the sections, was a convenient way to convert these length measurements from a plane to a three-dimensional volume. The risk of an overestimation introduced by this correction was minimal, since none of the sampled areas displayed numerous fibers running preferentially within the plane of the section, except for the narrow band in CA1, at the border between radiatum and lacunosum moleculare (see below).

Axon varicosities were defined as dilations 0.5 μm or more in transverse diameter, on the basis of prior electron microscopic measurements (Umbriaco et al., 1995). These had also shown that the average diameter of intervaricose ACh segments is about 0.2 μm, allowing for a clearcut distinction between the varicosities and the axons. The fixed ratio of 4 ACh varicosities per 10 μm of axon,

valid for mouse as well as rat hippocampus, allowed to directly infer the densities of varicosities from those of axon length. It also meant that both parameters were equally useful as indices of innervation density. Expressing length of axons and number of varicosities as densities (length or number per mm^3) facilitates correlations with other measurable parameters of cholinergic function and with cytometric data regarding this and other chemically defined systems.

Topographical features of the ACh innervation

The present study extended earlier observations on the distributional features of the hippocampal ACh innervation in adult mouse and rat made with AChE-histo- or immunocytochemistry (mouse: Slomianka and Geneser, 1991, 1993; rat: Storm-Mathisen and Blackstad, 1964), ChAT-immunocytochemistry (mouse: Kitt et al., 1994; rat: Lysakowski et al., 1989) and immunoctytochemistry of the vesicular transporter for ACh (rat: Arvidsson et al., 1997; Ichikawa et al., 1997; Schäfer et al., 1998). At variance with some early ChAT-immunocytochemical reports, however, we did not detect immunoreactive pyramidal cells in rat (Nishimura et al. 1988), nor numerous interneurons in either species (Kitt et al., 1994; Matthews et al., 1987). According to an earlier description (Frotscher et al., 1986), it could be assumed that the morphology and distribution of ACh interneurons here observed in the dorsal hippocampus was representative of the whole region, at least for rat. Although in low number, hippocampal ACh interneurons appeared slightly more numerous in rat than mouse, perhaps due to the greater volume of this region in the rat. In both species, the predilection of these cells for both lips of the hippocampal fissure – lacunosum moleculare of CA1 and moleculare of DG – was suggestive of some preferential relationship

with the perforant and temporo-ammonic pathways (Frotscher et al., 1986). The extent of the axonal arborization of these neurons, the nature of their putative coexistent transmitter(s) and the ultrastructural features of their terminals remain to be defined (Freund and Buzsaki, 1996).

In both species, there were particular aspects of the topographic distribution of the ACh innervation which were beyond the limits of resolution of the quantitative analysis, and yet of interest in terms of functional significance. For example, the three-layered pattern in the stratum pyramidale of CA1, with two denser bands of ACh innervation on either side of the thin and compact layer of pyramidal cell bodies, raised the question of a targeted versus non targeted innervation. This pattern could reflect some preferential relationships with the proximal dendrites of pyramidal neurons, and/or the GABA and glutamate synaptic inputs to these dendrites (Freund and Buzsaki, 1996). Yet, it was not observed in the equally densely innervated stratum pyramidale of CA3, in which the more loosely grouped pyramidal cells form a thicker layer. Thus, this layering pattern could merely be the result of the particularly high packing density of pyramidal cell bodies in CA1. As for the dense narrow band of longitudinally oriented ACh fibers observed at the interface of the strata radiatum and lacunosum moleculare of CA1, it could represent a pathway for ACh axons entering the densely innervated stratum lacunosum moleculare of CA3 from the subiculum. Interestingly, this band coincides with the presence of interneurons which, upon activation by ACh, are known to be involved in the pacing of theta activity in CA1 pyramidal cells (Chapman and Lacaille, 1999).

In the DG, the granular layer also displayed a three-layered pattern of innervation, which was reminiscent of the pyramidal layer in CA1. The relatively thicker and darker rim, orthogonal to the apical dendrites of granular cells, seemed to relate more with the density of innervation of the adjacent neuropil (stratum moleculare). The discrete three-sublayer pattern in the molecular layer of the DG was more obvious in rat than mouse, but not as clear as initially described with AChE-histochemistry (Lysakowski et al., 1989). This pattern might be related to the particular distribution of some afferents to this layer, such as the innervation of its outer and middle thirds by the lateral and medial entorhinal cortex, respectively (Witter et al., 2000).

Quantified distributional features of the ACh innervation

The fixed ratio of 4 varicosities per 10 μm of ACh axon measured throughout mouse as well as rat hippocampus was the same as previously determined for the ACh innervation in the different layers of three neocortical areas (frontal, parietal, occipital) in adult rat (Mechawar et al., 2000). Such a constancy is suggestive of intrinsic determinants and conversely supports the view that the density of ACh innervation, which varies between layers and regions, must be regulated by local cues controlling the extent of axonal arborization (e.g. Super et al., 1998; Skutella and Nitsch, 2001).

Many distributional features of this ACh innervation, common to both species, were revealed by the quantitative analysis. A first was its ubiquity, with laminar densities (per mm^3) ranging from 10.4 to 20.2 meters of axons and 4.2 to 8.1 million axon varicosities in mouse, and from 6.4 to 20.4 meters of axons and 2.6 to 8.2 million axon varicosities in rat. These relatively high densities suggest that

all hippocampal neurons in the rat and mouse might be within reach of ACh (see Descarries et al., 1997; Descarries and Mechawar 2000), in keeping with immunocytochemical observations that nearly all hippocampal interneurons and principal cells express cholinergic receptors (e.g., van der Zee and Luiten, 1999).

In accordance with earlier suggestions based on a quantification of AChE fibers in mouse (Schwegler et al., 1996) and rat (Matthews et al., 1987), the present study also indicated that, in spite of similar patterns of laminar distribution, the average density of ACh innervation in CA3 was significantly higher than in CA1, and in fact closer to that of DG. The 16% (mouse) and 33% (rat) differences between the two sectors of Ammon's horn were largely accounted for by the 87% (mouse) and 194% (rat) higher densities of ACh innervation in the stratum lacunosum moleculare of CA3 compared to CA1. Anatomical studies in rat have shown that the stratum lacunosum moleculare of CA3 and CA1 are differentially innervated by layer II and III neurons of the entorhinal cortex (Amaral and Witter, 1995; Witter et al., 2000). The entorhinal cortex, which receives input from the perirhinal and postrhinal cortex (Burwell and Amaral, 1998; Burwell, 2000) has been implicated in both object recognition (Wan et al., 1999) and spatial memory (Aggleton et al., 2000; Vann et al., 2000a). Interestingly, the lacunosum moleculare of CA1 also receives afferents from the midline nucleus reuniens of thalamus (Amaral and Witter, 1995), another pathway implicated in spatial memory (Vann et al., 2000b). This nucleus has been shown to influence hippocampal transmission through activation of local inhibitory interneurons (Dolleman-Van der Weel et al., 1997, 2000), much as demonstrated for hippocampal ACh (Ji and Dani, 2000; McQuiston and Madison, 1999a). It may

thus be speculated that the lower density of ACh innervation in the lacunosum moleculare of CA1 reflects a lesser role for ACh in the modulation of this type of information in this region. This would be consistent with computational models of CA1 predicting that, for effective associative memory, cholinergic suppression of intrinsic synaptic transmission should be weaker in lacunosum moleculare than stratum radiatum, in order to favour the treatment of extrinsic inputs (Hasselmo and Bower, 1992, 1993; Hasselmo and Schnell, 1994).

Also characteristic of both species was the low density of ACh innervation in the stratum lucidum of CA3. In CA3, mossy fibers represent one of the main inputs to this layer, and direct modulation of their activity by exogenous ACh has been shown to be relatively weak (Vogt and Regehr, 2001). Taken together, these and the above data seem to relate the laminar density of innervation with the degree of influence exerted locally by ACh. Such a link would be in line with the largely asynaptic nature of this innervation (Umbriaco et al., 1995), and the potential importance of an ambient level of extracellular ACh in its functioning (Descarries et al., 1997). It will be for future studies to determine if and how the greater density of ACh innervation in mice versus rat strata radiatum (+ 25%) and lacunosum moleculare (+ 69%) of CA1, which is the major interspecies difference measured in the present study, might translate into species-specific physiological and behavioral traits.

Other parameters of ACh function in hippocampus

Previous autoradiographic and immunocytochemical descriptions of muscarinic receptor subtypes and nicotinic subunits in hippocampus have revealed similar widespread and complementary laminar distributions for mouse

and rat (Hill et al., 1993; Sargent, 1993; Séguéla et al., 1993; Dominguez del Toro et al., 1994; Hohmann et al., 1995; Levey et al., 1995; Aubert et al., 1996; Schwegler et al., 1996). In both species, the most widely expressed $\alpha 7$ and $\beta 2$ nicotinic subunits (Sargent, 1993) were mainly found in the principal cell layers (Séguéla et al., 1993; Dominguez del Toro et al., 1994; Hill et al., 1993). In rat, m1, m3 and m4 subtypes have been shown to be expressed by principal cells, and m2 by interneurons (Freund and Buzsaki, 1996) and axon terminals (Levey et al., 1995). The apparent match between the distribution of m2 receptors and the ACh innervation of CA1 and CA3 is consistent with the recent anatomical demonstration of a terminal autoreceptor as well as heteroreceptor location for hippocampal m2 (Rouse et al., 1999, 2000). Conversely, its relatively low expression in the DG (Levey et al., 1995), in which the ACh innervation is dense, suggests a lesser role as autoreceptor and its predominance as terminal heteroreceptor in this region.

The mean overall densities of 6.1 million ACh varicosities per mm^3 in mouse hippocampus, and 5.9 million in rat, represent the densest neuromodulatory inputs thus far described in cerebral cortex (e.g., noradrenaline: Oleskevich et al., 1989; serotonin: Oleskevich and Descarries, 1990). Assuming that the density of ACh innervation measured in the dorsal hippocampus is representative of the whole region, and based on hippocampal volumes of 21.3 mm^3 for mouse (West, 1990) and 56 mm^3 for rat (Coleman et al., 1987), the total length of ACh axons in one hippocampus may be extrapolated at 326 (mouse) and 823 meters (rat), and the corresponding numbers of varicosities at 130 and 329 x 10^6. It is currently estimated that some 250 ACh nerve cell bodies in the septum and diagonal band of Broca project to mouse hippocampus (Schwegler et al., 1996), and 385 in the rat

(McKinney et al., 1983). Thus, these ACh neurons should be endowed with an axonal arborization averaging 1.3 meter in length and bearing 520 x 10^3 axon varicosities in mouse, compared to 2.1 meters of axon and 840 x 10^3 varicosities in rat. The latter values are twice higher than previously extrapolated for nucleus basalis ACh neurons projecting to adult rat neocortex (Mechawar et al., 2000), which, in itself, provides compelling structural evidence for a crucial role of ACh in hippocampal function.

Acknowledgments

Supported by grant MT-3544 from the MRC of Canada. N.A. holds a PhD studentship from the Groupe de recherche sur le système nerveux central (FCAR) and N.M. a research studentship from the Medical Research Council of Canada. The authors are grateful to Jean-Claude Lacaille for fruitful discussions and a critical revision of the manuscript. They also thank Gaston Lambert for photographic work.

References

Acquas E, Wilson C, Fibiger HC. 1996. Conditioned and unconditioned stimuli increase frontal cortical and hippocampal acetylcholine release: effects of novelty, habituation, and fear. J Neurosci 16:3089-3096.

Adler LE, Olincy A, Waldo M, Harris JG, Griffith J, Stevens K, Flach K, Nagamoto H, Bickford P, Leonard S, Freedman R. 1998. Schizophrenia, sensory gating, and nicotinic receptors. Schizophr Bull 24: 189-202.

Aggleton JP, Vann SD, Oswald CJ, Good M. 2000. Identifying cortical inputs to the rat hippocampus that subserve allocentric spatial processes: a simple problem with a complex answer. Hippocampus 10: 466-474.

Alkondon M, Pereira EF, Eisenberg HM, Albuquerque EX. 1999. Choline and selective agonists identify two subtypes of nicotinic acetylcholine receptors that modulate GABA release from CA1 interneurons in rat hippocampal slices. J Neurosci 19: 2693-2705.

Amaral DG and Kurz J. 1985. An analysis of the origins of the cholinergic and noncholinergic septal projections to the hippocampal formation of the rat. J Comp Neurol 240: 37-59.

Amaral DG and Witter MP. 1995. Hippocampal formation. In: Paxinos G, editor. The rat nervous system. San Diego : Academic Press. p 443-493

Arvidsson U, Riedl M, Elde R, Meister B. 1997. Vesicular acetylcholine transporter (VAChT) protein: a novel and unique marker for cholinergic neurons in the central and peripheral nervous systems. J Comp Neurol 378: 454-467.

Aubert I, Cecyre D, Gauthier S, Quirion R. 1996. Comparative ontogenic profile of cholinergic markers, including nicotinic and muscarinic receptors, in the rat brain. J Comp Neurol 369: 31-55.

Aznavour N, Mechawar N, Descarries L. 2000. Quantitative distribution of the cholinergic innervation in adult mouse hippocampus. Soc Neurosci Abstr 26: 2141.

Bartus RT, Dean RL, Beer B, Lippa AS. 1982. The cholinergic hypothesis of geriatric memory dysfunction. Science 217: 408-414.

Becker JT, Olton DS, Anderson CA, Breitinger ER. 1981. Cognitive mapping in rats: the role of the hippocampal and frontal system in retention and reversal. Behav Brain Res 3: 1-22.

Benes FM, Lange N. 2001. Two-dimensional versus three-dimensional cell counting: a practical perspective. Trends Neurosci 24: 11-17.

Benson DM, Blitzer RD, Landau EM. 1988. An analysis of the depolarization produced in guinea-pig hippocampus by cholinergic receptor stimulation. J Physiol (Lond) 404: 479-496.

Berkovic SF and Steinlein OK. 1999. Genetics of partial epilepsies. Adv Neurol 79: 375-381.

Bertrand D and Changeux JP. 1999. Nicotinic receptor: a prototype of allosteric ligand-gated ion channels and its possible implications in epilepsy. Adv Neurol 79: 171-188.

Blaker SN, Armstrong DM and Gage FH. 1988. Cholinergic neurons within the rat hippocampus: response to fimbria-fornix transection. J Comp Neurol 272: 127-138.

Breese CR, Lee MJ, Adams CE, Sullivan B, Logel J, Gillen KM, Marks MJ, Collins AC, Leonard S. 2000. Abnormal regulation of high affinity nicotinic receptors in subjects with schizophrenia. Neuropsychopharmacology 23: 351-364.

Burwell RD. 2000. The parahippocampal region: corticocortical connectivity. Ann NY Acad Sci 911: 25-42.

Burwell RD and Amaral DG. 1998. Perirhinal and postrhinal cortices of the rat: interconnectivity and connections with the entorhinal cortex. J Comp Neurol 391: 293-321.

Butcher LL, Talbot K, Bilezikjian L. 1975. Acetylcholinesterase neurons in dopamine-containing regions of the brain. J Neural Transm 37: 127-153.

Chapman CA and Lacaille JC. 1999. Cholinergic induction of theta-frequency oscillations in hippocampal inhibitory interneurons and pacing of pyramidal cell firing. J Neurosci 19: 8637-8645.

Cobb SR, Bulters DO, Suchak S, Riedel G, Morris RG, Davies CH. 1999. Activation of nicotinic acetylcholine receptors patterns network activity in the rodent hippocampus. J Physiol (Lond) 518: 131-140.

Cole AE and Nicoll RA. 1984. The pharmacology of cholinergic excitatory responses in hippocampal pyramidal cells. Brain Res 305: 283-290.

Coleman PD, Flood DG, West MJ. 1987. Volumes of the components of the hippocampus in the aging F344 rat. J Comp Neurol 266: 300-306.

Cozzari C, Howard J, Hartman B. 1990. Analysis of epitopes of choline acetyltransferase (ChAT) using monoclonal antibodies (Mabs). Soc Neurosci Abstr 16:200.

Davies P and Maloney AJ. 1976. Selective loss of central cholinergic neurons in Alzheimer's disease [letter]. Lancet 2: 1403.

Deller T, Katona I, Cozzari C, Frotscher M, Freund TF. 1999. Cholinergic innervation of mossy cells in the rat fascia dentata. Hippocampus 9: 314-320.

Descarries L. and Mechawar N. 2000. Ultrastructural evidence for diffuse transmission by monoamine and acetylcholine neurons of the central nervous system. Prog Brain Res 125: 27-47.

Descarries L, Gisiger V, Steriade M. 1997. Diffuse transmission by acetylcholine in the CNS. Prog Neurobiol 53: 603-625.

Dolleman-Van der Weel MJ and Witter MP. 2000. Nucleus reuniens thalami innervates gamma aminobutyric acid positive cells in hippocampal field CA1 of the rat. Neurosci Lett 278: 145-148.

Dolleman-Van der Weel, MJ, Lopes da Silva FH, Witter MP. 1997. Nucleus reuniens thalami modulates activity in hippocampal field CA1 through excitatory and inhibitory mechanisms. J Neurosci 17: 5640-5650.

Dominguez del Toro E, Juiz JM, Peng X, Lindstrom J, Criado M. 1994. Immunocytochemical localization of the alpha 7 subunit of the nicotinic acetylcholine receptor in the rat central nervous system. J Comp Neurol 349: 325-342.

Franklin KBJ, and Paxinos G. 1997. The Mouse Brain in Stereotaxic Coordinates. San Diego: Academic Press.

Freedman R, LE Adler, Leonard S. 1999. Alternative phenotypes for the complex genetics of schizophrenia. Biol Psychiatry 45: 551-558.

Freedman R, Coon H, Myles-Worsley M, Orr-Urtreger A, Olincy A, Davis A, Polymeropoulos M, Holik J, Hopkins J, Hoff M, Rosenthal J, Waldo MC, Reimherr F, Wender P, Yaw J, Young DA, Breese CR, Adams C, Patterson D, Adler LE, Kruglyak L, Leonard S, Byerley W. 1997. Linkage of a neurophysiological deficit in schizophrenia to a chromosome 15 locus. Proc Natl Acad Sci USA 94: 587-592.

Freund TF and Buzsaki G 1996. Interneurons of the hippocampus. Hippocampus 6: 347-470.

Frotscher M 1988. Cholinergic neurons in the rat hippocampus do not compensate for the loss of septohippocampal cholinergic fibers. Neurosci Lett 87: 18-22.

Frotscher M, Schlander M, Leranth C. 1986. Cholinergic neurons in the hippocampus. A combined light- and electron-microscopic immunocytochemical study in the rat. Cell Tissue Res 246: 293-301.

Fujii S, Jia Y, Yang A, Sumikawa K. 2000. Nicotine reverses GABAergic inhibition of long-term potentiation induction in the hippocampal CA1 region. Brain Res 863: 259-265.

Gage FH, Bjorklund A, Stenevi U. 1983. Reinnervation of the partially deafferented hippocampus by compensatory collateral sprouting from spared cholinergic and noradrenergic afferents. Brain Res 268: 27-37.

Hasselmo ME and Bower JM. 1992. Cholinergic suppression specific to intrinsic not afferent fiber synapses in rat piriform (olfactory) cortex. J Neurophysiol 67: 1222-1229.

Hasselmo ME and Bower JM. 1993. Acetylcholine and memory. Trends Neurosci 16: 218-222.

Hasselmo ME and Schnell E. 1994. Laminar selectivity of the cholinergic suppression of synaptic transmission in rat hippocampal region CA1: computational modeling and brain slice physiology. J Neurosci 14: 3898-3914.

Henderson Z, Harrison PS, Jagger E, Beeby JH. 1998. Density of choline acetyltransferase-immunoreactive terminals in the rat dentate gyrus after entorhinal cortex lesions: a quantitative light microscope study. Exp Neurol 152: 50-63.

Hill JA, Zoli M, Bourgeois JP, Changeux JP. 1993. Immunocytochemical localization of a neuronal nicotinic receptor: the beta 2-subunit. J Neurosci 13: 1551-1568.

Hohmann CF, Potter ED, Levey AI. 1995. Development of muscarinic receptor subtypes in the forebrain of the mouse. J Comp Neurol 358: 88-101.

Houser CR, Crawford GD, Barber RP, Salvaterra PM, Vaughn JE. 1983. Organization and morphological characteristics of cholinergic neurons: an immunocytochemical study with a monoclonal antibody to choline acetyltransferase. Brain Res 266: 97-119.

Ichikawa T, Ajiki K, Matsuura J, Misawa H. 1997. Localization of two cholinergic markers, choline acetyltransferase and vesicular acetylcholine transporter in the central nervous system of the rat: in situ hybridization histochemistry and immunohistochemistry. J Chem Neuroanat 13: 23-39.

Ji D and Dani JA. 2000. Inhibition and disinhibition of pyramidal neurons by activation of nicotinic receptors on hippocampal interneurons. J Neurophysiol 83: 2682-2690.

Jones S and Yakel JL. 1997. Functional nicotinic ACh receptors on interneurones in the rat hippocampus. J Physiol (Lond) 504: 603-610.

Kim JS and Levin ED. 1996. Nicotinic, muscarinic and dopaminergic actions in the ventral hippocampus and the nucleus accumbens: effects on spatial working memory in rats. Brain Res 725: 231-240.

Kitt CA, Hohmann C, Coyle J T, Price DL. 1994. Cholinergic innervation of mouse forebrain structures. J Comp Neurol 341: 117-129.

Leonard S, Breese C, Adams C, Benhammou K, Gault J, Stevens K, Lee M, Adler L, Olincy A, Ross R, Freedman R. 2000. Smoking and schizophrenia: abnormal nicotinic receptor expression. Eur J Pharmacol 393: 237-242.

Levey AI, Edmunds SM, Koliatsos V, Wiley RG, Heilman CJ. 1995. Expression of m1-m4 muscarinic acetylcholine receptor proteins in rat hippocampus and regulation by cholinergic innervation. J Neurosci 15: 4077-4092.

Lindstrom J. 1997. Nicotinic acetylcholine receptors in health and disease. Mol Neurobiol 15: 193-222.

Lysakowski A, Wainer BH, Bruce G, Hersh LB. 1989. An atlas of the regional and laminar distribution of choline acetyltransferase immunoreactivity in rat cerebral cortex. Neuroscience 28: 291-336.

Madison DV, Lancaster B, Nicoll RA. 1987. Voltage clamp analysis of cholinergic action in the hippocampus. J Neurosci 7: 733-741.

Maeda, T, Kaneko S, Satoh M. 1994. Roles of endogenous cholinergic neurons in the induction of long-term potentiation at hippocampal mossy fiber synapses. Neurosci Res 20: 71-78.

Matthews DA, Salvaterra PM, Crawford GD, Houser CR, Vaughn JE. 1987. An immunocytochemical study of choline acetyltransferase-containing neurons and axon terminals in normal and partially deafferented hippocampal formation. Brain Res 402: 30-43.

McKinney M, Coyle JT, Hedreen JC. 1983. Topographic analysis of the innervation of the rat neocortex and hippocampus by the basal forebrain cholinergic system. J Comp Neurol 217: 103-121.

McQuiston AR and Madison DV. 1999a. Muscarinic receptor activity has multiple effects on the resting membrane potentials of CA1 hippocampal interneurons. J Neurosci 19: 5693-5702.

McQuiston AR and Madison DV. 1999b. Nicotinic receptor activation excites distinct subtypes of interneurons in the rat hippocampus. J Neurosci 19: 2887-2896.

Mechawar N and Descarries L. 2001. The cholinergic innervation develops early and rapidly in the rat cerebral cortex: A quantitative immunocytochemical study. J Neurosci, submitted.

Mechawar N, Cozzari C, Descarries L. 2000. Cholinergic innervation in adult rat cerebral cortex: A quantitative immunocytochemical description. J Comp Neurol 428: 305-318.

Mizuno T and Kimura F. 1996. Medial septal injection of naloxone elevates acetylcholine release in the hippocampus and induces behavioral seizures in rats. Brain Res 713: 1-7.

Nishimura Y, Natori M, Mato M. 1988. Choline acetyltransferase immunopositive pyramidal neurons in the rat frontal cortex. Brain Res 440: 144-148.

Nyakas C, Luiten PG, Spencer DG, Traber J. 1987. Detailed projection patterns of septal and diagonal band efferents to the hippocampus in the rat with emphasis on innervation of CA1 and dentate gyrus. Brain Res Bull 18: 533-545.

Oleskevich S and Descarries L. 1990. Quantified distribution of the serotonin innervation in adult rat hippocampus. Neuroscience 34: 19-33.

Oleskevich S, Descarries L, Lacaille JC. 1989. Quantified distribution of the noradrenaline innervation in the hippocampus of adult rat. J Neurosci 9: 3803-3815.

Radcliffe KA and Dani JA. 1998. Nicotinic stimulation produces multiple forms of increased glutamatergic synaptic transmission. J Neurosci 18: 7075-7083.

Radcliffe KA, Fisher JL, Gray R, Dani JA. 1999. Nicotinic modulation of glutamate and GABA synaptic transmission of hippocampal neurons. Ann NY Acad Sci 868: 591-610.

Robertson RT and Gorenstein C. 1987. 'Non-specific' cholinesterase-containing neurons of the dorsal thalamus project to medial limbic cortex. Brain Res 404: 282-292.

Roghani A, Shirzadi A, Kohan SA, Edwards RH, Butcher LL. 1996. Differential distribution of the putative vesicular transporter for acetylcholine in the rat central nervous system. Brain Res Mol Brain Res 43: 65-76.

Rouse ST, Edmunds SM, Yi H, Gilmor ML, Levey AI. 2000. Localization of M(2) muscarinic acetylcholine receptor protein in cholinergic and non-cholinergic terminals in rat hippocampus. Neurosci Lett 284: 182-186.

Rouse ST, Marino MJ, Potter LT, Conn PJ, Levey AI. 1999. Muscarinic receptor subtypes involved in hippocampal circuits. Life Sci 64: 501-509.

Rye DB, Wainer BH, Mesulam MM, Mufson EJ, Saper CB. 1984. Cortical projections arising from the basal forebrain: a study of cholinergic and noncholinergic components employing combined retrograde tracing and immunohistochemical localization of choline acetyltransferase. Neuroscience 13: 627-643.

Sargent PB 1993. The diversity of neuronal nicotinic acetylcholine receptors. Annu Rev Neurosci 16: 403-443.

Schäfer MK, Eiden LE, Weihe E. 1998. Cholinergic neurons and terminal fields revealed by immunohistochemistry for the vesicular acetylcholine transporter. I. Central nervous system. Neuroscience 84: 331-359.

Schwegler H, Boldyreva M, Linke R, Wu J, Zilles K, Crusio WE. 1996. Genetic variation in the morphology of the septo-hippocampal cholinergic and GABAergic systems in mice: II. Morpho-behavioral correlations. Hippocampus 6: 535-545.

Séguéla P, Wadiche J, Dineley-Miller K, Dani JA, Patrick JW. 1993. Molecular cloning, functional properties, and distribution of rat brain alpha 7: a nicotinic cation channel highly permeable to calcium. J Neurosci 13: 596-604.

Shi ZR, Itzkowitz SH, Kim YS. 1988. A comparison of three immunoperoxidase techniques for antigen detection in colorectal carcinoma tissues. J Histochem Cytochem 36: 317-322.

Shimono K, Brucher F, Granger R, Lynch G,. Taketani M. 2000. Origins and distribution of cholinergically induced beta rhythms in hippocampal slices. J Neurosci 20: 8462-8473.

Skutella T and Nitsch R. 2001. New molecules for hippocampal development. Trends Neurosci 24: 107-113.

Slomianka, L and Geneser FA. 1991. Distribution of acetylcholinesterase in the hippocampal region of the mouse: II. Subiculum and hippocampus. J Comp Neurol 312:525-36.

Slomianka, L and Geneser FA. 1993. Distribution of acetylcholinesterase in the hippocampal region of the mouse: III. The area dentata. J Comp Neurol 331: 225-235.

Soghomonian J-J, Doucet G, Descarries L. 1987. Serotonin innervation in adult rat neostriatum. I. Quantified regional distribution. Brain Res 425: 85-100.

Steinlein OK. 2000. Neuronal nicotinic receptors in human epilepsy. Eur J Pharmacol 393: 243-247.

Storm-Mathisen JS and Blackstad TW. 1964. Cholinesterase in the hippocampal region. Acta Anat 56: 216-253.

Super H, Martinez A, Del Rio JA, Soriano E. 1998. Involvement of distinct pioneer neurons in the formation of layer- specific connections in the hippocampus. J Neurosci 18: 4616-4626.

Swanson LW. 1992. Brain Maps: Structure of the Rat Brain. Amsterdam: Elsevier.

Umbriaco D, Watkins KC, Descarries L, Cozzari C, Hartman BK. 1994. Ultrastructural and morphometric features of the acetylcholine innervation in adult rat parietal cortex: an electron microscopic study in serial sections. J Comp Neurol 348: 351-373.

Umbriaco D, Garcia S, Beaulieu C, Descarries L. 1995. Relational features of acetylcholine, noradrenaline, serotonin and GABA axon terminals in the stratum radiatum of adult rat hippocampus (CA1). Hippocampus 5: 605-620.

van der Zee EA and Luiten PG. 1999. Muscarinic acetylcholine receptors in the hippocampus, neocortex and amygdala: a review of immunocytochemical localization in relation to learning and memory. Prog Neurobiol 58: 409-471.

Vann SD, Brown MW, Aggleton JP. 2000a. Fos expression in the rostral thalamic nuclei and associated cortical regions in response to different spatial memory tests. Neuroscience 101: 983-991.

Vann SD, Brown MW, Erichsen JT, Aggleton JP. 2000b. Fos imaging reveals differential patterns of hippocampal and parahippocampal subfield activation in rats in response to different spatial memory tests. J Neurosci 20: 2711-2718.

Vogt KE and Regehr WG. 2001. Cholinergic Modulation of Excitatory Synaptic Transmission in the CA3 Area of the Hippocampus. J Neurosci 21: 75-83.

Wan H, Aggleton JP, Brown MW. 1999. Different contributions of the hippocampus and perirhinal cortex to recognition memory. J Neurosci 19: 1142-1148.

Weihe E, Tao-Cheng JH, Schafer MK, Erickson JD, Eiden LE. 1996. Visualization of the vesicular acetylcholine transporter in cholinergic nerve terminals and its targeting to a specific population of small synaptic vesicles. Proc Natl Acad Sci USA 93: 3547-3552.

West MJ. 1990. Stereological studies of the hippocampus: a comparison of the hippocampal subdivisions of diverse species including hedgehogs, laboratory rodents, wild mice and men. Prog Brain Res 83: 13-36.

Williams JH and Kauer JA. 1997. Properties of carbachol-induced oscillatory activity in rat hippocampus. J Neurophysiol 78: 2631-2640.

Witter MP, Naber PA, van Haeften T, Machielsen WC, Rombouts SA, Barkhof F, Scheltens P, Lopes da Silva FH. 2000. Cortico-hippocampal communication by way of parallel parahippocampal- subicular pathways. Hippocampus 10: 398-410.

Wong TP, Debeir T, Duff K, Cuello AC. 1999. Reorganization of cholinergic terminals in the cerebral cortex and hippocampus in transgenic mice carrying mutated presenilin-1 and amyloid precursor protein transgenes. J Neurosci 19: 2706-2716.

Woolf NJ. 1991. Cholinergic systems in mammalian brain and spinal cord. Prog Neurobiol 37: 475-524.

Wyble BP, Linster C, Hasselmo ME. 2000. Size of CA1-evoked synaptic potentials is related to theta rhythm phase in rat hippocampus. J Neurophysiol 83: 2138-2144.

Yun SH, Cheong MY, Mook-Jung I, Huh K, Lee C, Jung MW. 2000. Cholinergic modulation of synaptic transmission and plasticity in entorhinal cortex and hippocampus of the rat. Neuroscience 97: 671-676.

Table 1. Laminar and regional density of ACh axons and varicosities in the dorsal hippocampus of adult mouse and rat

		MOUSE		RAT	
		Axons (m/mm^3)	Varicosities ($10^6/mm^3$)	Axons (m/mm^3)	Varicosities ($10^6/mm^3$)
CA1	Oriens	13.7 ± 0.9	5.5 ± 0.3	14.8 ± 1.1	5.9 ± 0.5
	Pyramidale	17.9 ± 1.0	7.2 ± 0.4	17.0 ± 1.8	6.8 ± 0.7
	Radiatum	13.3 ± 1.6	5.3 ± 0.6	10.6 ± 1.6 *	4.2 ± 0.6 *
	L. Moleculare	10.8 ± 1.3	4.3 ± 0.5	6.4 ± 1.2 ***	2.6 ± 0.5 ***
	Mean	13.9 ± 0.7	5.6 ± 0.3	12.2 ± 1.0	4.9 ± 0.4
CA3	Oriens	16.7 ± 0.9	6.7 ± 0.3	17.8 ± 1.4	7.1 ± 0.6
	Pyramidale	19.6 ± 0.9	7.8 ± 0.4	20.4 ± 1.3	8.2 ± 0.5
	Lucidum	10.4 ± 1.2	4.2 ± 0.5	10.7 ± 1.6	4.3 ± 0.7
	Radiatum	13.7 ± 0.9	5.5 ± 0.3	13.2 ± 1.2	5.3 ± 0.5
	L. Moleculare	20.2 ± 1.0	8.1 ± 0.4	18.8 ± 1.4	7.5 ± 0.5
	Mean	16.1 ± 0.7	6.4 ± 0.3	16.2 ± 0.8	6.6 ± 0.3
DG	Moleculare	19.9 ± 1.2	8.0 ± 0.5	19.5 ± 1.2	7.8 ± 0.5
	Granulare	13.6 ± 1.6	5.4 ± 0.6	13.4 ± 1.7	5.4 ± 0.7
	Polymorph	13.9 ± 2.4	5.6 ± 1.0	13.8 ± 1.8	5.5 ± 0.7
	Mean	15.8 ± 1.2	6.2 ± 0.6	15.6 ± 1.2	6.2 ± 0.5
HIPPOCAMPUS		15.3 ± 0.7	6.1 ± 0.7	14.7 ± 0.7	5.9 ± 0.3

Data from 6 mice and 6 rats. Means ± s.d. in meters of axon and millions of axon varicosities per mm^3. See Figs. 5 and 6 for statistical analysis of differences between layers in each species. * $p < 0.05$, *** $p < 0.001$ indicate interspecies differences by Student t test.

Figure 1 Low and high power views from mouse (**A**,**B**) and rat (**C**,**D**) dorsal hippocampus. **A** and **C** illustrate the overall distribution of the ACh (ChAT-immunostained) innervation in the plane of section examined (interaural A 1.98 mm in mouse and bregma – 3.7 mm in rat). The three regions in which the ACh innervation was quantified are outlined: CA1, CA3 and DG. In each region, three rows of squares, disposed in the various layers, represent the sampling windows, 50 μm in side, from which length measurements of the ChAT-immunostained axon network were obtained, as described in Materials and Methods. See Results for a detailed description of the layered pattern of ACh innervation, and Table 1 for quantitative data on the density of ACh innervation in each layer and hippocampal region. The adjacent enlargements (**B** and **D**) are digitized light microscopic images of one of the sampling windows in the stratum radiatum of CA1. Note the greater density of ACh innervation in mouse than rat. Scale bars: for **A** and **C**, 0.5 mm in **C**; for **B** and **D**, 10 μm in **D**.

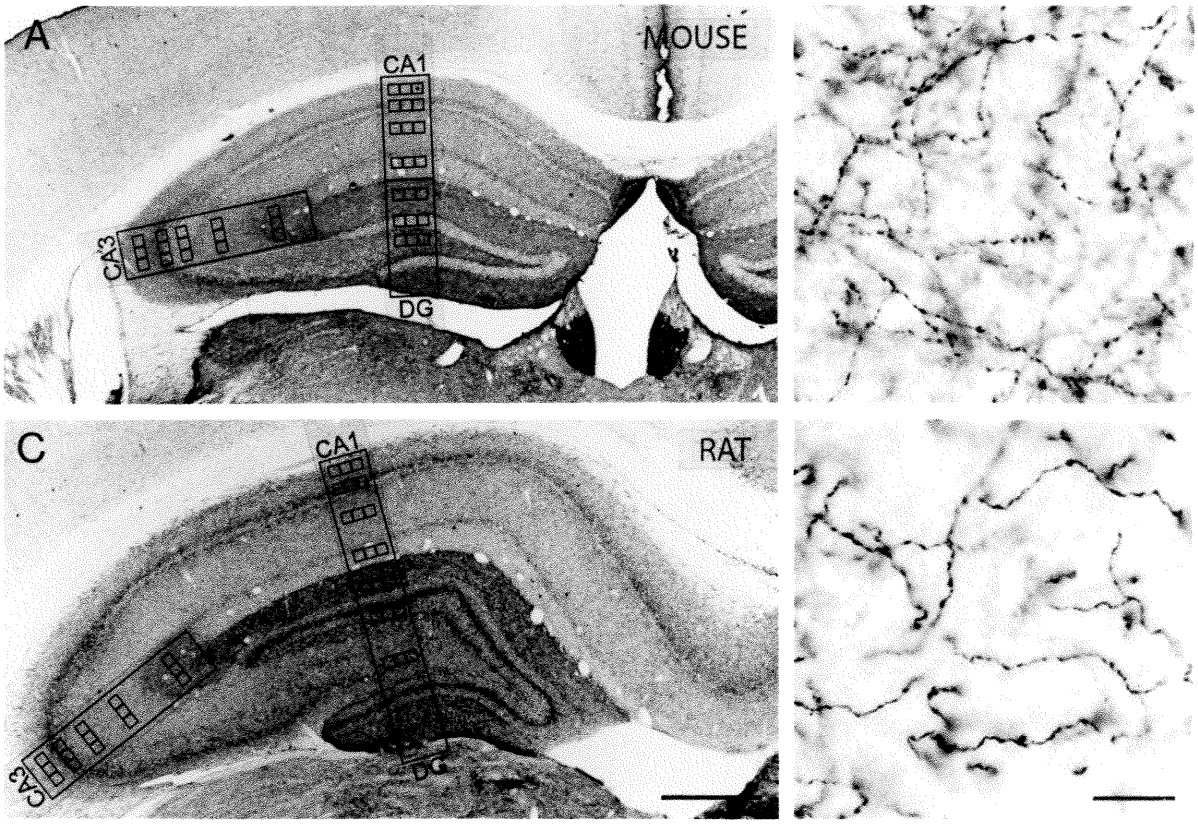
A
MOUSE
CA1
CA3
DG
C
RAT
CA1
CA3
DG

Figure 2 Laminar distribution of the ACh innervation in the dorsal hippocampus of adult mouse: CA1 and DG (**A**), CA3 (**B**); (see Table 1 and Fig. 4 for quantitative data). The density of ACh innervation is obviously much less in CA1 than in DG or CA3. In CA1 (**A**), note the three layered pattern in the stratum pyramidale (pyr), and the presence of two interneurons (arrows) within the band of slightly denser innervation (asterisks) at the border of stratum radiatum (rad) and lacunosum moleculare (lm). One of these two ACh interneurons is shown at higher magnification in **C**, among trajectories of fine varicose axons many of which appear to run medio-laterally. In the DG (**A**), the layered pattern formed by the alternation of strata moleculare (mol), granulare (gr) and polymorph (pm) is accentuated by the narrow bands of denser innervation on either side of the stratum granulare. CA3 (**B**) is rotated more than 90° for presentation. Note the dense innervation, but lack of stratification, in its widened pyramidal layer (pyr), contrasting with the low density in the underlying stratum lucidum (luc). The density in stratum radiatum (rad) is equivalent to that in CA1, whereas both oriens (or) and lacunosum moleculare (lm) are much more densely innervated in CA3 than CA1. Scale bars: for **A** and **B**, 100 μm in **B**; for **C**, 50 μm.

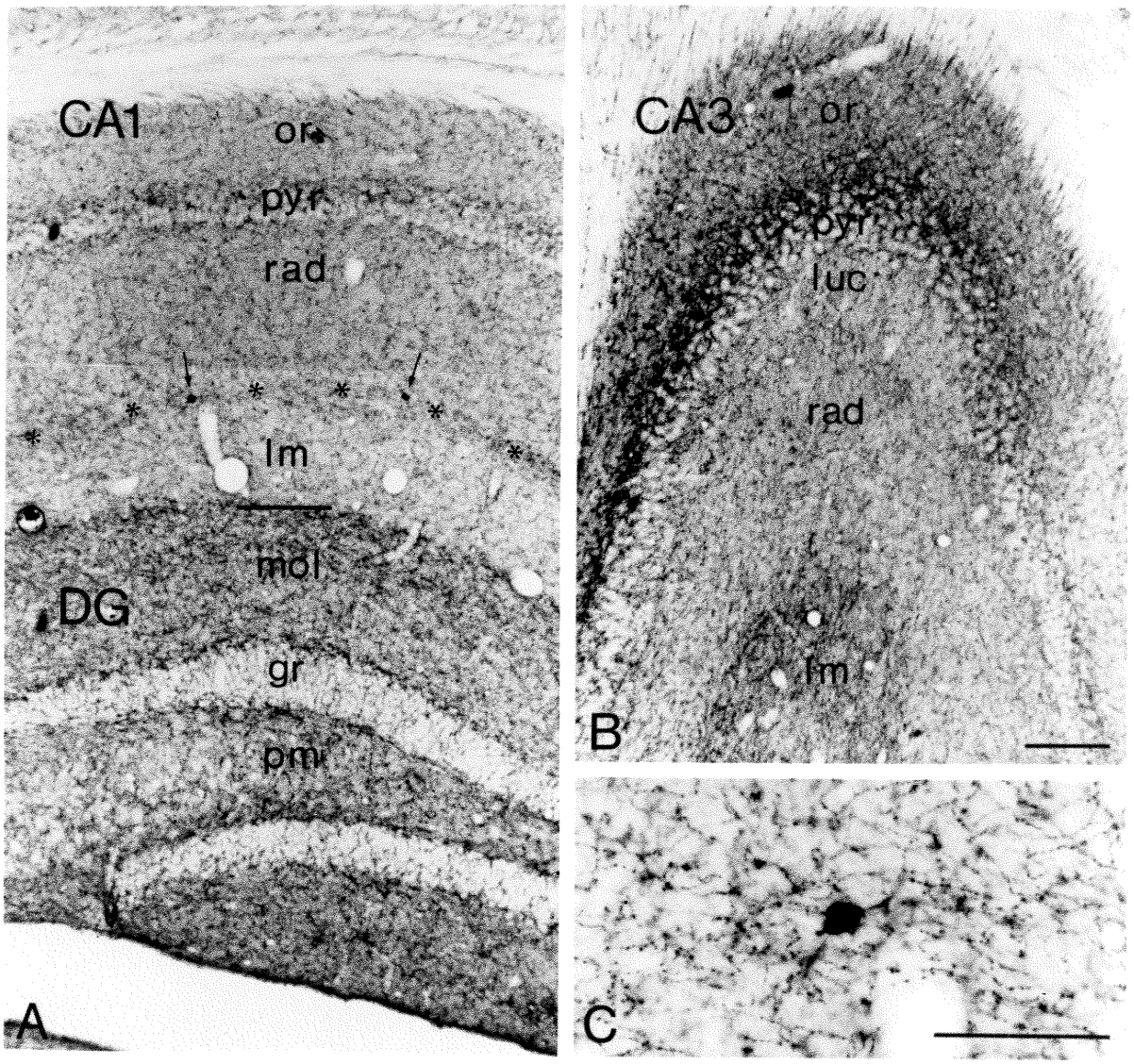
CA1
or
pyr
rad
lm
mol
DG
gr
pm
A
CA3
or
pyr
luc
rad
lm
B
C

Figure 3 Laminar distribution of the ACh innervation in the dorsal hippocampus of adult rat: CA1 and DG (**A**), CA3 (**B**); (see Table 1 and Fig. 5 for quantitative data). Same magnifications as in Fig. 2, for purposes of comparison. The contrast between the density of ACh innervation in CA1 versus DG or CA3 is greater than in mouse. In CA1 (**A**), the three layered pattern in the stratum pyramidale (pyr) resembles that in mouse, but the innervation of stratum radiatum (rad) and particularly of lacunosum moleculare (lm) is much less dense. Note the bipolar interneuron (arrow), and its thick proximal dendrites, near the border of lacunosum moleculare and radiatum (enlarged in **C**). In DG (**A**), the overall density of innervation is very similar to that in mouse, whereas the layering patterns on either side of the stratum granulare (gr) and within the stratum moleculare (mol) are more prominent. In CA3 (**B**) the laminar distribution and density of innervation is almost identical to that in mouse. Note the axon with a string of relatively large varicosities running above the horizontal portion of the upper dendrite in **C**. luc, lucidum. Scale bars: for **A** and **B**, 100 μm in **B**; for **C**, 50 μm.

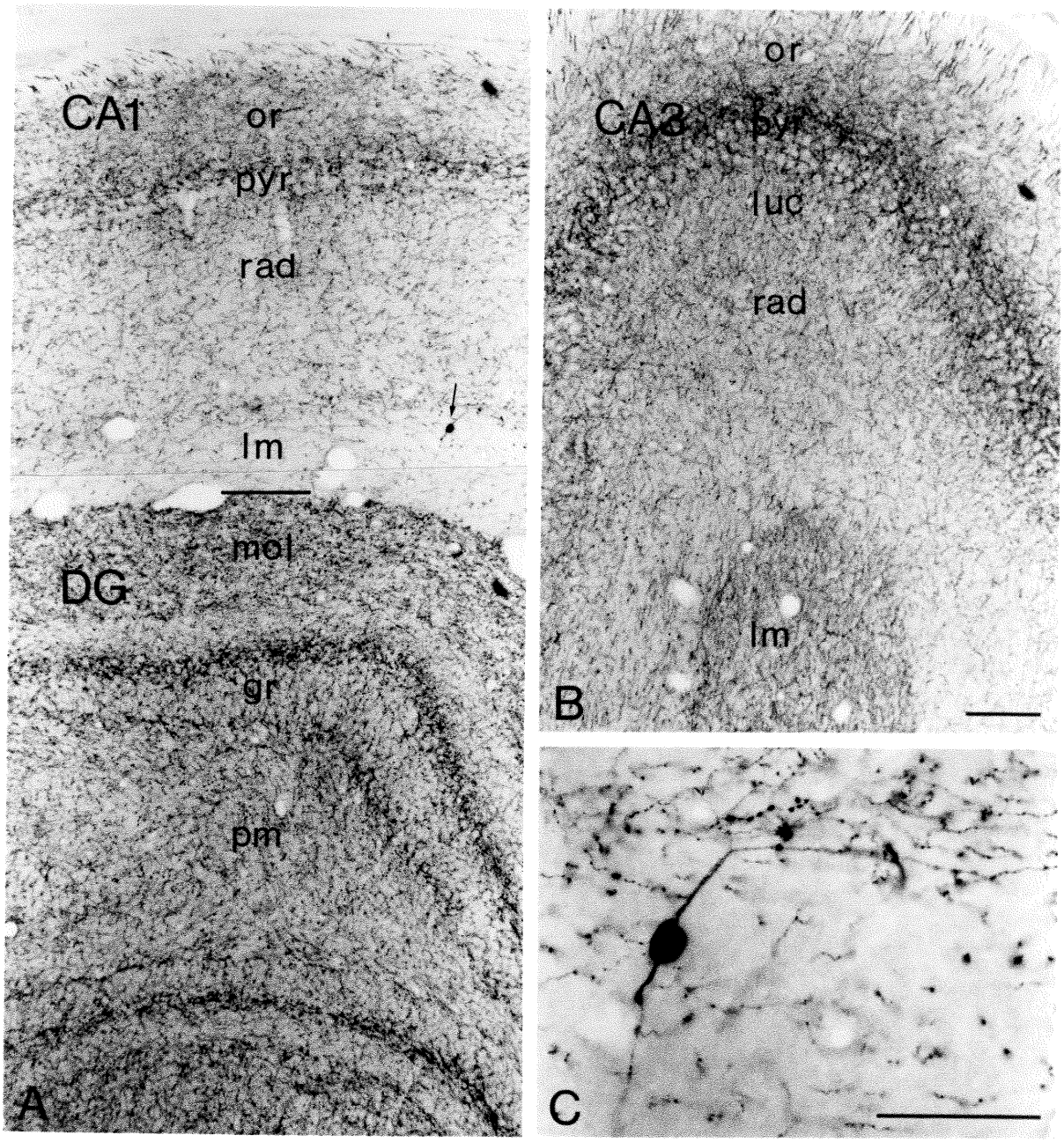
CA1
or
pyr
rad
lm
mol
DG
gr
pm
A
or
CA3
pyr
luc
rad
lm
B
C

Figure 4 Laminar and regional density of ACh axons and axon varicosities in the dorsal hippocampus of adult mouse (CA1, CA3 and DG). Data derived from the values in Table 1, as explained in Materials and Methods. Means ± s.e.m. in meter of axons or millions of axon varicosities per mm^3. The layers showing statistically significant differences are linked by hooks with asterisks in front of the differing layer(s). * ($p < 0.05$), ** ($p < 0.01$) and *** ($p < 0.001$) indicate significant differences between layers by Student t test.

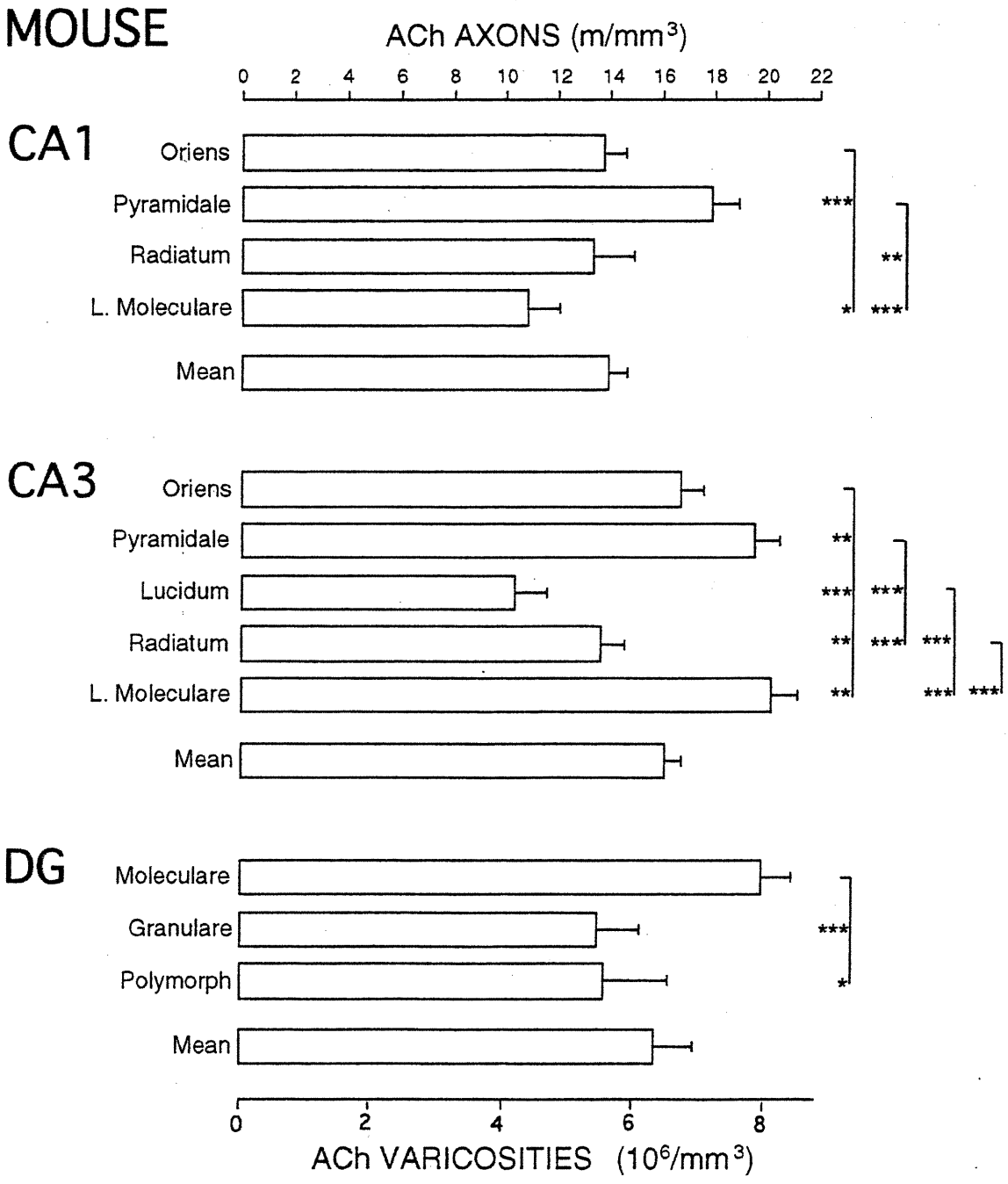
MOUSE
ACh AXONS (m/mm3)
0 2 4 6 8 10 12 14 16 18 20 22
CA1
Oriens
Pyramidale
Radiatum
L. Moleculare
Mean
***
**
*
***
CA3
Oriens
Pyramidale
Lucidum
Radiatum
L. Moleculare
Mean
**
***
***
**
***
**
***
***
***
DG
Moleculare
Granulare
Polymorph
Mean
***
*
0 2 4 6 8
ACh VARICOSITIES (10⁶/mm3)

Figure 5 Laminar and regional density of ACh axons and axon varicosities in the dorsal hippocampus of adult rat (CA1, CA3 and DG). Data derived from the values in Table 1, as explained in Materials and Methods. Means ± s.e.m. in meter of axons or millions of axon varicosities per mm3. The layers showing statistically significant differences are linked by hooks with asterisks in front of the differing layer(s). * ($p < 0.05$), ** ($p < 0.01$) and *** ($p < 0.001$) indicate significant differences between layers by Student t test.

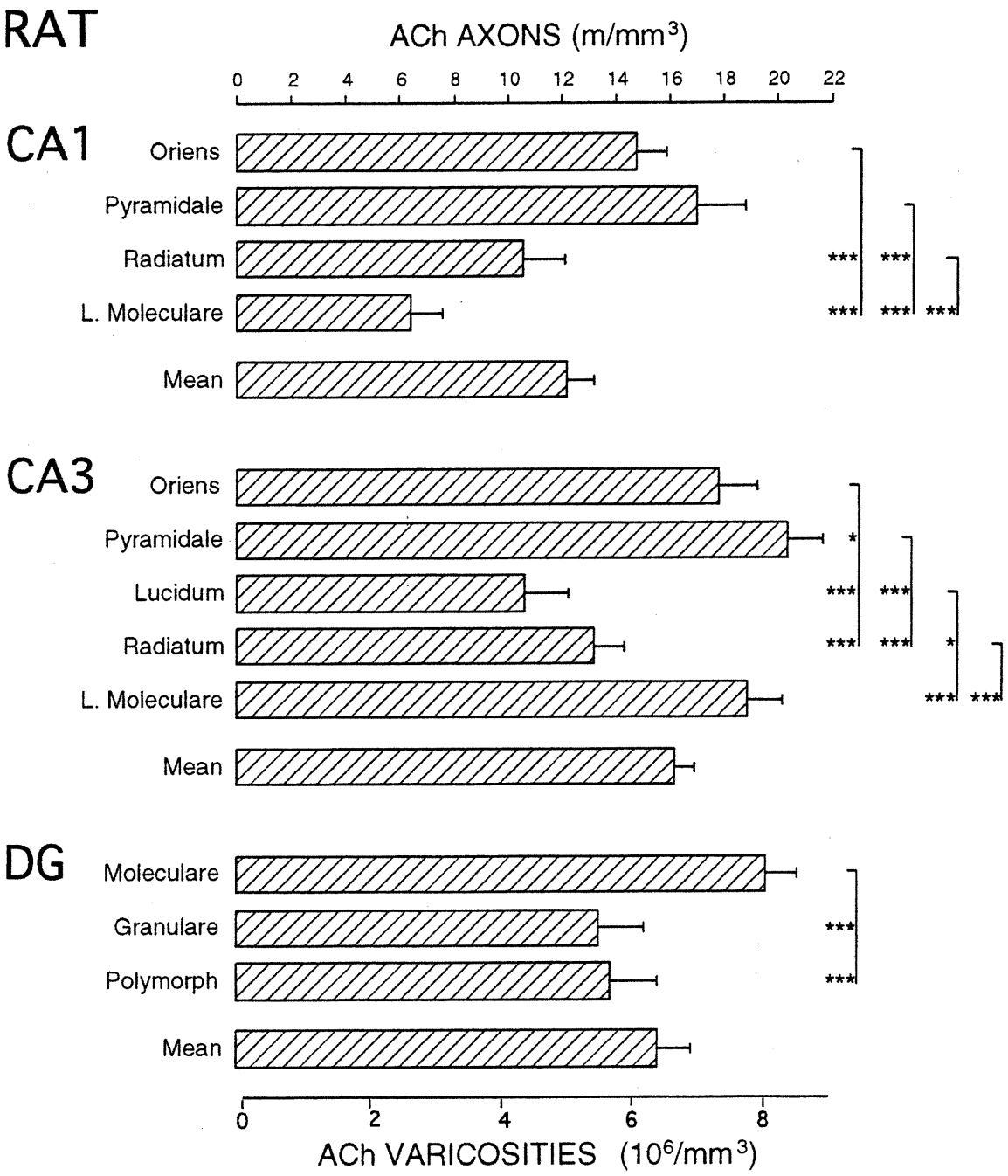
RAT
ACh AXONS (m/mm3)
0 2 4 6 8 10 12 14 16 18 20 22
CA1
Oriens
Pyramidale
Radiatum
L. Moleculare
Mean
***
***
***
***
***
CA3
Oriens
Pyramidale
Lucidum
Radiatum
L. Moleculare
Mean
*
***
***
***
***
*
***
***
DG
Moleculare
Granulare
Polymorph
Mean
***
***
0 2 4 6 8
ACh VARICOSITIES (10⁶/mm3)